ABC Imagem Cardiovascular

Volume 38 | Number 3

July/August/September 2025

Sociedade Brasileira de Cardiologia
ISSN-2675-312X

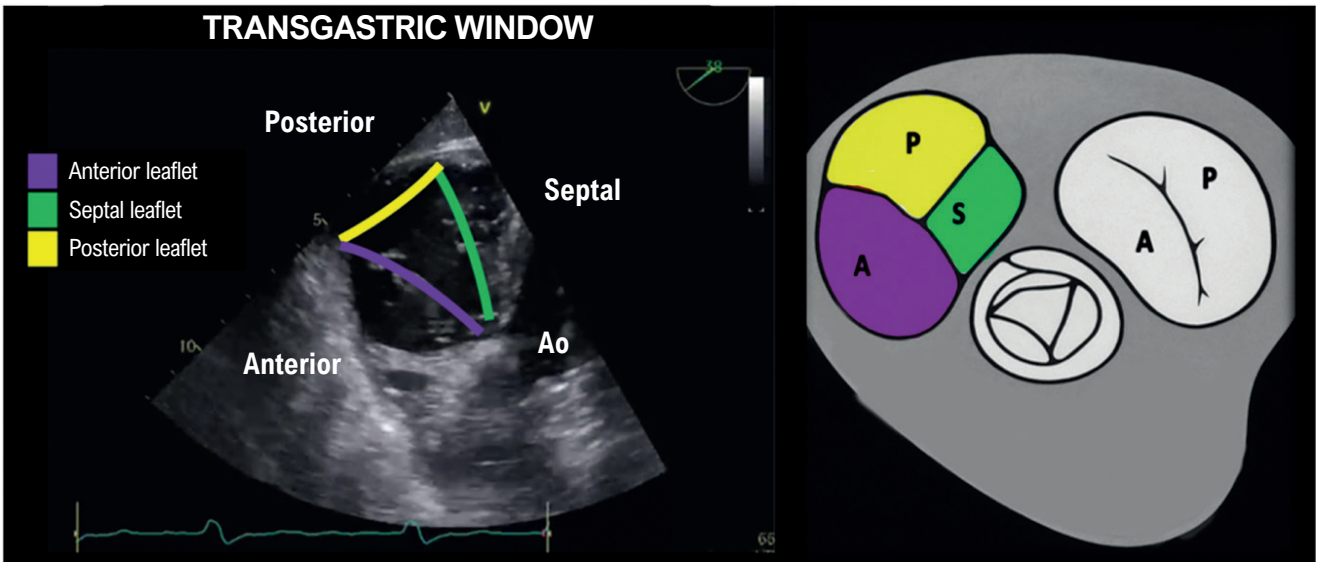

Figure 6 of the article 2025-0064: Tricuspid Valve: Anatomical Basis and Patient Selection Criteria for Transcatheter Structural Interventions.

DIC | SBC Sociedade Brasileira de Cardiologia 1943 | ABC Imagem Cardiovascular

Contents

Click on the title to read the article

Departament of Cardiovascular Imaging

President
Silvio Henrique Barberato - PR

Vice President of Echocardiography
Daniela do Carmo Rassi Frota - GO

Vice President of Nuclear Cardiology
Cláudio Tinoco Mesquita – RJ

Vice President of Vascular Echography
Salomon Israel do Amaral – RJ

Vice President of Magnetic Resonance Imaging
Isabela Bispo Santos da Silva Costa – SP

Vice President of Computed Tomography
Jorge Andion Torreão – BA

Vice President of Congenital Heart Disease and Pediatric Cardiology
Andressa Mussi Soares – ES

Managing Director
Adenalva Lima de Souza Beck – DF

Financial Director
Gláucia Maria Penha Tavares - SP

Journal Editor
Marcelo Dantas Tavares de Melo – PB

Consulting Board

Members
André Luiz Cerqueira de Almeida - BA
Arnaldo Rabischoffsky - RJ
Carlos Eduardo Rochitte - SP
Marcelo Luiz Campos Vieira - SP
Samira Saady Morhy - SP

Scientific Committee

Coordinator
Daniela do Carmo Rassi Frota - GO

Members
Andressa Mussi Soares - ES
Cláudio Tinoco Mesquita - RJ
Isabela Bispo Santos da Silva Costa - SP
Jorge Andion Torreão - BA
Salomon Israel do Amaral - RJ

Echocardiography Certification Committee

Coordinator
Tatiane Mascarenhas Santiago Emerich - ES
Andrea de Andrade Vilela - SP

Adult Echo Members
Antonio Amador Calvilho JR. - SP
Antonio Tito Paladino Filho - SP
Eliza de Almeida Gripp - RJ
Jaime Paula Pessoa Linhares Filho - CE
João Carlos Moron Saes Braga - SP
Marcio Mendes Pereira - MA
Paulo Henrique Nunes Pereira - PA
Renato de Aguiar Hortegal - SP
Tiago Costa Bignoto - SP
Wanessa Nakamura Guimarães - DF

Congenital Echo Members
Barbara Neiva Tanaka - MA
Daniela Lago Kreuzig - SP
Danielle Lopes Rocha - ES
Halsted Alarcao Gomes Pereira da Silva - SP
Leandro Alves Freire - SP
Marcio Miranda Brito - TO
Maria Elisa Martini Albretch - SP

Seniors
Andrea de Andare Vilela - SP
Glaucia Maria Penha Tavares - SP
José Luiz Barros Pena - MG
Maria Estefania Bosco Otto - DF
Mohamed Hassan Saleh - SP
Solange Bernardes Tatani - SP

Social Media Committee

Coordinator
Alex dos Santos Félix - RJ
Antonio Carlos Leite de Barros Filho - SP

Members
Barbara Athayde Linhares Martins Vrandecic - MG
Cristiane Nunes Martins - MG
José Roberto Matos Souza - SP
Simone Cristina Soares Brandão - PE

Professional Defense and Institutional Relations Committee

Members
Fabio Cañellas Moreira - RS
Jorge Yussef Afiune - DF
Marcelo Haertel Miglioranza - RS
Mohamed Hassan Saleh - SP
Wagner Pires de Oliveira Júnior - DF

Committee of Education and Accreditation

Coordinator
Edgar Bezerra de Lira Filho - SP

Members
Andrea de Andare Vilela - SP
Sandra Nívea dos Reis Saraiva Falcão - CE

Intersociety Committee

Coordinator
Marcelo Luiz Campos Vieira - SP

Members
Ana Cristina de Almeida Camarozano - PR
José Luiz Barros Pena - MG
Marcelo Haertel Miglioranza - RS

DIC Youth Committee

Coordinator
Bruna Morhy Borges Leal Assunção - SP
Márcio Miranda Brito - TO

Adult Echo Members
Carolina da Costa Mendes - SP
Manoela Falsoni - SP
Talita Beithum Ribeiro Mialski - PR
Tauin Raoni Do Couto - PA

CR/MR Members
Maria Júlia Silveira Souto - SP

Vascular Ultrasound Member
Larissa Chaves Nunes de Carvalho - SP

Member Of Congenital Heart Diseases
Isabela de Sousa Lobo Silva - SP

Committee on Echocardiography, Congenital and Pediatric Cardiology

Coordinator
Andressa Mussi Soares - ES

Members
Cláudia Regina Pinheiro de Castro Grau - SP
Laura Mercer Rosa - USA
Márcia Ferreira Alves Barberato - PR

PORTAL DIC

Coordinator
Alex dos Santos Félix - RJ

Administrative Council – Year 2025 (Brazilian Society of Cardiology)

North/Northeast
Nivaldo Menezes Filgueiras Filho (BA) – Vice-President of the Administrative Council of SBC
Sérgio Tavares Montenegro (PE)

East
Denilson Campos de Albuquerque (RJ)
Evandro Tinoco Mesquita (RJ)

State of São Paulo
Ricardo Pavanello (SP)
Miguel Moretti (SP)

Center
Carlos Eduardo de Souza Miranda (MG)
Renault M. Ribeiro Junior (DF)

South
Paulo Ricardo Avancini Caramori (RS) – President of the Administrative Council of SBC
Gerson Luiz Bredt Júnior (PR)

Scientific Committee
Sérgio Tavares Montenegro (PE)
Miguel Moretti (SP)
Angelo de Paola (SP)

National Editorial Board

ABC Imagem Cardiovascular

Volume 38, Nº 3, July/August/September 2025

Indexing: Lilacs (Latin American and Caribbean Health Sciences Literature), Latindex (Regional Cooperative Online Information System for Scholarly Journals from Latin America, the Caribbean, Spain and Portugal) and DOAJ (Directory of Open Access Journals)

Address: Av. Marechal Câmara, 160 - 3º andar - Sala 330
20020-907 • Centro • Rio de Janeiro, RJ • Brazil
Phone.: (21) 3478-2700
E-mail: abcimaging@cardiol.br
https://www.abcimaging.org/

Commercial Department
Phone: (11) 3411-5500
E-mail: comercialsp@cardiol.br

Editorial Production
SBC - Scientific Department

Graphic Design and Diagramming
SBC - Scientific Department

Editorial

Between the Physiological and the Pathological Spectra: When the Athlete's Heart Demands More Than Admiration

Antonio Amador Calvilho Júnior,[1,2] *Julia Galetto Nisgoski,*[2] *Maria Eduarda da Silva Pires,*[2] *Joao Nádson Granja Nunes,*[2] *Beatriz Moraes dos Santos Branco*[2]

Instituto Dante Pazzanese de Cardiologia,[1] *São Paulo SP – Brazil*

Universidade Paulista – Medicina,[2] *São Paulo, SP – Brazil*

The increasing participation in high-intensity sports has expanded the role of cardiology in athlete screening and monitoring. Although Sudden Cardiac Death (SCD) is rare, it has a deep impact on society as a whole. Echocardiography is central in this setting, serving as the primary imaging modality to distinguish physiological remodeling in the athlete's heart from structural cardiomyopathies.

Prolonged and intense exercise induces adaptive phenotypic and physiological changes that enhance myocardial performance. These adaptations, known as "athlete's heart," are extensively studied because they need to be differentiated from potentially fatal cardiovascular diseases.[1-3] The Athlete's Heart shares phenotypic characteristics with several pathological conditions, such as Hypertrophic Cardiomyopathy (HCM), Dilated Cardiomyopathy (DCM), and Arrhythmogenic Right Ventricular Cardiomyopathy (ARVC).[4] Cardiologists need to be aware of these overlaps to correctly diagnose and prevent serious outcomes, especially in young, apparently healthy individuals, who may not experience symptoms until they engage in intense exercise. Equally important is the ability to identify normal adaptive cardiac remodeling, thereby enabling precise screening and appropriate guidance for elite athletes.

Pre-participation sports evaluation is recommended as a preventive measure for athletes' SCD and begins with clinical evaluation and electrocardiography. However, up to 16% of SCD cases are linked to structural heart disease without electrocardiographic abnormalities.[5] Many of these conditions could be detected earlier through cardiovascular imaging. For this reason, some professional sports organizations have incorporated echocardiography, a low-cost and widely accessible tool, into initial screening protocols, and in some cases, as the only test performed at baseline evaluation. [6, 7]

This editorial underscores the importance of identifying echocardiographic "red flags" in athletes, findings that may warrant further investigation or temporary restriction from competition. These borderline features, situated between physiological adaptation and early disease, demand both high-quality image acquisition and expert interpretation. Therefore, defining the scope of relevant echocardiographic parameters in this population, as well as clarifying when adaptations should raise suspicion of pathology, remains a key priority.

Keywords

Echocardiography; Exercise-Induced Cardiomegaly; Cardiomyopathies

Mailing Address: Antonio Amador Calvilho Júnior •
Instituto Dante Pazzanese de Cardiologia – Ecocardiografia. Av. Dante Pazzanese, 500, Postal Code: 04012-909. São Paulo, SP – Brazil
E-mail: dr.calvilho@gmail.com

DOI: https://doi.org/10.36660/abcimg.20250059i

Comprehensive Echocardiographic Evaluation in Athletes

A well-conducted echocardiogram should follow minimum quality protocols and be tailored to the athlete's clinical context.[8] To increase sensitivity in detecting structural heart disease, it is recommended that athletes' echocardiograms include:

1. Multiple short-axis views to assess ventricular wall thickness in all segments.
2. Detailed assessment of the presence of myocardial trabeculations.
3. Visualization of the origin of the left and right coronary arteries.
4. Measurement of Left ventricular Global Longitudinal Strain (GLS) and Left Atrial Strain (LAS) whenever possible.

Echocardiography in Athletes: What is Expected?

Evaluating an athlete's heart requires not only technical expertise from the echocardiographer but also clinical sensitivity to recognize the complexities and nuances of physiological remodeling. Recognizing that there will often be uncertainties in the interpretation of the findings is important, which may require more specific and targeted additional investigations. To achieve this, the health professional must fully understand the expected cardiac adaptations, the variability of findings according to the type and volume of exercise, and the impact of factors such as the athlete's ethnicity, sex, age, and body composition.[8]

Structural and functional changes in the athlete's heart vary widely according to the predominant type of effort involved in the sport. Endurance sports, for example, tend to cause greater dilation of the cardiac chambers, while strength sports can lead to a more pronounced increase in ventricular wall thickness. Table 1 summarizes the main echocardiographic characteristics expected in the normally adapted athlete's heart.

Echocardiographic Red Flags: How to Recognize Suspicious Alterations in an Athlete's Heart

Certain echocardiographic findings should raise suspicion of pathology in athletes because they deviate from typical

physiological adaptations. A septal wall thickness > 15 mm or significant asymmetry points to possible HCM. Left Atrial dilation disproportionate to ventricular dilation indicates chronic overload or diastolic dysfunction. E/e' values greater than 14 suggest elevated ventricular filling pressure, which is unusual in normal adaptations. A reduction in GLS (< -16%) may reveal subclinical dysfunction even with preserved ejection fraction, while a LA reservoir strain measurement below 38% is an early sign of impaired atrial compliance. Furthermore, the presence of excessive trabeculations, apical aneurysms, or segmental dysfunction deviates from the physiological pattern. These criteria justify the need for further investigation.[2]

Table 2 summarizes the main echocardiographic red flags, their related entities, and the rationale for each to be considered a warning sign.

Table 1 – Normal echocardiographic findings in the athlete's heart[2]

Echocardiographic finding	Description in athletes
Cardiac chamber dilation	Symmetrical dilatation of LV and RV; common in several modalities.
Left ventricular thickening	Slight increase in wall thickness, especially in endurance athletes.
Eccentric LV remodeling	Increased LV volume without disproportionate thickness.
LV systolic function	Preserved or increased when assessed by specific methods, such as longitudinal strain by speckle tracking, this is evident even when the ejection fraction is slightly reduced.
Diastolic function	LV diastolic function is usually preserved or even optimized in adaptive states, as is the case with the "supernormal" pattern with a mitral inflow E/A ratio >2.
Atrial dilation	Frequent biatrial dilation, especially in men.
Aortic root	Slight dilation of the aortic root may occur within physiological limits.

AE: Átrio esquerdo; VD: Ventrículo direito; VE: ventrículo esquerdo.

Table 2 – Echocardiographic Red flags[2,4,8-10]

Red Flag Ecocardiográfica	Possível Entidade Associada	Justificativa Clínica
Septal thickness ≥ 15 mm or Septal thickness between 13–15 mm and associated with LVDD ≤ 53 mm, LA anteroposterior diameter ≤ 39 mm, diastolic dysfunction, concentric geometry, or hypertrophy asymmetry (IVS: PP ratio ≤ 1.3).	Hypertrophic cardiomyopathy	Values above physiological limits suggest structural pathology. Values that fall in the gray zone (13–15 mm) when associated with small chambers and/or asymmetry and/or diastolic dysfunction also suggest hypertrophic cardiomyopathy.
Isolated Left Ventricular Dilation	Dilated cardiomyopathy	Isolated left ventricular dilation should not be considered physiological and should raise immediate suspicion of dilated cardiomyopathy.
Disproportionate left atrial dilation or pronounced increase in LA anteroposterior diameter (men > 50 mm, women > 45 mm)	Hypertrophic Cardiomyopathy or Early Diastolic Dysfunction	Although it can occur in isolation, in physiological adaptive situations, it tends to coexist with ventricular enlargement, therefore, isolated or disproportionate LA enlargement should raise suspicion of a pathological cause.
E/e' > 14	Increased Ventricular Filling Pressure	Indicator of elevated filling pressure, an unusual condition in healthy athletes, and indicative of the presence of myocardial disease.
LVEF ≤ 47%	Dilated cardiomyopathy	There is indeed a decrease in resting LVEF in athletes (between 53-48%), but values below this range raise suspicion of cardiomyopathy.

GLS < -16%	Hypertrophic cardiomyopathy (if associated with LV hypertrophy) or subclinical LV dysfunction of any etiology	Early functional alteration, even with preserved ejection fraction. Adaptive LV hypertrophy does not reduce GLS.
RAS < 38%	Diastolic dysfunction or chronic overload	Early sign of loss of atrial compliance.
Excessive trabeculations + segmental dysfunction and/or myocardial wall thinning (end-diastolic thickness < 5 mm)	Non-compaction myocardium	Prominent trabeculations may occur in healthy athletes, but concomitant segmental dysfunction and/or myocardial wall thinning indicate a pathological origin.
Significant LV dilation + systolic dysfunction	Dilated cardiomyopathy	Combination incompatible with isolated physiological adaptation.
RV dilation* + contractile abnormalities or aneurysms (including in the LV)	Arrhythmogenic RV cardiomyopathy	Suggests RV structural involvement outside the athlete's spectrum.
Coronary artery origin anomalies	Malignant coronary artery course susceptible to ischemia	Abnormalities indicating an interarterial or intramural course are susceptible to coronary obstruction and, therefore, a risk of sudden death. Even non-classically malignant anomalies (retroaortic and prepulmonary courses) should indicate further evaluation.

** The presence of RV longitudinal dysfunction (S' ≤ 9 cm/s and/or TAPSE ≤ 16 mm) or reduced RV FAC (< 31%) is not normal in athletes and indicates further evaluation with stress echocardiography. LA: Left atrium; LVDD: Left ventricular diastolic diameter; LVEF: Left ventricular ejection fraction; PP: Posterior wall; GLS: Global longitudinal strain; IVS: Ventricular septum; RAS: Left atrial reservoir strain; RV: Right ventricle.*

How to Manage Suspicious Findings on Athletes' Echocardiograms?

The identification of a red flag on echocardiography should not, by itself, justify the athlete's immediate disqualification. Any isolated abnormality must be interpreted within a broader clinical context that considers symptoms, family history of sudden cardiac death or cardiovascular disease, electrocardiographic findings, and the nature of the sport involved. Within this integrated framework, the echocardiographer plays a pivotal role, not only in documenting structural or functional alterations but also in identifying patterns that warrant further investigation. This may call for additional testing, including three-dimensional echocardiography, cardiac magnetic resonance imaging, exercise stress testing, or genetic analysis.

Conclusion

Echocardiography remains the cornerstone for structural and functional evaluation of the athlete's heart. A clear understanding of its strengths and limitations, combined with the expertise of the echocardiographer, is essential to distinguish true warning signs from benign findings, safeguarding the athlete's health while avoiding unnecessary restriction from sports participation.

References

1. Maron BJ. Structural Features of the Athlete Heart as Defined by Echocardiography. J Am Coll Cardiol. 1986;7(1):190-203. doi: 10.1016/s0735-1097(86)80282-0.
2. Flanagan H, Cooper R, George KP, Augustine DX, Malhotra A, Paton MF, et al. The Athlete's Heart: Insights from Echocardiography. Echo Res Pract. 2023;10(1):15. doi: 10.1186/s44156-023-00027-8.
3. Maron BJ, Pelliccia A, Spirito P. Cardiac Disease in Young Trained Athletes. Insights Into Methods for Distinguishing Athlete's Heart from Structural Heart Disease, with Particular Emphasis on Hypertrophic Cardiomyopathy. Circulation. 1995;91(5):1596-601. doi: 10.1161/01.cir.91.5.1596.
4. Albaeni A, Davis JW, Ahmad M. Echocardiographic Evaluation of the Athlete's Heart. Echocardiography. 2021;38(6):1002-16. doi: 10.1111/echo.15066.
5. Maron BJ, Doerer JJ, Haas TS, Tierney DM, Mueller FO. Sudden Deaths in Young Competitive Athletes: Analysis of 1866 Deaths in the United States, 1980-2006. Circulation. 2009;119(8):1085-92. doi: 10.1161/CIRCULATIONAHA.108.804617.
6. Niederseer D, Rossi VA, Kissel C, Scherr J, Caselli S, Tanner FC, et al. Role of Echocardiography in Screening and Evaluation of Athletes. Heart. 2020:heartjnl-2020-317996. doi: 10.1136/heartjnl-2020-317996.

7. Mont L, Pelliccia A, Sharma S, Biffi A, Borjesson M, Terradellas JB, et al. Pre-Participation Cardiovascular Evaluation for Athletic Participants to Prevent Sudden Death: Position Paper from the EHRA and the EACPR, Branches of the ESC. Endorsed by APHRS, HRS, and SOLAECE. Europace. 2017;19(1):139-63. doi: 10.1093/europace/euw243. Epub 2016 Nov 4. PMID: 27815371.

8. Oxborough D, George K, Cooper R, Bhatia R, Ramcharan T, Zaidi A, et al. Echocardiography in the Cardiac Assessment of Young Athletes: A 2025 Guideline from the British Society of Echocardiography (Endorsed by Cardiac Risk in the Young). Echo Res Pract. 2025;12(1):7. doi: 10.1186/s44156-025-00069-0.

9. Mancuso FJN. My Approach to "Athlete'S Heart": Evaluation of the Different Types of Adaptation to Exercise. Arq Bras Cardiol: Imagem Cardiovasc. 2023;36(1):e20230002. doi:10.36660/abcimg.20230002.

10. Pelliccia A, Maron BJ, Di Paolo FM, Biffi A, Quattrini FM, Pisicchio C, et al. Prevalence and Clinical Significance of Left Atrial Remodeling in Competitive Athletes. J Am Coll Cardiol. 2005;46(4):690-6. doi: 10.1016/j.jacc.2005.04.052.

Editorial

Transesophageal Echocardiogram Always Before TAVI?

Jairo Alves Pinheiro,[1,2,3] João Lucas Pinheiro,[4] Lucas Velloso Dutra,[1,4,5] Luciano Holanda,[2,3] Renata de Sá Cassar,[2,6]

Hospital Sirio-Libanes,[1] São Paulo, SP – Brazil
Hospital do Coração,[2] São Paulo, SP – Brazil
Hospital Samaritano de São Paulo,[3] São Paulo, SP – Brazil
Instituto Dante Pazzanese de Cardiologia,[4] São Paulo, SP – Brazil
Hospital Edmundo Vasconcelos,[5] São Paulo, SP – Brazil
Instituto do Coração (Incor) do Hospital das Clínicas da Faculdade de Medicina da Universidade de São Paulo (HCFMUSP),[6] São Paulo, SP – Brazil

Cardiovascular imaging is crucial in the selection and planning of interventions for structural heart disease.[1]

Transcatheter aortic valve implantation (TAVI) has transformed the management of severe aortic stenosis (AS) in high-risk surgical populations and is currently being expanded to intermediate- and low-risk populations.[2]

Transesophageal echocardiography (TEE) offers high spatial resolution and excellent anatomical characterization of the aortic valve. However, it is a semi-invasive examination that requires preparation, fasting, and sedation. Furthermore, it can cause discomfort and poses risks, albeit low, such as esophageal perforation and bronchoaspiration.[1]

Despite the historical importance of TEE in TAVI, its routine use prior to the procedure has been questioned. In general, in this scenario, TTE is the initial examination in the evaluation of severity quantification, ventricular function, and other associated valvular pathologies, while computed tomography angiography (CT angiography) has become the standard for planning and choosing the prosthesis.[3]

The current ACC/AHA (2020) and ESC (2021) guidelines do not recommend the systematic use of TEE before TAVI. Therefore, the flowchart focuses on TTE and CT angiography, with TEE reserved for specific situations such as: suboptimal TTE images or inconclusive CT angiography, diagnostic uncertainty or discrepancy in the severity of AS, presence of aortic regurgitation disproportionate to the degree of valve calcification, evaluation of associated valvular diseases, evaluation of suspected endocarditis, severe renal failure, allergy to iodinated contrast, and presence of atrial fibrillation where left atrial appendage occlusion is considered in combination with TAVI. In these contexts, TEE adds essential clinical information and can change the management.[4,5,6]

Another relevant point is the use of TEE during the procedure, as it is useful in assessing prosthesis positioning, residual periprosthetic regurgitation, ventricular function, and immediate complications (annular rupture, aortic dissection, and early prosthetic dysfunction).[1,7]

However, in cases selected by the Heart Team, the TAVI "minimalist approach" has become increasingly common. In these cases, monitoring and evaluation are performed with TTE, with TEE reserved for support in the assessment of complications, such as localization and quantification of periprosthetic regurgitation, aortic dissection, and acquired Gerbode defects.[1,7]

In the context of the "Heart Team," the echocardiographer is an integral part and must adopt a critical and selective approach, opting for TEE before TAVI and/or intraprocedurally only when its contribution is clear.[1]

Therefore, the answer to the initial question is NO.

TEE should not be mandatory before TAVI, but rather reserved for select cases in which TTE or CT angiography cannot provide sufficient information for safe and effective planning.[3,6]

In a value-based medicine environment, the performance of exams should be guided by real clinical benefit, not by automatic institutional protocols.

Rational use preserves their high clinical utility and avoids unnecessary risks to patients.[6]

Keywords

Transcatheter Aortic Valve Replacement; Transesophageal Echocardiography; Aortic Valve Stenosis; Magnetic Resonance Imaging

Mailing Address: Jairo Alves Pinheiro •
Hospital Sirio-Libanes – Ecocardiografia. Rua Dona Adma Jafet, 115. Postal Code: 01308-050, Bela Vista, São Paulo, SP – Brazil
E-mail: jairoanapinheiro@gmail.com

DOI: https://doi.org/10.36660/abcimg.20250060i

References

1. Hahn RT, Little SH, Monaghan MJ, Kodali SK, Williams M, Leon MB, et al. Recommendations for Comprehensive Intraprocedural Echocardiographic Imaging During TAVR. JACC Cardiovasc Imaging. 2015;8(3):261-87. doi: 10.1016/j.jcmg.2014.12.014.
2. Mack MJ, Leon MB, Thourani VH, Pibarot P, Hahn RT, Genereux P, et al. Transcatheter aortic-valve replacement in low-risk patients at five years. N Engl J Med. 2023;389(21):1949-60. doi:10.1056/NEJMoa2307447.
3. Blanke P, Weir-McCall JR, Achenbach S, Delgado V, Hausleiter J, Jilaihawi H, Marwan M, Nørgaard BL, Piazza N, Schoenhagen P, Leipsic JA. Computed tomography imaging in the context of transcatheter aortic valve implantation/transcatheter aortic valve replacement: An expert consensus document of the Society of Cardiovascular Computed Tomography. JACC Cardiovasc Imaging. 2019;12(1):1-24. doi:10.1016/j.jcmg.2018.06.003.
4. Zoghbi WA, Adams D, Bonow RO, Enriquez-Sarano M, Foster E, Grayburn PA, et al. Recommendations for Noninvasive Evaluation of Native Valvular Regurgitation. A Report from the American Society of Echocardiography Developed in Collaboration with the Society for Cardiovascular Magnetic Resonance. J Am Soc Echocardiogr. 2017;30(4):303-71. doi: 10.1016/j.echo.2017.01.007.
5. Cahill TJ, Baddour LM, Habib G, Hoen B, Salaun E, Pettersson GB, Schäfers HJ, Prendergast BD. Challenges in infective endocarditis. J Am Coll Cardiol. 2017;69(3):325-344. doi:10.1016/j.jacc.2016.10.066.Otto CM, Nishimura RA, Bonow RO, Carabello BA, Erwin JP, Gentile F, et al. 2020 ACC/AHA Guideline for the Management of Patients with Valvular Heart Disease: A Report of the American College of Cardiology/American Heart Association Joint Committee on Clinical Practice Guidelines. Circulation. 2021;143:e72–e227. doi: 10.1161/CIR.0000000000000923.
6. Vahanian A, Beyersdorf F, Praz F, Milojevic M, Baldus S, Bauersachs J, et al. 2021 ESC/EACTS Guidelines for the Management of Valvular Heart Disease. Eur Heart J. 2022;43(7):561-632. doi: 10.1093/eurheartj/ ehab395.
7. Alkhouli M, Hijazi ZM, Holmes DR, Rihal CS, Wiegers SE. Intracardiac echocardiography in structural heart disease interventions. JACC Cardiovasc Interv. 2018;11(21):2135-2148. doi:10.1016/j.jcin.2018.06.056.

Left Atrium Reservoir Strain and Cardiovascular Hemodynamics: the Hidden Truths Reveal Far More Than What is Readily Apparent

Renato A. Hortegal,[1,2] *David Le Bihan,*[1,2] *Rodrigo Barretto,*[1] *Wilson Mathias Jr.*[1,2]

Instituto do Coração (Incor) do Hospital das Clínicas da Faculdade de Medicina da Universidade de São Paulo (HCFMUSP),[1] *São Paulo, SP – Brazil*
Grupo Fleury,[2] *São Paulo, SP – Brazil*

"If it is any point requiring reflection,
we shall examine it to better purpose in the dark."
— Edgar Allan Poe, The Purloined Letter (1844)

Over the past 15 years, Speckle-tracking Echocardiography has evolved into a robust technique for assessing both global and regional myocardial function. Among its expanding applications, Left Atrial (LA) strain, particularly in the reservoir phase, has emerged as a clinically relevant parameter. A reduced Left Atrial Strain reservoir (LASr) has been independently associated with elevated Left Ventricular (LV) filling pressures, recurrence of atrial fibrillation, heart failure hospitalizations, and overall cardiovascular mortality.[1,2] Reflecting this growing body of evidence, LASr has been formally incorporated into clinical practice in the recently published *"Recommendations for the Evaluation of Left Ventricular Diastolic Function by Echocardiography and for Heart Failure With Preserved Ejection Fraction Diagnosis: An Update From the American Society of Echocardiography."*[3]

Despite this, the complexity of LA mechanics has largely followed an oversimplified approach: it is often treated as a surrogate marker of filling pressures, evaluated in isolation and interpreted using fixed cut-off values, without integrating the hemodynamic and mechanical context in which the atrium operates. While such an approach has facilitated its clinical adoption, it may obscure important physiological nuances and lead to misinterpretation in complex scenarios.

The LA wall is histologically similar to the pulmonary veins, with a mean thickness ranging from 2.3 to 4.4 mm, which can be less than 30% of the LV wall thickness.[4] This makes it highly sensitive to the mechanical influence of adjacent structures that operate at a much higher force scale. Therefore, from a physiological standpoint, LA reservoir strain is a composite biomarker, shaped by at least three major components:[5,6]

1. Early atrial relaxation, shown by the S1-wave of pulmonary venous flow, which indicates the initial suction phase of the reservoir function. This is best appreciated when LA volume changes are analyzed alongside LA pressure waveforms, and occasionally appears as a subtle notch at the onset of the LASr curve.
2. Longitudinal systolic function of the ventricle, responsible for the apical displacement of the Atrioventricular (AV) plane during systole. This component stretches the LA wall and directly contributes to reservoir strain amplitude.
3. Left atrial pressure, particularly the V-wave, which modulates atrial wall tension and LA compliance.

These three forces interact dynamically and define the shape and magnitude of the LASr curve. This concept has been supported by physiological studies showing that acute changes in afterload, such as those induced by isometric handgrip, can significantly impact LA reservoir strain.[7] In this setting, increased LV pressure results in altered LASr patterns, even in the absence of changes in intrinsic atrial function — highlighting the load dependency of this metric (Figure 1).

Such physiological interplay may yield practical clinical insights. Consider patients with non-severe mitral regurgitation undergoing Cardiac Resynchronization Therapy (CRT). Improvement in mitral regurgitation often reduces LA preload[8] and subsequently decreases LASr, despite favorable LV remodeling and decreased LV end-systolic volume. Without hemodynamic contextualization, this apparent paradox might be misinterpreted as functional worsening, when in fact it reflects normalization of loading conditions.

A second, more complex scenario involves patients with paradoxical low-flow, low-gradient aortic stenosis, a subgroup that often overlaps with HFpEF physiology. In such cases, low-dose nitroprusside infusion has been explored as a hemodynamic tool to assess contractile reserve and guide treatment. Simultaneous assessment of Pulmonary Capillary Wedge Pressure (PAWP) and Left Atrial (LA) strain during vasodilation can provide further insights: a reduction in PAWP accompanied by an increase in LASr, in response to reduced LA pressure, may indicate a load-sensitive phenotype with increased afterload-mediated systolic and diastolic dysfunction, which supports prioritizing guideline-directed medical therapy for HFpEF and provides caution and concerns towards more invasive treatment as Transcatheter Aortic Valve Implantation (TAVI), that could potentially lead to further increase in pulsatile vascular load and thus worsening abnormal ventricular-vascular coupling.[9] While these strategies remain exploratory, they reflect a growing recognition that dynamic assessment of atrial mechanics can enrich the diagnostic and therapeutic process.

Another fact that we need to consider is the interplay that exists between the different phases of Left Atrial physiology. In

Keywords

Echocardiography; Hemodynamics; Heart Atria; Atrial Function

Mailing Address: David Le Bihan •
Instituto do Coração (Incor) do Hospital das Clínicas da Faculdade de Medicina da Universidade de São Paulo (HCFMUSP) – Av. Dr. Enéas Carvalho de Aguiar, 44. Postal Code: 05403-900, Cerqueira César, São Paulo, SP – Brazil
E-mail: david.bihan@hc.fm.usp.br

DOI: https://doi.org/10.36660/abc.20250068i

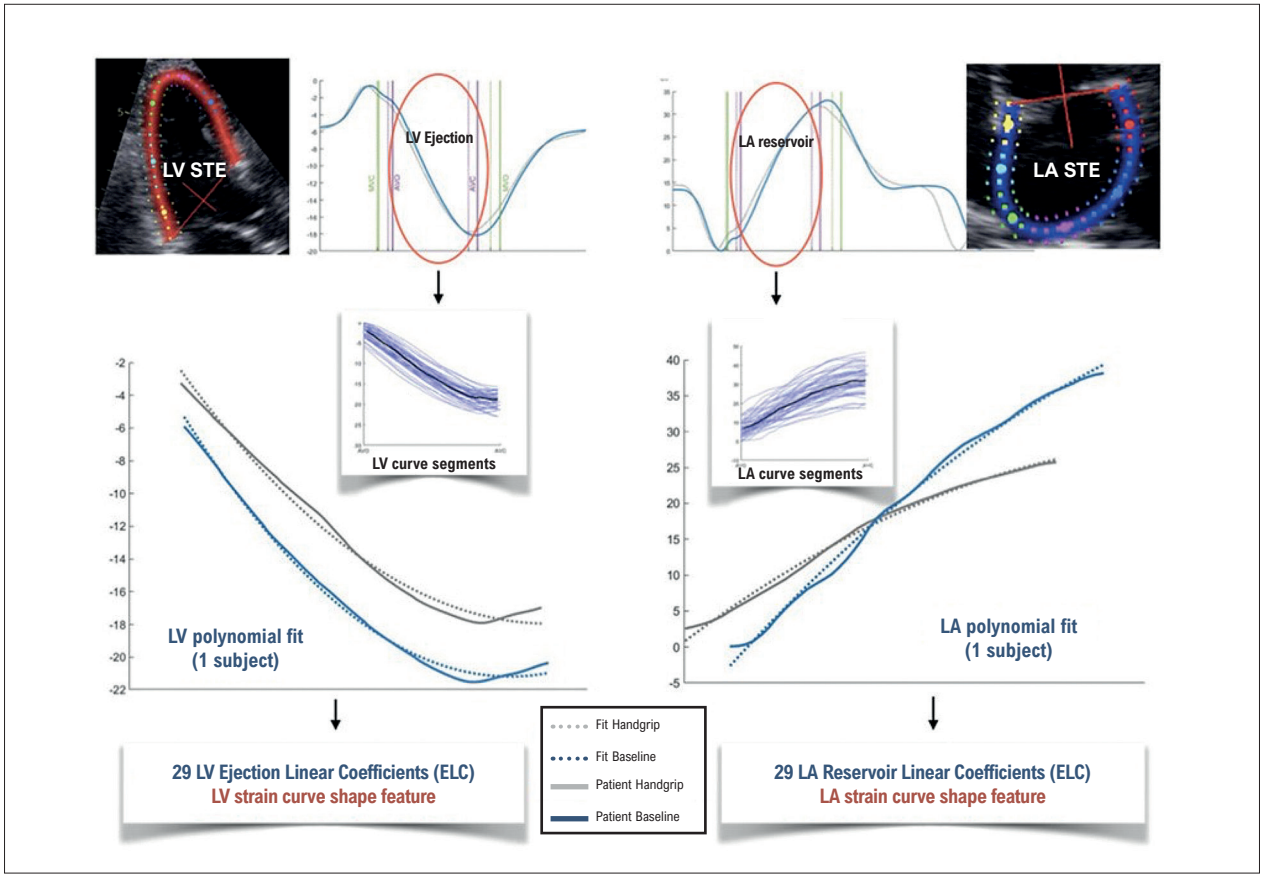

Figure 1 – *Speckle-tracking Echocardiography (STE) was used to extract strain curve segments from the left Ventricle (LV) during the ejection phase and from the Left Atrium (LA) during the reservoir phase. Polynomial regression was applied to each segment, generating 29 shape coefficients per phase: LV Ejection Linear Coefficients (ELC) and LA Reservoir Linear Coefficients (RLC). Curves from a representative subject (in blue) are displayed alongside population-level polynomial fits for baseline and isometric handgrip conditions (dotted lines). This approach was used to quantitatively assess ventricular and atrial myocardial mechanics beyond peak strain values. The acute increase in afterload induced by the handgrip maneuver mobilizes the contractile reserve of the LV and, in ventricles with limited reserve, reduces the velocity and magnitude of contraction. This imbalance may result in afterload-mediated LV systolic dysfunction and modify the slope of the LA reservoir strain curve, thereby altering its overall shape. These changes are quantitatively captured by shifts in the polynomial coefficients,[6] providing a quantitative marker of atrioventricular coupling and functional reserve under stress.*

some circumstances, a decrease in LA pressure could not affect the reservoir phase. This is probably because this phase also reflects the rigidity of the Left Atrium, which can be impacted by the chronicity of the disease. In these cases, the active contractile function of the left atrium may more accurately indicate improvements in hemodynamics.[10]

In conclusion, LASr should be interpreted not merely as a static marker of atrial function, but rather as a dynamic signal, modulated by ventricular mechanics and loading conditions. It is not so much what is revealed by absolute LASr values, but what is concealed within its shape, context, and variation under stress, that demands investigation. Future studies should aim to refine its application through integrated multiparametric approaches, incorporating both strain and hemodynamic markers. Such strategies may enhance the diagnostic precision of echocardiography in complex conditions like HFpEF, valvular disease, and atrial cardiomyopathy — where understanding the heart as a system, rather than as isolated chambers, is critical.

References

1. Almeida ALC, Melo MDT, Bihan DCSL, Vieira MLC, Pena JLB, Del Castillo JM, et al. Position Statement on the Use of Myocardial Strain in Cardiology Routines by the Brazilian Society of Cardiology's Department Of Cardiovascular Imaging - 2023. Arq Bras Cardiol. 2023;120(12):e20230646. doi: 10.36660/abc.20230646.
2. Thomas L, Marwick TH, Popescu BA, Donal E, Badano LP. Left Atrial Structure and Function, and Left Ventricular Diastolic Dysfunction: JACC State-of-the-Art Review. J Am Coll Cardiol. 2019;73(15):1961-77. doi: 10.1016/j.jacc.2019.01.059.

3. Nagueh SF, Sanborn DY, Oh JK, Anderson B, Billick K, Derumeaux G, et al. Recommendations for the Evaluation of Left Ventricular Diastolic Function by Echocardiography and for Heart Failure with Preserved Ejection Fraction Diagnosis: An Update from the American Society of Echocardiography. J Am Soc Echocardiogr. 2025;38(7):537-69. doi: 10.1016/j.echo.2025.03.011.

4. Ho SY, Cabrera JA, Sanchez-Quintana D. Left Atrial Anatomy Revisited. Circ Arrhythm Electrophysiol. 2012;5(1):220-8. doi: 10.1161/CIRCEP.111.962720.

5. Hoit BD, Gabel M. Influence of Left Ventricular Dysfunction on the Role of Atrial Contraction: An Echocardiographic-Hemodynamic Study in Dogs. J Am Coll Cardiol. 2000;36(5):1713-9. doi: 10.1016/s0735-1097(00)00922-0.

6. Nishimura RA, Abel MD, Hatle LK, Tajik AJ. Relation of Pulmonary Vein to Mitral Flow Velocities by Transesophageal Doppler Echocardiography. Effect of Different Loading Conditions. Circulation. 1990;81(5):1488-97. doi: 10.1161/01.cir.81.5.1488.

7. Uemoto RV, Cancellier R, Hortegal R, Freitas RV, Maduro Y, Paganelli M, et al. The Impact of Isometric Handgrip Testing in Left Atrial Reservoir Function. Eur Heart J Cardiovasc Imaging. 2022;23(Suppl 1):jeab289.104. doi:10.1093/ehjci/jeab289.104.

8. Russo E, Russo G, Cassese M, Braccio M, Carella M, Compagnucci P, et al. The Role of Cardiac Resynchronization Therapy for the Management of Functional Mitral Regurgitation. Cells. 2022;11(15):2407. doi: 10.3390/cells11152407.

9. Reddy YNV, Nishimura RA. Paradox of Low-Gradient Aortic Stenosis. Circulation. 2019;139(19):2195-7. doi: 10.1161/CIRCULATIONAHA.118.038252.

10. Le Bihan DC, Togna DJD, Barretto RB, Assef JE, Machado LR, Ramos AI, et al. Early Improvement in Left Atrial Remodeling and Function after Mitral Valve Repair or Replacement in Organic Symptomatic Mitral Regurgitation Assessed by Three-Dimensional Echocardiography. Echocardiography. 2015;32(7):1122-30. doi: 10.1111/echo.12817.

Original Article

Overview of Professional Practice in Computed Tomography and Cardiac Magnetic Resonance Imaging in Brazil

Isabela Bispo Santos da Silva Costa,[1] Jorge Andion Torreão,[2] Juliano de Lara Fernandes,[3] Henrique Trad,[4] Gabriela Liberato,[5] Roberto Sasdelli Neto,[6] Silvio Henrique Barberato,[7,8] Ibraim Masciarelli Pinto,[9] Tiago Senra[9]

Universidade de São Paulo, Instituto do Câncer do Estado de São Paulo,[1] São Paulo, SP – Brazil
Hospital Santa Izabel,[2] Salvador, BA – Brazil
Instituto de Ensino e Pesquisa Jose Michel Kalaf,[3] Campinas, SP – Brazil
Lotus Radiologia,[4] Ribeirão Preto, SP – Brazil
Instituto do Coração (Incor) do Hospital das Clínicas da Faculdade de Medicina da Universidade de São Paulo (HCFMUSP),[5] São Paulo, SP – Brazil
Hospital Israelita Albert Einstein,[6] Paulo, SP – Brazil
CardioEco Centro de Diagnostico Cardiovascular,[7] Curitiba, PR – Brazil
Quanta Diagnóstico e Terapia – Ecocardiografia,[8] Curitiba, PR – Brazil
Instituto Dante Pazzanese de Cardiologia,[9] São Paulo, SP – Brazil

Abstract

Background: Non-invasive imaging for cardiovascular disease diagnosis has grown in volume and relevance in recent years, and it is important for early detection of cardiovascular diseases. There is a lack of data from Brazil on the availability of methods such as computed tomography (CT) and cardiac magnetic resonance imaging (CMR).

Objective: This study assessed the regional distribution of professional practice and the exams performed, correlating these factors with population data and the number of active professionals.

Methods: A nationwide survey was conducted by means of an online questionnaire applied to professionals who perform CT and CMR, compared with demographic data and the number of scans performed within Brazilian public and private healthcare systems.

Results: A total of 219 professionals filled out the questionnaire, 139 (63.8%) male, 161 (73.9%) cardiologists, and 46 (21.1%) radiologists. Regarding regional distribution, the Southeast had 125 professionals (57.3%), the Northeast 35 (16.1%), the South 30 (13.8%), the Central-West 22 (10.1%), and the North 6 (2.8%). The profile of these professionals in Brazilian regions was similar, with no statistical differences observed regarding the proportion of men ($p = 0.2451$), cardiologists ($p = 0.1325$), radiologists ($p = 0.4564$), or training time > 2 years ($p = 0.8519$). The Southeast had the highest absolute number of exams, and the North had the lowest.

Conclusion: The data revealed structural disparities in access to cardiovascular imaging throughout Brazil, in terms of both number of professionals and number of exams performed. The regional discrepancies observed in this study reflect distinct demographic and economic circumstances in Brazilian regions.

Keywords: X-Ray Computed Tomography; Magnetic Resonance Imaging; Cardiovascular Diseases; Unified Health System; Supplemental Health.

Introduction

Cardiovascular diseases remain the leading cause of mortality worldwide.[1,2] A study conducted in the United States based on data from the National Center for Health Statistics (NCHS) showed a total of 10,951,403 cardiovascular deaths in adults over 35 years of age from 2010 to 2022.[3] Brazilian data are similar, with cardiovascular mortality accounting for approximately 30% of all deaths in the country.[4] Early and accurate diagnosis is a fundamental part of cardiovascular disease investigation, and it assists in decision-making regarding the most appropriate treatment, thus preventing cardiovascular complications such as infarction, stroke, revascularization, and cardiovascular mortality. Accordingly, advanced imaging methods such as computed tomography (CT) and cardiac magnetic resonance imaging (CMR) have gained prominence worldwide, with exponential growth in recent years.[5]

Advances in devices, contrast media, organization of services, increased clinical applicability of exams, and greater availability have created an extremely favorable scenario for growth in this field. In Brazil, there is a lack of available data

Mailing Address: Isabela Bispo Santos da Silva Costa •
Universidade de São Paulo Instituto do Câncer do Estado de São Paulo. Av. Dr. Arnaldo, 251. Postal Code: 01246-000, São Paulo, SP – Brazil
E-mail: isabelabispo@yahoo.com.br
Manuscript received August 4, 2025; revised August 21, 2025; accepted August 21, 2025
Editor responsible for the review: Marcelo Tavares

DOI: https://doi.org/10.36660/abcimg.20250053i

Central Illustration: Overview of Professional Practice in Computed Tomography and Cardiac Magnetic Resonance Imaging in Brazil

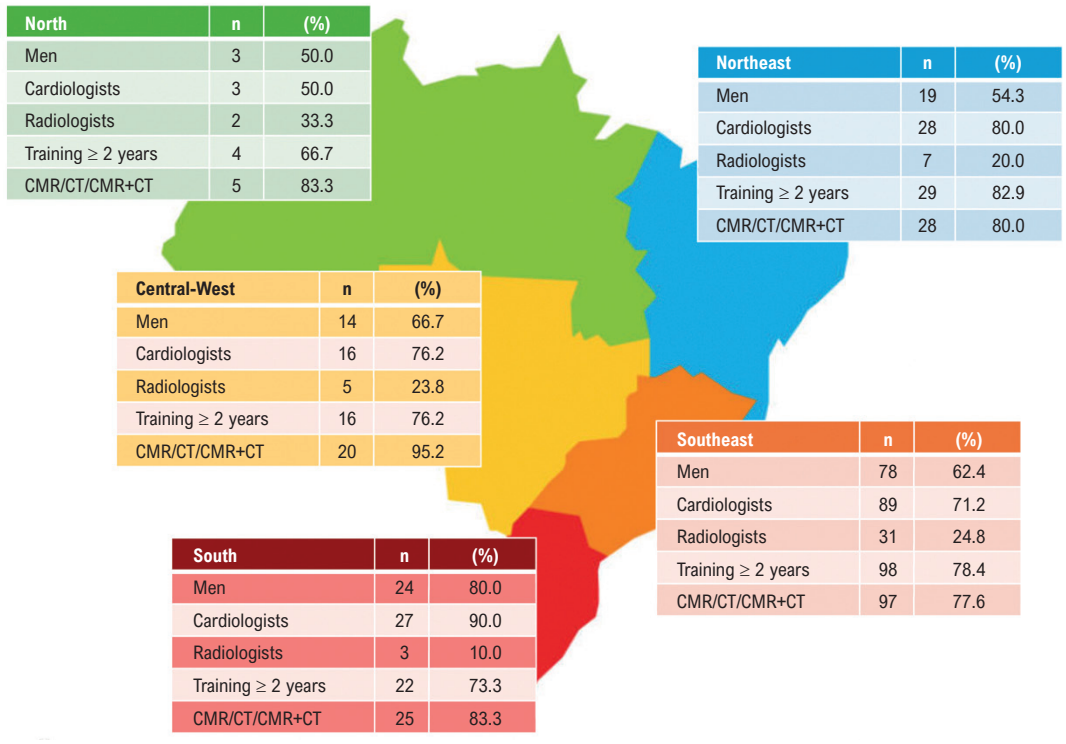

North	n	(%)
Men	3	50.0
Cardiologists	3	50.0
Radiologists	2	33.3
Training ≥ 2 years	4	66.7
CMR/CT/CMR+CT	5	83.3

Northeast	n	(%)
Men	19	54.3
Cardiologists	28	80.0
Radiologists	7	20.0
Training ≥ 2 years	29	82.9
CMR/CT/CMR+CT	28	80.0

Central-West	n	(%)
Men	14	66.7
Cardiologists	16	76.2
Radiologists	5	23.8
Training ≥ 2 years	16	76.2
CMR/CT/CMR+CT	20	95.2

Southeast	n	(%)
Men	78	62.4
Cardiologists	89	71.2
Radiologists	31	24.8
Training ≥ 2 years	98	78.4
CMR/CT/CMR+CT	97	77.6

South	n	(%)
Men	24	80.0
Cardiologists	27	90.0
Radiologists	3	10.0
Training ≥ 2 years	22	73.3
CMR/CT/CMR+CT	25	83.3

Arq Bras Cardiol: Imagem cardiovasc. 2025;38(3):e20250053

Professional profile by Brazilian region. CMR: cardiac magnetic resonance imaging; CT: computed tomography.

on these exams in the literature. Given Brazil's continental size and population and the heterogeneous nature of healthcare access within both the Brazilian Unified Health System (SUS, acronym in Portuguese) and private health insurance (PHI), it is important to understand distinct Brazilian realities. To this end, a survey of professionals involved in Brazilian cardiovascular imaging was designed.

We believe that this survey makes it possible to identify regions with a shortage of professionals, which will allow for targeted policies to encourage training and qualification, in addition to facilitating the planning of infrastructure investments, for example, installation of advanced equipment in areas with higher demand. Moreover, the survey can help identify gaps in the training profile of professionals, indicating the need to enhance academic curricula and training programs to further align them with current technological and clinical requirements, in accordance with the guidelines of the field, thus developing a comprehensive overview of the Brazilian situation.[6]

Methods

The objectives of this survey were to identify the profile of medical professionals working in cardiovascular imaging, in 2024, with a focus on CT and CMR; to assess their geographic distribution in Brazil; to assess the length of training in cardiovascular imaging; and to correlate the data obtained with the number of exams performed through the SUS and PHI in the same year.

This cross-sectional study was conducted by means of an online questionnaire applied to healthcare professionals who perform CT and CMR scans in Brazil. This survey is a partnership between the Department of Cardiovascular Imaging (DIC) of the Brazilian Society of Cardiology (SBC) and the Radiological and Diagnostic Imaging Society of São Paulo (SPR).

The questionnaire consists of the following four questions:

What is/are your medical specialty/ies (multiple choice):

1. Cardiologist
2. Radiologist
3. Pediatrician
4. Heart surgeon

Where do you practice?

1. Southeast
2. Northeast

3. Central-West
4. North
5. South

How many years of training did you complete in CT/CMR?

1. < 1 year
2. 1 year
3. 2 years
4. > 2 years

What methods do you work with (multiple choice)?

1. Computed tomography
2. Magnetic resonance imaging
3. Echocardiography
4. Nuclear medicine

The questionnaire was posted on the websites of participating medical societies, in message boards, medical conferences, and webinars whose target audience was healthcare professionals who perform CT/CMR in Brazil. The questionnaire was available from October 2024 to January 2025 at: https://docs.google.com/forms/d/e/1FAIpQLSchvk0lti_TbezPstpC9PK3Qz_KuU5zyd79MwYama2M6vbDng/viewform?usp=sf_link.

The total number of exams performed within the SUS in outpatient and inpatient settings by Brazilian region was obtained by consulting DATASUS (https://datasus.saude.gov.br/home/tabnet) in May 2025, searching for code 0207020019 (magnetic resonance imaging of the heart/aorta w/ cine). It was not possible to estimate the number of cardiac CT scans for calcium score assessment or coronary computed tomography angiography (CCTA) due to the lack of specific codes for these exams in the SUS.

The total number of exams performed through PHI in outpatient and inpatient settings by Brazilian region was obtained by consulting the website of the National Supplementary Health Agency (ANS), the regulatory body responsible for private health plans in Brazil. The website (https://www.gov.br/ans/pt-br/acesso-a-informacao/perfil-do-setor/dados-e-indicadores-do-setor/d-tiss-painel-dos-dados-do-tiss) was accessed in May 2025 to search for the following codes:

- 41101138 MRI – heart – morphological and functional
- 41101146 MRI – heart – morphological and functional + perfusion + stress
- 41101154 MRI – heart – morphological and functional + perfusion + myocardial viability
- 41001087 CT – heart – for coronary calcium score assessment
- 41001230 CT – coronary computed tomography angiography

Codes 41101138, 41101146, and 41101154 were grouped under the classification CMR.

This survey did not include out-of-network exams.

Brazilian demographic data were obtained from the last census, available at: https://www.ibge.gov.br/estatisticas/todos-os-produtos-estatisticas.html (see Supplementary Material).

The information collected by the questionnaire was analyzed in conjunction with data on the number of exams performed in Brazil by region and demographic data.

Statistical Analysis

Normally distributed continuous variables were presented as mean and standard deviation, and non-normally distributed continuous variables were presented as median and interquartile range. Categorical variables were presented as absolute and relative frequencies (percentages). Continuous variables were analyzed using Student's t test or Mann-Whitney U test, and categorical variables were analyzed using the chi-squared test or Fisher's exact test. P values < 0.05 were considered significant, and SPSS (Statistical Package for the Social Sciences), version 18.0 (SPSS Inc., Chicago, IL, USA) was used to analyze the data.

Results

A total of 219 professionals responded to the questionnaire, 139 (63.8%) male and 80 (36.7%) female. In relation to medical specialty, 161 (73.9%) were cardiologists, and 46 (21.1%) were radiologists. The distribution of these professionals was heterogeneous throughout Brazilian regions. There were 125 (57.3%) professionals in the Southeast, 35 (16.1%) in the Northeast, 30 (13.8%) in the South, 22 (10.1%) in the Central-West, and 6 (2.8%) in the North. The majority of professionals had completed 2 or more years of training in cardiovascular imaging (169 professionals, 77.5%), and they worked with CT (219 professionals; 100%) and CMR (210 professionals; 96.3%). A minority also worked with echocardiography (39 professionals; 17.9%) or nuclear medicine (12 professionals; 5.5%). Table 1 summarizes the baseline data described.

Regarding sex, women and men were similar in their medical specialty of origin, but differed in the length of training in cardiac imaging (Table 2). The proportion of men who responded that they had 2 or more years of training was lower than that of women (100 [72.5%] versus 69 [86.3%], respectively; $p = 0.029$).

Proportional analysis of the number of professionals in relation to the percentage distribution of the Brazilian population showed that, in the North and Northeast regions, the proportion of professionals was lower than the percentage distribution of the Brazilian population, suggesting a shortage of professionals in those regions. In the Southeast region, the concentration of professionals was higher than the distribution of the Brazilian population (Figure 1). The profile of these professionals in the different regions of the country was similar, with no statistical differences observed regarding the proportion of men ($p = 0.2451$), cardiologists ($p = 0.1325$), radiologists ($p = 0.4564$), training time greater than or equal to 2 years ($p = 0.8519$), and additional imaging methods ($p = 0.4361$) (Central Figure).

In relation to the volume of exams in Brazil in 2024, 14,966 CMR scans were performed within the SUS. Within

Table 1 – Profile of professionals who perform computed tomography and cardiac magnetic resonance imaging in Brazil

Variables	n	%
Sex		
Male	139	63.8
Female	80	36.7
Medical training		
Cardiologist	161	73.9
Radiologist	46	21.1
Pediatric cardiologist	8	3.7
Heart surgeon	1	0.5
Cardiologist/radiologist	2	0.9
Brazilian region		
North	6	2.8
Northeast	35	16.1
Central-West	22	10.1
Southeast	125	57.3
South	30	13.8
Training time		
< 1 year	12	5.5
1 year	37	17.0
2 years	130	59.6
> 2 years	39	17.9
Imaging methods		
Computed tomography	219	100
Magnetic resonance imaging	210	96.3
Nuclear medicine	12	5.5
Echocardiography	39	17.9

private healthcare, there were 44,382 CMR scans, 130,189 CCTA exams, and 2,629 calcium score assessments. Table 3 displays the distribution of exams by region. Analysis of the distribution of cardiovascular imaging exams in Brazil revealed significant disparities between regions and between the public and private healthcare systems. Considering the CMR exams performed within the SUS, a pronounced concentration was observed in the Southeast region, with 9,404 exams, followed by the Northeast (2,855), South (1,759), Central-West (849), and North (99).

In data on PHI, regional inequality persists, but with considerably higher absolute numbers in all regions. The Southeast region stood out again with 22,492 CMR scans, representing greater availability through PHI. The South (13,955) and Central-West (3,318) also had significant volumes, in contrast to the North (1,130) and Northeast (3,487), which continued to have lower access, although higher than that observed within the SUS.

CCTA exams were also largely concentrated in the Southeast (66,304) and South (35,152) regions, with much lower numbers in the North (3,209), Northeast (10,902), and Central-West (14,622). Calcium score assessments followed a similar pattern, with emphasis on the South (1,095) and Southeast (1,041), demonstrating the greater presence of these cardiovascular risk stratification tools in areas with a higher density of specialized services.

The Southeast region, with 36% of the population using the SUS and 59.7% using PHI, disproportionately accounted for 62.8% of CMR scans performed within the SUS and 50.7% of CCTA and CMR scans within PHI, as well as 57.3% of professionals specializing in cardiovascular imaging. Conversely, the North region, with 10.4% of the population using the SUS and 3.7% using PHI, accounted for only 0.7% of CMR scans performed within the SUS, 2.4% of CCTA exams within PHI, and 2.8% of professionals in this field, representing a scenario of significant healthcare shortages. Meanwhile, the South, with approximately 14% of the population in each system, accounted for 27.3% of CT scans and 31.4% of CMR scans within PHI, although it concentrated only 13.8% of specialized professionals. This suggests a high density of exams per professional in this region. These data are detailed in Figure 2.

Table 4 shows the relationship between the total number of cardiovascular imaging exams performed and regional structural variables, such as population, gross domestic product (GDP),

Table 2 – Professional profile according to sex

Category	Women (n, %)	Men (n, %)	P value
Cardiologist	58 (72.5%)	104 (75.4%)	0.7601
Radiologist	14 (17.5%)	32 (23.2%)	0.4123
Training ≥ 2 years	69 (86.3%)	100 (72.5%)	0.0291
CMR/CT/CMR+CT	63 (78.8%)	110 (79.7%)	1.0

CMR: cardiac magnetic resonance imaging; CT: computed tomography.

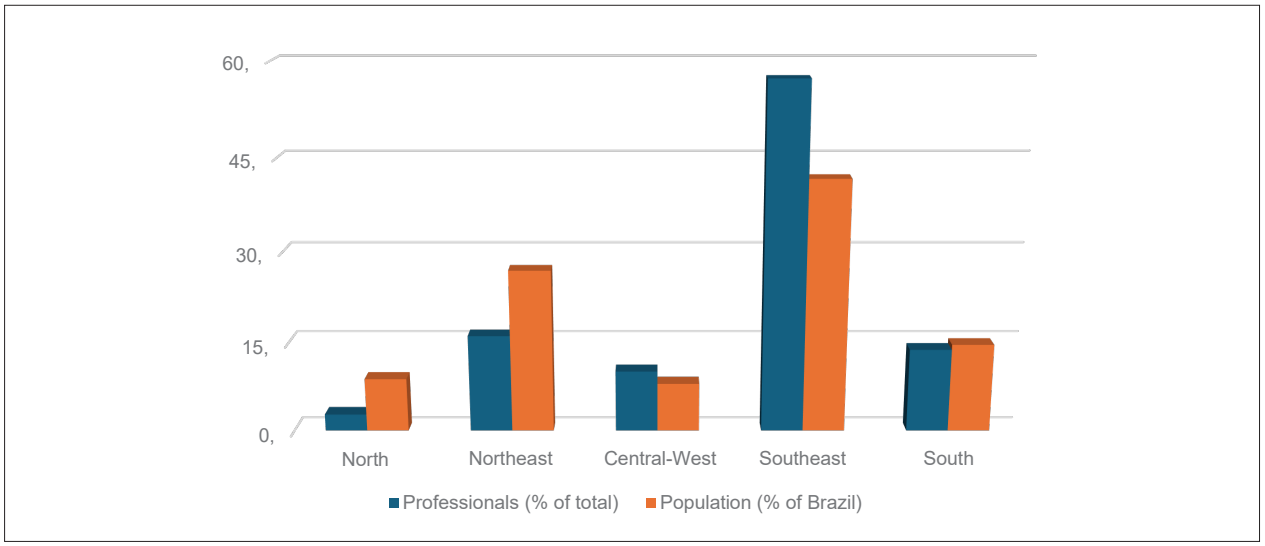

Figure 1 – *Proportion of cardiovascular imaging professionals in Brazil and percentage distribution of the Brazilian population.*

Table 3 – Number of cardiac magnetic resonance and computed tomography scans by region and healthcare system

Exams	Number by Brazilian region				
SUS	**North**	**Northeast**	**Central-West**	**Southeast**	**South**
CMR	99	2,855	849	9,404	1,759
PHI	**North**	**Northeast**	**Central-West**	**Southeast**	**South**
CMR	1,130	3,487	3,318	22,492	13,955
CCTA	3,209	10,902	14,622	66,304	35,152
Calcium score	12	363	118	1,041	1,095

CCTA: coronary computed tomography angiography; CMR: cardiac magnetic resonance imaging; PHI: private health insurance; SUS: Brazilian Unified Health System.

and number of active professionals. The South region, with 31.1 million inhabitants and a GDP of 1.56 trillion Brazilian reals (BRL), had the highest rate of exams per 100,000 inhabitants (167,007) and the highest productivity relative to GDP (33,312 exams per billion BRL), despite a moderate number of professionals (n = 30). The Southeast region, with a larger population (88.6 million), higher GDP (4.71 trillion BRL), and absolute number of professionals (n = 125), had the second-highest rate of exams per 100,000 inhabitants (111,988) and high efficiency relative to GDP (21,056.94 exams/billion BRL). In contrast, the North region, with only 6 professionals and the lowest GDP, performed the lowest absolute and proportional number of exams (22,275/100,000 inhabitants; 7,889.17 exams/billion BRL), demonstrating significant underutilization of diagnostic resources. The Northeast and Central-West regions had intermediate results, with increasing rates of exams per inhabitant and per billion BRL of GDP, consistent with their respective professional density. These findings should certainly be analyzed with caution, but they demonstrate the influence of economic infrastructure on regional access to cardiovascular imaging methods in Brazil. Regional economic capacity and population size appear to influence the availability and use of exams; these data may indirectly reflect the population's access to PHI, not just the availability of professionals in a given region.

Discussion

The growth of non-invasive diagnostic methods in cardiology assessment has become a global reality.[5] This increase has resulted from the growing body of scientific evidence published in the literature, reinforcing the importance of these methods in cardiovascular disease diagnosis.[7] The main national and international guidelines on the subject highlight the role of CCTA, calcium score, and CMR in the diagnosis of cardiovascular disease and cardiovascular involvement in systemic diseases.[6,8-10]

The incorporation of CCTA as the initial approach for investigating patients with coronary artery disease in the United Kingdom has yielded noticeable results more than half a decade

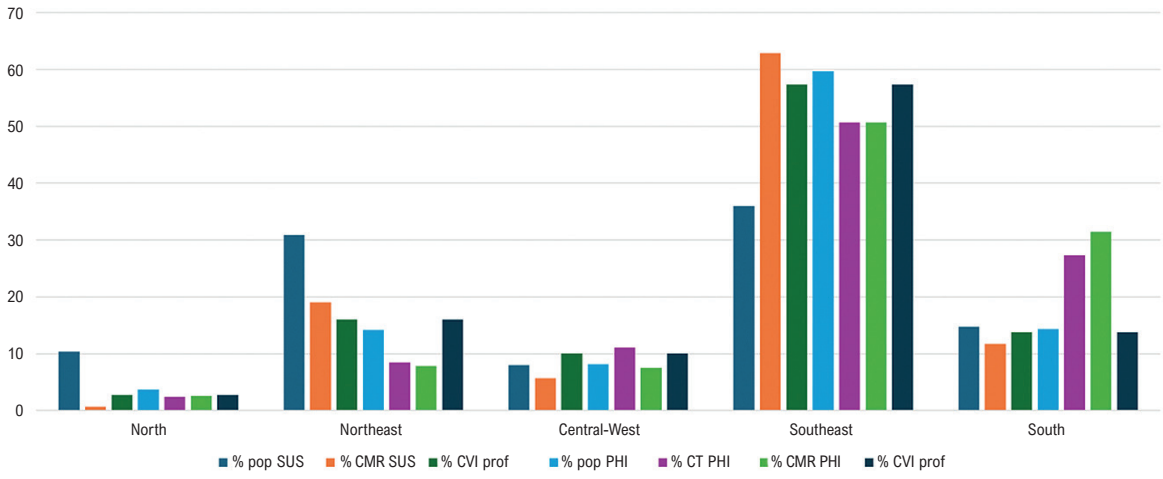

	% pop SUS	% CMR SUS	% CVI prof	% pop PHI	% CT PHI	% CMR PHI	% CVI prof
North	10.4	0.7	2.8	3.7	2.4	2.5	2.8
Northeast	30.9	19.1	16.1	14.2	8.5	7.9	16.1
Central-West	8.0	5.7	10.1	8.1	11.1	7.5	10.1
Southeast	36.0	62.8	57.3	59.7	50.7	50.7	57.3
South	14.7	11.8	13.8	14.3	27.3	31.4	13.8

Figure 2 – *Percentage distribution of the number of exams, population served by the Unified Health System and private health insurance, and proportion of cardiovascular imaging professionals in Brazil. % CMR PHI: percentage of cardiac magnetic resonance imaging scans performed through private health insurance; % CMR SUS: percentage of cardiac magnetic resonance imaging scans performed within the Unified Health System; % CT PHI: percentage of cardiac computed tomography scans performed through private health insurance; % CVI prof: percentage of cardiovascular imaging professionals in the region; % pop PHI: percentage of the population served by private health insurance; % pop SUS: percentage of the population served by the Unified Health System.*

Table 4 – Relationship between number of exams performed according to local population, gross domestic product, and number of professionals per Brazilian region

	Population	GDP (bi)	Professionals	Total exams	Exams/100,000 inhabitants	Exams/bi PIB
North	19,977,877	0.564064	6	4,450	22.275	7,889.17
Northeast	57,112,096	1.243104	35	17,607	30.829	14,163.74
Central-West	16,289,538	0.932166	22	18,907	60.769	20,282.86
Southeast	88,617,693	4.712982	125	99,241	111.988	21,056.94
South	31,113,021	1.559828	30	51,961	167.007	33,312.00

bi: billion Brazilian reals; GDP: gross domestic product.

after implementation. The National Institute for Health and Care Excellence (NICE), the body responsible for quality, evidence-based decision-making in the National Health Service (NHS), recommended the use of CCTA as the preferred diagnostic test for evaluating chest pain.[11] The study revealed that, in regions that fully adopted the recommendation, there was a significant reduction in the number of myocardial scintigraphy tests. The change in investigation strategy was also associated with a slight reduction in invasive coronary angiography and a reduction in cardiovascular mortality. Moreover, a decreasing trend in all-cause mortality was identified, reinforcing the effectiveness of the proposed model. These data confirm the central role of CCTA, not only in improving clinical outcomes, but also its potential to optimize resources within the United Kingdom's public health system.[11]

In Brazil, circumstances are different, as this test is not widely available with the Brazilian SUS. Even when available, we are not able to quantify its use due to the lack of coding. In the context of PHI, prior evaluation is frequently requested due to positive ischemia tests, in addition to criteria that often limit its use, which should be reviewed. The data presented reveal important inequality in the provision and use of advanced cardiovascular imaging tests in Brazil, both between the different regions of the country and between the SUS and PHI. The concentration of tests in the Southeast and South regions, especially in the private sector, contrasts with the low provision observed in the North, Northeast, and Central-West regions, highlighting structural and healthcare limitations in these areas.

These regional inequalities in access to cardiovascular imaging exams indicate structural limitations and historical asymmetries in the distribution of resources within the Brazilian healthcare system. Although most exams are concentrated in the most economically developed regions, the high relative productivity observed in the South suggests a possible optimization of the existing infrastructure, or even a more consolidated private market, with greater access to PHI. On the other hand, the limited performance observed in the North region, even when adjusted for GDP and number of inhabitants, highlights additional barriers, such as a lack of equipment, low PHI coverage, and shortage of trained professionals. The discrepancy between regions reinforces the need for specific public policies that promote development of professional training in interior regions, investment in diagnostic infrastructure in the SUS, and more equitable regulation of access to imaging methods, in order to ensure minimum fair coverage in all Brazilian regions.

The findings of this analysis dialogue with those presented by Monti et al.,[12] in a survey conducted by the CMR working group of the Italian Society of Cardiology. The study identified structural and operational barriers similar to those observed in Brazil, including limited access to CMR, regional disparities, and underutilization of the technique, even in centers with installed capacity. Furthermore, the study highlighted the shortage of professionals with specific training as one of the main obstacles to expanding the clinical use of CMR. These challenges, shared across different health systems, reinforce the importance of coordinated strategies to expand specialist training, optimize the use of available resources, and integrate CMR into care guidelines more broadly and equitably.

Data from Germany's national certification program and the European Society of Cardiovascular Radiology (ESCR) registry revealed pronounced heterogeneity in the provision and use of cardiovascular imaging, among both institutions and medical specialties. The study underscored the need for standardization in training, certification, and quality control processes, indicating that, even in a country with broad technological availability, the lack of uniformity in professional qualifications and the incorporation of imaging into clinical workflows limits systematic use.[13] Similarly, a recent analysis on the use of CCTA in different regions of the United States and the United Kingdom revealed significant inequalities in access and adoption of the exam, associated with the availability of equipment, the presence of trained specialists, and variations in regional clinical guidelines.[14] These findings reinforce that, even in advanced healthcare systems, the consolidation of cardiovascular imaging as a routine diagnostic tool requires structured policies for training, professional accreditation, and technical governance. These challenges are particularly critical in Brazil, where they are characterized by even more pronounced regional inequalities.

Based on the findings presented, it is possible to propose strategies to mitigate regional inequalities in access to cardiovascular imaging in Brazil. The creation of regional training and qualification centers dedicated to CCTA and CMR, especially in the North, Northeast, and Central-West regions, can promote the development of expertise in interior regions and contribute to the retention of professionals. Accordingly, retention scholarships linked to medical residency, master's, or doctoral programs, funded by Brazilian agencies such as the Coordination for the Improvement of Higher Education Personnel (CAPES) and the National Council for Scientific and Technological Development (CNPq), should be offered based on epidemiological and structural data obtained by means of national censuses in the field. Additionally, public-private partnerships for the acquisition and maintenance of advanced imaging equipment can be strategic for regions with low technological coverage, provided that they are accompanied by clear regulatory protocols that guarantee priority use by the SUS. These integrated measures can contribute to greater equity in the provision of exams, expanding the clinical and social impact of cardiovascular imaging in Brazil.

Our data have important limitations. We believe that the number of imaging professionals in this survey is an underestimate, especially regarding the participation of radiologists. International data have shown that radiologist participation is higher.[5] These limitations were due to the voluntary participation of the professionals involved, as well as the fact that the majority of radiologists represented are affiliated with the SPR, which operates in São Paulo. Lack of coding in the SUS prevented us from accessing the number of CCTA scans and calcium scores. The lack of data on out-of-network exams performed in Brazil was a limitation, whose impact was likely not significant on this survey, given their low proportion in the Brazilian context.

In conclusion, our results demonstrated pronounced inequality in the provision and use of cardiovascular imaging in Brazil, with a greater concentration of resources and procedures in the Southeast and South regions, and marked shortages in other regions. This asymmetry is not limited to technological and economic infrastructure; it also reflects a shortage of qualified professionals in the field, especially in more vulnerable regions. Given this scenario, there is an evident need for strategies focused on training, ongoing development, and retention of cardiovascular imaging specialists, as an essential component to expanding access and ensuring more equitable care. Investment in human capital development is an indispensable step toward consolidating cardiovascular imaging as a routine diagnostic tool and improving the quality of care nationwide.

Acknowledgments

The authors would like to thank all the professionals who responded to the questionnaire and the DIC and SPR teams who supported the initiative

Author Contributions

Conception and design of the research: Costa IBSS, Torreão JA, Fernandes JL, Trad H, Liberato G, Sasdelli Neto R, Pinto IM, Senra T. Acquisition of data: Costa IBSS, Torreão JA, Fernandes JL, Trad H, Liberato G, Sasdelli Neto R, Senra T. Analysis and interpretation of the data: Costa IBSS, Pinto IM, Senra T. Statistical analysis: Costa IBSS, Senra T. Writing of the manuscript: Costa IBSS, Torreão JA, Fernandes JL, Trad H, Liberato G, Sasdelli Neto R, Senra T. Critical revision of the manuscript for intellectual content: Barberato SH, Pinto IM, Senra T.

Potential conflict of interest

No potential conflict of interest relevant to this article was reported.

Sources of funding

There were no external funding sources for this study.

Study association

This study is not associated with any thesis or dissertation work.

Ethics approval and consent to participate

This study was approved by the Ethics Committee of the Instituto Dante Pazzanese under the protocol number CAAE 85943025.6.0000.5462. All the procedures in this study were in accordance with the 1975 Helsinki Declaration, updated in 2013. Informed consent was obtained from all participants included in the study.

Use of Artificial Intelligence

The authors did not use any artificial intelligence tools in the development of this work.

Data Availability

The underlying content of the research text is contained within the manuscript.

References

1. Ahmad FB, Anderson RN. The Leading Causes of Death in the US for 2020. JAMA. 2021;325(18):1829-30. doi: 10.1001/jama.2021.5469.
2. Rache B, Rocha R, Medeiros LA, Okada LM, Ferrari G, Zeng H, et al. Transition Towards Cancer Mortality Predominance Over Cardiovascular Disease Mortality in Brazil, 2000-2019: A Population-Based Study. Lancet Reg Health Am. 2024;39:100904. doi: 10.1016/j.lana.2024.100904.
3. Woodruff RC, Tong X, Khan SS, Shah NS, Jackson SL, Loustalot F, et al. Trends in Cardiovascular Disease Mortality Rates and Excess Deaths, 2010-2022. Am J Prev Med. 2024;66(4):582-9. doi: 10.1016/j.amepre.2023.11.009.
4. Oliveira GMM, Brant LCC, Polanczyk CA, Malta DC, Biolo A, Nascimento BR, et al. Cardiovascular Statistics - Brazil 2023. Arq Bras Cardiol. 2024;121(2):e20240079. doi: 10.36660/abc.20240079.
5. Catapano F, Moser LJ, Francone M, Catalano C, Vliegenthart R, Budde RPJ, et al. Competence of Radiologists in Cardiac CT and MR Imaging in Europe: Insights from the ESCR Registry. Eur Radiol. 2024;34(9):5666-77. doi: 10.1007/s00330-024-10644-4.
6. Magalhães TA, Carneiro ACC, Moreira VM, Trad HS, Lopes MMU, Cerci RJ, et al. Cardiovascular Computed Tomography and Magnetic Resonance Imaging Guideline of the Brazilian Society of Cardiology and the Brazilian College of Radiology - 2024. Arq Bras Cardiol. 2024;121(9):e20240608. doi: 10.36660/abc.20240608.
7. Dewey M. Competence and Contributions of Radiologists to Cardiac CT and MR Imaging Across Europe. Eur Radiol. 2024;34(10):6578-80. doi: 10.1007/s00330-024-10741-4.
8. Nieman K, García-García HM, Hideo-Kajita A, Collet C, Dey D, Pugliese F, et al. Standards for Quantitative Assessments by Coronary Computed Tomography Angiography (CCTA): An Expert Consensus Document of the Society of Cardiovascular Computed Tomography (SCCT). J Cardiovasc Comput Tomogr. 2024;18(5):429-43. doi: 10.1016/j.jcct.2024.05.232.
9. Ommen SR, Ho CY, Asif IM, Balaji S, Burke MA, Day SM, et al. 2024 AHA/ACC/AMSSM/HRS/PACES/SCMR Guideline for the Management of Hypertrophic Cardiomyopathy: A Report of the American Heart Association/American College of Cardiology Joint Committee on Clinical Practice Guidelines. Circulation. 2024;149(23):e1239-311. doi: 10.1161/CIR.0000000000001250.
10. Leiner T, Bogaert J, Friedrich MG, Mohiaddin R, Muthurangu V, Myerson S, et al. SCMR Position Paper (2020) on Clinical Indications for Cardiovascular Magnetic Resonance. J Cardiovasc Magn Reson. 2020;22(1):76. doi: 10.1186/s12968-020-00682-4.
11. Moss AJ, Williams MC, Newby DE, Nicol ED. The Updated NICE Guidelines: Cardiac CT as the First-Line Test for Coronary Artery Disease. Curr Cardiovasc Imaging Rep. 2017;10(5):15. doi: 10.1007/s12410-017-9412-6.
12. Monti L, Ricci F, Baggiano A, Barison A, Carrabba N, Figliozzi S, et al. Current Trends and Challenges in the Clinical Use of Cardiovascular Magnetic Resonance: A Survey from the Italian Society of Cardiology. Eur Heart J Imaging Methods Pract. 2025;3(1):qyaf046. doi: 10.1093/ehjimp/qyaf046.
13. Sieren MM, Maintz D, Gutberlet M, Krombach GA, Bamberg F, Hunold P, et al. Current Status of Cardiovascular Imaging in Germany: Structured Data from the National Certification Program, ESCR Registry, and Survey among Radiologists. Rofo. 2022;194(2):181-91. doi: 10.1055/a-1554-9236.
14. Banashefski B, Ji R, Dhruva SS, Neuhaus J, Redberg RF. Cardiac Coronary Tomography Angiography (CCTA) Use Across Geographical Regions in the USA and the UK: A Cross-Sectional Study. BMJ Surg Interv Health Technol. 2023;5(1):e000201. doi: 10.1136/bmjsit-2023-000201.

***Supplemental Materials**

For additional information, please click here.

Safety of dobutamine stress echocardiography using a modified protocol in a large unselected population

José Sebastião de Abreu,[1] Tereza Cristina Pinheiro Diógenes,[1] Marília Esther Benevides Abreu,[1] Isadora Sucupira Machado Chagas,[1] Sarah Gomes Diógenes,[1] Ana Gardenia Liberato Ponte Farias,[1] Marcia Maria Carneiro[1]

Universidade Estadual do Ceará,[1] Fortaleza, CE – Brazil

Abstract

Background: Dobutamine stress echocardiography (DSE) using the conventional protocol (CP-DSE) may lead to important adverse effects.

Objective: This study was aimed at assessing the safety of DSE using a modified protocol (MP-DSE).

Methods: Data were collected from our institutional database to compare MP-DSE with the CP-DSE. In the CP-DSE, atropine could be administered during the fourth stage or its extension. In the MP-DSE, atropine was initiated at the beginning of the third stage, and there was no stage extension. Upon completion of DSE or for arrhythmia control, metoprolol was administered in the CP-DSE and esmolol in the MP-DSE. In cases of typical angina, nitroglycerin was administered at the examiner's discretion in the CP-DSE, whereas its use was predetermined in the MP-DSE. A p-value < 0.05 was considered statistically significant.

Results: Of 17,811 tests performed, 9,121 were conducted using the MP-DSE. During DSE, myocardial oxygen consumption, represented by the rate-pressure product, was significantly higher in the MP-DSE group (22,530 ± 4,575 vs 23,037 ± 4,072 bpm.mmHg; p < 0.001). Hypertensive peak (1% vs 0.4%; p = 0.0001) and nonsustained ventricular tachycardia (0.6% vs 0.1%; p = 0.0001) were more frequent in the CP-DSE, while supraventricular tachyarrhythmia (2.1% vs 3.78%; p = 0.0001) and atrial fibrillation (0.8% vs 1.3%; p = 0.003) were more common in the MP-DSE. These arrhythmias resolved spontaneously or with medication. In the CP-DSE, two patients had ventricular fibrillation and one, acute coronary syndrome.

Conclusion: In our study, the modified protocol for DSE proved to be a safe option, with no severe adverse effects observed, despite the presence of an elevated rate-pressure product.

Keywords: Stress Echocardiography; Safety; Drug-Related Side Effects and Adverse Reactions.

Introduction

Dobutamine stress echocardiography (DSE) protocols have traditionally involved exposure to large doses of dobutamine and a significant incidence of adverse effects. However, the development of newer protocols for this diagnostic method has progressively reduced these risks.[1-6]

The addition of atropine to DSE protocols at an earlier stage has enhanced the test's sensitivity without compromising its specificity and safety. As a result, current guidelines limit the maximum dose of dobutamine and atropine is initiated before or even during the last stage of dobutamine infusion.[6,7]

The intravenous administration of an ultra-short-acting beta-blocker at the end of the DSE is essential for controlling heart rate (HR), arrhythmias and myocardial ischemia, and may even enhance the accuracy of the test.[2,3-8] However, the literature does not indicate a preference between esmolol and metoprolol. Ischemia occurring during DSE might require the use of coronary vasodilator, administered either orally or intravenously, although current guidelines do not specify the drug formulation or route of administration.[3-6]

Reports of adverse effects associated with DSE have been essential to establish contraindications to the test, emphasizing its higher risk compared to echocardiography with other stressors, such as exercise, dipyridamole, or adenosine.[9-11] Thus, ongoing monitoring and the development of new protocols are necessary to minimize complications, particularly considering that dobutamine is the most widely available pharmacologic agent for stress echocardiography. Therefore, this study aimed at assessing the safety of DSE by applying a modified protocol to a large, unselected population.

Methods

This retrospective study compared the conventional protocol for DSE (CP-DSE) with a modified protocol (MP-DSE),

Mailing Address: José Sebastião de Abreu •
Clinicárdio de Fortaleza e Cardioexata. Rua Doutor Jose Lourenço, 500. Postal Code: 60115-280, Fortaleza, CE – Brazil
E-mail: jsabreu10@yahoo.com.br
Manuscript received August 04, 2025; revised September 08, 2025; accepted September 08, 2025
Editor responsible for the review: Marcelo Tavares

DOI: https://doi.org/10.36660/abcimg.20250054i

Central Illustration: Safety of dobutamine stress echocardiography using a modified protocol in a large unselected population

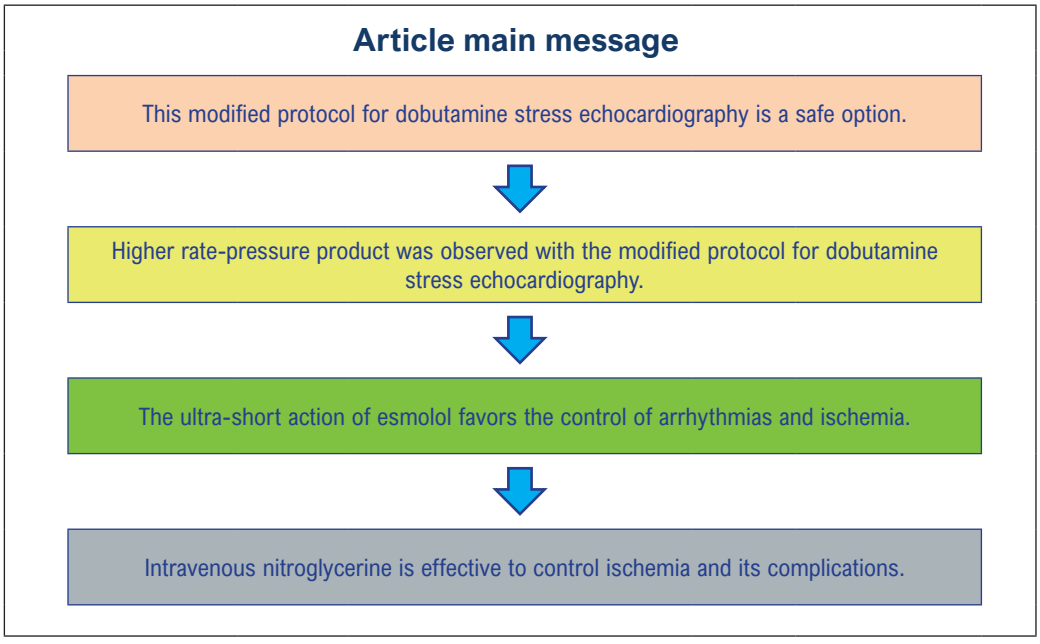

Arq Bras Cardiol: Imagem cardiovasc. 2025;38(3):e20250054

using data collected from our institutional database about patients referred for DSE to assess myocardial ischemia with an adequate echocardiographic window. Patients submitted to the CP-DSE, constituting the CP-DSE group, were enrolled between 1997 and 2007, and those who underwent MP-DSE, constituting the MP-DSE group, were enrolled between 2008 and 2021.

Patient demographic data, coronary artery disease risk factors and history of myocardial revascularization were assessed through medical history, clinical evaluation and laboratory tests. All patients were informed about the objectives and potential risks of DSE and provided consent to undergo the procedure. Patients referred for myocardial viability assessment were excluded from the analysis.

This study's protocol complies with the ethical principles outlined in the 1975 Declaration of Helsinki ethical principles and was submitted to and approved by our institutional Human Research Ethics Committee.

In both groups, dobutamine was continuously infused in up to four stages at incremental doses of 10, 20, 30 and 40 μcg.kg^{-1}.min^{-1}. When indicated, atropine was administered in boluses of 0.25- to 0.50-mg, up to the maximum cumulative dose of 2 mg.[2-4,12] In cases of paradoxical sinus deceleration, defined as a 5- to 10- beat reduction in HR, atropine could be administered during the initial stages, at the examiner's discretion. Upon test conclusion, an intravenous beta-blocker or coronary vasodilator was used according to each group's protocol. However, when coronary spasm was suspected, priority was given to vasodilator administration.

Absolute contraindications to dobutamine use were unstable angina, recent myocardial infarction, severe and symptomatic aortic stenosis, acute aortic dissection, decompensated heart failure, ventricular pseudoaneurysm and obstructive hypertrophic cardiomyopathy. Atropine was contraindicated in cases of myasthenia gravis, pyloric stenosis, prostate disease determining urinary retention and narrow-angle glaucoma.[9,11]

To increase the number of tests completed, beta-blocker withdrawal was recommended two to three days before the test for CP-DSE patients and 5 days before for MP-DSE patients. A quad-screen display was used for comparative analysis, with CX 200 (Apogee) and Vingmed System Five (General Electric) equipment utilized in the CP-DSE group, and Vivid 7 and Vivid E9 (General Electric) equipment in the MP-DSE group.

Regarding important adverse effects, hypertensive peak was defined as blood pressure higher than 230/120 mm Hg, while hypotension was defined as systolic blood pressure (SBP) lower than 100 mm Hg. We retrieved the following arrhythmias from the database: supraventricular tachyarrhythmia (junctional or atrial), atrial fibrillation, sustained ventricular tachycardia (duration > 30 seconds), nonsustained ventricular tachycardia and ventricular fibrillation. Additional events recorded included paradoxical sinus deceleration, acute coronary syndrome, acute

myocardial infarction, ventricular rupture, asystole and death. DSE should be discontinued in cases of potential life-threatening conditions or intolerance to the test medications.

Blood pressure was measured at the beginning of each stage and during the recovery phase. Electrocardiographic monitoring was continuous, and 12-lead electrocardiography was performed before and throughout the procedure. DSE was considered complete when at least 85% of the age-predicted maximal HR (220 minus age in years) was achieved and/or myocardial ischemia was detected. Ischemia was defined as either the appearance of wall motion abnormalities in at least two contiguous myocardial segments that were previously normal, or the worsening of a preexisting abnormality – excluding cases where an akinetic segment became dyskinetic.

In the early version of the CP-DSE, dobutamine was infused in three-minute stages and atropine was initiated at the end of the fourth stage (40-μcg.kg^{-1}.min^{-1} of dobutamine), which was then extended to allow for atropine bolus administration. However, the CP-DSE protocol evolved over time, and in its later version, atropine began to be administered starting from the fourth stage.[13]

An intravenous bolus of metoprolol (5 to 10 mg) was administered upon DSE completion, regardless of whether the result was positive or negative for myocardial ischemia, or in the presence of tachyarrhythmias. Additional boluses could be given if arrhythmias or angina persisted. If angina continued, nitroglycerin could be administered as a sublingual spray or tablet, or as an intravenous infusion, at the examiner's discretion.

In the MP-DSE protocol, all stages had a maximum duration of three minutes, and atropine infusion began during the third stage alongside dobutamine administration – except in cases where the examiner identified an exaggerated chronotropic response to dobutamine.[13]

Upon DSE completion, esmolol was intravenously administered in 30-mg bolus, independently of a positive or negative result for myocardial ischemia. If arrhythmia or typical angina occurred, additional bolus could be repeated at 3-minute intervals. When typical angina did not subside within six minutes, nitroglycerin solution (100 μcg/mL) would be intravenously administered in 3-mL bolus, followed by intravenous infusion (1 mL/minute) that would be maintained while angina persisted, as long as SBP > 110 mm Hg.[14,15]

For the statistical analysis, categorical variables were presented in tables as point estimates of prevalence, and quantitative variables were expressed as mean ± standard deviation, and minimum and maximum values. The variables "adverse effects", "risk factors" and "type of therapy" were organized in contingency tables according to protocol groups, test results (negative or positive for myocardial ischemia) and age ranges. Associations between protocol groups and these variables were analyzed using Pearson's chi-square test or Fisher's exact test, as appropriate. For the quantitative variables, normal distribution was analyzed using Shapiro-Wilk test, and then, bivariate analysis was performed using Mann-Whitney test. A 5% significance level was adopted for all statistical tests, and analyses were performed using SPSS version 20.

Results

This study assessed 17,811 completed DSE out of 18,531 tests performed. The sample was distributed as follows: 8,690 tests in the CP-DSE group and 9,121 in the MP-DSE group. Female sex and young patients predominated in both groups. In the MP-DSE group, older men (≥65 years), use of antihypertensive, lipid-lowering and hypoglycemic medications, as well as known coronary artery disease, were more common than in the CP-DSE group. Discontinuation of oral beta-blocker prior to testing was more frequent in the MP-DSE group, while CP-DSE patients more often underwent DSE while still on beta-blocker therapy (Table 1). In the CP-DSE group, 14.4% of the tests (n = 1,251) were concluded before the fourth stage, compared to 66% (n = 5,994) in the MP-DSE group. There were 434 (4.99%) inconclusive tests in the CP-DSE group and 286 (3.1%) in the MP-DSE group. None of the inconclusive tests reached the target HR or met the criteria for myocardial ischemia (Figure 1).

In the entire sample and considering both positive and negative DSE results for myocardial ischemia, HR was higher in the CP-DSE group at baseline, but, during stress, HR did not differ between the groups. At baseline, SBP and rate-pressure product (HR x SBP) of negative and positive DSE results for myocardial ischemia were higher in the CP-DSE group. However, during stress, both SBP and rate-pressure product were higher in the MP-DSE group in both negative and positive tests for myocardial ischemia (Table 2).

In the CP-DSE group, as compared to the MP-DSE group, peak hypertensive effect, typical angina and nonsustained ventricular tachycardia were more frequently found in both positive and negative tests for myocardial ischemia. Isolated ventricular ectopics, supraventricular tachyarrhythmias and atrial fibrillation were more frequently found in the positive tests of the CP-DSE group and in the negative tests of the MP-DSE group (Table 3).

The most severe adverse effects occurred in the CP-DSE patients with positive test results for ischemia and included ventricular fibrillation (2 patients) and acute coronary syndrome (1 patient). These patients were admitted for hemodynamic evaluation and subsequently underwent surgical myocardial revascularization, with no complications reported (Table 3). In the MP-DSE group, nitroglycerin solution was administered to 76 patients presenting with typical angina.

Atropine was administered to 83% of CP-DSE patients and 92.6% of MP-DSE patients. The mean dose of atropine was higher in the MP-DSE group, including among patients with negative ischemia results, regardless of age, and among non-elderly patients with positive ischemia results. However, the mean dose of atropine did not differ between groups among elderly patients with positive ischemia results. Lower doses of atropine were administered to elderly patients, regardless of ischemia status (Table 4). Early administration of atropine to reverse paradoxical sinus deceleration occurred in 16 CP-DSE patients and 64 MP-DSE patients.

Discussion

In this study with two large unselected populations, we assessed the safety of two protocols for DSE. In the modified

Table 1 – Baseline characteristics: demographic data, risk factors, and type of therapy

Variables	CP-DSE	MP-DSE	p
Number of tests	8,690 (100%)	9,121 (100%)	
Mean age (years)	61 ± 11.73	62.71 ± 2.05	< 0.001
Number of tests in patients aged ≤65 years	5,487 (66.1%)	5,182 (56.8%)	< 0.001
Number of tests in patients aged >65 years	3,203 (33.9%)	3,939 (43.2%)	
Men	3,723 (42.8%)	4,150 (45.5%)	< 0.001
Women	4,967 (57.2%)	4,971 (54.5%)	
Hypertension	4,608 (53%)	6,243 (68.4%)	< 0.001
Dyslipidemia	3,755 (43.2%)	5,228 (57.3%)	< 0.001
Diabetes	1,415 (16.3%	2,476 (27.1%)	< 0.001
Known coronary artery disease	1,635 (18.8%)	1,838 (20.2%)	< 0.001
Previous myocardial revascularization			
stent	438 (5.0%)	1,167 (12.8%)	< 0.001
mammary or saphenous bypass graft	1,108 (12.8%)	538 (5.9%)	< 0.001
mammary bypass graft	830 (9.6%)	426 (4.7%)	< 0.001
Oral beta-blocker			
on	408 (4.7%)	197 (2.2%)	< 0.001
suspended	1,420 (16.3%)	2,770 (30.4%)	< 0.001

Data expressed as mean ± standard deviation, absolute numbers, and percentages; PC-DSE: conventional protocol for dobutamine stress echocardiography; MP-DSE: modified protocol for dobutamine stress echocardiography.

protocol, a lower amount of dobutamine was administered and esmolol was established as the ultra-short-acting beta-blocker to control arrhythmia or ischemia. In patients with persistent angina, the control was achieved with predetermined doses of nitroglycerin, as shown in the Central Illustration.

Over the past four decades, dobutamine infusion duration and dosage have varied. The frequent use of high doses has led to high dobutamine exposure and important adverse effects. Subsequent protocols have maintained 3-minute intervals per stage, and atropine administration could be initiated along with the 20-, 30-, or 40-μcg.kg^{-1}.min^{-1} dobutamine infusion.[1,3,4,6,7,12,16] In the CP-DSE group, there was greater exposure to dobutamine, and the test was concluded from the fourth stage on in 85.6% of the patients, while, in the MP-DSE group, only 44% needed to reach the fourth stage for conclusion.

According to Anthenoffer et al.,[13] paradoxical sinus deceleration during DSE may represent the Bezold-Jarisch reflex, triggered by parasympathetic stimulation in the posterior wall of the left ventricle or by baroreceptor activation. This deceleration can be either gradual or sudden and abrupt. Based on data retrieved from the database, this reflex was observed in the CP-DSE group and was followed by atropine administration at the examiner's discretion to reverse the deceleration. However, only 16 such cases were recorded, suggesting possible underreporting or a less stringent diagnostic criterion. In the MP-DSE group, early and immediate administration of atropine was strictly implemented in 64 patients to prevent atrioventricular block or asystole.

Intravenous administration of an ultra-short-acting beta-blocker at the end of DSE is essential for controlling or preventing arrhythmias and ischemic manifestations, as well as for facilitating a rapid return to baseline heart rate. Either esmolol or metoprolol may be used, although current guidelines do not specify a preferred agent.[2,6]

In the CP-DSE group, metoprolol was used, and its effectiveness in controlling arrhythmias, ischemic manifestations and reducing HR was confirmed.[1,7,17] However, we observed that in the MP-DSE group, esmolol not only contributed to the control of ischemic manifestations and arrhythmias but also appeared to reduce HR more rapidly. Notably, in the management of supraventricular arrhythmias, esmolol has been shown to act faster and more effectively than amiodarone in cases of acute atrial fibrillation.[3,18,19]

Metoprolol administered at the end of the test enhances the sensitivity of DSE for diagnosing myocardial ischemia

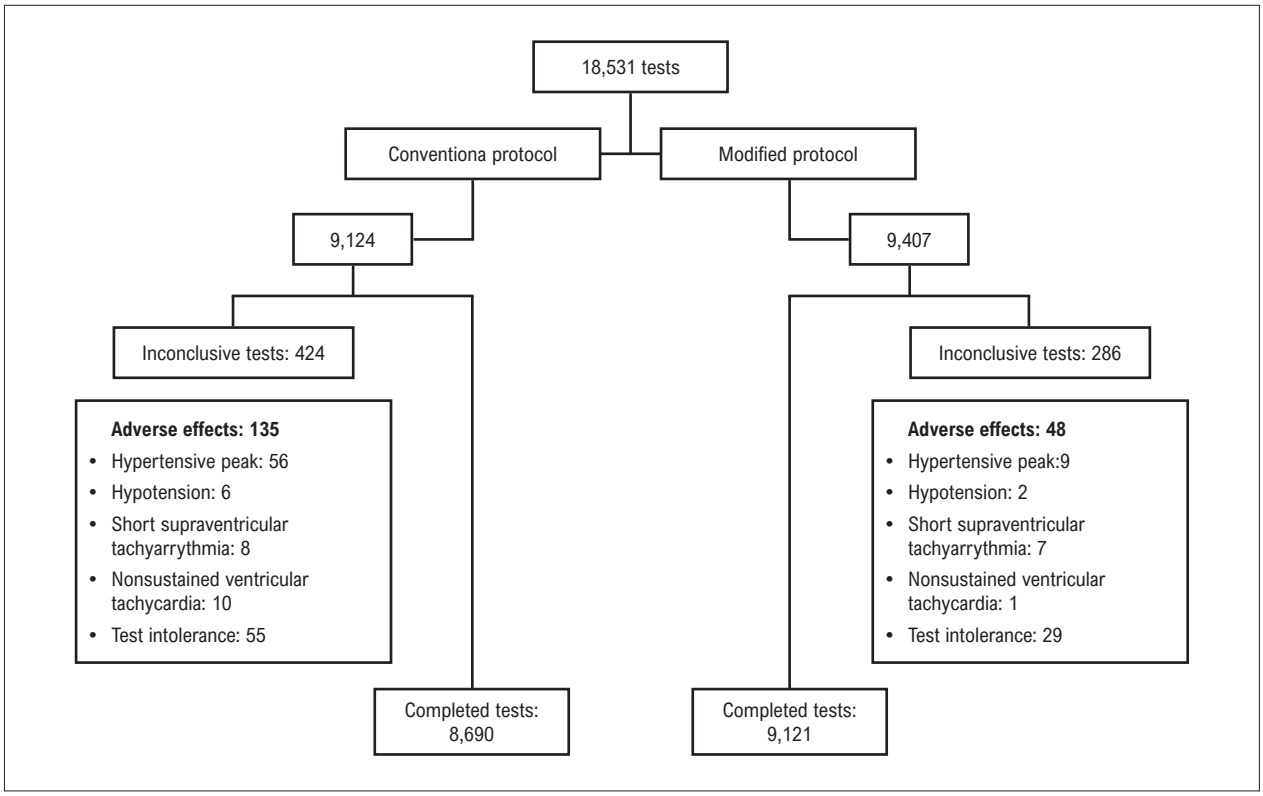

Figure 1 – *Flowchart of the patients; none of the inconclusive tests reached the target heart rate nor met the criteria for myocardial ischemia.*

without compromising specificity.[8,20] In our study, esmolol revealed wall motion abnormalities consistent with ischemia during the recovery phase (Video 1), which may suggest a class effect of ultra-short-acting beta-blockers.

When myocardial ischemia presents with ST-segment elevation or is not promptly controlled with a beta-blocker, the use of nitrates becomes essential.[21] In the CP-DSE group, sublingual nitrate was administered; however, its effect was not always sufficiently rapid due to impaired absorption caused by mouth dryness – a common side effect of atropine, particularly in elderly patients. Therefore, we opted to use lingual spray nitrate or intravenous isosorbide mononitrate. When these options were unavailable, intravenous nitroglycerin was administered at the examiner's discretion. In the MP-DSE group, nitroglycerin infusion was routinely implemented with predetermined timing and dosage, which may have contributed to the prevention of potential ischemic complications.[14,15,22]

In our study, during stress, the rate-pressure product was higher in the MP-DSE group for both positive and negative ischemia results. This may have been influenced by a greater number of hypertensive patients, a lower proportion of patients on oral beta-blockers and earlier administration of atropine in this group. The rate-pressure product is known to correlate with myocardial oxygen consumption; therefore, when this parameter is elevated, the likelihood of ischemia increases. In the MP-DSE group, the higher rate-pressure product indicated increased oxygen demand. Evidence suggests that the rate-pressure product is a more reliable indicator of the adequacy of dobutamine stress than the achievement of target HR.[23]

It is worth noting that, despite higher systolic blood pressure (SBP) during stress in the MP-DSE group, hypertensive peaks were more frequent in the CP-DSE group. This may be related to alpha-adrenergic stimulation secondary to greater exposure to dobutamine. Similar findings were reported by Lee et al.[24] in their study involving 3,129 patients, in which atropine was administered at a later stage.

Typical angina is a late and less frequent manifestation than wall motion abnormalities in the ischemic cascade.[3] Although the MP-DSE group had a higher percentage of patients with risk factors for probable or known coronary artery disease, typical angina was more frequent in the CP-DSE group, which may be consistent with the higher incidence of positive DSE results for ischemia observed in that group.

Isolated ectopic beats are common during DSE and become clinically relevant when they occur in bursts, as tachyarrhythmias, or as fibrillation. However, the vast majority can be suppressed following test completion and administration of a beta-blocker bolus. Supraventricular ectopic beats in recurrent bursts,

Table 2 – Values of the hemodynamic variables in the stress echocardiography protocols used and number of tests performed (N) according to negative or positive results for myocardial ischemia

Results / Variables	Protocol	N	Mean ± SD	p
Baseline heart rate (bpm)				
Negative	CP-DSE MP-DSE	7,313 8,375	76.55 ± 15.614 75.35 ± 15.614	< 0.001
Positive	CP-DSE MP-DSE	1,380 753	73.66 ± 15.614 73.75 ± 15.614	0.820
Negative and positive	CP-DSE MP-DSE	8,690 9,121	76.09 ± 14.078 75.21 ± 14.280	< 0.001
Heart rate under stress (bpm)				
Negative	CP-DSE MP-DSE	7,313 8,375	149.94 ± 15.635 149.62 ± 14.153	< 0.001
Positive	CP-DSE MP-DSE	1,380 753	144.69 ± 21.402 144.39 ± 18.726	0.097
Negative and positive	CP-DSE MP-DSE	8,690 9,121	149.11 ± 16.793 149.18 ± 14.654	0.155
Baseline systolic blood pressure (mm Hg)				
Negative	CP-DSE MP-DSE	7,313 8,374	134.93 ± 20.085 129.18 ± 15.614	< 0.001
Positive	CP-DSE MP-DSE	7,313 8,375	136.43 ± 22.889 132.72± 16.204	< 0.001
Negative and positive	CP-DSE MP-DSE	8,690 9,121	135.17 ± 20.562 129.48 ± 15.693	< 0.001
Systolic blood pressure under stress (mm Hg)				
Negative	CP-DSE MP-DSE	7,313 8,375	150.20 ± 25.758 153.67 ± 22.665	< 0.001
Positive	CP-DSE MP-DSE	1,380 753	152.24 ± 29.472 159.63 ± 22.980	< 0.001
Negative and positive	CP-DSE MP-DSE	8,690 9,121	150.53 ± 26.391 154.16 ± 22.749	< 0.001
Baseline heart rate x baseline systolic blood pressure (bpm . mm Hg)				
Negative	CP-DSE MP-DSE	7,313 8,376	10,394 ± 2,599 9,766 ± 2,259	< 0.001
Positive	CP-DSE MP-DSE	1,380 753	10,142 ± 2,615 9,801 ± 2,109	0.006
Negative and positive	CP-DSE MP-DSE	8,690 9,121	10,354 ± 2,603 9,769 ± 2,247	< 0.001
Heart rate under stress x systolic blood pressure under stress (bpm . mm Hg)				
Negative	CP-DSE MP-DSE	7,313 8,376	22,596 ± 4,445 23,034 ± 4,031	< 0.001
Positive	CP-DSE MP-DSE	1,380 753	22,177 ± 5,194 23,077 ± 4,504	< 0.001
Negative and positive	CP-DSE MP-DSE	8,690 9,121	22,530 ± 4,575 23,037 ± 4,072	< 0.001

Data expressed as mean ± SD and absolute numbers. SD: standard deviation; PC-DSE: conventional protocol for dobutamine stress echocardiography; MP-DSE: modified protocol for dobutamine stress echocardiography; bpm: beats per minute.

Table 3 – Adverse effects of dobutamine stress echocardiography according to the protocols used and the results (negative or positive) for myocardial ischemia

Variables / Results	CP-DSE	MP-DSE	p
Total sample	8,690 (100%)	9,121 (100%)	
Hypertensive peak			
Negative	62 (0.71%)	32 (0.35%)	< 0.001
Positive	29 (0.33%)	2 (0.02%)	< 0.001
All	91 (1.04%)	34 (0.37%)	< 0.001
Typical angina			
Negative	301 (3.46%)	128 (1.4%)	< 0.001
Positive	532 (6.12%)	336 (3.7%)	< 0.001
All	833 (9.58%)	464 (5.1%)	< 0.001
Isolated ventricular ectopics			
Negative	2,243 (25.8%)	2,721 (29.8%)	< 0.001
Positive	472 (5.43%)	289 (3.17%)	< 0.001
All	2,715 (31%)	3,010 (33%)	< 0.001
Supraventricular tachyarrhythmia			
Negative	124 (1.43%)	239 (2.62%)	< 0.001
Positive	38 (0.43%)	34 (0.37%)	< 0.001
All	162 (2.11%)	273 (3.78%)	< 0.001
Atrial fibrillation			
Negative	54 (0.62%)	107 (1.17%)	< 0.001
Positive	17 (0.2%)	9 (0.1%)	0.001
All	71 (0.82%)	116 (1.27%)	< 0.001
Nonsustained ventricular tachycardia			
Negative	20 (0.23%)	8 (0.1%)	< 0.001
Positive	28 (0.32%)	3 (0.03%)	< 0.001
All	48 (0.55%)	11 (0.13%)	< 0.001
Acute coronary syndrome			
Positive	1 (0.01%)	-	
Ventricular fibrillation			
Positive	2 (0.02%)	-	

Data expressed as absolute numbers and percentages; PC-DSE: conventional protocol for dobutamine stress echocardiography; MP-DSE: modified protocol for dobutamine stress echocardiography.

nonsustained tachyarrhythmias and atrial fibrillation were more frequently observed in the MP-DSE group, particularly in tests with negative results for ischemia.

The incidence of atrial fibrillation during DSE has varied, on average, from 1% to 4%, with rates reported as 0.86% among 4,818 patients in the meta-analysis by Mansencal et al.[25] and 2% among 3,800 patients in the study by Carasso et al.[26] Some publications have not associated atropine use with a higher incidence of arrhythmia.[1] Tsutsui et al.[16] found no significant difference in atrial fibrillation incidence during DSE with or without early atropine administration (0.8% vs. 1.2%; p = NS). These percentages are very similar to those observed in our study (0.82% vs. 1.27%; p < 0.001), although we found a statistically significant difference in the MP-DSE group, which involved lower doses of dobutamine and more frequent use of atropine. This finding does not rule out a potential association between atropine use and atrial fibrillation, which warrants further investigation.

Considering the higher mean dose of atropine and the greater number of patients who had discontinued oral beta-blockers prior to testing, as previously recommended, the higher percentage of completed tests in the MP-DSE group was expected. Consistent with a previous study involving octogenarians, our findings showed that elderly patients required lower doses of atropine.[10] Furthermore, supporting published data, reduced atropine use in elderly patients was observed in both positive and negative ischemia results.

Nonsustained ventricular tachycardia was more frequently observed in the CP-DSE group, regardless of whether the test result was positive or negative for ischemia, suggesting an effect related to the higher doses of dobutamine. At the examiner's discretion, the test was interrupted and a beta-blocker bolus was administered, effectively preventing the progression to sustained ventricular tachycardia.

The most severe complications occurred exclusively in the CP-DSE group. One patient developed acute coronary syndrome during DSE, requiring prolonged intravenous nitroglycerin infusion. This patient subsequently underwent coronary angiography, which revealed severe coronary artery disease. Ventricular fibrillation was observed in two other patients – one during the fourth stage and the other during the recovery phase – both of whom tested positive for myocardial ischemia and had severe coronary artery disease. Defibrillation was successfully performed in both cases without sequelae, and surgical myocardial revascularization was carried out thereafter. No cases of cardioversion or electrical defibrillation were reported in the MP-DSE group.

In this study, none of the following complications was observed: Takotsubo syndrome, acute myocardial infarction, atrioventricular dissociation, asystole, cardiac rupture, death or sustained ventricular tachycardia. Geleijnse et al.[11] reported that, in the absence of sustained ventricular tachycardia, the risk of severe complications during stress testing – whether with a vasodilator, dobutamine or exercise – is comparable.

Table 4 – Dose of atropine administered according to protocol, age group, and results for myocardial ischemia (negative or positive)

Variable	Protocol	Mean	SD	Minimum	Maximum	p
Mean dose (mg)	CP-DSE	0.540	0.433	0	2 mg	< 0.001
	MP-DSE	0.602	0.488	0	2 mg	
Age < 65 years	CP-DSE	0.642	0.441	0	2 mg	< 0.001
	MP-DSE	0.740	0.513	0	2 mg	
Age ≥ 65 years	CP-DSE	0.360	0.356	0	2 mg	< 0.001
	MP-DSE	0.417	0.380	0	2 mg	
Negative for ischemia	CP-DSE	0.547	0.437	0	2 mg	< 0.001
	MP-DSE	0.607	0.488	0	2 mg	
Positive for ischemia	CP-DSE	0.495	0.411	0	2 mg	0.070
	MP-DSE	0.552	0.476	0	2 mg	
Negative < 65 years	CP-DSE	0.655	0.442	0	2 mg	< 0.001
	MP-DSE	0.745	0.513	0	2 mg	
Negative ≥ 65 years	CP-DSE	0.360	0.357	0	2 mg	< 0.001
	MP-DSE	0.420	0.381	0	2 mg	
Positive < 65 years	CP-DSE	0.580	0.427	0	2 mg	0.014
	MP-DSE	0.682	0.515	0	2 mg	
Positive ≥ 65 years	CP-DSE	0.367	0.349	0	2 mg	0.216
	MP-DSE	0.405	0.377	0	2 mg	

SD: standard deviation; CP-DSE: conventional protocol for dobutamine stress echocardiography; MP-DSE: modified protocol for dobutamine stress echocardiography.

The study by Rozanski et al.,[27] using nuclear medicine imaging, demonstrated that over two decades, the percentage of tests yielding positive results for ischemia declined to 5%. Other studies have shown that, over four decades, the rate of inducible myocardial ischemia during stress echocardiography dropped from 60% to less than 10%, likely due to changes in patient profiles and improvements in anti-ischemic therapy.[28,29] This may explain the lower percentage of positive ischemia tests in the MP-DSE group in our study. Additionally, it is worth noting the higher rate-pressure product observed in that group during stress. The decline in positive test rates has prompted the incorporation of new tools to enhance the diagnostic accuracy of stress echocardiography.

The potential occurrence of significant adverse effects should never be underestimated. Based on the findings of our study, we believe that the implementation of a well-defined protocol and prompt action to manage adverse events are essential for ensuring the safety of DSE. Key safety measures include strict attention to DSE contraindications, minimizing dobutamine exposure, immediate reversal of paradoxical sinus deceleration, use of esmolol as an ultra-short-acting beta-blocker, and intravenous nitroglycerin administration when necessary.

Our study has several limitations. It is a retrospective analysis, and neither the pretest probability of coronary artery disease nor its influence on test outcomes was calculated.[27-30] Regarding the use of beta-blockers and coronary vasodilators, ischemia severity was not quantified when comparing the groups. There was no standardization of coronary vasodilator use, although this limitation was mitigated in the MP-DSE group. Hemodynamic assessment to evaluate DSE accuracy was not performed, and patients were not followed longitudinally to compare the prognostic value of CP-DSE versus MP-DSE; however, these were beyond the scope of this study. Although, in practice, heart rate reduction occurred more rapidly with esmolol than with metoprolol, a comparative study is needed to confirm this observation. Myocardial contrast echocardiography could potentially increase the number of diagnostic tests, but due to its cost, it remains uncommon in our setting.

In conclusion, the modified DSE protocol, featuring early administration of atropine and intravenous use of esmolol and nitroglycerin, proved to be a safe approach,

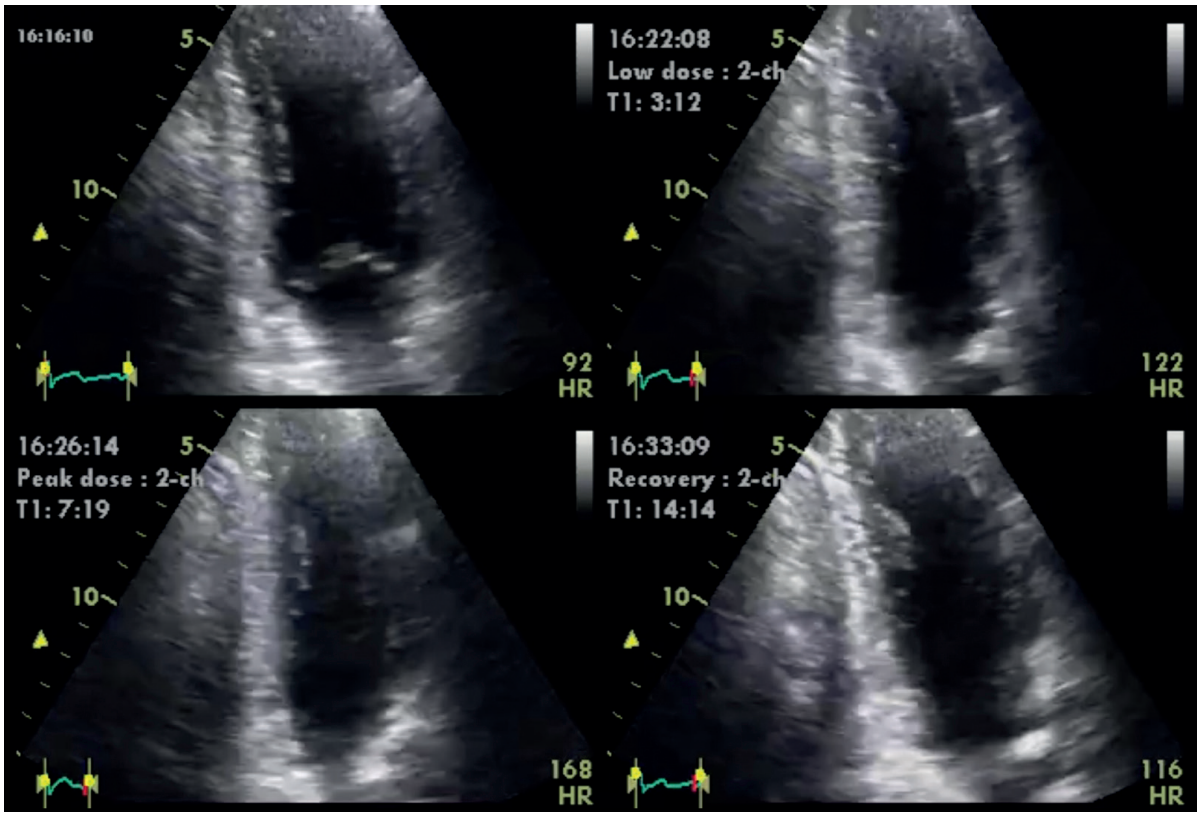

Video 1 – *In the two-chamber apical view, during the peak of dobutamine stress echocardiography (168 bpm), a subtle contractility abnormality can be observed. Following the intravenous infusion of an esmolol bolus, during the recovery phase (116 bpm), the area of wall motion abnormality extends to the anterior and inferior walls, indicating intense and unequivocal myocardial ischemia. Watch in: http://abcimaging.org/supplementary-material/2025/3803/ABCImag-2025-0054_AO_video_1.mp4*

with no severe adverse effects reported. It resulted in reduced exposure to dobutamine and a higher rate-pressure product, contributing to both safety and diagnostic efficacy.

Author Contributions

Conception and design of the research: Abreu JS, Diógenes TC, Abreu MEB. Acquisition of data: Abreu JS, Diógenes TC, Abreu MEB. Analysis and interpretation of the data: Abreu JS, Abreu MEB, Diógenes SG, Carneiro MM. Statistical analysis: Abreu JS. Writing of the manuscript: Abreu JS, Farias AGLP, Carneiro MM. Critical revision of the manuscript for intellectual content: Abreu JS, Machado IS, Farias AGLP.

Potential Conflict of Interest

No potential conflict of interest relevant to this article was reported.

Sources of Funding

There were no external funding sources for this study.

Study Association

This study is not associated with any thesis or dissertation work.

Ethics Approval and Consent to Participate

This study was approved by the Ethics Committee of the Nome da Instituição under the protocol number CAAE: 70990923.6.0000.5534, opinion number 6.312.526. All the procedures in this study were in accordance with the 1975 Helsinki Declaration, updated in 2013. Informed consent was obtained from all participants included in the study.

Use of Artificial Intelligence

The authors did not use any artificial intelligence tools in the development of this work.

Availability of Research Data

The underlying content of the research text is contained within the manuscript.

References

1. Poldermans D, Fioretti PM, Boersma E, Forster T, van Urk H, Cornel JH, et al. Safety of Dobutamine-Atropine Stress Echocardiography in Patients with Suspected or Proven Coronary Artery Disease. Am J Cardiol. 1994;73(7):456-9. doi: 10.1016/0002-9149(94)90675-0.
2. Pellikka PA, Roger VL, Oh JK, Miller FA, Seward JB, Tajik AJ. Stress Echocardiography. Part II. Dobutamine Stress Echocardiography: Techniques, Implementation, Clinical Applications, and Correlations. Mayo Clin Proc. 1995;70(1):16-27. doi: 10.1016/S0025-6196(11)64660-0.
3. Krahwinkel W, Ketteler T, Gödke J, Wolfertz J, Ulbricht LJ, Krakau I, et al. Dobutamine Stress Echocardiography. Eur Heart J. 1997;18(Suppl D):D9-15. doi: 10.1093/eurheartj/18.suppl_d.9.
4. Pellikka PA, Nagueh SF, Elhendy AA, Kuehl CA, Sawada SG; American Society of Echocardiography. American Society of Echocardiography Recommendations for Performance, Interpretation, and Application of Stress Echocardiography. J Am Soc Echocardiogr. 2007;20(9):1021-41. doi: 10.1016/j.echo.2007.07.003.
5. Sicari R, Nihoyannopoulos P, Evangelista A, Kasprzak J, Lancellotti P, Poldermans D, et al. Stress Echocardiography Expert Consensus Statement--Executive Summary: European Association of Echocardiography (EAE) (a Registered Branch of the ESC). Eur Heart J. 2009;30(3):278-89. doi: 10.1093/eurheartj/ehn492.
6. Pellikka PA, Arruda-Olson A, Chaudhry FA, Chen MH, Marshall JE, Porter TR, et al. Guidelines for Performance, Interpretation, and Application of Stress Echocardiography in Ischemic Heart Disease: From the American Society of Echocardiography. J Am Soc Echocardiogr. 2020;33(1):1-41.e8. doi: 10.1016/j.echo.2019.07.001.
7. Steeds RP, Wheeler R, Bhattacharyya S, Reiken J, Nihoyannopoulos P, Senior R, et al. Stress Echocardiography in Coronary Artery Disease: A Practical Guideline from the British Society of Echocardiography. Echo Res Pract. 2019;6(2):G17-G33. doi: 10.1530/ERP-18-0068.
8. Mathias W Jr, Tsutsui JM, Andrade JL, Kowatsch I, Lemos PA, Leal SM, et al. Value of Rapid Beta-Blocker Injection at Peak Dobutamine-Atropine Stress Echocardiography for Detection of Coronary Artery Disease. J Am Coll Cardiol. 2003;41(9):1583-9. doi: 10.1016/s0735-1097(03)00242-0.
9. Varga A, Garcia MA, Picano E; International Stress Echo Complication Registry. Safety of Stress Echocardiography (from the International Stress Echo Complication Registry). Am J Cardiol. 2006;98(4):541-3. doi: 10.1016/j.amjcard.2006.02.064.
10. Abreu JS, Diógenes TC, Farias AG, Morais JM, Paes JN Jr. Safety and Feasibility of Dobutamine-Atropine Stress Echocardiography in Octogenarian Patients. Arq Bras Cardiol. 2005;85(3):198-204. doi: 10.1590/s0066-782x2005001600009.
11. Geleijnse ML, Krenning BJ, Nemes A, van Dalen BM, Soliman OI, Ten Cate FJ, et al. Incidence, Pathophysiology, and Treatment of Complications during Dobutamine-Atropine Stress Echocardiography. Circulation. 2010;121(15):1756-67. doi: 10.1161/CIRCULATIONAHA.109.859264.
12. Geleijnse ML, Fioretti PM, Roelandt JR. Methodology, Feasibility, Safety and Diagnostic Accuracy of Dobutamine Stress Echocardiography. J Am Coll Cardiol. 1997;30(3):595-606. doi: 10.1016/s0735-1097(97)00206-4.
13. Attenhofer CH, Pellikka PA, McCully RB, Roger VL, Seward JB. Paradoxical Sinus Deceleration during Dobutamine Stress Echocardiography: Description and Angiographic Correlation. J Am Coll Cardiol. 1997;29(5):994-9. doi: 10.1016/s0735-1097(97)00030-2.
14. Abrams J. A Reappraisal of Nitrate Therapy. JAMA. 1988;259(3):396-401.
15. Curry SH, Lopez LM, Lambert CR, Kwon HR, Stack RK. Plasma Concentrations and Hemodynamic effects of Intravenous, Sublingual, and Aerosolized Nitroglycerin in Patients Undergoing Cardiac Catheterization. Biopharm Drug Dispos. 1993;14(2):107-18. doi: 10.1002/bdd.2510140203.
16. Tsutsui JM, Osório AF, Lario FA, Fernandes DR, Sodre G, Andrade JL, et al. Comparison of Safety and Efficacy of the Early Injection of Atropine during Dobutamine Stress Echocardiography with the Conventional Protocol. Am J Cardiol. 2004;94(11):1367-72. doi: 10.1016/j.amjcard.2004.07.141.
17. Mathias W Jr, Arruda A, Santos FC, Arruda AL, Mattos E, Osório A, et al. Safety of Dobutamine-Atropine Stress Echocardiography: A Prospective Experience of 4,033 Consecutive Studies. J Am Soc Echocardiogr. 1999;12(10):785-91. doi: 10.1016/s0894-7317(99)70182-3.
18. Maurovich-Horvat P, Károlyi M, Horváth T, Szilveszter B, Bartykowszki A, Jermendy ÁL, et al. Esmolol is Noninferior to Metoprolol in Achieving a Target Heart Rate of 65 Beats/Min in Patients Referred to Coronary CT Angiography: A Randomized Controlled Clinical Trial. J Cardiovasc Comput Tomogr. 2015;9(2):139-45. doi: 10.1016/j.jcct.2015.02.001.
19. Milojevic K, Beltramini A, Nagash M, Muret A, Richard O, Lambert Y. Esmolol Compared with Amiodarone in the Treatment of Recent-Onset Atrial Fibrillation (RAF): An Emergency Medicine External Validity Study. J Emerg Med. 2019;56(3):308-18. doi: 10.1016/j.jemermed.2018.12.010.
20. Karagiannis SE, Bax JJ, Elhendy A, Feringa HH, Cokkinos DV, van Domburg R, et al. Enhanced Sensitivity of Dobutamine Stress Echocardiography by Observing Wall Motion Abnormalities during the Recovery Phase after Acute Beta-Blocker Administration. Am J Cardiol. 2006;97(4):462-5. doi: 10.1016/j.amjcard.2005.09.075.
21. Haouzi AJ, Schwartz S, Liszka E. Coronary Artery Spasm Following Dobutamine Stress Echocardiogram. BMJ Case Rep. 2020;13(8):e235206. doi: 10.1136/bcr-2020-235206.
22. Kim C, Ha M, Kim W, Park SJ, Hwang SH, Yong HS, et al. Nitrates Administered by Spray versus Tablet: Comparison of Coronary Vasodilation on CT Angiography. Eur Radiol. 2021;31(1):515-24. doi: 10.1007/s00330-020-07104-0.
23. Sawada SG. A Reappraisal of Dobutamine Echocardiography for Risk Stratification before Noncardiac Surgery. J Am Soc Echocardiogr. 2020;33(4):433-7. doi: 10.1016/j.echo.2020.01.017.
24. Lee CY, Pellikka PA, Shub C, Sinak LJ, Seward JB. Hypertensive Response during Dobutamine Stress Echocardiography. Am J Cardiol. 1997;80(7):970-1. doi: 10.1016/s0002-9149(97)00561-4.
25. Mansencal N, Mustafic H, Hauguel-Moreau M, Lannou S, Szymanski C, Dubourg O. Occurrence of Atrial Fibrillation during Dobutamine Stress Echocardiography. Am J Cardiol. 2019;123(8):1277-82. doi: 10.1016/j.amjcard.2019.01.022.
26. Carasso S, Sandach A, Kuperstein R, Schwammenthal E, Glikson M, Luria D, et al. Atrial Fibrillation in Dobutamine Stress Echocardiography. Int J Cardiol. 2006;111(1):53-8. doi: 10.1016/j.ijcard.2005.07.001.
27. Rozanski A, Gransar H, Hayes SW, Min J, Friedman JD, Thomson LE, et al. Temporal Trends in the Frequency of Inducible Myocardial Ischemia during Cardiac Stress Testing: 1991 to 2009. J Am Coll Cardiol. 2013;61(10):1054-65. doi: 10.1016/j.jacc.2012.11.056.
28. Carpeggiani C, Landi P, Michelassi C, Sicari R, Picano E. The Declining Frequency of Inducible Myocardial Ischemia during Stress Echocardiography Over 27 Consecutive Years (1983-2009). Int J Cardiol. 2016;224:57-61. doi: 10.1016/j.ijcard.2016.08.313.
29. Picano E, Pierard L, Peteiro J, Djordjevic-Dikic A, Sade LE, Cortigiani L, et al. The Clinical Use of Stress Echocardiography in Chronic Coronary Syndromes and Beyond Coronary Artery Disease: A Clinical Consensus Statement from the European Association of Cardiovascular Imaging of the ESC. Eur Heart J Cardiovasc Imaging. 2024;25(2):e65-e90. doi: 10.1093/ehjci/jead250.
30. Cortigiani L, Bigi R, Bovenzi F, Molinaro S, Picano E, Sicari R. Prognostic Implication of Appropriateness Criteria for Pharmacologic Stress Echocardiography Performed in an Outpatient Clinic. Circ Cardiovasc Imaging. 2012;5(3):298-305. doi: 10.1161/CIRCIMAGING.111.971242.

My Approach to Three-Dimensional Echocardiography in Mitral Stenosis: How and When?

Alexandre Costa Souza,[1,2] *Marcus Vinicius Silva Freire de Carvalho,*[1] *Marco André Moraes Sales*[1]
Hospital São Rafael,[1] *Salvador, BA – Brazil*
Instituto D'Or de Pesquisa e Ensino (IDOR),[2] *Rio de Janeiro, RJ – Brazil*

Central Illustration: My Approach to Three-Dimensional Echocardiography in Mitral Stenosis: How and When?

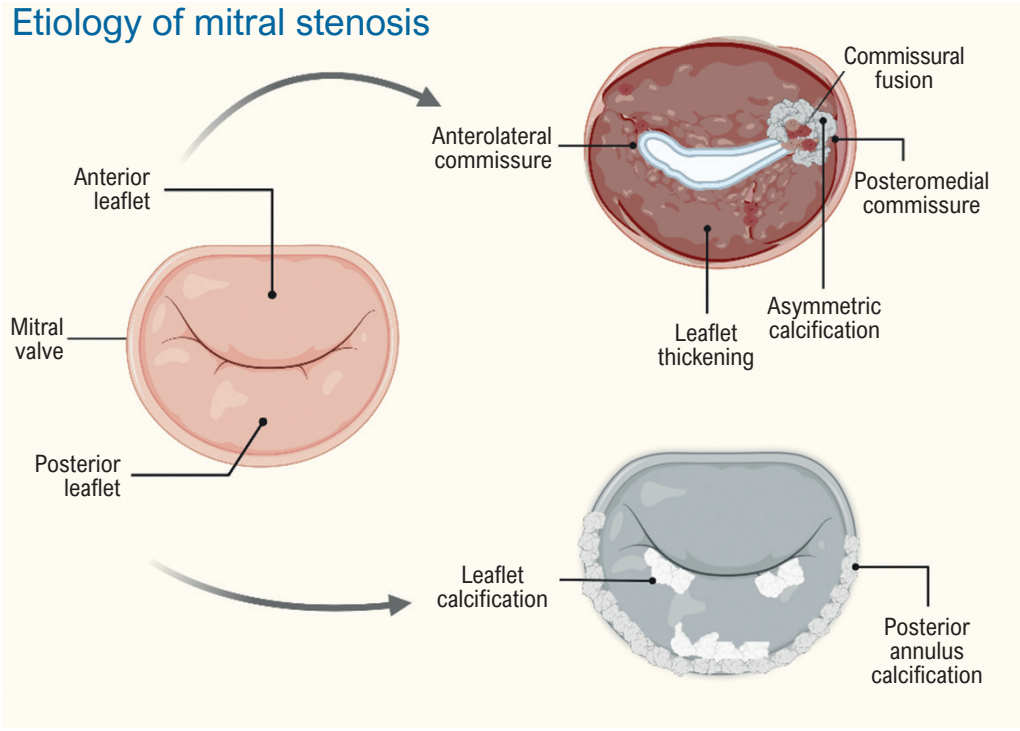

Arq Bras Cardiol: Imagem cardiovasc. 2025;38(3):e20250057

Schematic illustration of the anatomical manifestations of mitral stenosis according to etiology. On the left, a normal mitral valve. In the upper right quadrant, the rheumatic pattern shows diffuse leaflet thickening with fusion and asymmetric calcification of one commissure. In the lower right quadrant, the degenerative calcific pattern shows extensive calcium deposition in the posterior annulus and the leaflet bases.

Keywords

Three-Dimensional Echocardiography; Mitral Valve Stenosis; Three-Dimensional Imaging

Mailing Address: Alexandre Costa Souza •
Hospital São Rafael – Ecocardiografia. Avenida São Rafael, 2152. Postal Code: 41253-190, Salvador, BA – Brazil
E-mail: alexandrecostahsr@gmail.com
Manuscript received August 13, 2025; revised August 29, 2025; accepted August 29, 2025
Editor responsible for the review: Marcelo Tavares

DOI: https://doi.org/10.36660/abcimg.20250057i

Abstract

Three-dimensional echocardiography has become an essential tool in the assessment of mitral stenosis, allowing detailed anatomical analyses and reliable measurements, even in complex anatomies or extensive calcification. Based on daily clinical experience in an imaging laboratory, this article offers a practical guide for image acquisition and optimization, multiplanar reconstruction, and three-dimensional planimetry, focusing on technical adjustments, the use of tools such as rotation and cropping, and strategies for integrating the method into the routine workflow of cardiovascular imaging centers.

SUMÁRIO

Introduction

Mitral stenosis remains a clinically relevant condition worldwide. It is associated with significant morbidity, and it impacts patient quality of life and survival. Moreover, in older populations in developed countries, degenerative etiologies have become progressively more frequent, reflecting population aging and increased life expectancy.[1] International guidelines emphasize that mitral stenosis, regardless of etiology, is associated with severe complications, such as pulmonary hypertension, atrial fibrillation, and heart failure, requiring accurate diagnostic and therapeutic strategies to provide details on disease progression and improve prognosis.[1]

Two-dimensional (2D) echocardiography is still the primary method for quantifying valve area in mitral stenosis. However, 2D planimetry is highly dependent on an exact orthogonal slice over the leaflet tips, and slight deviations in the plane or the presence of acoustic shadowing due to calcification can lead to overestimation of the area and even make it impossible to measure.[2]

Recognizing these limitations, European guidelines recommend the complementary use of three-dimensional (3D) planimetry, which improves the definition of the smallest functional orifice when 2D imaging is suboptimal.[3] Additionally, area calculation by pressure half-time (PHT) is directly influenced by atrial and ventricular compliance, transient hemodynamic conditions (e.g., aortic regurgitation, diastolic dysfunction), and associated lesions, such as mitral regurgitation, which shorten or lengthen PHT and lead to errors in valve area estimation. These factors explain why, in complex clinical scenarios, the integration of additional parameters such as 3D planimetry may be relevant for accurate classification of mitral stenosis severity.[2,3]

My Approach in Practice

Given these limitations and the need for more accurate measurements, 3D echocardiography has become increasingly integral to mitral stenosis assessment, not only as a supplement but also as a central tool in complex scenarios, especially due to the fact that it allows for orthogonal alignment of the pyramidal beam in relation to the valve plane and due to its high spatial resolution. Below, we describe our approach to this assessment in daily practice.

The first step is always to optimize 2D acquisition. An inadequate 2D image directly compromises the quality of 3D reconstruction. Adjustments such as gain, compression, and alignment should be made before activating 3D mode. A quality 3D assessment cannot be achieved without a stable and well-oriented 2D basis.

Following image optimization, we use 2D multiplane mode to align the orthogonal axes and correctly identify the plane of the leaflet tips. Subsequently, we activate 3D zoom mode to obtain an en face view of the valve orifice, positioning the cutting plane at the smallest diameter during diastole. When necessary, we apply color Doppler, integrated with the reconstruction to assess residual flow or associated regurgitation. Leaflet mobility, symmetry of commissural fusion, and the presence of calcification or subvalvular alterations are assessed by means of multiplanar reconstructions and en face views obtained in 3D mode, allowing detailed analysis of the mitral apparatus in different orthogonal planes.[4]

The Role of 3D Transthoracic Echocardiography

Three-dimensional transthoracic echocardiography (TTE) represents a strategic initial phase in mitral stenosis assessment, especially due to the fact that it provides real-time images with good spatial resolution in patients with a favorable acoustic window.[4] Its main contribution is quick, noninvasive acquisition of the mitral valve. Furthermore, 3D TTE facilitates the morphological characterization of the valve regarding symmetry of commissural fusion, leaflet thickening, and extent of calcifications; this information is relevant to etiological diagnosis and selection of candidates for percutaneous valvotomy. Although it has limitations in complex anatomies or in patients with inadequate windows, this step can anticipate relevant data and more efficiently guide the planning of transesophageal assessment.[4] Figure 1 displays an example of 3D TTE in severe rheumatic mitral stenosis with tunneling, demonstrating the morphological alterations that are typical of this etiology in atrial and ventricular views.

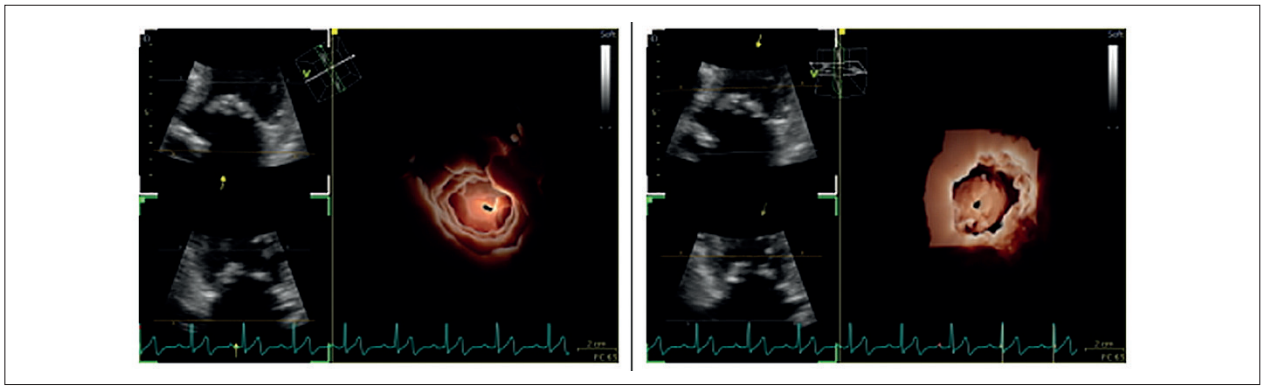

Figure 1 – *Three-dimensional transthoracic echocardiography of the mitral valve in severe rheumatic mitral stenosis with tunneling. On the left, atrial view with the tunneled valve orifice, typical of severe rheumatic anatomies. On the right, ventricular view showing the elongated, narrow trajectory of the functional orifice, with commissural fusion and associated subvalvular restriction.*

In a prospective study involving 105 patients with severe mitral stenosis, despite the lower image resolution of 3D TTE compared to 3D transesophageal echocardiography, both techniques showed excellent agreement (significant correlation; mean bias < 0.01 cm^2), confirming the reliability of 3D TTE for quantifying valve area.[5]

Although the role of 3D TTE is relevant and can provide reliable data, especially in favorable acoustic windows, transesophageal echocardiography is still an indispensable step for detailed assessment. It is during this phase that we systematically apply the following acquisition and optimization parameters.

Image Assessment and Optimization Parameters

3D Planimetry

Three-dimensional planimetry is currently considered the most accurate method for determining mitral valve area in mitral stenosis, as it reduces errors related to oblique views and dependence on acoustic windows that limit 2D planimetry. Using multiplanar reconstructions and en face visualization in 3D transesophageal mode, it is possible to accurately identify the smallest orifice in diastole, even in complex anatomies with calcification or asymmetric commissural fusion.[2,3]

In addition to greater accuracy in measuring valve area, 3D planimetry has demonstrated relevance in prognostic stratification. In a comparative study, the method consistently yielded smaller valve areas than PHT and 2D planimetry, reclassifying mitral stenosis severity in nearly 20% of cases.[6] More importantly, only classifications of severe stenosis obtained by 3D planimetry were significantly associated with clinical outcomes, such as the need for valvotomy, valve surgery, or hospitalization for heart failure; it also showed better correlation with hemodynamic markers, such as right ventricular systolic pressure and left atrial volume.[7,8] These findings reinforce the value of 3D planimetry not only in anatomical assessment but also in identifying patients at higher risk of clinical events.[6]

Figure 2 illustrates an example of 3D planimetry obtained by 3D transesophageal echocardiography, highlighting multiplanar reconstruction and en face visualization for precise plane positioning in the smallest functional orifice during diastole. FlexiSlice® (GE Healthcare) was used for precise plane alignment and visual optimization.

Comparison with PHT and 2D Planimetry

When compared to traditional methods, 3D planimetry shows lower interobserver variability and avoids biases associated with the method of PHT and 2D planimetry.[2,4] Whereas PHT is directly influenced by atrial and ventricular compliance, the presence of associated regurgitation, and transient hemodynamic conditions, compromising the accuracy of valve area estimation, 2D planimetry can overestimate or underestimate stenosis severity when there are non-orthogonal slices or acoustic shadowing.[2,3] Therefore,

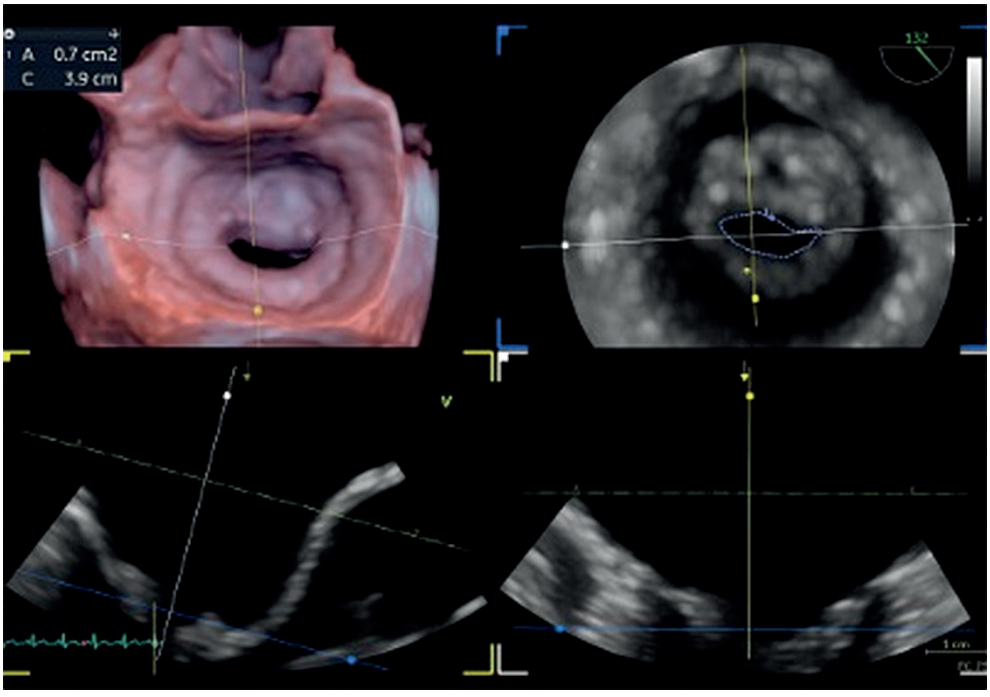

Figure 2 – *Multiplanar reconstruction by three-dimensional transesophageal echocardiography in mitral stenosis, allowing precise positioning of the plane in the narrowest portion of the valve orifice during diastole, facilitating reliable anatomical measurement of the functional area.*

the integration of 3D planimetry into the diagnostic workflow has a significant clinical impact, allowing more accurate stratification of disease severity and assisting in decision-making and planning of interventions, such as percutaneous valvotomy or surgery.[2-4]

Multiplanar Alignment in Volume Acquisition

Before capturing 3D volume, whether in zoom or full-volume mode, it is essential to use 2D multiplanar mode in order to correctly align the orthogonal axes to the mitral valve plane. This alignment during the acquisition phase is especially important in cases of mitral stenosis, where anatomy is often asymmetrical, and the minimum functional area may not coincide with a standard anatomical plane. Adjusting the lateral-medial and anteroposterior planes over the leaflet ends ensures that the plane of maximum diastolic opening is recorded, thus reducing errors and facilitating post-processing.

For rheumatic valves, it is recommended to align the coronal plane between the commissures (anterolateral and posteromedial), respecting any eventual asymmetries. The axial (transverse) plane should be verified to ensure that the functional orifice is centered and avoid tangential cuts. When there is asymmetric calcification or anatomical distortion, small adjustments to probe tilt can reposition the beam in a more favorable manner. The presence of an irregular rhythm, such as in atrial fibrillation, justifies the preference for 3D zoom mode with single-beat acquisition, avoiding stitch artifacts, which are common in full-volume images.

During 3D zoom acquisition, it is important to maintain a reasonable frame rate, ideally above 20 volumes per second (VPS), in order to preserve temporal clarity. Single-beat acquisition modes can reach up to 25 VPS, improving definition in patients with irregular rhythms, whereas multiple beats can increase the frame rate to even higher values (such as 80 VPS), but they require regular rhythm and pose the risk of artifacts. Very low rates can make it difficult to identify the smallest functional diameter, especially in complex anatomies.

The systematic adoption of these strategies during acquisition provides volumes that are more representative of functional anatomy, reduces the need for extensive corrections in post-processing, and increases the accuracy of valve area measurement by 3D planimetry.

Post-processing and Optimization of 3D Images

High-quality 3D images for mitral stenosis assessment directly depend on appropriate gain, brightness, and compression settings during acquisition and post-processing. Gain should be adjusted to enhance the echogenicity of the leaflets and commissures without saturating the image or introducing artifacts. Excessive gain amplifies low-intensity echoes, which can generate artificial shadows, whereas insufficient gain compromises visualization of the valve edges and valve orifice. A proper balance ensures that anatomical boundaries are clear, facilitating multiplanar reconstruction and 3D planimetry.[4]

Brightness and compression (contrast adjustment) also play a fundamental role. In the analysis of mitral stenosis, low- to medium-intensity compression is recommended, preserving the contrast necessary to clearly differentiate the edges of the functional orifice and commissures, without saturating echogenic areas. Excessive compression reduces the grayscale range, which can mask fine calcifications or partial fusions; very low compression excessively increases the dynamic range, resulting in reduced margin definition. Adjustment should be performed progressively during post-processing, verifying sharpness and anatomical continuity in multiplanar reconstructions before planimetry, in order to highlight the valve apparatus without distorting morphology.[4]

Smoothing is another available feature, which acts to reduce the graininess of a reconstructed surface. Although it is useful for creating a more homogeneous appearance of the valve and facilitating visual analysis, excessive use of this tool can distort irregular surfaces and attenuate the perception of critical structures, such as punctual calcifications or areas of fusion. In mitral stenosis, smoothing should be applied cautiously, only to improve image uniformity without compromising anatomical accuracy. Similarly, a well-optimized 2D image prior to volume capture is indispensable, given that any artifacts that arise during acquisition propagate to the 3D dataset, compromising multiplanar analysis and subsequent measurement of the valve area.[7,8]

Gamma adjustment can also be used to balance the distribution of grayscale in 3D imaging. Lower values increase contrast in darker areas, enhancing edges and fine calcifications, whereas higher values facilitate the visualization of less echogenic structures. Adjustments should be moderate in order to avoid loss of detail or distortion of anatomical perception.

In 3D analysis of mitral stenosis, features such as Clarity can be used to enhance edges and reduce noise, improving valve contour definition and facilitating planimetry, especially in complex anatomies or those with calcification. Adjustments should be moderate in order to avoid artifacts or artificial highlights. As a complementary and optional feature, HD Live can be used for volumetric rendering with lighting simulation, altering depth perception and 3D realism. Although this feature does not directly influence measurement accuracy, it can assist in spatial understanding and visual communication of anatomical findings.

Artifact and Noise Correction

High-quality 3D images for mitral stenosis assessment do not depend only on appropriate gain, brightness, and compression adjustments, as mentioned above, but also on strategies to reduce artifacts and noise that can compromise valve area measurement. A frequent challenge is acoustic shadowing caused by extensive calcification, which leads to loss of definition in the leaflets and subvalvular region. In order to mitigate this, the following are recommended:

- Slightly reduce the gain and adjust the compression to enhance valve edges without saturating calcified areas.
- Experiment with small changes in the probe angle, seeking windows with lower acoustic interference.

- In persistent cases, apply 3D zoom mode with a restricted focus on the valve, minimizing the need for extensive reconstructions and areas affected by shadowing.

Speckle noise is another issue that can make accurate identification of the valve contour difficult. Smoothing or noise suppression filters may be applied, provided that they are used moderately, given that excessive use tends to distort the actual geometry, especially in areas with calcification or commissural fusion.

In full-volume acquisitions, motion artifacts, for example, stitch artifacts, are common in patients with atrial fibrillation or tachycardia. In these cases, the use of smaller volumes or single-beat acquisition is preferable to avoid loss of anatomical continuity, even with lower spatial resolution.

Careful application of these techniques, combined with proper alignment of orthogonal planes and rational use of rotation and cropping tools, is essential to ensure that the final dataset faithfully represents anatomy, enabling reliable and reproducible planimetry.

Finally, it is important to bear in mind that all 3D analyses depend on the quality of the original 2D image. Artifacts acquired in the 2D base propagate to the reconstructed volume, impacting the accuracy of planimetry. A stable, well-centered, and distortion-free acquisition is the first step to effective post-processing.

Rotation and Cropping Functions in Post-processing

During 3D analysis of mitral stenosis, volume manipulation with the rotation and cropping functions is applied to optimize visualization of the valve orifice and mitral apparatus. Rotation of the volumetric block along orthogonal axes allows for precise alignment of the plane of view with the leaflet tips, facilitating an en face view of valve opening during diastole. This step is particularly important in complex anatomies, where asymmetric commissural fusions or calcifications can distort the standard orientation, making it difficult to measure the functional area.[6,8]

The cropping feature makes it possible to remove portions of the 3D volume that do not contribute to analysis, for example, adjacent cavities or redundant portions of the left atrium, allowing for exclusive focus on the mitral valve and its orifice. This cleaning process improves image clarity and structural definition, in addition to facilitating multiplanar reconstruction and planimetry.[4] Careful use of the cropping function also reduces artifacts and avoids overlapping structures, especially in cases with significant atrial dilation or multiple flow planes that could interfere with interpretation.[8]

The combination of these techniques, in conjunction with previously applied gain, brightness, compression, and smoothing adjustments, results in a more stable reconstruction that is faithful to the actual anatomy. Accordingly, systematic use of rotation and cropping tools not only improves visual quality but also increases the accuracy of valve area measurement and anatomical characterization, contributing to more reliable diagnostic analysis in mitral valve stenosis.

Systematic application of appropriate acquisition strategies, in association with image optimization techniques in post-processing and careful volume manipulation with tools such as rotation and cropping, improves the quality of 3D reconstruction and diagnostic reliability in mitral stenosis. Table 1 summarizes the main recommendations for reducing artifacts and obtaining accurate measurements. When the technical stage is optimized, it is possible to advance to individualized assessment of mitral stenosis according to etiology.

Individual Assessment According to Etiology

Mitral Stenosis of Rheumatic Etiology

Mitral stenosis of rheumatic etiology is characterized by commissural fusion, leaflet thickening that begins at the ends and extends toward the base, and fusion of the subvalvular apparatus, resulting in an orifice with a "fish mouth" appearance and diastolic doming motion of the anterior leaflet[2,8] (Figure 3). Echocardiographic assessment should document not only the extent of commissural fusion but also the presence and distribution of calcium in the commissures, which are fundamental parameters for determining the feasibility and safety of percutaneous balloon valvotomy.[8,9] Asymmetric commissural involvement or the presence of extensive calcification in the commissures are associated with lower hemodynamic success of percutaneous balloon valvotomy and greater risk of significant post-procedural mitral regurgitation[6,8] (Figure 4).

Recent studies show that 3D scores, such as the Anwar score, better capture the severity of commissural calcification and subvalvular involvement. These elements are directly related to the occurrence of suboptimal outcomes, such as final valve area < 1.5 cm^2 or significant post-procedural mitral regurgitation.[10] In a study by Farrag et al., the 3D-Anwar score was superior to the traditional Wilkins 2D score in predicting adverse outcomes, with a more robust negative correlation between the score and the valve area obtained.[9] Therefore,

Table 1 – Practical strategies to minimize artifacts in acquisition and post-processing of 3D volumes in mitral stenosis assessment

Reduce gain and adjust contrast in regions with calcification to avoid saturation and acoustic shadowing.
If there is loss of definition due to acoustic shadowing, adjust the probe angle slightly.
Give preference to 3D zoom mode when full-volume mode generates artifacts, especially in irregular rhythms.
Use smoothing moderately, only to homogenize the image, without losing anatomical definition.
In patients with atrial fibrillation, avoid multi-beat acquisition; single-beat mode is preferable for reduced volumes.
Ensure a good 2D image before capturing volume, as initial artifacts compromise the entire reconstruction.

2D: two-dimensional; 3D: three-dimensional.

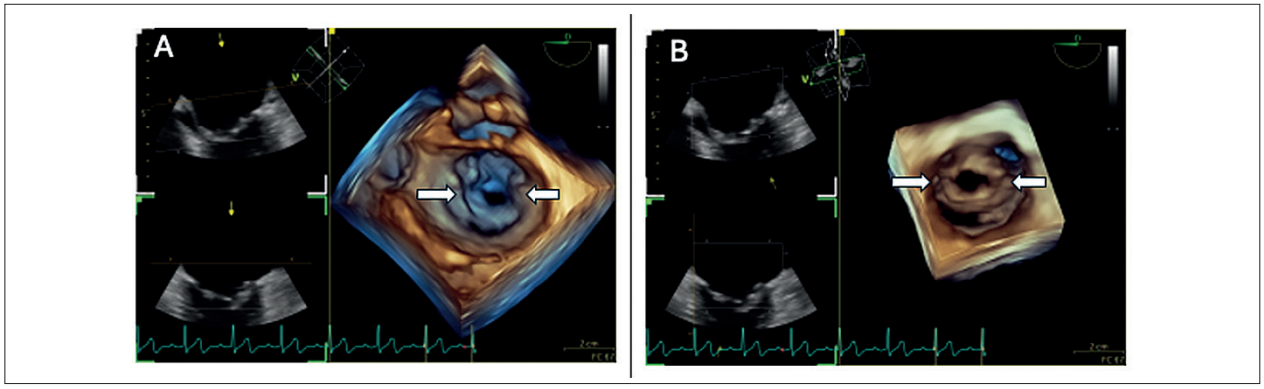

Figure 3 – *Three-dimensional images obtained by transesophageal echocardiography demonstrating commissural fusion, a characteristic of rheumatic mitral stenosis. (A) Atrial view. (B) Ventricular view.*

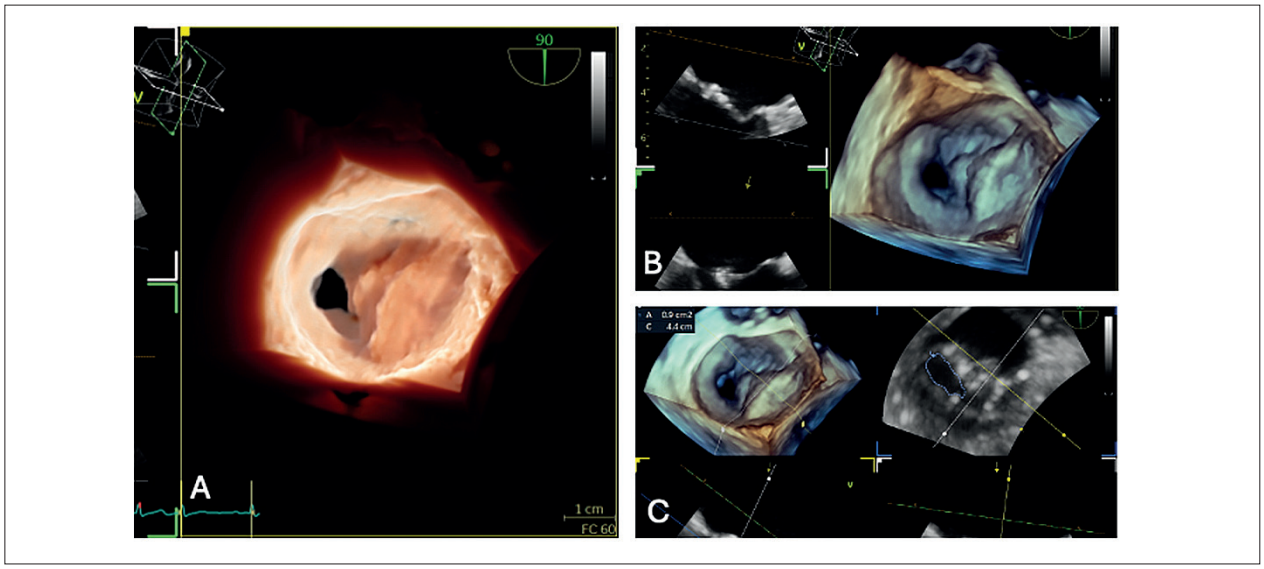

Figure 4 – *Images obtained by three-dimensional transesophageal echocardiography demonstrating partial commissural fusions and asymmetric calcification in rheumatic mitral stenosis. (A) Transillumination image, highlighting extensive calcification and asymmetric fusion of the posteromedial commissure. (B) Three-dimensional en face view of the mitral valve, highlighting the fusion and asymmetric distribution of calcium between the commissures. (C) Three-dimensional transesophageal planimetry showing severe stenosis.*

3D assessment of commissures not only enhances the accuracy of planimetry and anatomical characterization but also also provides fundamental prognostic parameters for candidate selection and planning of percutaneous interventions, reducing the risk of complications such as residual mitral regurgitation (Figure 5).

Mitral stenosis of degenerative etiology

Mitral stenosis of degenerative etiology predominantly occurs in elderly patients, and it results from progressive calcification of the mitral annulus, with frequent extension to the base of the leaflets. This configuration leads to the formation of a tubular or tunnel-shaped orifice, generally without significant commissural fusion, and it usually generates lower transmitral gradients for the same valve area when compared to the rheumatic form.[11,12] These anatomical peculiarities make conventional 2D echocardiography assessment challenging, given that the presence of extensive calcium often produces acoustic shadowing, making accurate 2D planimetry difficult or impossible.[11]

In this scenario, 3D echocardiography also plays an important role in calcific degenerative etiology, as it allows multiplanar reconstructions and en face visualization of the valve orifice, overcoming limitations imposed by acoustic shadowing and providing more reproducible and accurate measurements of mitral valve area.[1,2]

In addition to accurately measuring the valve area, 3D echocardiography allows for characterization of the distribution and extent of calcification, detailing annular involvement and calcium penetration in the leaflet bases.[11,12] This analysis is particularly relevant because the tubular geometry that is typical in this etiology tends to generate smaller gradients for the same

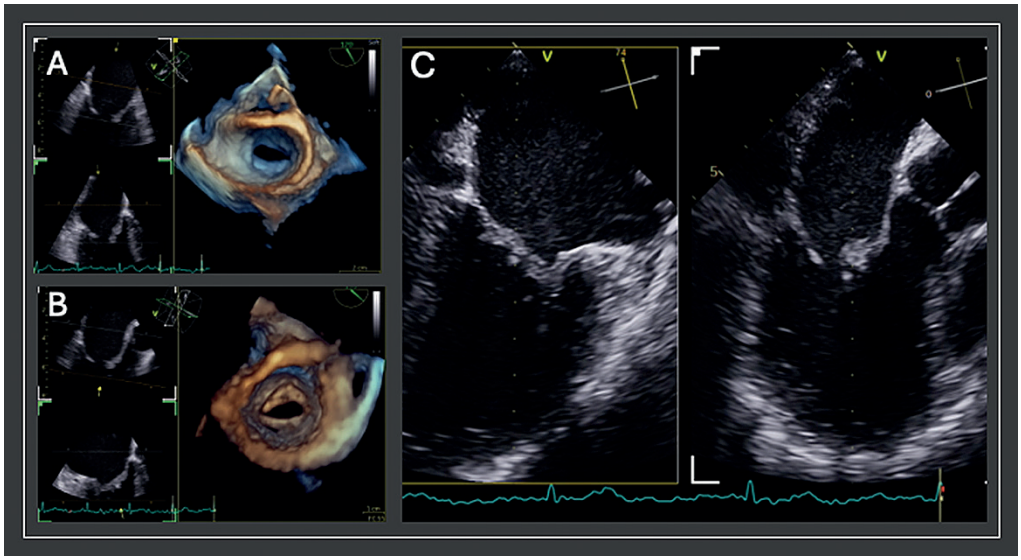

Figure 5 – *Images obtained by three-dimensional transesophageal echocardiography, representing a mitral valve with rheumatic anatomy that is favorable for percutaneous balloon valvotomy. (A) Three-dimensional atrial en face view demonstrating symmetrical commissural fusion with reduced valve area. (B) Three-dimensional ventricular en face view, with typical restricted posterior mobility and absence of significant subvalvular calcification. (C) Multiplanar (Multi-D) reconstruction integrating orthogonal slices for complementary mitral valve assessment.*

valve area, which can mask the severity of the obstruction when only hemodynamic parameters are considered.[11] The use of 3D assessment helps differentiate between low gradients due to reduced flow and those related to valve anatomy, avoiding underdiagnosis of significant stenosis.[10] In cases with extensive calcification or complex anatomical deformity, the integration of 3D assessment with computed tomography has been recommended to complement anatomical definition and guide therapeutic planning.[12]

The Central Illustration displays a comparative summary of the main anatomical characteristics with therapeutic implications for rheumatic and degenerative forms of mitral stenosis.

Conclusion

Three-dimensional planimetry is currently the most reliable method for estimating mitral valve area, especially in scenarios with complex anatomy, asymmetric commissural fusion, or extensive calcification. Even though 2D echocardiography continues to play a central role in the initial assessment, the systematic use of 3D echocardiography should be recommended in both the pre-procedure phase and the follow-up of patients with significant mitral stenosis, contributing to greater diagnostic accuracy and improved therapeutic guidance.

Author Contributions

Conception and design of the research: Costa A; Acquisition of data: Costa A, Sales MAM. Analysis and interpretation of the data: Carvalho MVSF; Writing of the manuscript: Costa A, Sales MAM, Carvalho MVSF; Critical revision of the manuscript for intellectual content: Costa A.

Potential conflict of interest

No potential conflict of interest relevant to this article was reported.

Sources of funding

There were no external funding sources for this study.

Study association

This study is not associated with any thesis or dissertation work.

Ethics approval and consent to participate

This article does not contain any studies with human participants or animals performed by any of the authors.

Use of Artificial Intelligence

The authors did not use any artificial intelligence tools in the development of this work.

Data Availability

The underlying content of the research text is contained within the manuscript.

References

1. Coisne A, Lancellotti P, Habib G, Garbi M, Dahl JS, Barbanti M, et al. ACC/AHA and ESC/EACTS Guidelines for the Management of Valvular Heart Diseases: JACC Guideline Comparison. J Am Coll Cardiol. 2023;82(8):721-34. doi: 10.1016/j.jacc.2023.05.061.

2. Silbiger JJ. Advances in Rheumatic Mitral Stenosis: Echocardiographic, Pathophysiologic, and Hemodynamic Considerations. J Am Soc Echocardiogr. 2021;34(7):709-22.e1. doi: 10.1016/j.echo.2021.02.015.

3. Vahanian A, Beyersdorf F, Praz F, Milojevic M, Baldus S, Bauersachs J, et al. 2021 ESC/EACTS Guidelines for the Management of Valvular Heart Disease. Eur Heart J. 2022;43(7):561-632. doi: 10.1093/eurheartj/ehab395.

4. Lang RM, Badano LP, Tsang W, Adams DH, Agricola E, Buck T, et al. EAE/ASE Recommendations for Image Acquisition and Display Using Three-Dimensional Echocardiography. J Am Soc Echocardiogr. 2012;25(1):3-46. doi: 10.1016/j.echo.2011.11.010.

5. Fard MS, Rezaeian N, Pourafkari L, Erami S, Nader ND. Level of Agreement in Three-Dimensional Planimetric Measurement of Mitral Valve Area between Transthoracic and Transesophageal Echocardiography. Echocardiography. 2019;36(8):1501-8. doi: 10.1111/echo.14431.

6. Bleakley C, Eskandari M, Aldalati O, Moschonas K, Huang M, Whittaker A, et al. Impact of 3D Echocardiography on Grading of Mitral Stenosis and Prediction of Clinical Events. Echo Res Pract. 2018;5(4):105-11. doi: 10.1530/ERP-18-0031.

7. Vegas A. Three-Dimensional Transesophageal Echocardiography: Principles and Clinical Applications. Ann Card Anaesth. 2016;19(Suppl 1):S35-S43. doi: 10.4103/0971-9784.192622.

8. Faletra FF, Agricola E, Flachskampf FA, Hahn R, Pepi M, Marsan NA, et al. Three-Dimensional Transoesophageal Echocardiography: How to Use and When to Use-a Clinical Consensus Statement from the European Association of Cardiovascular Imaging of the European Society of Cardiology. Eur Heart J Cardiovasc Imaging. 2023;24(8):e119-97. doi: 10.1093/ehjci/jead090.

9. Wunderlich NC, Beigel R, Siegel RJ. Management of Mitral Stenosis Using 2D and 3D Echo-Doppler Imaging. JACC Cardiovasc Imaging. 2013;6(11):1191-205. doi: 10.1016/j.jcmg.2013.07.008.

10. Farrag HMA, Setouhi AM, El-Mokadem MO, El-Swasany MA, Mahmoud KS, Mahmoud HB, et al. Additive Value of 3D-Echo in Prediction of Immediate Outcome after Percutaneous Balloon Mitral Valvuloplasty. Egypt Heart J. 2019;71(1):19. doi: 10.1186/s43044-019-0019-x.

11. Ruiz JMM, Gómez JLZ. The Role of 2D and 3D Echo in Mitral Stenosis. J Cardiovasc Dev Dis. 2021;8(12):171. doi: 10.3390/jcdd8120171.

12. Kato N, Watanabe H, Pellikka PA, Guerrero M. Clinical Challenges in Calcific Mitral Stenosis from Diagnosis to Management. J Cardiol. 2025:S0914-5087(25)00167-4. doi: 10.1016/j.jjcc.2025.06.014.

My approach to optimize my equipment for the use of ultrasound contrast agents

Marcio S. M. Lima[1,2]
Instituto do Coração (InCor), Faculdade de Medicina da Universidade de São Paulo,[1] *São Paulo, SP – Brazil*
Grupo Fleury,[2] *São Paulo, SP – Brazil*

Central Illustration: My approach to optimize my equipment for the use of ultrasound contrast agents

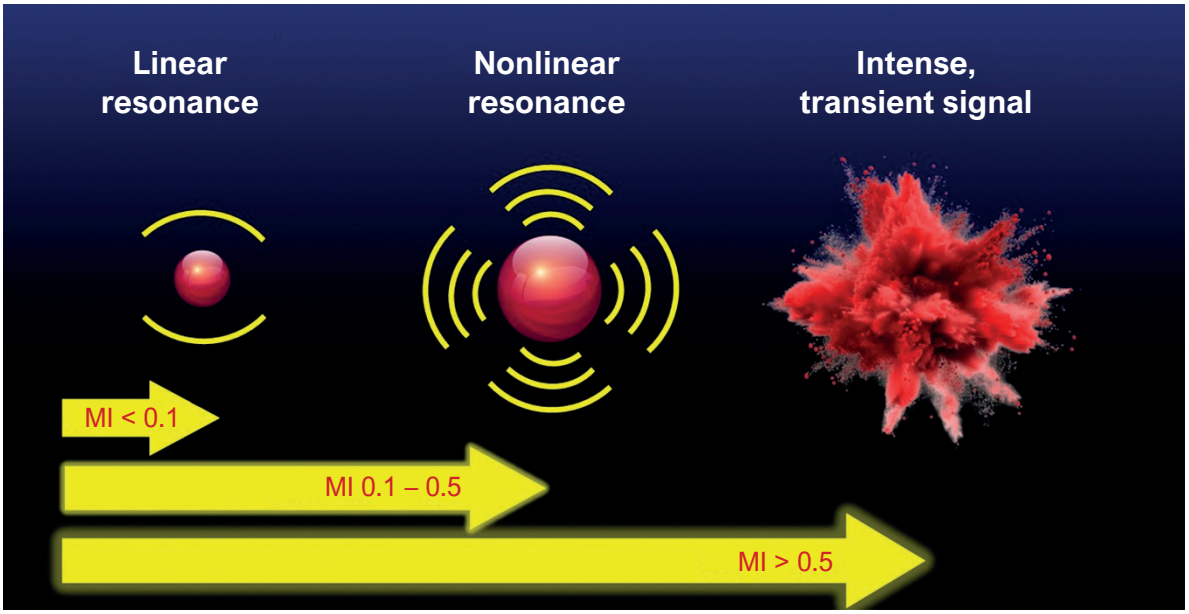

Arq Bras Cardiol: Imagem cardiovasc. 2025;38(3):e20250061

Resonance of microbubbles in response to the energy transmitted by the echocardiography equipment transducer. MI: mechanical index.

Abstract

Contrast echocardiography, based on ultrasound contrast agents composed of microbubbles, has been increasingly incorporated into echocardiography labs. It involves the infusion of compounds that enhance the visualization of various cardiac and vascular structures. The multiple adjustments required are usually included in pre-configured packages (presets) installed by manufacturers on the equipment. However, it is possible – and sometimes necessary – to make modifications to optimize image generation and, guided by the objective of the echocardiographic study, to achieve the full potential this technique can offer.

Keywords

Echocardiography; Contrast Media; Diagnostic Equipment

Mailing Address: Marcio S. M. Lima •
Instituto do Coração (Incor) do Hospital das Clínicas da Faculdade de Medicina da Universidade de São Paulo (HCFMUSP). Av. Dr. Eneas de Carvalho Aguiar, 44. Postal Code: 05403-000, São Paulo, SP – Brazil
E-mail: marcio.lima@incor.usp.br
Manuscript received August 17, 2025; revised August 29, 2025; accepted August 29, 2025
Editor responsible for the review: Marcelo Tavares

DOI: https://doi.org/10.36660/abcimg.20250061i

Introduction

Contrast echocardiography (CE) is based on the use of ultrasound contrast agents (UCAs), or echocardiographic contrast, for the purpose of opacifying cardiac structures. It is a safe, cost-effective technique that significantly aids the diagnostic process and, consequently, guides treatment, improving patient outcomes across various clinical scenarios.[1-4]

In this advanced echocardiographic technique, microbubble-based compounds are used – microspheres composed of high molecular weight gas (perfluorocarbon or sulfur hexafluoride) encapsulated by an albumin or lipid shell. In addition to being smaller than red blood cells, this composition gives microbubbles some unique properties. For

SUMÁRIO

example, they have lower solubility and diffusibility in blood, meaning greater compound stability, which allows them to cross the pulmonary capillary barrier.[5] Another very important aspect is the rheology of the microbubble when interacting with ultrasound (US) waves. Depending on the amount of transmitted energy, there may be linear or nonlinear radial oscillation, or even microbubble destruction. Therefore, energy adjustment is crucial in CE (Central Figure).

The opacification of structures occurs through the interaction between US waves and microbubbles, generating a powerful reflected signal – approximately 135 times stronger – that is captured by the echocardiography equipment. At this stage, to maximize the effectiveness of the technique, it is essential to optimize the settings of the device being used. The multiple adjustments required are typically included in preconfigured packages provided by manufacturers (presets), and the main variable is the transmitted energy, measured by the so-called Mechanical Index (MI). This adjustment should be guided primarily by the specific objective of the echocardiographic examination being performed.

Ultrasound Contrast Agents and Contrast Echocardiography

The main and most frequent indications for the use of UCAs are:

- Poor acoustic image quality: the use of UCAs can "rescue" exams that would otherwise require additional, more complex and costly imaging methods (Figure 1);[6,8]
- Volume quantification and assessment of left ventricular (LV) systolic function: This estimation shows excellent correlation with cardiac magnetic resonance imaging, improving interobserver reproducibility (Figure 2);[9,10]
- Optimization of Doppler signal for evaluating valvular gradients and estimating pulmonary artery systolic pressure;
- Stress echocardiography: enhances the analysis of segmental wall motion and allows for myocardial perfusion assessment (Figure 3);
- Investigation of thrombi and evaluation of cardiac masses;
- Detection of LV rupture;
- Area delimitation during septal alcoholization for hypertrophic cardiomyopathy.

There are numerous benefits to using UCAs in echocardiographic examinations. Some of the main advantages include:

- They are safe and cost-effective;
- Administration is relatively simple and quick;
- They are non-nephrotoxic;
- They do not accumulate in various tissues;
- They are associated with improved diagnostic accuracy in multiple clinical scenarios and better outcomes in critically ill patients.

Although relatively straightforward, certain steps are essential for the proper administration of UCAs. The key steps are outlined below:

1. A peripheral venous access should be obtained, preferably in the antecubital fossa, with a gauge of at least 20G, along with the installation of a three-way stopcock. This access must be tested for patency to ensure proper infusion.
2. The UCA should be prepared according to the manufacturer's specifications. Sonovue, an agent approved by ANVISA and authorized for routine use in Brazil, consists of a kit containing a vial with lyophilized microbubbles of sulfur hexafluoride at a

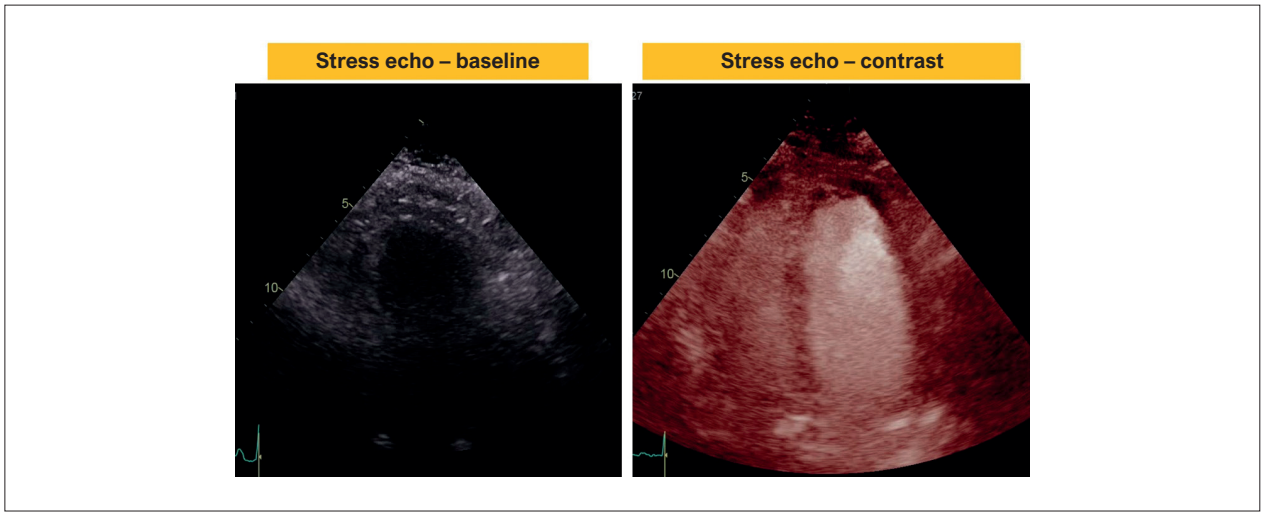

Figure 1 – *Patient with chronic obstructive pulmonary disease and obesity referred for a pharmacological stress echocardiogram using dobutamine. Baseline imaging showed reduced quality. Improvement was observed with the use of an ultrasound contrast agent, allowing the exam to be successfully performed.*

concentration of 8 μL/mL and a syringe with a 0.9% sodium chloride diluent solution. After dilution, the compound should be manually and gently homogenized.

3. Sonovue can be administered in small boluses or, much less frequently, via continuous infusion. Bolus doses typically range from 0.5 to 1.0 mL, followed by a 5 mL flush of 0.9% saline infused over 5 to 10 seconds, or by elevating the limb. It is recommended to use the smallest bolus that ensures adequate opacification, thereby conserving contrast for the entire echocardiographic study. Optimal contrast of the left ventricle is achieved when the cavity is well opacified and the endocardial-cavity interface (endocardial border) is clearly defined. Administering an excessive dose of the contrast agent may result in a "blooming" artifact – an intense apical brightness that distorts adjacent structures – and acoustic shadowing with image attenuation in the basal segments. Conversely, using a lower dose may lead to suboptimal contrast in the apical region, producing a "swirling" appearance, as well as myocardial attenuation that may be generalized or segmental, mimicking perfusion defects.

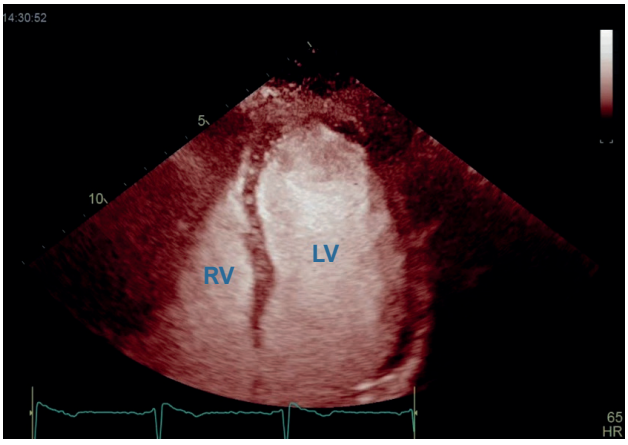

Figure 2 – *Clearer visualization of the borders allows a more accurate measurement of left ventricular volumes and calculation of ejection fraction, reducing interobserver variability. LV: left ventricle; RV: right ventricle.*

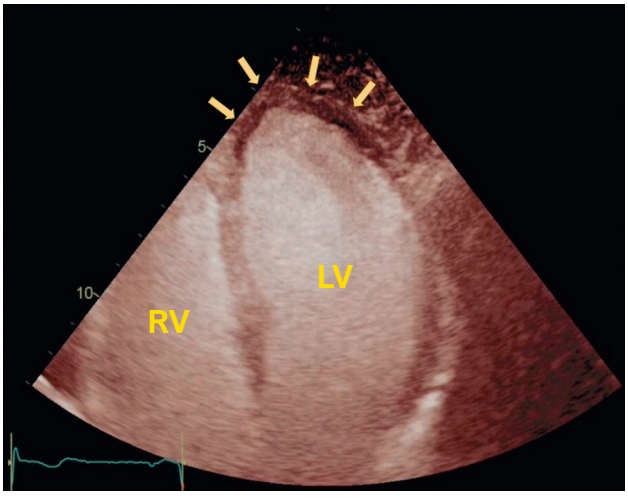

Figure 3 – *A 60-year-old woman underwent contrast echocardiography under pharmacological stress with dobutamine. She experienced chest discomfort and ST-segment depression in the precordial leads on the electrocardiogram. An area of myocardial perfusion deficit was observed at the apex of the left ventricle, associated with localized hypokinesia (arrows). The test was positive for the presence of myocardial ischemia. LV: left ventricle; RV: right ventricle.*

Optimizing my equipment for contrast echocardiography

The rheology of microbubbles and the high reflectivity of US waves are the core of the image opacification technique in CE. The structural composition of the microsphere leads to different bubble behaviors when interacting with US beams at varying levels of transmitted energy.

The MI is a measure that expresses the energy transmitted to tissues, *i.e.*, the acoustic power. Conceptually, it corresponds to the peak negative pressure of the US wave divided by the square root of the central frequency (P- /$\sqrt{f}$), and it is typically greater than 0.8 in most non-contrast images. This is the primary parameter to be adjusted in CE. A very low MI (< 0.2) causes asymmetric and nonlinear radial oscillation of the microbubbles, characterized by greater expansion during the rarefaction phase of the US wave compared to compression at the peak acoustic pressure. This phenomenon is highly relevant in CE, as it not only reflects the fundamental frequency of the US beam transmitted by the transducer but also generates multiple harmonic frequencies – especially the second harmonic.[5] The resulting signal is intense and forms the basis of image opacification in CE. Simultaneously, CE equipment is equipped with specific image cancellation algorithms that filter the received signals. Two of the most common technologies for this purpose are pulse amplitude modulation and pulse inversion, the latter illustrated in Figure 4.

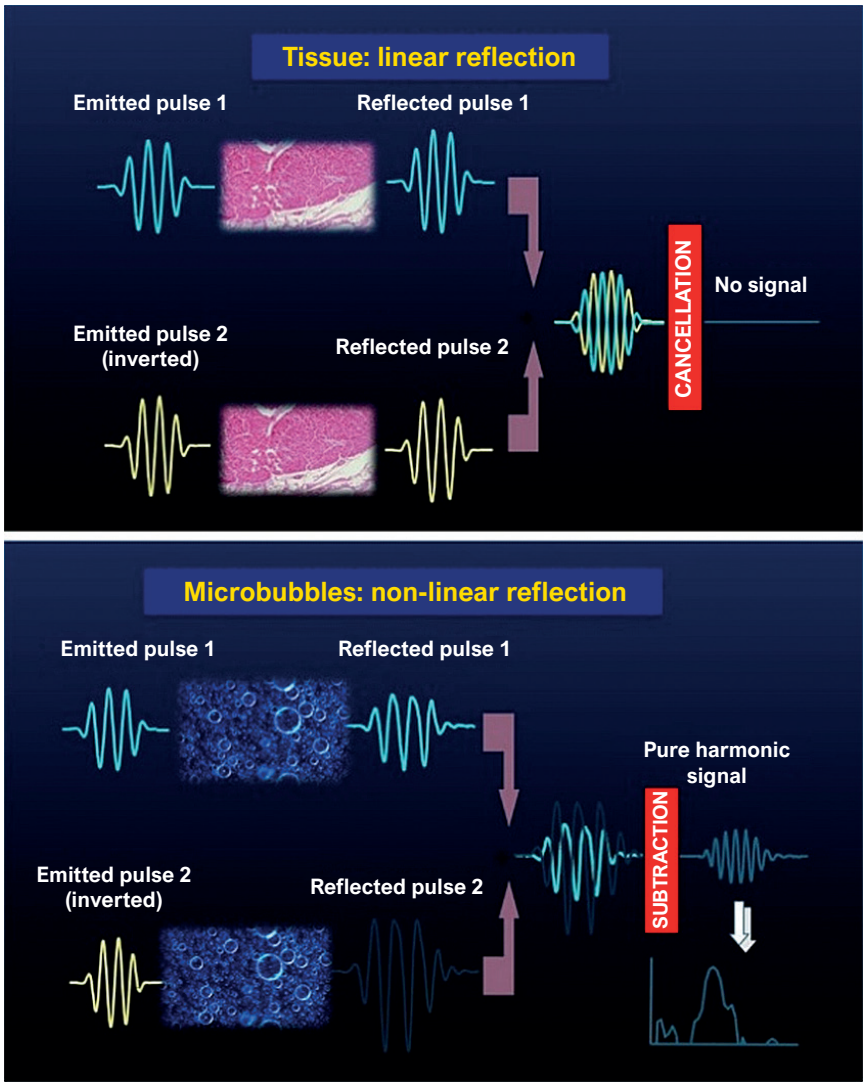

Figure 4 – *Pulse inversion algorithm for image cancellation. Two ultrasound pulses are emitted at the fundamental frequency, one normal and one inverted. Top panel: In tissue, these pulses are reflected similarly (linear reflection). Subtracting the received pulses results in a null signal (no output), leading to image cancellation and reduced brightness in that sector. Bottom panel: The pulses are reflected by microbubbles at both the fundamental and harmonic frequencies. Subtracting these reflected pulses removes the fundamental frequency, resulting in a "pure" harmonic signal, which appears as a bright intensity in the image.*

Another important point is that with the low amount of transmitted energy, there is minimal destruction of microbubbles within the myocardial microvasculature. This allows not only enhanced visualization of the LV cavity but also for the assessment of myocardial perfusion (MP). Following the recommendation to use imaging in fundamental mode (although harmonic mode may also be used), with a very low Mechanical Index (MI < 0.2), an excellent contrast-to-noise ratio is achieved, along with clear delineation of the interface between the myocardium and the LV cavity (endocardial borders), as well as the ability to evaluate MP. Therefore, setting a very low MI (< 0.20) combined with image cancellation algorithm technology represents the optimal parameters for assessing volumes, ejection fraction, segmental contraction, and MP – even in real time, both at rest and under stress.[4,11-13]

Specifically for the assessment of MP, the use of high-energy pulse "flashes" (MI: 0.8–1.2; 5–15 frames) is recommended to destroy microbubbles within the myocardium while preserving opacification within the cardiac chamber. The replenishment time should be less than five seconds at rest and less than two seconds under stress. Typically, this function is already included in the equipment's preset and can be easily activated.

Intermediate MI levels (0.2–0.5) may be used, offering improved image resolution, though at the cost of increased microbubble destruction. MI values above 0.5 should not be used in CE. Situations where this energy level may be appropriate include the investigation of thrombi and masses, as well as the diagnosis of non-compacted cardiomyopathy.

Regarding image generation technology, although harmonic imaging is currently available in CE transducers, the use of nonlinear fundamental frequency is recommended. This approach ensures a better contrast-to-noise ratio, with the frame rate adjusted to approximately 25–35 Hz and the transducer transmission frequency kept below 2.0 MHz.

In patients with a larger body surface area, it may be necessary to adjust to an even lower transmission frequency to allow greater penetration of the ultrasound beam into the tissues. It is possible to use either grayscale imaging or apply color mapping ("chroma"), such as red ruby, to the generated images.

Image depth should be adjusted according to the objective of the examination. If the focus is on LV opacification for volume quantification, systolic function assessment, and delineation of endocardial borders for segmental contraction analysis, the image depth should be set to visualize the mitral valve and approximately 1 to 2 cm of the left atrium.

Image attenuation in the basal segments of the LV may occur, especially when an excessive amount of UCA is used. This can lead to a misdiagnosis of perfusion deficits in these regions. Some strategies can be adopted to improve image definition, such as centering the basal segments in the image – since axial resolution is superior to lateral resolution in the ultrasound field – positioning the focus at the level of the mitral valve, and increasing the gain in this area using the time gain compensation adjustment. An example of these adjustments is illustrated in Figure 5.

If the goal is to investigate a possible apical thrombus, non-compacted cardiomyopathy, or evaluate an apical aneurysm (Figure 6), it is necessary to reduce the image depth and adjust the focus to that specific region. Setting the Mechanical Index (MI) to an intermediate level (2.0–3.0) may help improve spatial resolution, although this comes at the cost of increased microbubble destruction.

Attenuation may also occur in the myocardium of the apical region of the left ventricle, due to higher acoustic power in that area and, occasionally, a higher frame rate, which leads to greater microbubble destruction. Recommended adjustments to optimize the image in these cases include reducing the frame rate and adjusting the gain locally.[4]

Finally, UCAs can also be used to assist in estimating valvular gradients and systolic pressure in the pulmonary

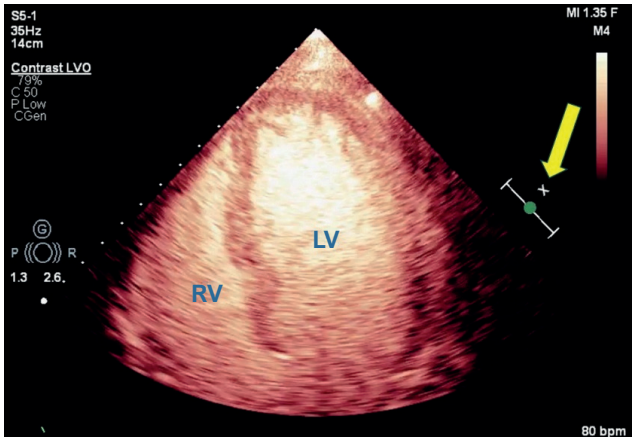

Figure 5 – *Contrast echocardiography. Recommended adjustments to optimize this image include: positioning the focus (yellow arrow) at the level of the mitral valve to improve acoustic resolution of the basal segments and reducing the gain to enhance delineation of the endocardial borders. LV: left ventricle; RV: right ventricle.*

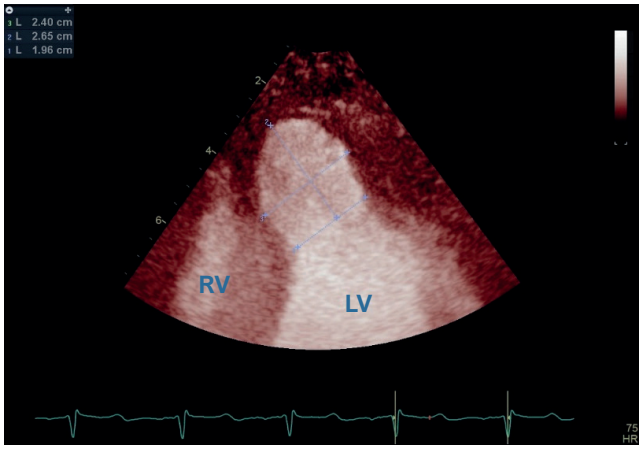

Figure 6 – *Apical aneurysm image better visualized with the use of an ultrasound contrast agent, allowing clear definition of the endocardial borders and more accurate measurement. LV: left ventricle; RV: right ventricle.*

artery. In such cases, the signal (and noise) generated may be intense. The recommendation is to reduce the gain until clear spectral curves with well-defined envelopes are obtained.[4]

Conclusion

CE, based on the opacification of cardiac structures using UCAs composed of microbubbles, has been increasingly adopted across various echocardiography labs. This procedure offers numerous benefits, but to fully achieve its potential, certain equipment adjustments are necessary. Typically, adjustment packages (presets) come pre-configured and installed by manufacturers, and their use is recommended. The primary adjustment involves the level of energy transmitted by the transducer, represented by the MI, which is crucial for minimizing microbubble destruction. This ensures proper opacification of the left ventricle and enables the assessment of MP. Other recommended adjustments include place the image focus at the level of the mitral valve, modifying overall and/or sectoral gain to enhance visualization of apical and basal segments, reducing the frame rate, adjusting the US beam depth, and selecting either fundamental or harmonic imaging modes for image generation.

Author Contributions

Conception and design of the research; Acquisition of data; Analysis and interpretation of the data; Statistical analysis; Writing of the manuscript; Critical revision of the manuscript for intellectual content: Lima MSM.

Potential conflict of interest

I declare no relevant conflict of interest.

Sources of funding

This study had no external funding sources

Study association

This study is not affiliated with any graduate programs.

Ethics approval and consent to participate

This article does not contain any studies with human or animal subjects performed by any of the authors.

Use of Artificial Intelligence

The authors did not use artificial intelligence tools in the development of this work.

Data Availability

The underlying content of the research text is contained in the manuscript.

References

1. Porter TR, Mulvagh SL, Abdelmoneim SS, Becher H, Belcik JT, Bierig M, et al. Clinical Applications of Ultrasonic Enhancing Agents in Echocardiography: 2018 American Society of Echocardiography Guidelines Update. J Am Soc Echocardiogr. 2018;31(3):241-74. doi: 10.1016/j.echo.2017.11.013.
2. Porter TR, Feinstein SB, Senior R, Mulvagh SL, Nihoyannopoulos P, Strom JB, et al. CEUS Cardiac Exam Protocols International Contrast Ultrasound Society (ICUS) Recommendations. Echo Res Pract. 2022;9(1):7. doi: 10.1186/s44156-022-00008-3.

3. Senior R, Becher H, Monaghan M, Agati L, Zamorano J, Vanoverschelde JL, et al. Clinical Practice of Contrast Echocardiography: Recommendation by the European Association of Cardiovascular Imaging (EACVI) 2017. Eur Heart J Cardiovasc Imaging. 2017;18(11):1205-1205af. doi: 10.1093/ehjci/jex182.

4. Porter TR, Abdelmoneim S, Belcik JT, McCulloch ML, Mulvagh SL, Olson JJ, et al. Guidelines for the Cardiac Sonographer in the Performance of Contrast Echocardiography: A Focused Update from the American Society of Echocardiography. J Am Soc Echocardiogr. 2014;27(8):797-810. doi: 10.1016/j.echo.2014.05.011.

5. Burns PN. Harmonic Imaging with Ultrasound Contrast Agents. Clin Radiol. 1996;51(Suppl 1):50-5.

6. Costa JM, Tsutsui JM, Nozawa E, Morhy SS, Andrade JL, Ramires JF, et al. Contrast Echocardiography Can Save Nondiagnostic Exams in Mechanically Ventilated Patients. Echocardiography. 2005;22(5):389-94. doi: 10.1111/j.1540-8175.2005.03176.x.

7. Makaryus AN, Zubrow ME, Gillam LD, Michelakis N, Phillips L, Ahmed S, et al. Contrast Echocardiography Improves the Diagnostic Yield of Transthoracic Studies Performed in the Intensive Care setting by Novice Sonographers. J Am Soc Echocardiogr. 2005;18(5):475-80. doi: 10.1016/j.echo.2004.10.004.

8. Kurt M, Shaikh KA, Peterson L, Kurrelmeyer KM, Shah G, Nagueh SF, et al. Impact of Contrast Echocardiography on Evaluation of Ventricular Function and Clinical Management in a Large Prospective Cohort. J Am Coll Cardiol. 2009;53(9):802-10. doi: 10.1016/j.jacc.2009.01.005.

9. Saloux E, Labombarda F, Pellissier A, Anthune B, Dugué AE, Provost N, et al. Diagnostic Value of Three-Dimensional Contrast-Enhanced Echocardiography for Left Ventricular Volume and Ejection Fraction Measurement in Patients with Poor Acoustic Windows: A Comparison of Echocardiography and Magnetic Resonance Imaging. J Am Soc Echocardiogr. 2014;27(10):1029-40. doi: 10.1016/j.echo.2014.06.006.

10. Hoffmann R, von Bardeleben S, ten Cate F, Borges AC, Kasprzak J, Firschke C, et al. Assessment of Systolic Left Ventricular Function: A Multi-Centre Comparison of Cineventriculography, Cardiac Magnetic Resonance Imaging, Unenhanced and Contrast-Enhanced Echocardiography. Eur Heart J. 2005;26(6):607-16. doi: 10.1093/eurheartj/ehi083.

11. Sieswerda GT, Yang L, Boo MB, Kamp O. Real-Time Perfusion Imaging: A New Echocardiographic Technique for Simultaneous Evaluation of Myocardial Perfusion and Contraction. Echocardiography. 2003;20(6):545-55. doi: 10.1046/j.1540-8175.2003.03093.x.

12. Muskula PR, Main ML. Safety with Echocardiographic Contrast Agents. Circ Cardiovasc Imaging. 2017;10(4):e005459. doi: 10.1161/CIRCIMAGING.116.005459.

13. Kaufmann BA, Wei K, Lindner JR. Contrast Echocardiography. Curr Probl Cardiol. 2007;32(2):51-96. doi: 10.1016/j.cpcardiol.2006.10.004.

Assessment of Acute Chest Pain in the Emergency Department: How Point-of-Care Ultrasound Can Assist the Cardiologist

Alexandre de Matos Soeiro,[1,2,3] Lucas Lentini Herling de Oliveira,[1] Rômulo Fonseca de Moraes,[1] Tatiana de Carvalho Andreucci Torres Leal[1]

Universidade de São Paulo, Instituto do Coração,[1] São Paulo, SP – Brazil
HCor,[2] São Paulo, SP – Brazil
BP Mirante,[3] São Paulo, SP – Brazil

Abstract

The use of point-of-care ultrasound (POCUS) in emergency settings is now well established as part of the initial assessment of critically ill patients. In cases of acute chest pain, POCUS plays a significant role in differential diagnosis, helping to reduce diagnostic errors and, most importantly, preventing the discharge of patients with potentially life-threatening conditions. In this context, the main diagnostic considerations include acute coronary syndrome (ACS), pericarditis, pulmonary thromboembolism (PTE), and acute aortic syndromes (AAS). POCUS has proven effective in all of these scenarios and can be widely applied with proper training, both by novice physicians and experienced echocardiographers. This article aims to discuss the key ways in which POCUS can specifically aid in the differential diagnosis of chest pain.

Introduction

The use of point-of-care ultrasound (POCUS) in emergency settings is now well established as an integral part of the initial assessment of critically ill patients. In cases of acute chest pain, POCUS has proven to be a valuable tool in differential diagnosis, helping reduce diagnostic errors and, most importantly, preventing the discharge of patients with potentially life-threatening conditions.[1,2] Among the main differential diagnoses in this scenario are acute coronary syndrome (ACS), pericarditis, pulmonary thromboembolism (PTE), and acute aortic syndromes (AAS).

a) ACS

The diagnosis of ACS is primarily based on clinical history, electrocardiography (ECG), and troponin levels. Although these tools are simple and widely used, the increasing adoption of POCUS raises questions about its potential to improve diagnostic accuracy, shorten time to diagnosis, assist in risk stratification, and detect complications associated with ACS.[1,2]

Following clinical assessment, patients with suspected ACS in the emergency department (ED) can be pragmatically classified into three groups:[1,2]

- Definitive or highly probable diagnosis of ACS (e.g., typical clinical presentation with ST-segment elevation and/or troponin elevation);
- Ruled-out diagnosis (e.g., low-suspicion presentation with normal ECG and troponin levels);
- Indeterminate diagnosis.

In confirmed cases, POCUS can be helpful in identifying complications in unstable patients, such as acute pulmonary edema or cardiogenic shock. When the diagnosis of ACS is ruled out, POCUS may assist in the differential diagnosis, such as AAS, pericarditis, or PTE.[1,2]

The indeterminate diagnosis group includes, for instance, patients with initially negative troponins but at intermediate risk for adverse events (e.g., a History, ECG, Age, Risk factors, Troponin [HEART] score between 4 and 6, or a 0/1-hour algorithm from the European Society of Cardiology [ESC] falling into the observation zone). In such cases, POCUS may reveal signs of poor prognosis and support the decision to conduct an earlier inpatient investigation. This group also includes patients presenting to the ED with a clinical or electrocardiographic presentation suggestive of acute coronary occlusion (ACO). If uncertainty remains, POCUS may help to increase or decrease the pretest probability of ACO.[1-3]

In recent years, there has been a growing recognition of the limitations of using ST-segment elevation as a dichotomous criterion to define ACO. Consequently, greater importance is being placed on clinical presentation and other ECG findings. In this context, POCUS emerges as a valuable complementary tool for detecting regional wall motion abnormalities (RWMA). As with ECG findings, echocardiographic findings should not be interpreted in a binary manner but rather as part of a broader process of clinical reasoning.[3]

A recent study evaluated whether the presence of RWMA on POCUS could predict obstructive coronary artery disease (CAD) in patients presenting to the ED with chest pain. Among the 657 participants with suspected ACS, approximately 11% showed RWMA. These findings were significantly more frequent in those who required

Keywords

Emergencies; Acute Coronary Syndrome; Pulmonary Embolism; Aortic Dissection

Mailing Address: Alexandre de Matos Soeiro •
Universidade de São Paulo, Instituto do Coração. Av. Dr Eneas de Carvalho Aguiar, 44. Postal code: 05403-000. São Paulo, SP – Brazil
E-mail: alexandre.soeiro@bol.com.br
Manuscript received May 25, 2025; revised May 29, 2025; accepted June 2, 2025
Editor responsible for the review: Marcelo Tavares

DOI: https://doi.org/10.36660/abcimg.20250045i

Central Illustration: Assessment of Acute Chest Pain in the Emergency Department: How Point-of-Care Ultrasound Can Assist the Cardiologist

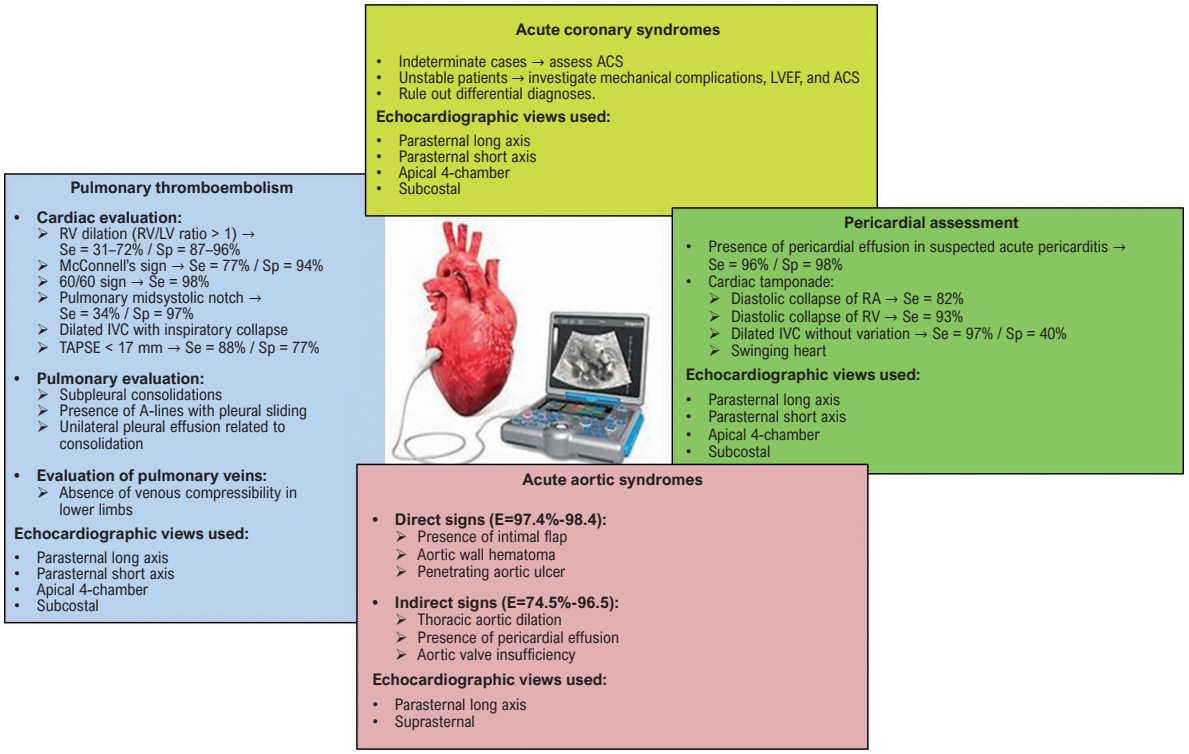

Arq Bras Cardiol: Imagem cardiovasc. 2025;38(3):e20250045

Use of POCUS in the differential diagnosis of acute chest pain. IVC: inferior vena cava; LVEF: left ventricular ejection fraction; LV: left ventricle; RA: right atrium; RV: right ventricle; RWMA: regional wall motion abnormality; Se: sensitivity; Sp: specificity; TAPSE: tricuspid annular plane systolic excursion.

revascularization (26.2% vs. 7.6%), with odds ratios ranging from 3.16 to 3.68 depending on the statistical adjustment. The analysis included all three risk groups of the ESC 0/1-hour algorithm (rule-in, observe, and rule-out), demonstrating that the presence or absence of RWMA influenced CAD risk across all categories. These findings reinforce that POCUS can help identify higher-risk patients, even without offering a definitive diagnosis. However, the accuracy of the method in detecting acute myocardial infarction (AMI) varies depending on the population studied.[4]

Another retrospective study examined whether the detection of RWMA on POCUS could accelerate the indication for revascularization in patients with possible ACO. The study included 234 patients presenting to the ED with chest pain and negative troponins, excluding those with ST-segment elevation. Among the 23 patients who underwent revascularization, 14 had RWMA on POCUS, which was performed on average 36 minutes before the first troponin result. The mean time to revascularization was 432 minutes in patients with RWMA, compared to 2,158 minutes in those without. Despite methodological limitations, the study suggests that POCUS may provide relevant information in less time than troponin testing.[5]

RWMA may represent either an acute coronary event or sequelae of prior events. Some studies on the topic choose to exclude patients with a history of AMI from their analyses. Although this distinction is not always possible based solely on clinical history, the presence of RWMA supports clinical reasoning and risk stratification by identifying patients with a higher likelihood of adverse outcomes. These patients should therefore be considered for hospital admission and further investigation, taking into account other factors that contribute to pretest probability.[4]

Several studies have investigated the value of POCUS performed by emergency physicians. A study published in 2020 compared trained emergency physicians with experienced echocardiographers, evaluating the accuracy of the former in detecting RWMA in patients with chest pain in the ED. A total of 89 patients were assessed, and the emergency physicians achieved a sensitivity of 76.9% and a specificity of 92.1%. The professionals evaluated were three in-hospital physicians with approximately 5 years of POCUS

experience who underwent a specific 3-hour training on RWMA detection conducted by a cardiologist.[6]

Another similar study compared RWMA assessments performed by emergency medicine residents with formally conducted echocardiograms in the context of ST-elevation AMI. The study included five first-year residents, three second-year residents, and one third-year resident, all of whom underwent video-based training focused on RWMA identification. These residents had prior experience with at least 25 cardiac POCUS exams and 150 general POCUS exams, although they had no specific training in RWMA detection before the study. A total of 75 patients were included, 62% of whom showed RWMA on formal echocardiography. POCUS performed by the residents achieved a sensitivity of 88% and a specificity of 92% compared to the gold standard used in the study (formal echocardiography or, in some cases, ventriculography).[7]

These studies highlight several important points. First, it appears feasible to train physicians who are not echocardiography specialists to assess RWMA using POCUS. However, the accuracy achieved by these professionals tends to be lower than that of experienced echocardiographers. Moreover, findings observed in studies using echocardiograms performed by specialists are likely not fully reproducible when POCUS is used by less experienced operators. The level of agreement, as well as the sensitivity and specificity of the exam, can vary significantly depending on the clinical context and the provider's level of training. Prospective studies incorporating POCUS into clinical decision-making may help clarify its true impact on the assessment of patients with chest pain.[6,7]

Finally, in unstable patients — such as those with acute pulmonary edema or cardiogenic shock — POCUS can aid in the differential diagnosis by enabling the assessment of biventricular function, volume status, and the identification of mechanical complications such as mitral regurgitation and/or pericardial effusion.[2]

b) Pericardial assessment

In the systematic evaluation of the heart using POCUS, visualization of the pericardium plays a key role in hemodynamic characterization and the differential diagnosis of chest pain.[8,9]

In particular, when managing pericardial effusions, POCUS offers healthcare professionals a fast, accurate, and bedside-available diagnostic tool. Its use enables not only precise estimation of effusion volume but also early detection of cardiac tamponade and appropriate guidance for interventions such as pericardiocentesis, significantly contributing to improved clinical outcomes.[8,9]

Under physiological conditions, the pericardial space contains approximately 15 to 50 mL of fluid, a volume that is generally undetectable by simpler ultrasound machines. A pericardial effusion is defined as the abnormal accumulation of fluid in this space, becoming more easily visualized on ultrasound examination.[8,9]

Among the differential diagnoses of chest pain, pericarditis accounts for approximately 5% of ED visits. Its clinical criteria include chest pain with features typical of pericardial involvement, suggestive ECG findings, presence of a pericardial friction rub, and evidence of pericardial effusion or an increase in the volume of a previously known effusion.[9]

Performing POCUS at the bedside facilitates the diagnosis of both pericarditis and pericardial effusion, as even small abnormal fluid collections in the pericardial space can be detected and considered diagnostic. The method has high accuracy, with sensitivity reaching up to 96% and specificity up to 98% when performed by adequately trained emergency physicians — not necessarily cardiologists.[10]

Pericardial effusion can be measured using several basic echocardiographic windows, such as parasternal long and short axes, apical four-chamber, and subcostal views. Based on the observed thickness of the fluid layer, the effusion can be classified as minimal, small, moderate, or large (Table 1).[10]

The presence of abnormal fluid in the pericardial space — its volume and rate of accumulation — may exert extrinsic compression on the cardiac chambers, directly affecting atrial and ventricular relaxation. This restriction depends not only on the absolute fluid volume but also on the pericardium's elasticity to accommodate it. In cases of rapid accumulation, even small volumes may significantly increase intrapericardial pressure. On the other hand, in cases of slow and progressive accumulation, the pericardium can adapt due to its distensibility, accommodating volumes exceeding 500 mL.[10]

The echocardiographic findings most commonly identified on POCUS in patients with cardiac tamponade include:[8-10]

b.1) Late diastolic collapse of the right atrium (RA)

Diastolic collapse of the RA is one of the most important and earliest echocardiographic signs of cardiac tamponade.[9] This phenomenon occurs during atrial relaxation, when RA volume is reduced and intrapericardial pressure peaks, causing the atrial wall to invaginate into the chamber. It is a highly sensitive finding, particularly when the collapse lasts for more than one-third of the cardiac cycle. However, its specificity is moderate (approximately 82%), as brief RA collapses can also occur in other conditions, such as elevated intrathoracic pressure. Nevertheless, sustained RA collapse is a strong indicator of cardiac tamponade. [9,10]

b.2) Diastolic collapse of the right ventricle (RV)

Diastolic collapse of the RV is typically observed during early diastole, when the chamber volume is still

Table 1 – Classification of pericardial effusion according to thickness and estimated fluid volume

Pericardial effusion measurement	Approximate fluid volume
< 5 mm	50–100 mL (minimal)
5–10 mm	100–250 mL (small)
10–20 mm	250–500 mL (moderate)
> 20 mm	> 500 mL (large)

reduced. Although its sensitivity is slightly lower than that of RA collapse (approximately 93%), this finding is highly specific for tamponade. It is important to note that in certain clinical scenarios—such as RV hypertrophy or elevated diastolic pressure in the RV (e.g., acute or chronic cor pulmonale)—this collapse may be absent even in the presence of tamponade.[9,10]

b.3) Dilated inferior vena cava (IVC) with minimal or absent respiratory variation

In cases of cardiac tamponade, the RA becomes unable to adequately accommodate venous return due to the compression caused by increased intrapericardial pressure. As a result, the IVC remains dilated, with minimal or absent respiratory variation. This finding has high sensitivity for cardiac tamponade (95–97%) and a high negative predictive value (NPV). However, its specificity is low (around 40%), as it can also be seen in other conditions such as chronic lung disease, heart failure, tricuspid regurgitation, and other cardiopathies.[9,10]

The IVC is typically visualized in a sagittal subcostal view, just below the xiphoid process. The diameter should be measured approximately 2 to 3 cm before its junction with the RA, near the confluence with the hepatic vein. In some cases, M-mode can be used to improve measurement accuracy. The IVC is considered abnormal when its diameter exceeds 2.1 cm and inspiratory variation is less than 50%.[9,10]

b.4) Swinging heart

This finding is characteristic of large pericardial effusions and refers to the pendular movement of the heart within the pericardial sac.

The integration of POCUS into routine clinical practice has been shown to improve diagnostic accuracy and enable timely interventions, optimizing care for patients with pericardial involvement. However, it is essential to recognize the limitations of this modality. The effectiveness of POCUS is highly dependent on the operator's experience and training, which can lead to variability in results. In addition, limited access to ultrasound equipment and trained personnel remains a significant barrier, particularly in resource-constrained settings.[9,10]

c) PTE

PTE is one of the leading causes of chest pain in ED s, accounting for 5% to 10% of cases. Without treatment, its mortality rate is approximately 30%, but this can be reduced to 3%–8% with early therapy.[1,11] Early diagnosis is essential but challenging. POCUS has proven to be a valuable bedside tool, allowing for rapid and integrated evaluation of cardiac, pulmonary, and vascular findings, with reported specificity as high as 96.7%.[12]

The ultrasound assessment of patients with suspected PTE should include three main regions: the heart, lungs, and deep venous system of the lower limbs. The combination of findings across these areas increases diagnostic accuracy and can support early therapeutic decisions, including the initiation of reperfusion therapy even in the absence of a pulmonary CT angiogram.

c.1) Cardiac assessment

In the context of PTE, cardiac POCUS aims to identify signs of acute RV strain and dysfunction. In the absence of such findings, the exam can help rule out PTE in hemodynamically unstable patients and assist in identifying alternative causes of instability, such as left ventricle (LV) dysfunction or valvular disease. The main echocardiographic findings associated with PTE include:

- RV dilation: RV/LV ratio > 1 in apical or subxiphoid views and/or end-diastolic diameter > 30 mm in the parasternal long-axis view. Sensitivity: 31%–72%; specificity: 87%–96%.[1,12]
- McConnell's sign: hypokinesia of the RV free wall with preserved apical motion. Sensitivity: 77%; specificity: 94%.[12]
- Interventricular septal flattening ("D-sign"): characterized by flattening of the septum toward the LV, predominantly during diastole, observed in the parasternal short-axis view.[1]
- 60/60 sign: pulmonary artery acceleration time (PAT) < 60 ms combined with tricuspid regurgitation gradient (TRG) < 60 mmHg. This pattern is suggestive of acute PTE, with sensitivity up to 98% when associated with RV overload (Figure 1).[12,13]
- Pulmonary midsystolic notch: a Doppler finding in the RV outflow tract, characterized by a pronounced notch after a sharp initial peak, followed by a dome-shaped waveform. Alerhand et al. reported 92% sensitivity and 99% specificity for massive or submassive PTE; for PTE in general, sensitivity was 34% and specificity 97%.[13]
- Dilated IVC with inspiratory collapse < 50%.[1]
- Tricuspid annular plane systolic excursion (TAPSE) < 17 mm, indicating RV systolic dysfunction. Sensitivity: 88%; specificity: 77%.[1,13]

c.2) Pulmonary assessment

Pulmonary POCUS can be performed using either a convex or linear transducer, scanning the intercostal spaces in the anterior, lateral, and posterior regions of the chest. The main findings suggestive of pulmonary infarction secondary to PTE include (Figure 2):

- Triangular subpleural consolidations (the most common, seen in approximately 85% of cases) or, less frequently, rounded or polygonal consolidations (3%).[1]
- Presence of A-lines associated with pleural sliding.
- Pleural effusion, usually unilateral and associated with the area of consolidation.[1]

When combined with cardiac findings and evidence of deep vein thrombosis (DVT), these ultrasound patterns

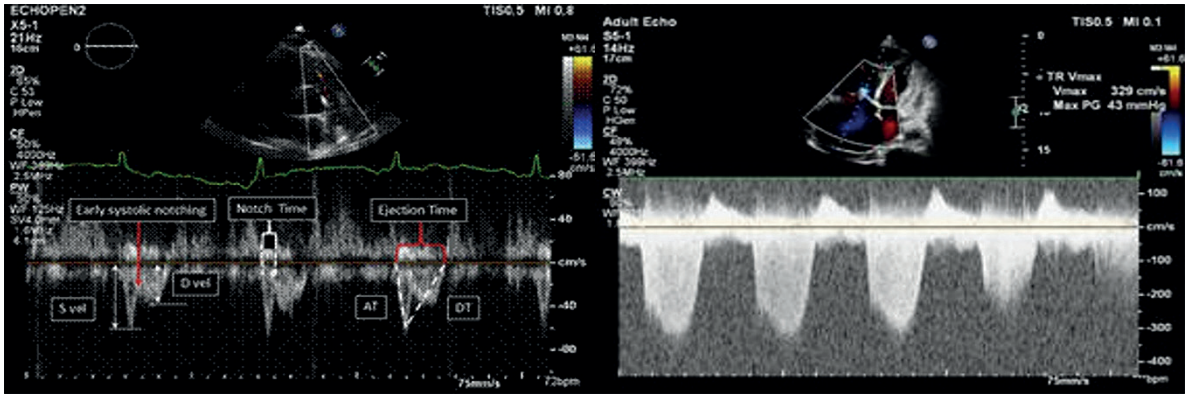

Figure 1 – *Doppler showing pulmonary midsystolic notch and 60/60 sign (reduced PAT and TRG). TRG: tricuspid regurgitation gradient; PAT: pulmonary artery acceleration time.*

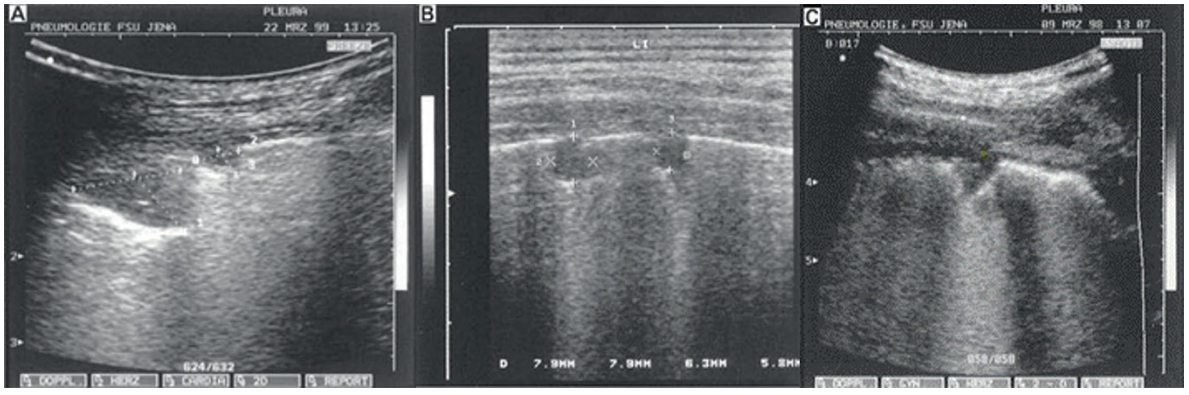

Figure 2 – *Pulmonary consolidations: A – triangular; B – rounded; C – polygonal with adjacent pleural effusion.*

significantly increase clinical suspicion for PTE, with specificity reaching up to 99%.[13]

c.3) Deep vein assessment

Ultrasound evaluation of the deep venous system of the lower limbs is a key component of the POCUS protocol in patients with suspected PTE. The absence of venous compressibility is highly suggestive of DVT. When identified in patients with compatible clinical signs or in those with suggestive cardiac and pulmonary POCUS findings, it may justify the immediate initiation of anticoagulant therapy.[1]

The multi-organ POCUS approach allows for the integration of both direct and indirect signs of PTE, providing a rapid assessment with high sensitivity and specificity.[8] The simultaneous presence of RV dysfunction, pulmonary consolidations, and DVT carries high predictive value. Recent studies highlight the growing role of POCUS, especially in emergency settings and resource-limited environments. In addition, POCUS enables the exclusion of other critical differential diagnoses, such as pneumothorax, cardiac tamponade, and aortic dissection. Thus, POCUS is increasingly recognized as an essential tool in the evaluation of patients with chest pain and suspected PTE — particularly when pulmonary CT angiography is not available.[1]

d) Aortic assessment

AAS should always be considered key differential diagnoses in the evaluation of chest pain in emergency settings. As with other conditions discussed, visualization of the ascending aorta should be part of the initial POCUS assessment, forming an integral part of the diagnostic algorithm for patients presenting with chest pain.[14,15]

The ADvISED study (Diagnostic Accuracy of the Aortic Dissection Detection Risk Score Plus D-Dimer for Acute Aortic Syndromes), which evaluated patients with chest pain in the ED, applied a protocol combining the Aortic Dissection

Detection Risk Score (ADD-RS) with D-dimer testing. The results demonstrated a negative predictive value (NPV) of 99.7% for ruling out AAS, although the specificity of the model alone was limited (57.3%) for positive diagnosis.[16]

A subanalysis of that study incorporated POCUS into the algorithm and showed that the presence of direct signs of AAS raised the diagnostic specificity to 97.4%. Even indirect signs performed well, with specificity of 74.5%. The inclusion of POCUS increased the NPV to 100% and improved overall diagnostic accuracy, with the area under the curve (AUC) rising from 0.77 to 0.88.[17]

The PROFUNDUS study, conducted prospectively with over 1,900 patients, also evaluated the use of POCUS combined with D-dimer for AAS investigation in emergency settings. In that study, the presence of direct signs on POCUS showed 98.4% specificity for diagnosing AAS, while indirect signs reached specificity between 88% and 96.5%. As with ADvISED, the combined use of POCUS and D-dimer achieved an NPV of 100%.[18]

In clinical practice, the key question becomes: "Which echocardiographic views should be used, and what findings should be sought?" The preferred views include:

- Parasternal long-axis view: allows assessment of the LV outflow tract and ascending aorta;
- Suprasternal view (at the suprasternal notch): provides visualization of the aortic arch and descending thoracic aorta.[14,15]

During the evaluation, physicians should actively search for direct and indirect signs of AAS, as outlined below:

Direct signs:

- Presence of an intimal flap (dissection of the tunica intima);
- Aortic wall hematoma;
- Penetrating aortic ulcer.

Indirect signs:

- Aortic dilation;
- Pericardial effusion;
- Aortic valve insufficiency.

Author Contributions

Conception and design of the research, analysis and interpretation of the data and critical revision of the manuscript for intellectual content: Soeiro AM; acquisition of data and writing of the manuscript: Soeiro AM, Leal TCAT, Oliveira LLH, Moraes RF.

Potential Conflict of Interest

No potential conflict of interest relevant to this article was reported.

Sources of Funding

There were no external funding sources for this study.

Study Association

This study is not associated with any thesis or dissertation work.

Ethics Approval and Consent to Participate

This article does not contain any studies with human participants or animals performed by any of the authors.

Use of Artificial Intelligence

The authors did not use any artificial intelligence tools in the development of this work.

Availability of Research Data

The underlying content of the research text is contained within the manuscript.

References

1. Ha YR, Toh HC. Clinically Integrated Multi-Organ Point-Of-Care Ultrasound for Undifferentiated Respiratory Difficulty, Chest Pain, or Shock: A Critical Analytic Review. J Intensive Care. 2016;4:54. doi: 10.1186/s40560-016-0172-1.
2. Byrne RA, Rossello X, Coughlan JJ, Barbato E, Berry C, Chieffo A, et al. 2023 ESC Guidelines for the Management of Acute Coronary Syndromes. Eur Heart J. 2023;44(38):3720-826. doi: 10.1093/eurheartj/ehad191.
3. McLaren J, Alencar JN, Aslanger EK, Meyers HP, Smith SW. From ST-Segment Elevation MI to Occlusion MI: The New Paradigm Shift in Acute Myocardial Infarction. JACC Adv. 2024;3(11):101314. doi: 10.1016/j.jacadv.2024.101314.
4. Xu C, Melendez A, Nguyen T, Ellenberg J, Anand A, Delgado J, et al. Point-of-Care Ultrasound May Expedite Diagnosis and Revascularization of Occult Occlusive Myocardial Infarction. Am J Emerg Med. 2022;58:186-91. doi: 10.1016/j.ajem.2022.06.010.
5. Roggel A, Jehn S, Dykun I, Balcer B, Al-Rashid F, Totzeck M, et al. Regional Wall Motion Abnormalities on Focused Transthoracic Echocardiography in Patients Presenting with Acute Chest Pain: A Predefined Post Hoc Analysis of the Prospective Single-Centre Observational EPIC-ACS study. BMJ Open. 2024;14(9):e085677. doi: 10.1136/bmjopen-2024-085677.
6. Croft PE, Strout TD, Kring RM, Director L, Vasaiwala SC, Mackenzie DC. WAMAMI: Emergency Physicians Can Accurately Identify Wall Motion Abnormalities in Acute Myocardial Infarction. Am J Emerg Med. 2019;37(12):2224-8. doi: 10.1016/j.ajem.2019.03.037.
7. Sağlam C, Ünlüer EE, Yamanoğlu NGÇ, Kara PH, Ediboğlu E, Bektaşlı R, et al. Accuracy of Emergency Physicians for Detection of Regional Wall Motion Abnormalities in Patients with Chest Pain Without ST-Elevation Myocardial Infarction. J Ultrasound Med. 2021;40(7):1335-42. doi: 10.1002/jum.15513.

8. Mandavia DP, Hoffner RJ, Mahaney K, Henderson SO. Bedside Echocardiography by Emergency Physicians. Ann Emerg Med. 2001;38(4):377-82. doi: 10.1067/mem.2001.118224.

9. Imazio M, De Ferrari GM. Cardiac Tamponade: An Educational Review. Eur Heart J Acute Cardiovasc Care. 2021;10(1):102-9. doi: 10.1177/2048872620939341.

10. Chiabrando JG, Bonaventura A, Vecchié A, Wohlford GF, Mauro AG, Jordan JH, et al. Management of Acute and Recurrent Pericarditis: JACC State-of-the-Art Review. J Am Coll Cardiol. 2020;75(1):76-92. doi: 10.1016/j.jacc.2019.11.021.

11. Konstantinides SV, Meyer G, Becattini C, Bueno H, Geersing GJ, Harjola VP, et al. 2019 ESC Guidelines for the Diagnosis and Management of Acute Pulmonary Embolism Developed in Collaboration with the European Respiratory Society (ERS). Eur Heart J. 2020;41(4):543-603. doi: 10.1093/eurheartj/ehz405.

12. Daley JI, Dwyer KH, Grunwald Z, Shaw DL, Stone MB, Schick A, et al. Increased Sensitivity of Focused Cardiac Ultrasound for Pulmonary Embolism in Emergency Department Patients with Abnormal Vital Signs. Acad Emerg Med. 2019;26(11):1211-20. doi: 10.1111/acem.13774.

13. Albricker ACL, Freire CMV, Santos SND, Alcantara ML, Saleh MH, Cantisano AL, et al. Joint Guideline on Venous Thromboembolism - 2022. Arq Bras Cardiol. 2022;118(4):797-857. doi: 10.36660/abc.20220213.

14. Bernett J, Strony R. Diagnosing Acute Aortic Dissection with Aneurysmal Degeneration with Point of Care Ultrasound. Am J Emerg Med. 2017;35(9):1384.e3-1384.e4. doi: 10.1016/j.ajem.2017.05.052.

15. Lee PY, Saad K, Hossain A, Lieu I, Allencherril J. Initial Evaluation and Management of Patients Presenting with Acute Chest Pain in the Emergency Department. Curr Cardiol Rep. 2023;25(12):1677-86. doi: 10.1007/s11886-023-01984-6.

16. Nazerian P, Mueller C, Soeiro AM, Leidel BA, Salvadeo SAT, Giachino F, et al. Diagnostic Accuracy of the Aortic Dissection Detection Risk Score Plus D-Dimer for Acute Aortic Syndromes: The ADvISED Prospective Multicenter Study. Circulation. 2018;137(3):250-8. doi: 10.1161/CIRCULATIONAHA.117.029457.

17. Nazerian P, Mueller C, Vanni S, Soeiro AM, Leidel BA, Cerini G, et al. Integration of Transthoracic Focused Cardiac Ultrasound in the Diagnostic Algorithm for Suspected Acute Aortic Syndromes. Eur Heart J. 2019;40(24):1952-60. doi: 10.1093/eurheartj/ehz207.

18. Morello F, Bima P, Castelli M, Capretti E, Soeiro AM, Cipriano A, et al. Diagnosis of Acute Aortic Syndromes with Ultrasound and D-Dimer: The PROFUNDUS Study. Eur J Intern Med. 2024;128:94-103. doi: 10.1016/j.ejim.2024.05.029.

Convolutional Neural Network Applications In Cardiac Imaging

Luiz Henrique Cartaxo Fernandes,[1] José Lucas Formiga Dantas,[1] Marilia Graziela Vieira de Macena Lima,[1] Glaudir Donato,[1] Marcelo Dantas Tavares de Melo[2]

Centro de Ciências Médicas, Universidade Federal da Paraíba,[1] João Pessoa, PB – Brasil

Departamento de Medicina Interna, Universidade Federal da Paraíba,[2] João Pessoa, PB – Brasil

Central Illustration: Convolutional Neural Network Applications In Cardiac Imaging

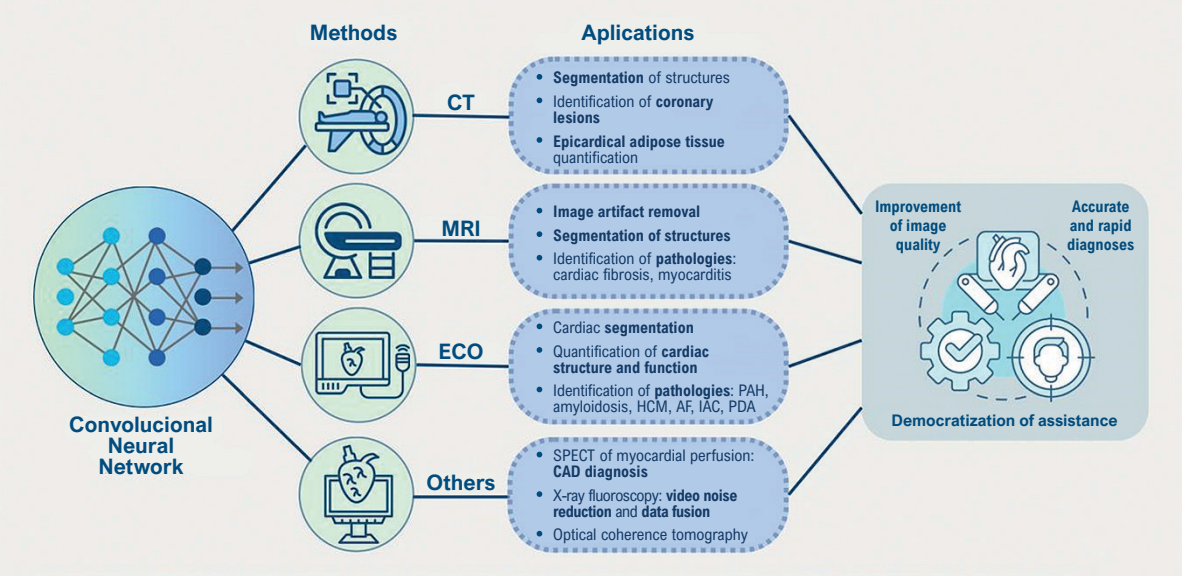

Arq Bras Cardiol: Imagem cardiovasc. 2025;38(3):e20250058

Applications of Convolutional Neural Networks in different types of diagnostic imaging methods in cardiology. AF: Atrial Fibrilation; CAD: Coronary artery disease; CT: Computed Tomography; ECO: Echocardiography; HCM: Hypertrophic Cardiomyopathy; IAC: Interatrial Communication; MRI: Magnetic Imaging Resonance; OCT: Optical Coherence Tomography; PAH: Pulmonary Arterial Hypertension; PDA: Patent Ductus Arteriosus; SPECT-MPI: Single Photon Emission Computed Tomography – Myocardial Perfusion Imaging.

Abstract

Neural networks are computer models that mimic the workings of the human brain, learning from large volumes of data to perform increasingly complex tasks. This is done by means of interconnected artificial neurons that propagate information from raw layers to refined layers, sometimes of a weighted nature, weaving in the classification or identification of non-linear patterns. The Convolutional Neural Network (CNN) is a specialized deep learning architecture designed to extract and analyze spatial patterns within images, enabling applications in diagnostic decision-making and longitudinal clinical monitoring. Its use in Computed Tomography and Magnetic Resonance Imaging through cardiac image segmentation makes it possible to quickly and efficiently define cardiac structures, playing an important role in the reconstruction of three-dimensional images and in supporting preoperative procedures. In addition, compared to other forms of conventional analysis, it guarantees objective interpretations and superior image quality, based on the removal of artifacts from the studied segment. Echocardiograms have shown good results in identifying pathologies such as pulmonary hypertension, amyloidosis, hypertrophic cardiomyopathy

Keywords

Computer Neural Networks; Artificial Intelligence; Cardiac Imaging Techniques

Mailing Address: Luiz Henrique Cartaxo Fernandes •
Universidade Federal da Paraíba – Centro de Ciências Médicas. Cidade Universitária, s/n – Conj. Pres. Castelo Branco III. Postal Code: 58051-900. João Pessoa, PB – Brazil
E-mail: luiz.cartaxo@academico.ufpb.br
Manuscript received August 13, 2025; revised August 29, 2025; accepted August 29, 2025
Editor responsible for the review: Marcelo Tavares

DOI: https://doi.org/10.36660/abcimg.20250058i

SUMÁRIO

and congenital diseases, and studies on the automation of these exams have shown an opening for what could be a dissemination framework in more remote areas where manual operators are not available. Consequently, CNN-based approaches have the potential to streamline cardiovascular imaging workflows, minimize inter-observer variability, and expand diagnostic capabilities to underserved and remote regions with limited access to specialized care.

Introduction

The human nervous system is one of the most efficient ways of capturing and interpreting data, reflecting the stimuli and experiences to which the body is subjected throughout life.[1] According to the phenomenon of neuroplasticity, all these interactions dictate brain modifications, being adapted for decision-making and allowing pre-existing knowledge to be learned and act as a basis for the creation of new information circuits.[2]

Neural networks have emerged as artificial models that try to recover this processing quickly and effectively in order to solve the problems raised, becoming important tools in the dynamic field of artificial intelligence (AI).[3] In order to overcome this challenge, networks are trained to identify recognition patterns from thousands or millions of examples, making it possible to build the system's own learning.[4] This happens through what is called "input", i.e. any new concept that is inserted into the ordering. The set of inputs generates a response, the "output", which can be influenced in a weighted way, always taking a reference standard as its essence.[5]

This can be exemplified simply: in the assessment of a patient with suspected atrial fibrillation (AF), when an electrocardiogram is requested for investigation, each voltage in the tracing can take on the role of an input neuron, which can continue to influence the cascade and serve as a new input for the next neuron, solidifying the final response.[6] Thus, if the diagnosis is AF when there is no corresponding tracing, the weights that led to that result are reduced. On the other hand, if there is a match, they are strengthened and reused in subsequent analyses.[7] In addition, extra notions can be added, such as the patient's age, gender and comorbidities.

The application of AI in the medical field has been widely explored and, in recent years, has become a disruptive technology for interpreting images.[8] Within this context, the Convolutional Neural Network (CNN) has emerged as a version of this processing aimed at recognizing and classifying images, reducing the computational effort and improving its robustness.[8] The hierarchical arrangement of multiple convolutional layers allows CNNs to progressively transform low-level features – such as pixel intensity gradientes – into increasingly abstract and clinically relevant representations.[9] During the training period, the CNN exercises and individualizes its filters according to the task to be performed. In a way, image classification starts by detecting the edges of coarser pixels in the initial layer, using this to detect simple shapes in the second layer and so on, allowing more complex features to be distinguished. Finally, the last layer is responsible for advanced image reading, based on the filters built.[10]

The advantages of CNN over other neural networks is that it establishes the vital resources for successful prediction, reducing the dimensionality of the resources in the previous layer.[11]

Accurate segmentation of cardiac images is essential for clinical decision making, and Deep Learning techniques and the use of CNN have shown remarkable results in this area, although their quantification and analysis remains an ongoing challenge due to the complexity of cardiac substructures and existing anatomical variability. The individualization of this analysis is essential to solidify objective evidence of the most varied pathologies investigated, facilitating diagnosis, monitoring and clinical follow-up of the patient.[12]

In this approach, through the image segmentation method, the convolutional neural network enables fast and efficient responses. This is because in certain situations, the presence of certain features is more important than others. Sometimes recognizing the location of an alteration in the heart chamber is the only essential objective, and it is not necessary to see these structures with high pixel definition.[13]

The application scenario covers a wide range of imaging exams, from use in echocardiography to calculate end-systolic and end-diastolic volume, through to the ability to assess the ventricular or atrial space in multiple slices, as well as the observation of coronary calcification plaques through CT-guided coronary angiography (CCTA). The range of applications of CNNs in cardiac imaging is highlighted in the Central Illustration. For the most part, these aspects are supported by figures and engravings from atlases or other documents that are included in the model's database. Another interesting point is that there are already studies using the system itself to weave in and ensure the quality of ultrasounds and other tests made available.[5]

Applications of CNN in CT

The use of convolutional neural networks has excelled in automating the segmentation of cardiac and vascular structures in computed tomography (CT) images, a process by which cardiac structures or pathological lesions are delimited.[5,12,13] The segmentation of cardiac images by CT has clinical relevance in the identification of valvular heart disease, evaluation of coronary artery disease, diagnosis of congenital heart disease, preoperative planning and in extracardiac indications.[12] The application of CNNs has brought speed and efficiency to the cardiac segmentation process, since it was previously carried out manually and subjectively by radiologists. In a study of the segmentation of cardiac chambers and great vessels, Sharkey et al. presented results indicating that the variability of analysis between observers is similar to the variability between the observer and the CNN.[14] These findings support the premise that CNN-based segmentation can deliver reproducible, objective, and diagnostically accurate results, comparable to expert manual assessment.

With regard to the identification of anatomical structures, Chen, et al. showed that the convolutional neural network proved to be an accurate and efficient tool for assessing the volume and three-dimensional reconstruction of the left atrium.[15] The calculation of volume by CNN proved to be

capable of predicting the risk of recurrence of atrial fibrillation in patients after catheter ablation. Astudillo, et al. used a CNN technique to identify the coronary cusps and the right and left coronary ostia on multi-detector row computed tomography.[16] These structures are important reference points for defining the perimeter and area of the aortic annulus and, consequently, the aortic valve prostheses to be implanted by transcatheter means. The method proved to be reproducible and reliable, and could be applied in routine preoperative planning in order to reduce time spent and accuracy in defining reference points.

CNNs have also proved to be excellent tools for identifying pathological images in coronary angiography. Coronary computed tomography angiography is an important method for assessing the severity of arterial stenosis, as well as being highly accurate in quantifying atherosclerosis when compared to intravascular ultrasound. In a multicenter study, a neural network was trained to segment coronary plaques.[17] The study showed excellent agreement between the Deep Learning tool and the measurements of experienced readers regarding the volume of the atheroma plaque and the degree of arterial stenosis. There was also agreement with vascular ultrasound measurements, as well as prognostic value in terms of the risk of future acute myocardial infarction.

Quantification of epicardial adipose tissue can also be optimized through the use of CNNs. Epicardial adipose tissue is a metabolically active depot of visceral fat and may be related to visceral obesity and metabolic syndrome.[18] Coronary angiography is the gold standard for identifying epicardial adipose tissue, but its manual quantification is laborious and challenging. In this scenario, West et al. developed a CNN to automatically quantify epicardial adipose tissue and identify its clinical association with cardiac and non-cardiac diseases.[19] The method proved to be accurate, fast and reproducible for quantifying epicardial adiposity using coronary angiography. The tool was also able to show good prognostic value for mortality in general and for cardiovascular events.

Applications of CNN in MRI

In recent years, magnetic resonance imaging has become an excellent tool for investigating cardiovascular diseases, with a high capacity to provide complex diagnoses.[20,21] It is a non-invasive, versatile method free of ionizing radiation, capable of identifying structure, function, flow and characterization of cardiac tissue. Late gadolinium enhancement and T1/T2 mapping have added important information about cardiac viability and pathologies such as tissue infarction and diffuse myocardial fibrosis. The development of flow MRI has also brought major advances by providing blood flow information in several planes, which allows the identification of intracardiac shunts.[20] However, the lengthy scanning process and slow image production are disadvantages of MRI. MRI images must take cardiac and respiratory movement into account to avoid artifacts, which must be suppressed by reconstruction algorithms. In this scenario, Deep learning–based reconstruction methods have demonstrated superior performance compared with conventional algorithms, yielding higher-fidelity images, enhanced artifact suppression, and substantially reduced processing times.

Hauptmann, et al. trained a three-dimensional residual CNN in U-Net to remove spatio-temporal artifacts in subsampling real-time MRI data from images of patients with congenital heart disease.[22] Artifact removal by the CNN was compared with the conventional compression sensing technique, a tool that requires intense and time-consuming computational reconstruction. The CNN-based method achieved artifact suppression over five times faster than the compressed sensing approach, while delivering superior image quality and more accurate ventricular volumetric measurements. El-Rewaidy et al. also presented important results on the reconstruction of MRI images with delayed gadolinium enhancement using a convolutional neural network.[23] Compared to the compression sensing technique, image reconstruction using CNN was 300 times faster.

CNNs have influenced multiple stages of the MRI workflow, from image acquisition planning and real-time reconstruction to post-processing tasks such as quantitative analysis and prognostic modeling. Like CT, MRI also plays an important role in the segmentation and consequent identification of cardiac structures.[24] In this process using MRI, the use of CNNs has also been related to greater efficiency.[25] Sander et al. used a CNN to perform the segmentation of cardiac structures and another auxiliary CNN to automatically identify areas of segmentation failure.[26] The study showed that cardiac image segmentation using CNNs associated with the manual correction of detected segmentation failures resulted in increased performance.

In terms of disease identification, many studies have used conventional image indices as input data for neural networks to diagnose heart disease. For example, cardiac scarring identified on magnetic resonance imaging is associated with unfavorable cardiovascular outcomes. Bekheet, et al., developed a CNN called FibrosisNet to diagnose cardiac fibrosis on MRI, showing high diagnostic accuracy and precision.[27] Sharifrazi et al., obtained important results by combining a deep convolutional neural network with the K-means clustering technique, forming CNN-KCL, to diagnose and classify myocarditis based on MRI image data.[28] The technique using CNN outperformed other traditional Machine Learning algorithms in classifying myocarditis in terms of accuracy and precision.

Applications of CNN in echocardiography

Echocardiography is the most easily accessible and widely used imaging method for assessing cardiac structure and function. Its advantages include rapid image acquisition and the absence of ionizing radiation, which make it an efficient and democratic method. Echocardiography can be used both to screen asymptomatic patients and to diagnose and follow up cardiac conditions.[29,30] As it is an operator-dependent test, it requires a certain degree of experience on the part of the professional, and there can be variations in interpretation.[29,31]

When it comes to applying automated image interpretation to echocardiography, there are some intrinsic challenges to this method. The echocardiogram consists of generating both static images, as well as videos and

Doppler recordings collected from different points of view to obtain the desired parameters. In addition, the values obtained in the measurements can vary greatly due to the intrinsic variability of heartbeats. There is also the variation that already exists when extrapolating measurements from two-dimensional images to measurements of the three-dimensional object.[32,33]

Despite these impasses and given the complexity of the diagnostic method in question, an automated learning approach would bring many benefits and assist human interpretation, as it would allow automatic identification and classification of views. In fact, the use of Deep Learning (DL), and more specifically Convolutional Neural Networks (CNNs), to train artificial intelligence in the interpretation of echocardiograms would make it possible to reduce costs and, consequently, democratize this test. This technological integration could enable echocardiographic acquisition by operators with limited specialized training, thereby facilitating access to cardiac imaging in geographically remote or resource-limited settings.[32]

Several studies have shown the effectiveness of using CNNs in echocardiography. Among the applications observed, the majority are for quantifying the structure and function of the heart and for cardiac segmentation.[10,29,34-38] It has also been used in the detection of left ventricular hypertrophy,[39-41] aortic stenosis,[42,43] identification of cardiac phases,[44] early detection of acute myocardial infarction[45] and classification of cardiac visualizations.[46,47] The model used by Ghorbani et al, in addition to accurately identifying elements of cardiac structure and function, trained a CNN to predict systemic phenotypes that modify cardiovascular risk, such as age, gender, height and weight, from echocardiogram images.[29]

Zhang et al went further and trained a convolutional neural network for fully automated interpretation of echocardiograms, including visualization identification, image segmentation, quantification of heart structure and function, and disease detection. This study demonstrated success in the automated analysis of view type and image segmentation. With regard to the structure and function of the heart, there was some discrepancy between manual and automated measurements, especially of the structure, with a tendency to overestimate the values. Finally, the model was successful in identifying pulmonary arterial hypertension (PAH), amyloidosis and hypertrophic cardiomyopathy, based on analysis of the masses, structure and function of the heart chambers.[32]

Recent studies have also evaluated the capacity for automatic diagnosis of pulmonary arterial hypertension and,[48] according to the results obtained by DuBrock et al,[49] the algorithm used is capable of speeding up the diagnosis of PAH by 6 to 18 months, an extremely relevant aspect in a disease where early diagnosis is crucial for effective control of the condition.[48,49]

Another described pathology that can be identified by echocardiography using CNNs is occult atrial fibrillation (AF). Yuan et al developed a model that was able to distinguish between sinus rhythm and AF, as well as predicting the concomitant presence of paroxysmal AF in those with sinus rhythm. The model performed better than using clinical risk factors, transthoracic echocardiogram measurements, left atrial size or CHA_2DS_2VASc score.[50] Research using DL has also been carried out and obtained favorable results in the area of fetal and neonatal echocardiography, such as for the prenatal diagnosis of atrial septal defect[51] and for the identification of patent ductus arteriosus in neonates.[52]

Application of CNN in other methods

Single Photon Emission Computed Tomography (SPECT) of myocardial perfusion is a test that can identify the presence of myocardial ischemia and therefore coronary artery disease. Betancur et al analyzed the application of deep learning to this diagnostic method, aiming to verify the ability to automatically predict coronary disease through CNNs trained with myocardial perfusion images, compared to the usual method currently used. The result was greater efficacy and better detection sensitivity with the deep learning method.[53] Other studies have also evaluated the ability to automatically classify myocardial perfusion images. Papadrianos et al trained CNNs to identify three possible outputs - infarction, ischemia and normal perfusion - and all models evaluated presented positive and reliable results.[54] Su et al demonstrated the feasibility and accuracy of CNN-based diagnosis for CAD, with a system that is already used in practice and is capable of considerably reducing the time needed to interpret images.[55]

X-ray fluoroscopy allows real-time visualization of the cardiac structure, which makes it an indispensable method for performing image-guided procedures, such as cardiac resynchronization therapy, angiography and endovascular aortic repair. Deep learning has also been successfully tested to aid these procedures, either by reducing video noise or by fusing preoperative data with intraoperative x-ray images in order to guide the intervention and reduce contrast exposure.[56-59] Studies have also shown better sensitivity and specificity in characterizing coronary lesions using optical coherence tomography when deep learning is applied.[60-62]

Conclusion

The application of CNN in cardiac image analysis has emerged as a versatile tool, contributing to accurate and rapid diagnoses. Its incorporation into cardiovascular imaging makes it possible to remove the bias of inter-observer variability, reduce image artifacts, improve the automation of measurements and, finally, overcome geographical barriers by allowing the evaluation of images acquired remotely and thus democratizing care. Future perspectives should focus on large-scale validation studies to confirm the generalizability and clinical robustness of CNN-based approaches across diverse patient populations and imaging protocols. Furthermore, integrating these algorithms into routine workflows will require addressing regulatory and interoperability challenges to ensure safe and effective adoption in real-world cardiovascular practice.

Author Contributions

Conception and design of the research: Melo MDT. Acquisition of data: Fernandes LHC, Dantas JLF, Lima MGVM. Analysis and interpretation of the data: Fernandes LHC, Dantas JLF, Lima MGVM, Donato G. Writing of the manuscript: Fernandes LHC, Dantas JLF, Lima MGVM. Critical revision of the manuscript for intellectual content: Donato G, Melo MDT.

Potential conflict of interest

No potential conflict of interest relevant to this article was reported.

Sources of funding

There were no external funding sources for this study.

Study association

This study is not associated with any thesis or dissertation work.

Ethics approval and consent to participate

This article does not contain any studies with human participants or animals performed by any of the authors.

Use of Artificial Intelligence

The authors did not use any artificial intelligence tools in the development of this work.

Data Availability

The underlying content of the research text is contained within the manuscript.

References

1. Rotta NT, Ohlweiler L, Riesgo RS. Transtornos da Aprendizagem. Porto Alegre: Artmed; 2015.
2. Costa RLS. Neuroscience and Learning. Rev Bras Educ. 2023;28:e280010. doi: 10.1590/S1413-24782023280010.
3. Kriegeskorte N, Golan T. Neural Network Models and Deep Learning. Curr Biol. 2019;29(7):R231-6. doi: 10.1016/j.cub.2019.02.034.
4. Krittanawong C, Zhang H, Wang Z, Aydar M, Kitai T. Artificial Intelligence in Precision Cardiovascular Medicine. J Am Coll Cardiol. 2017;69(21):2657-64. doi: 10.1016/j.jacc.2017.03.571.
5. Litjens G, Ciompi F, Wolterink JM, de Vos BD, Leiner T, Teuwen J, et al. State-of-the-Art Deep Learning in Cardiovascular Image Analysis. JACC Cardiovasc Imaging. 2019;12(8 Pt 1):1549-65. doi: 10.1016/j.jcmg.2019.06.009.
6. Krittanawong C, Johnson KW, Rosenson RS, Wang Z, Aydar M, Baber U, et al. Deep Learning for Cardiovascular Medicine: A Practical Primer. Eur Heart J. 2019;40(25):2058-73. doi: 10.1093/eurheartj/ehz056.
7. El-Taraboulsi J, Cabrera CP, Roney C, Aung N. Deep Neural Network Architectures for Cardiac Image Segmentation. Artif Intell Life Sci. 2023;4:100083. doi: 10.1016/j.ailsci.2023.100083.
8. Johnson KW, Soto JT, Glicksberg BS, Shameer K, Miotto R, Ali M, et al. Artificial Intelligence in Cardiology. J Am Coll Cardiol. 2018;71(23):2668-79. doi: 10.1016/j.jacc.2018.03.521.
9. Bizopoulos P, Koutsouris D. Deep Learning in Cardiology. IEEE Rev Biomed Eng. 2019;12:168-93. doi: 10.1109/RBME.2018.2885714.
10. Lau ES, Di Achille P, Kopparapu K, Andrews CT, Singh P, Reeder C, et al. Deep Learning-Enabled Assessment of Left Heart Structure and Function Predicts Cardiovascular Outcomes. J Am Coll Cardiol. 2023;82(20):1936-48. doi: 10.1016/j.jacc.2023.09.800.
11. Wang P, Qiao J, Liu N. An Improved Convolutional Neural Network-Based Scene Image Recognition Method. Comput Intell Neurosci. 2022;2022:3464984. doi: 10.1155/2022/3464984.
12. Alnasser TN, Abdulaal L, Maiter A, Sharkey M, Dwivedi K, Salehi M, et al. Advancements in Cardiac Structures Segmentation: A Comprehensive Systematic Review of Deep Learning in CT Imaging. Front Cardiovasc Med. 2024;11:1323461. doi: 10.3389/fcvm.2024.1323461.
13. Lüscher TF, Wenzl FA, D'Ascenzo F, Friedman PA, Antoniades C. Artificial Intelligence in Cardiovascular Medicine: Clinical Applications. Eur Heart J. 2024;45(40):4291-304. doi: 10.1093/eurheartj/ehae465.
14. Sharkey MJ, Taylor JC, Alabed S, Dwivedi K, Karunasaagarar K, Johns CS, et al. Fully Automatic Cardiac Four Chamber and Great Vessel Segmentation on CT Pulmonary Angiography Using Deep Learning. Front Cardiovasc Med. 2022;9:983859. doi: 10.3389/fcvm.2022.983859.
15. Chen HH, Liu CM, Chang SL, Chang PY, Chen WS, Pan YM, et al. Automated Extraction of Left Atrial Volumes from Two-Dimensional Computer Tomography Images Using a Deep Learning Technique. Int J Cardiol. 2020;316:272-8. doi: 10.1016/j.ijcard.2020.03.075.
16. Astudillo P, Mortier P, Bosmans J, De Backer O, Jaegere P, Iannaccone F, et al. Automatic Detection of the Aortic Annular Plane and Coronary Ostia from Multidetector Computed Tomography. J Interv Cardiol. 2020;2020:9843275. doi: 10.1155/2020/9843275.
17. Lin A, Park C. HHS Public Access international multicentre study. 2022;4(4):10–1.
18. Oikonomou EK, Antoniades C. The Role of Adipose Tissue in Cardiovascular Health and Disease. Nat Rev Cardiol. 2019;16(2):83-99. doi: 10.1038/s41569-018-0097-6.
19. West HW, Siddique M, Williams MC, Volpe L, Desai R, Lyasheva M, et al. Deep-Learning for Epicardial Adipose Tissue Assessment with Computed Tomography: Implications for Cardiovascular Risk Prediction. JACC Cardiovasc Imaging. 2023;16(6):800-16. doi: 10.1016/j.jcmg.2022.11.018.
20. Oscanoa JA, Middione MJ, Alkan C, Yurt M, Loecher M, Vasanawala SS, et al. Deep Learning-Based Reconstruction for Cardiac MRI: A Review. Bioengineering. 2023;10(3):334. doi: 10.3390/bioengineering10030334.
21. Argentiero A, Muscogiuri G, Rabbat MG, Martini C, Soldato N, Basile P, et al. The Applications of Artificial Intelligence in Cardiovascular Magnetic Resonance-A Comprehensive Review. J Clin Med. 2022;11(10):2866. doi: 10.3390/jcm11102866.
22. Hauptmann A, Arridge S, Lucka F, Muthurangu V, Steeden JA. Real-Time Cardiovascular MR with Spatio-Temporal Artifact Suppression Using Deep Learning-Proof of Concept in Congenital Heart Disease. Magn Reson Med. 2019;81(2):1143-56. doi: 10.1002/mrm.27480.
23. El-Rewaidy H, Neisius U, Mancio J, Kucukseymen S, Rodriguez J, Paskavitz A, et al. Deep Complex Convolutional Network for Fast Reconstruction of 3D Late Gadolinium Enhancement Cardiac MRI. NMR Biomed. 2020;33(7):e4312. doi: 10.1002/nbm.4312.
24. Peng P, Lekadir K, Gooya A, Shao L, Petersen SE, Frangi AF. A Review of Heart Chamber Segmentation for Structural and Functional Analysis Using Cardiac Magnetic Resonance Imaging. MAGMA. 2016;29(2):155-95. doi: 10.1007/s10334-015-0521-4.

25. Xiong Z, Fedorov VV, Fu X, Cheng E, Macleod R, Zhao J. Fully Automatic Left Atrium Segmentation from Late Gadolinium Enhanced Magnetic Resonance Imaging Using a Dual Fully Convolutional Neural Network. IEEE Trans Med Imaging. 2019;38(2):515-24. doi: 10.1109/TMI.2018.2866845.

26. Sander J, de Vos BD, Išgum I. Automatic Segmentation with Detection of Local Segmentation Failures in Cardiac MRI. Sci Rep. 2020;10(1):21769. doi: 10.1038/s41598-020-77733-4.

27. Bekheet M, Sallah M, Alghamdi NS, Rusu-Both R, Elgarayhi A, Elmogy M. Cardiac Fibrosis Automated Diagnosis Based on FibrosisNet Network Using CMR Ischemic Cardiomyopathy. Diagnostics. 2024;14(3):255. doi: 10.3390/diagnostics14030255.

28. Sharifrazi D, Alizadehsani R, Joloudari JH, Band SS, Hussain S, Sani ZA, et al. CNN-KCL: Automatic Myocarditis Diagnosis Using Convolutional Neural Network Combined with K-Means Clustering. Math Biosci Eng. 2022;19(3):2381-402. doi: 10.3934/mbe.2022110.

29. Ghorbani A, Ouyang D, Abid A, He B, Chen JH, Harrington RA, et al. Deep Learning Interpretation of Echocardiograms. NPJ Digit Med. 2020;3:10. doi: 10.1038/s41746-019-0216-8.

30. American College of Cardiology Foundation Appropriate Use Criteria Task Force; American Society of Echocardiography; American Heart Association; American Society of Nuclear Cardiology; Heart Failure Society of America; Heart Rhythm Society; et al. ACCF/ASE/AHA/ASNC/HFSA/HRS/SCAI/SCCM/SCCT/SCMR 2011 Appropriate Use Criteria for Echocardiography. A Report of the American College of Cardiology Foundation Appropriate Use Criteria Task Force, American Society of Echocardiography, American Heart Association, American Society of Nuclear Cardiology, Heart Failure Society of America, Heart Rhythm Society, Society for Cardiovascular Angiography and Interventions, Society of Critical Care Medicine, Society of Cardiovascular Computed Tomography, Society for Cardiovascular Magnetic Resonance American College of Chest Physicians. J Am Soc Echocardiogr. 2011;24(3):229-67. doi: 10.1016/j.echo.2010.12.008.

31. De Geer L, Oscarsson A, Engvall J. Variability in Echocardiographic Measurements of Left Ventricular Function in Septic Shock Patients. Cardiovasc Ultrasound. 2015;13:19. doi: 10.1186/s12947-015-0015-6.

32. Zhang J, Gajjala S, Agrawal P, Tison GH, Hallock LA, Beussink-Nelson L, et al. Fully Automated Echocardiogram Interpretation in Clinical Practice. Circulation. 2018;138(16):1623-35. doi: 10.1161/CIRCULATIONAHA.118.034338.

33. Madani A, Arnaout R, Mofrad M, Arnaout R. Fast and Accurate View Classification of Echocardiograms Using Deep Learning. NPJ Digit Med. 2018;1:6. doi: 10.1038/s41746-017-0013-1.

34. Shi S, Alimu P, Mahemut P. The Study of Echocardiography of Left Ventricle Segmentation Combining Transformer and Convolutional Neural Networks. Int Heart J. 2024;65(5):889-97. doi: 10.1536/ihj.23-638.

35. Jiang J, Deng H, Xue Y, Liao H, Wu S. Detection of Left Atrial Enlargement Using a Convolutional Neural Network-Enabled Electrocardiogram. Front Cardiovasc Med. 2020;7:609976. doi: 10.3389/fcvm.2020.609976.

36. Painchaud N, Duchateau N, Bernard O, Jodoin PM. Echocardiography Segmentation with Enforced Temporal Consistency. IEEE Trans Med Imaging. 2022;41(10):2867-78. doi: 10.1109/TMI.2022.3173669.

37. Lei Y, Fu Y, Roper J, Higgins K, Bradley JD, Curran WJ, et al. Echocardiographic Image Multi-Structure Segmentation Using Cardiac-SegNet. Med Phys. 2021;48(5):2426-37. doi: 10.1002/mp.14818.

38. Wehbe RM, Katsaggelos AK, Hammond KJ, Hong H, Ahmad FS, Ouyang D, et al. Deep Learning for Cardiovascular Imaging: A Review. JAMA Cardiol. 2023;8(11):1089-98. doi: 10.1001/jamacardio.2023.3142.

39. Jian Z, Wang X, Zhang J, Wang X, Deng Y. Diagnosis of Left Ventricular Hypertrophy Using Convolutional Neural Network. BMC Med Inform Decis Mak. 2020;20(1):243. doi: 10.1186/s12911-020-01255-2.

40. Nazar W, Nazar K, Daniłowicz-Szymanowicz L. Machine Learning and Deep Learning Methods for Fast and Accurate Assessment of Transthoracic Echocardiogram Image Quality. Life. 2024;14(6):761. doi: 10.3390/life14060761.

41. Duffy G, Cheng PP, Yuan N, He B, Kwan AC, Shun-Shin MJ, et al. High-Throughput Precision Phenotyping of Left Ventricular Hypertrophy with Cardiovascular Deep Learning. JAMA Cardiol. 2022;7(4):386-95. doi: 10.1001/jamacardio.2021.6059.

42. Holste G, Oikonomou EK, Mortazavi BJ, Coppi A, Faridi KF, Miller EJ, et al. Severe Aortic Stenosis Detection by Deep Learning Applied to Echocardiography. Eur Heart J. 2023;44(43):4592-604. doi: 10.1093/eurheartj/ehad456.

43. Wessler BS, Huang Z, Long GM Jr, Pacifici S, Prashar N, Karmiy S, et al. Automated Detection of Aortic Stenosis Using Machine Learning. J Am Soc Echocardiogr. 2023;36(4):411-20. doi: 10.1016/j.echo.2023.01.006.

44. Farhad M, Masud MM, Beg A, Ahmad A, Ahmed LA, Memon S. Cardiac Phase Detection in Echocardiography Using Convolutional Neural Networks. Sci Rep. 2023;13(1):8908. doi: 10.1038/s41598-023-36047-x.

45. Muraki R, Teramoto A, Sugimoto K, Sugimoto K, Yamada A, Watanabe E. Automated Detection Scheme for Acute Myocardial Infarction Using Convolutional Neural Network and Long Short-Term Memory. PLoS One. 2022;17(2):e0264002. doi: 10.1371/journal.pone.0264002.

46. Naser JA, Lee E, Pislaru SV, Tsaban G, Malins JG, Jackson JI, et al. Artificial Intelligence-Based Classification of Echocardiographic Views. Eur Heart J Digit Health. 2024;5(3):260-9. doi: 10.1093/ehjdh/ztae015.

47. Østvik A, Smistad E, Aase SA, Haugen BO, Lovstakken L. Real-Time Standard View Classification in Transthoracic Echocardiography Using Convolutional Neural Networks. Ultrasound Med Biol. 2019;45(2):374-84. doi: 10.1016/j.ultrasmedbio.2018.07.024.

48. Sun D, Hu Y, Li Y, Yu X, Chen X, Shen P, et al. Chamber Attention Network (CAN): Towards Interpretable Diagnosis of Pulmonary Artery Hypertension Using Echocardiography. J Adv Res. 2024;63:103-15. doi: 10.1016/j.jare.2023.10.013.

49. DuBrock HM, Wagner TE, Carlson K, Carpenter CL, Awasthi S, Attia ZI, et al. An Electrocardiogram-Based AI Algorithm for Early Detection of Pulmonary Hypertension. Eur Respir J. 2024;64(1):2400192. doi: 10.1183/13993003.00192-2024.

50. Yuan N, Stein NR, Duffy G, Sandhu RK, Chugh SS, Chen PS, et al. Deep Learning Evaluation of Echocardiograms to Identify Occult Atrial Fibrillation. NPJ Digit Med. 2024;7(1):96. doi: 10.1038/s41746-024-01090-z.

51. Zhou X, Yang T, Ruan Y, Zhang Y, Liu X, Zhao Y, et al. Application of Neural Networks in Prenatal Diagnosis of Atrioventricular Septal Defect. Transl Pediatr. 2024;13(1):26-37. doi: 10.21037/tp-23-394.

52. Erno J, Gomes T, Baltimore C, Lineberger JP, Smith DH, Baker GH. Automated Identification of Patent Ductus Arteriosus Using a Computer Vision Model. J Ultrasound Med. 2023;42(12):2707-13. doi: 10.1002/jum.16305.

53. Betancur J, Commandeur F, Motlagh M, Sharir T, Einstein AJ, Bokhari S, et al. Deep Learning for Prediction of Obstructive Disease from Fast Myocardial Perfusion SPECT: A Multicenter Study. JACC Cardiovasc Imaging. 2018;11(11):1654-63. doi: 10.1016/j.jcmg.2018.01.020.

54. Papandrianos NI, Feleki A, Papageorgiou EI, Martini C. Deep Learning-Based Automated Diagnosis for Coronary Artery Disease Using SPECT-MPI Images. J Clin Med. 2022;11(13):3918. doi: 10.3390/jcm11133918.

55. Su TY, Chen JJ, Chen WS, Chang YH, Lu HH. Deep Learning for Myocardial Ischemia Auxiliary Diagnosis Using CZT SPECT Myocardial Perfusion Imaging. J Chin Med Assoc. 2023;86(1):122-30. doi: 10.1097/JCMA.0000000000000833.

56. Toth D, Miao S, Kurzendorfer T, Rinaldi CA, Liao R, Mansi T, et al. 3D/2D Model-to-Image Registration by Imitation Learning for Cardiac Procedures. Int J Comput Assist Radiol Surg. 2018;13(8):1141-9. doi: 10.1007/s11548-018-1774-y.

57. Breininger K, Albarqouni S, Kurzendorfer T, Pfister M, Kowarschik M, Maier A. Intraoperative Stent Segmentation in X-Ray Fluoroscopy for Endovascular Aortic Repair. Int J Comput Assist Radiol Surg. 2018;13(8):1221-31. doi: 10.1007/s11548-018-1779-6.

58. Sadda P, Qarni T. Real-Time Medical Video Denoising with Deep Learning: Application to Angiography. Int J Appl Inf Syst. 2018;12(13):22-8. doi: 10.5120/ijais2018451755.

59. Luo Y, Ma Y, O' Brien H, Jiang K, Kohli V, Maidelin S, et al. Edge-Enhancement Densenet for X-Ray Fluoroscopy Image Denoising in Cardiac Electrophysiology Procedures. Med Phys. 2022;49(2):1262-75. doi: 10.1002/mp.15426.

60. Abdolmanafi A, Duong L, Dahdah N, Adib IR, Cheriet F. Characterization of Coronary Artery Pathological Formations from OCT Imaging Using Deep Learning. Biomed Opt Express. 2018;9(10):4936-60. doi: 10.1364/BOE.9.004936.

61. Abdolmanafi A, Cheriet F, Duong L, Ibrahim R, Dahdah N. An Automatic Diagnostic System of Coronary Artery Lesions in Kawasaki Disease Using Intravascular Optical Coherence Tomography Imaging. J Biophotonics. 2020;13(1):e201900112. doi: 10.1002/jbio.201900112.

62. Gessert N, Lutz M, Heyder M, Latus S, Leistner DM, Abdelwahed YS, et al. Automatic Plaque Detection in IVOCT Pullbacks Using Convolutional Neural Networks. IEEE Trans Med Imaging. 2019;38(2):426-34. doi: 10.1109/TMI.2018.2865659.

Tricuspid Valve: Anatomical Basis and Patient Selection Criteria for Transcatheter Structural Interventions

Alexandre Costa Souza,[1,2] *Halsted Alarcão Gomes Pereira da Silva,*[3] *Alex dos Santos Felix*[4]
Hospital São Rafael/RedeD'or,[1] *Salvador, BA – Brazil*
Instituto D'Or de Pesquisa e Ensino (IDOR),[2] *Rio de Janeiro, RJ – Brazil*
Instituto Dante Pazzanese de Cardiologia,[3] *Sao Paulo, SP – Brazil*
Instituto Nacional de Cardiologia (INC),[4] *Rio de Janeiro, RJ – Brazil*

Central Illustration: Tricuspid Valve: Anatomical Basis and Patient Selection Criteria for Transcatheter Structural Interventions

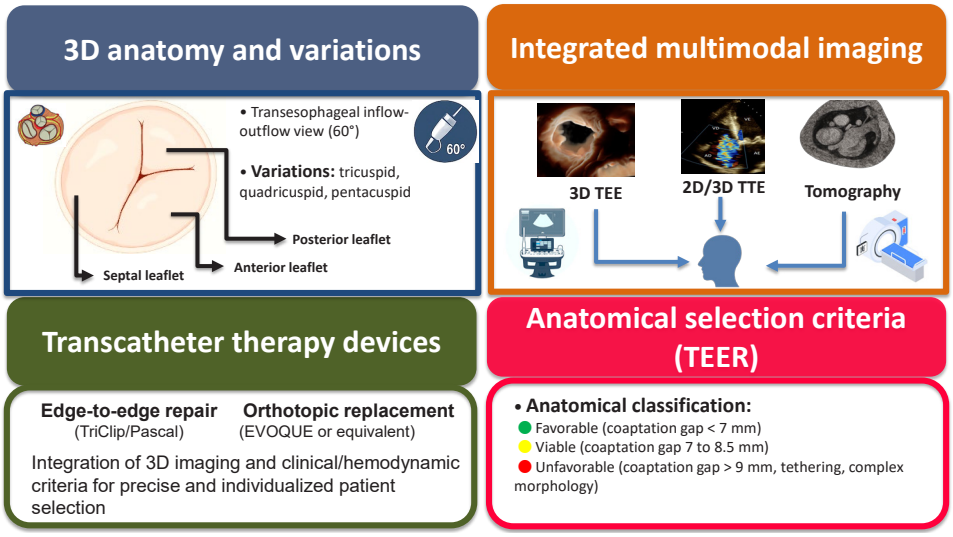

Arq Bras Cardiol: Imagem cardiovasc. 2025;38(3):e20250064

TEE: transesophageal echocardiography; TEER: transcatheter edge-to-edge repair; TTE: transthoracic echocardiography; 2D: two-dimensional; 3D: three-dimensional.

Abstract

Tricuspid regurgitation has been recognized as a relevant clinical entity, with a direct impact on morbidity and mortality. Recent advances in multimodal cardiovascular imaging have promoted more detailed anatomical and functional assessment of the tricuspid apparatus, guiding the indication and planning of transcatheter interventions. To provide a review of the anatomical basis of the tricuspid valve and discuss echocardiographic and clinical criteria for selecting candidates for transcatheter therapies. This narrative review of the anatomical variability of the tricuspid valve and its subvalvular apparatus incorporates recent recommendations from echocardiography societies and clinical evidence. Special emphasis has been given to three-dimensional echocardiography, transesophageal echocardiography, and computed tomography for morphological and functional characterization of tricuspid regurgitation. Contemporary evidence has demonstrated that up to 45% of patients present with non-classical morphologies (quadricuspid or pentacuspid valves), which impact the viability and outcomes of edge-to-edge repair. The integration of three-dimensional echocardiography enhances accuracy in grading regurgitation severity, enables precise measurement of the vena contracta area, and assists in device selection. Clinical factors including

Keywords

Tricuspid Valve; Tricuspid Valve Insufficiency; Three-Dimensional Echocardiography; Transesophageal Echocardiography

Mailing Address: Alexandre Costa Souza •
Hospital São Rafael – Ecocardiografia. Av. São Rafael, 2152. Postal Code: 41253-190, Salvador, BA – Brazil
E-mail: alexandrecostahsr@gmail.com
Manuscript received August 21, 2025; revised August 29, 2025; accepted August 29, 2025
Editor responsible for the review: Marcelo Tavares

DOI: https://doi.org/10.36660/abcimg.20250064i

SUMÁRIO

right ventricular function, pulmonary artery systolic pressure, and the presence of intracardiac devices also influence patient selection. Appropriate selection of candidates for transcatheter tricuspid valve therapies requires a systematic approach with integrated application of imaging methods and clinical parameters. Detailed echocardiographic characterization of leaflet morphology, coaptation gap, and annulus geometry is crucial for planning the procedure, selecting the device, and predicting outcomes.

Introduction

The tricuspid valve is an anatomical and functional complex that plays a fundamental role in adequate cardiac mechanics, influencing hemodynamics of both ventricles. The term "tricuspid" derives from the traditional anatomical description, composed of the anterior, septal, and posterior cusps, although we know that, in up to 45% of cases, the valve may be bicuspid or even have more than three cusps, with considerable anatomical variability.[1] Normal tricuspid valve area ranges from 7 to 9 cm^2; anatomically speaking, it is the most inferior valve in the heart. The more apical position in relation to the mitral valve, associated with the saddle-shaped, elliptical geometry of the valve annulus and the proximity of structures such as the coronary sinus and bundle of His, pose particular challenges to transcatheter structural procedures, making imaging-based definition extremely important. In addition to the tricuspid valve, the tricuspid complex is composed of the fibromuscular annulus and subvalvular apparatus (chordae tendineae and papillary muscles), whose dynamic interaction ensures correct valve coaptation during the cardiac cycle. Three-dimensional (3D) reconstruction studies, by means of 3D transthoracic or transesophageal echocardiography or even computed tomography, allow for more detailed visualization of the cusps (en face view on 3D echocardiography) and precise measurement of valve dimensions, reducing the subjectivity inherent to two-dimensional approaches.[1,2]

As a complement to anatomical visualization, functional assessment of the tricuspid valve is essential for determining the mechanism of dysfunction and planning the best therapeutic option. For this purpose, 3D echocardiography has emerged as a useful tool that allows for real-time volumetric imaging, using specific techniques to quantify valve annulus measurements and function. Furthermore, it enables rendered and realistic analysis of cardiac structures, allowing free navigation throughout the dataset, obtaining anatomical slices that show the relationship between the valve, the subvalvular apparatus, and other adjacent structures.[3] Direct measurement of the vena contracta area using 3D echocardiography increases the accuracy of tricuspid regurgitation (TR) quantification, overcoming technical limitations and measurement errors of two-dimensional methods, as it is able to capture the irregular geometry of the valve regurgitant orifice and reduce the need for geometric assumptions.[3] The integration of 3D Doppler also allows for more accurate estimation of regurgitant volume using techniques such as 3D proximal isovelocity surface area (PISA) radius and assessment of dynamic flow changes throughout the cardiac cycle, providing greater consistency in reflux grading and, consequently, supporting more accurate therapeutic decisions.[4]

Cardiovascular imaging specialists must have an integrated understanding of the following three fundamental pillars when selecting candidates for percutaneous tricuspid valve interventions:

1. Valve morphology: Anatomical variations that deviate from the classic "tricuspid" pattern can directly influence the choice of edge-to-edge devices, annuloplasty techniques, or prostheses.
2. Accurate quantification of regurgitation severity currently benefits from 3D methods to measure vena contracta area and regurgitant volume and to assess jet dynamics and multiple jets, thus avoiding underestimations that could delay treatment.
3. A patient's clinical and functional profile includes assessment of the right ventricle (RV), pulmonary artery systolic pressure, presence of intracardiac devices, and comorbidities that may alter the risk-benefit ratio.

In conjunction, these elements, obtained through conventional or 3D echocardiography, tomography, magnetic resonance imaging, and hemodynamic correlations, guide the definition of the optimal moment, the most appropriate strategy, and prognosis for each patient, supporting safe interventional practices focused on individualization.

Severity classification and correlation with candidate selection

It can be difficult to quantify TR for several reasons, including multiple regurgitant jets, respiratory-related changes, or blood volume. Characterization of TR severity depends on an integrative assessment of multiple parameters.

Current recommendations from the European Association for Cardiovascular Imaging (EACVI) and the American Society of Echocardiography (ASE) suggest using qualitative, semi-quantitative, and quantitative parameters to classify TR severity into three grades.

Important TR is defined as follows:

- Qualitative parameters: Leaflets with a large coaptation gap; on continuous Doppler, dense signal, often triangular with an early peak
- Semiquantitative parameters: Systolic flow reversal pattern in the hepatic vein; dominant E wave (≥ 1 m/s); PISA radius > 9 mm; vena contracta width > 7 mm
- Quantitative parameters: Effective regurgitant orifice area (EROA) ≥ 40 mm^2; regurgitant volume ≥ 45 ml or regurgitant fraction ≥ 50%.

More recently, a five-grade classification system was proposed by Hahn et al., including massive and torrential TR patterns, defined as follows: massive TR (vena contracta width: 14 to 20 mm, EROA: 60 to 79 mm^2, 3D vena contracta area 95 to 114 mm^2) and torrential TR (vena contracta width: ≥ 21 mm, EROA ≥ 80 mm^2, 3D vena contracta area ≥ 115 mm^2). This classification has demonstrated better risk stratification of patients with TR before and after percutaneous tricuspid valve intervention[5,6] (Table 1).

Transesophageal echocardiography (TEE) has also become an integral part of the assessment of candidates for transcatheter tricuspid valve therapy, complementing the

Table 1 – Echocardiography criteria for grading tricuspid insufficiency

	Mild	Moderate	Severe	Massive	Torrential
2D assessment (Semiquantitative)					
Vena contracta width, mm	< 3	3 to 6.9	7 to 13.9	14 to 20.9	≥ 21
PISA radius, mm	≤ 5.4	5.5 to 8.9	≥ 9	≥ 9	≥ 9
Hepatic vein flow	Systolic dominant	Systolic blunting	Systolic flow reversal	Systolic flow reversal	Systolic flow reversal
Tricuspid inflow	A-wave dominant	Variable	E-wave dominant (velocity ≥ 1 m/s)	E-wave dominant (velocity ≥ 1 m/s)	E-wave dominant (velocity ≥ 1 m/s)
2D assessment (Quantitative)					
EROA, mm²	< 20	20 to 39	40 to 59	60 to 79	≥ 80
Regurgitant volume, mL	< 30	30 to 44	45 to 59	60 to 74	≥ 75
Regurgitant fraction	< 15%	16% to 49%	≥ 50%	≥ 50%	≥ 50%
Quantitative Doppler EROA, mm²	–	–	75 to 94.9	95 to 114.9	≥ 115
3D assessment					
Vena contracta area, mm²	–	–	75 to 94.9	95 to 114.9	≥ 115

Adapted from Badano et al.[5] EROA: effective regurgitant orifice area; PISA: proximal isovelocity surface area; 2D: two-dimensional; 3D: three-dimensional.

information provided by transthoracic echocardiography (TTE). Whereas TTE allows for initial quantification of the degree of regurgitation and measurement of functional parameters, TEE, especially the 3D version, offers much higher spatial resolution, which allows for precise characterization of both the etiology (primary, functional, or device-related) and the morphology of leaflets and commissures. This more detailed anatomical definition facilitates confirmation of the severity of regurgitation, especially in situations involving multiple jets or hemodynamic variability related to volume and respiration. By means of TEE, it is also possible to accurately measure valve failure and assess the tricuspid valve's relationship with adjacent structures, especially cardiac implantable electronic device (CIED) leads. This information is crucial for selecting the transcatheter device (edge-to-edge clip versus orthotopic prosthesis) and defining appropriate positioning and diameter. Furthermore, by providing real-time images during procedure planning and execution, TEE guides the precise alignment of the clip arms or prosthesis seating, contributing to reduced mechanical complications and improved intervention efficacy. Thus, incorporating TEE into a heart team's assessment protocol significantly improves the safety, accuracy, and clinical success of transcatheter tricuspid valve therapies.

Three-dimensional TEE enhances anatomical and functional assessment of the tricuspid valve, enabling volumetric reconstructions of the valve apparatus and real-time visualization of its dynamics throughout the cardiac cycle. This 3D precision guides the choice of the optimal point of capture during the edge-to-edge procedure and helps determine the appropriate orthotopic prosthesis size, reducing the risk of oversizing. Additionally, 3D TEE facilitates intraprocedural monitoring of device positioning, allowing immediate adjustments to angulation and implantation depth, which result in greater efficacy and reduced periprocedural complications.

Anatomy and relationships of the tricuspid valve complex

Recent 3D TEE studies have proposed a morphological classification system that is capable of reflecting the true variability of the tricuspid leaflets and guiding interventional planning. Hahn et al. identified six distinct valve configurations (Figure 1), ranging from the classic three-leaflet pattern (type I) to quadricuspid variants with additional anterior (IIIA), posterior (IIIB), or septal (IIIC) leaflets, also including bicuspid (type II) and even pentacuspid (type IV) forms. They demonstrated that under 55% of patients exhibited the usual tricuspid form, and type IIIB (two posterior leaflets) was the most prevalent quadricuspid subtype. This standardized nomenclature not only facilitates communication between imaging teams and interventionalists but also highlights the need for dedicated 3D protocols for en face mapping and accurate assessment of valve morphology before attempting any transcatheter intervention.[6]

In this context, the description of the morphological subtype ceases to be a taxonomic exercise and begins to have a direct operational impact on the strategy of tricuspid transcatheter edge-to-edge repair (T-TEER). The greater

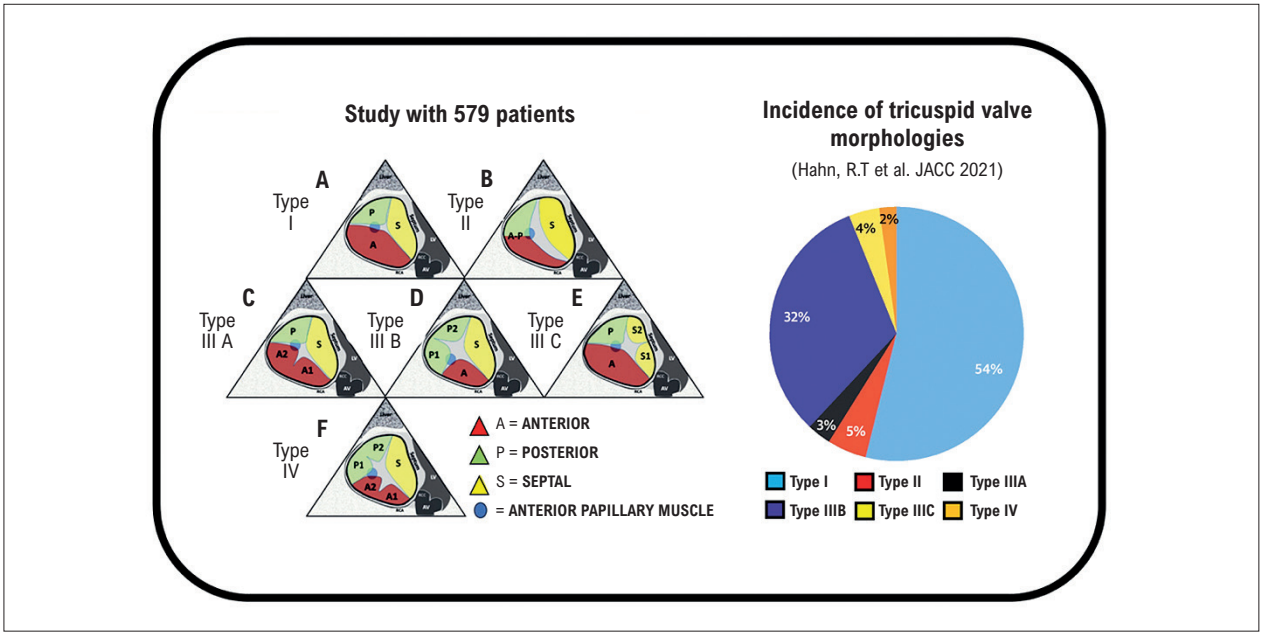

Figure 1 – *Standardized echocardiographic nomenclature of tricuspid valve leaflets. Adapted from Hahn RT et al.*[6]

the anatomical complexity, especially in quadricuspid and pentacuspid valves, where incisions longer than 10 mm define true commissures, and duplicate leaflets may be present in critical positions, the more difficult it becomes to align the clip arms, ensure adequate coaptation, and avoid significant residual regurgitation. Multicenter studies indicate that valves with four or more leaflets exhibit greater residual TR after the procedure, because the choice of safe clipping points, the number of clips required, and the risk of uneven leaflet tensioning vary according to the morphological pattern. Thus, the recently proposed morphological classification guides tactical decisions, from candidate selection to planning the catheter path and the number of clips to be used, increasing the likelihood of technically successful T-TEER.[6-8]

Retrospective multicenter data reinforce this relationship between anatomy and T-TEER efficacy. In a cohort of 145 patients undergoing T-TEER, Sugiura et al. identified a four-leaflet configuration in 29% of cases and demonstrated that this morphology increased the likelihood of ≥ moderate residual TR (≥ 3+) by 2.6, even after adjusting for baseline severity, coaptation gap width, and jet location. Furthermore, the presence of TR ≥ 3+ at 30 days doubled the combined risk of mortality or heart failure hospitalization at 1 year (56.1% versus 27.7%), demonstrating that reducing regurgitation below moderate is crucial to prognosis. The study also proposed a sequential evaluation combining morphology, coaptation gap > 7 mm, and noncentral jets, identifying subgroups with up to 45% of residual TR ≥ moderate at 30 days, a marker of adverse clinical outcome. These findings complement the classification proposed by Hahn by providing clear prognostic data, supporting careful patient selection and, when necessary, consideration of alternative approaches such as annuloplasty or valve replacement, in cases with more complex morphologies.[6,8]

Imaging techniques for selecting candidates and planning percutaneous tricuspid valve interventions

Echocardiographic assessment should include the transgastric short-axis view, acquired in the deep transgastric plane with a rotation of approximately 30° to 50°. In this view, the tricuspid valve is visualized en face, and the aorta is located at 5 o'clock, providing interventionalists with a direct anatomical reference to inspect the coaptation line, estimate tethering, classify morphology, and identify commissures.[6]

For 3D volumetric study, two 3D reconstructions are particularly useful. The surgeon's view (aorta at 11 o'clock) is derived from a midesophageal acquisition, and it uses the interatrial septum and aorta as anatomical landmarks. The interventionalist's view, generated from the same 3D acquisition, with the aorta rotated to 5 o'clock, reproduces the orientation of the transgastric window and, therefore, matches the fluoroscopic perspective in the catheterization laboratory. The equivalence between the transgastric and interventionalist views standardizes the clockwise and counterclockwise orientation of the leaflets, reducing intraprocedural orientation errors and errors in the anatomical assessment of candidates for dedicated devices (Figure 2).

Three-dimensional reconstruction of the tricuspid annulus, complemented by cardiac tomography, makes it possible to confirm annulus diameters, area, and perimeter; assess the relationship with the right coronary artery; and define optimal fluoroscopic projections, completing the multimodal imaging-guided selection and planning cycle.

Complementing the transgastric views and the surgeon and interventionalist 3D reconstructions described above, the RV inflow-outflow echocardiographic window, acquired in the mid-esophagus at approximately 60°, with progressive anteriorization of the probe until simultaneously encompassing

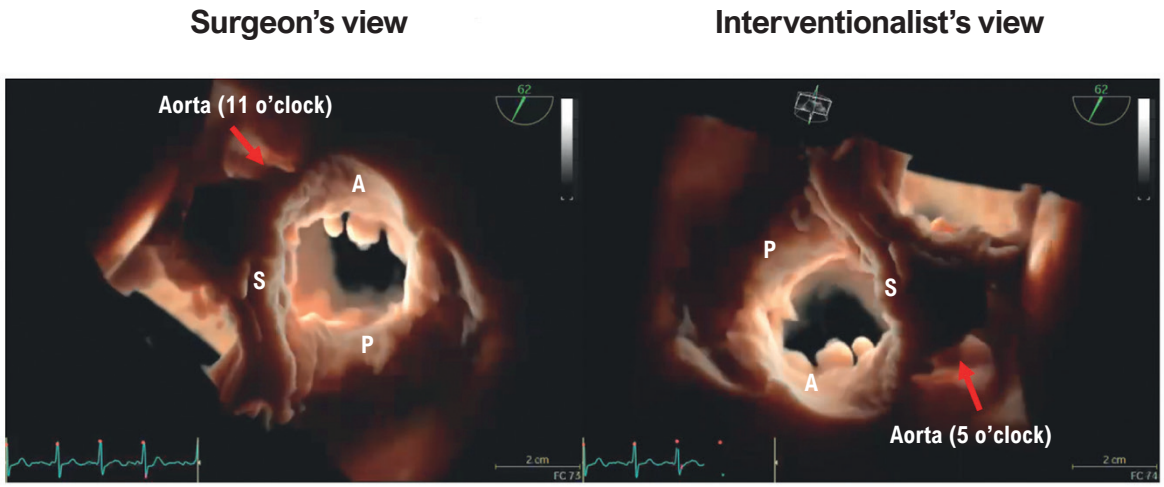

Figure 2 – *Three-dimensional reconstructions of the tricuspid valve applying transillumination in three-dimensional transesophageal echocardiography, highlighting two complementary orientations. On the left, the surgeon's view shows the valve en face with the aorta positioned at 11 o'clock, replicating the operative perspective. On the right, the interventionalist's view results from the rotation of the three-dimensional volume to position the aorta at 5 o'clock, corresponding to fluoroscopic view in the catheterization laboratory. The anterior, posterior, and septal cusps are delimited in both projections. A: anterior; P: posterior; S: septal.*

the inflow tract (septal and anterior leaflets) and the outflow tract (RV outflow tract and pulmonary valve), provides a relevant longitudinal view for selecting candidates for transcatheter tricuspid valve intervention. In this projection, it is possible to measure the angle between the tricuspid annulus and the catheter path, estimating the coaxiality of T-TEER systems; to assess the degree of tethering of the anterior leaflet, which is a decisive parameter for eligibility without overlapping the posterior leaflet; and to delineate the course of the right coronary artery, as well as the position of intracavitary electrodes in relation to the annulus, reducing the risk of conflict with implanted devices. During the procedure, the same view acts as a dynamic guide for interventionalists, allowing fine adjustments to the rotation of the clip or orthotopic replacement system, monitoring leaflet coaptation in real time and confirming that the device does not invade the RV outflow tract or distort the pulmonary valve. Thus, the inflow-outflow projection connects pre-procedure anatomical characterization with intra-procedure feedback, increasing precision in navigation, anchoring, and immediate verification of hemodynamic results.

For illustrative purposes contributing to a better understanding of the inflow-outflow echocardiographic window in the mid-esophagus at 60° and its related slice planes, the anterior cusp is represented in purple, the septal cusp in green, and the posterior cusp in yellow. In this window, the anterior cusp is presented in the position closest to the aortic valve, with the posterior cusp in the opposite position. By adding biplane technology such as X-plane (Philips) or Multi-D (GE), it is possible to acquire an orthogonal slice with the analysis plane directed toward both the anterior and posterior cusps. Figure 3 displays the biplane slice from the anterior cusp, with the formation of a simultaneous image corresponding to the inverted apical four-chamber window with the RV on the left, and the left ventricle on the right. If the coronary sinus ostium or the interventricular septum are visualized, the adjacent leaflet is most likely the septal leaflet. On the biplane image, the anterior leaflet will appear in a more distal position in relation to the transducer.

Figure 4 displays the biplane view, but from the posterior leaflet. In this case, the septal leaflet will be closer to the coronary sinus, and the posterior leaflet will be more distal to the transducer.

In Figure 5, adding a 3D analysis plane with the tricuspid valve in open and closed positions, with the biplane view orthogonal to the anterior leaflet clearly and precisely shows the correlation between the echocardiographic planes, thus providing correct spatial understanding of the analyzed leaflets without the need to memorize or infer the position of each tricuspid valve component, which is not always successful.

The transgastric window provides a short-axis view that integrates the tricuspid valve plane with its septal, anterior, and posterior leaflets and the RV cavity, making it possible to measure the gap between leaflets, characterize morphology, and quantify tethering without geometric assumptions. This perspective also facilitates the identification of residual clefts, providing essential information for planning a transcatheter strategy, as demonstrated in Figure 6.

With this anatomical basis, in candidates for T-TEER, the transgastric window displays all leaflets en face, guiding the

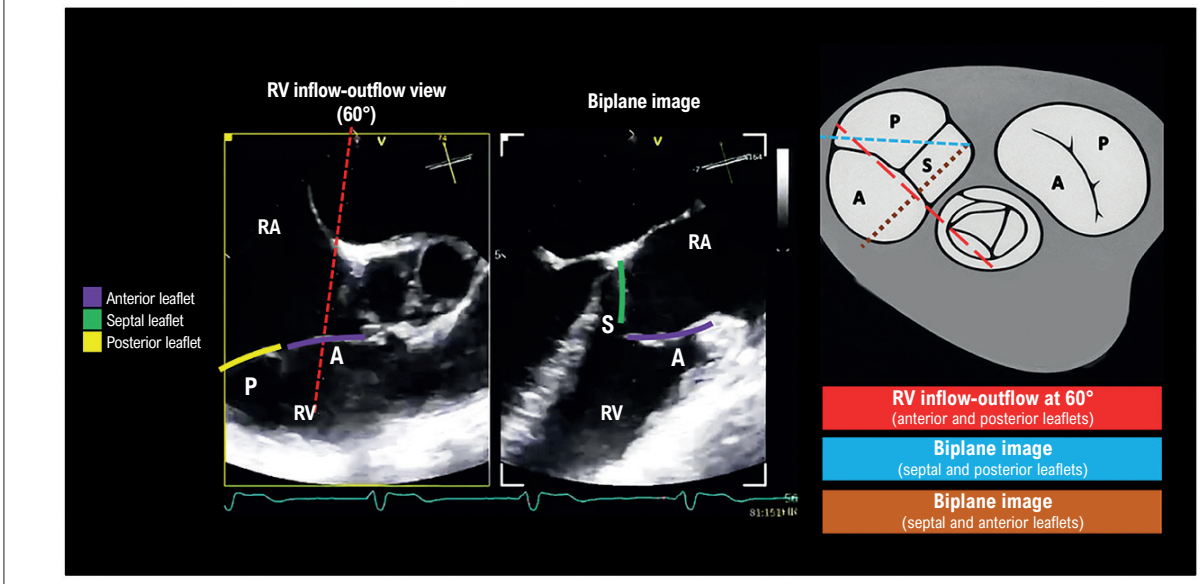

Figure 3 – *Echocardiographic representation of the tricuspid valve in the transesophageal right ventricular inflow-outflow window, complemented by biplane mode. On the left, the image obtained at 60° shows the anterior and posterior leaflets, useful in selecting candidates for transcatheter therapies. In the center, biplane mode allows simultaneous assessment of the orthogonal plane, identifying the septal leaflet in combination with the anterior leaflet. On the right, a schematic diagram relating the echocardiographic slice planes to the corresponding leaflets, indicating different pairs of leaflets visualized according to the angle and orientation of the transducer. A: anterior; P: posterior; RA: right atrium; RV: right ventricle; S: septal.*

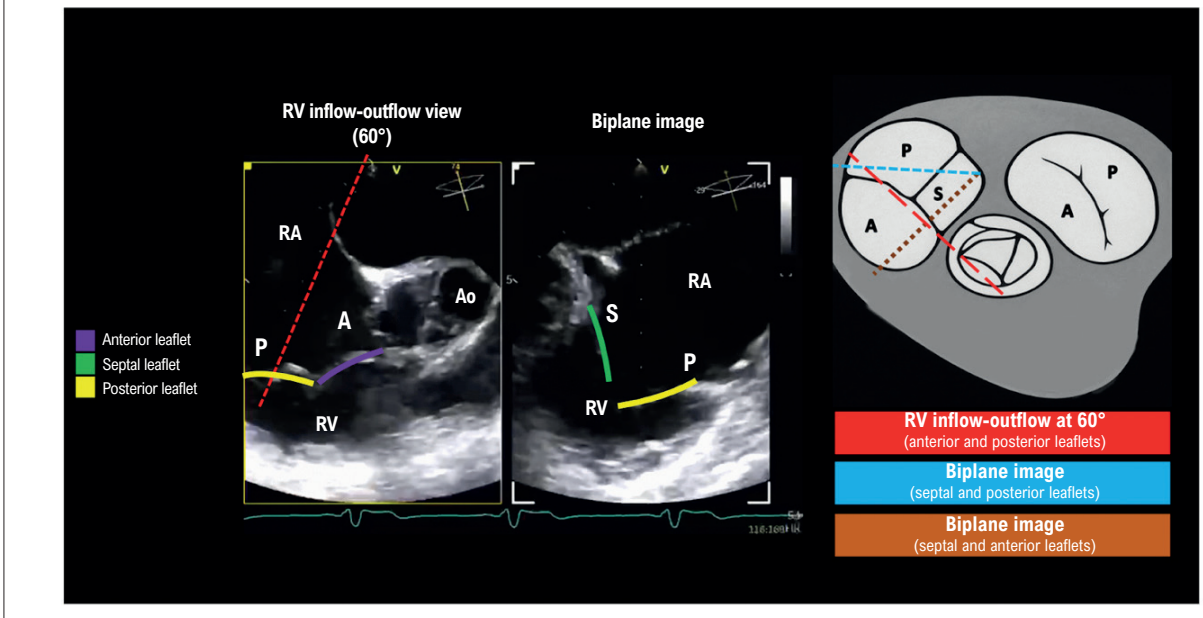

Figure 4 – *Image of the right ventricular inflow-outflow tract in the 60° plane, with the orthogonal section from the posterior leaflet, concomitant image of the anterior and posterior leaflets, and in parallel the septal and posterior leaflets, allowing for better anatomical detailing of the tricuspid valve. A: anterior; Ao: aorta; P: posterior; RA: right atrium; RV: right ventricle; S: septal.*

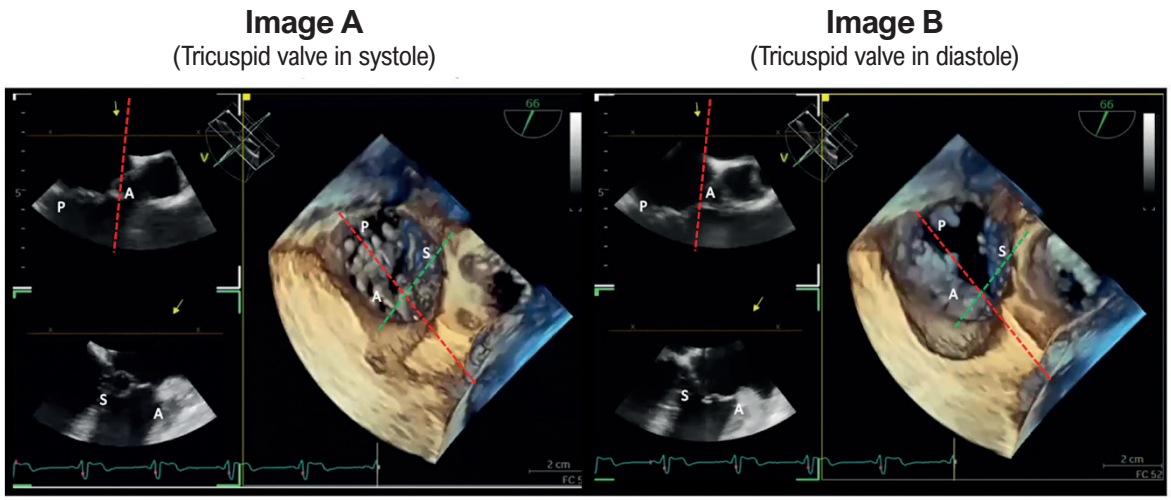

Figure 5 – *Three-dimensional transesophageal echocardiogram.* *Assessment of the tricuspid valve with biplane reconstruction in the systole (Image A) and diastole (Image B) phases, oriented according to the interventionalist's view, with the aorta positioned at 5 o'clock. The central images present volumetric reconstruction, displaying the valve en face. The dashed lines indicate the orthogonal planes used for multiplanar analysis. On the left of each block, the two-dimensional sections correspond to the inflow-outflow plane (top), highlighting the anterior and posterior leaflets, and the orthogonal plane (bottom), showing the anterior leaflet in relation to the septal leaflet. Comparison between the phases of the cardiac cycle allows for the assessment of the dynamics of leaflet opening and coaptation. A: anterior; P: posterior; S: septal.*

point of optimal grasping and ensuring clip coaxiality in relation to the interventricular septum. This perpendicular orientation in relation to the coaptation plane maximizes the coaptation area and reduces leaflet tension; the clip is only released after confirmation of adequate edge capture, which contributes to technical reproducibility and procedural success.

For orthotopic prosthesis implantation, the transgastric window allows direct measurement of tricuspid annulus diameter, guiding selection of appropriate prosthesis size and alignment along the aorta-tricuspid axis. During the procedure, real-time monitoring enables precise adjustments of device angulation and depth, reducing the risk of unwanted contact with adjacent structures and ensuring stable prosthesis positioning.

Eligibility criteria for transcatheter intervention

The most recent publication of the Tricuspid Valve Academic Research Consortium (TVARC) defines the criteria required for transcatheter device implantation to be considered successful.[9]

- Absence of significant tricuspid stenosis (tricuspid valve area ≥ 1.5 cm^2 or tricuspid valve area index ≥ 0.9 cm^2/m^2 [≥ 0.75 if body mass index > 30 kg/m^2])
- Doppler velocity index < 2.2
- Mean gradient < 5 mmHg
- Reduction of total TR to levels considered optimal (mild residual TR ≤ 1+) or acceptable (mild residual TR ≤ 2+)

Multiple studies have demonstrated worse outcomes in patients with more severe residual TR. According to the current consensus, eligibility for transcatheter repair is classified into the following three anatomical groups: favorable, viable, and unfavorable. This categorization derives from assessments of echocardiographic data that demonstrate greater or lesser likelihood of therapeutic success of the procedure, as displayed in Table 2.[10] With the development of new devices and improvements in their structure, feasibility parameters tend to expand over time.

Tricuspid transcatheter edge-to-edge repair

T-TEER is a catheter-based tricuspid valve repair technique that reduces TR by restoring coaptation by means of leaflet approximation, which indirectly reduces or stabilizes the valve annulus. T-TEER is currently the most commonly applied transcatheter tricuspid valve repair technique. It can be performed with TriClip (Abbott) or Pascal (Edwards Lifesciences), two guided systems that utilize a transvenous transfemoral approach to restore tricuspid valve coaptation with a valve clipping device.

In the majority of studies on T-TEER, procedural success is defined as a reduction in TR to ≤ moderate or 2+. In this context, multiple small studies have identified predictors of success, including the following:

- Jet location
- Coaptation gap size
- Valve morphology (number of leaflets)
- Valve thickness or calcification
- Valve mobility

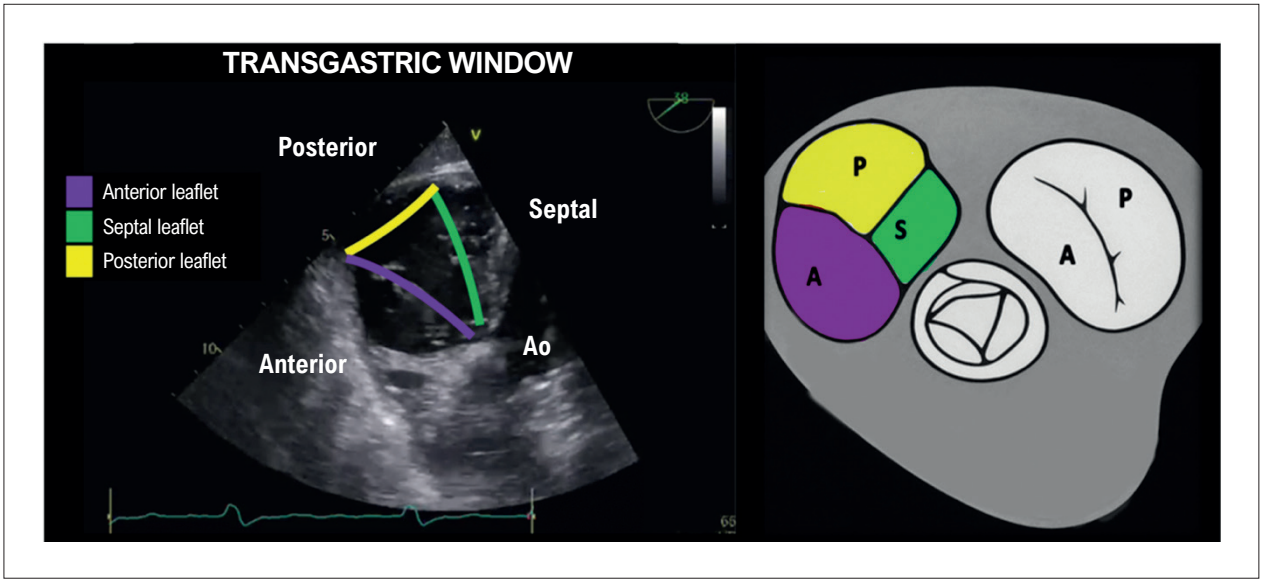

Figure 6 – *Two-dimensional transgastric view of transesophageal echocardiography in short-axis view (30° insonation angle), demonstrating the tricuspid valve in an anterior position to the aortic plane. Note the morphology of the tricuspid leaflets, with complete coaptation in diastole, and the contour of the aortic root just above the valve plane. A: anterior; Ao: aorta; P: posterior; S: septal.*

Table 2 – Echocardiographic eligibility criteria for percutaneous edge-to-edge tricuspid valve repair (TriClip)

	Transcatheter device repair (TriClip)		
	Favorable	**Feasible/viable**	**Unfavorable**
Valve morphology	3 leaflets	Non-tricuspid morphology	Non-tricuspid morphology with thickened valve and subvalvular complex
Coaptation gap, mm	< 7	7 to 8.5	> 8.5
Leaflets	Normal leaflet length (≥ 7 mm), normal mobility, no flail or tethering	Primary TR with flail gap (< 10 mm), secondary TR with tethering height < 9 mm	Primary TR with flail gap (≥ 10 mm); short (< 7 mm), thickened, or perforated leaflets; secondary TR with tethering height ≥ 9 mm or tenting area > 2.1 cm²
Jet location	Central and within the anteroseptal commissure	Central but not within the anteroseptal commissure	Massive, torrential, very eccentric, or multiple commissures
PM leads	No leads	Leads that do not participate in TR	Leads that cause impingement
Windows	Excellent transesophageal echocardiographic windows	Adequate windows with transesophageal or intracardiac echocardiography	Inadequate windows
RV remodeling	Normal, mildly dilated, or mildly dysfunctional	Moderate dilation or dysfunction	Severe dilation or dysfunction (LVEF < 45% on 3DE or NMR)
Pulmonary hemodynamics	Normal PASP, normal TPG, TAPSE/PASP > 0.41	PASP ≤ 60 to 65 mmHg, PVR ≤ 4 WU, MPAP ≤ 30 mmHg, TPG ≤ 17 mmHg	PASP > 60 to 65 mmHg, PVR > 4 WU, MPAP > 30 mmHg, TPG > 17 mmHg, TAPSE/PASP ≤ 0.41

Adapted from Hungerford SL et al.[11] LVEF: left ventricular ejection fraction; MPAP: mean pulmonary artery pressure; NMR: nuclear magnetic resonance; PASP: pulmonary artery systolic pressure; PM: pacemaker; PVR: pulmonary vascular resistance; TAPSE: tricuspid annular plane systolic excursion; TPG: transpulmonary gradient; TR: tricuspid regurgitation; WU: Wood units; 3DE: three-dimensional echocardiography.

- Complexity of the subvalvular apparatus
- TR severity
- Valve-to-annulus ratio
- Location and extent of CIED-related TR
- Tenting height
- Left atrial appendage volume.

Very large coaptation gaps, torrential TR, markedly thickened or immobile valves, and CIED-related TR in which the device adheres to the leaflets or subvalvular apparatus may be relative contraindications for the use of this technique. Furthermore, correct and adequate visualization of the leaflets during the procedure, through the use of TEE (with or without adjunctive intracardiac echocardiographic imaging), is also an important technical prerequisite for planning the intervention.

Transcatheter tricuspid valve replacement

Transcatheter tricuspid valve replacement (TTVR) involves the insertion of a bioprosthesis through a transvenous transcatheter approach. TTVR can be orthotopic or heterotopic; the latter is often used as a palliative procedure to relieve systemic venous congestion in patients who cannot undergo T-TEER or orthotopic TTVR. The anatomical requirements for TTVR are primarily related to the ability to position the device within the annular plane and the anchoring mechanism. Therefore, different devices will have different anatomical constraints. Initial TTVR implantations were performed through the implantation of a balloon-expandable prosthesis within a surgical valve prosthesis or in a prosthetic annulus. Due to the growing demand for implants in native valve disease, there has been progressive improvement in devices, in addition to optimization of access, which is currently transfemoral or transjugular. Unlike T-TEER devices, large coaptation gaps, torrential TR, complex morphologies, markedly thickened or immobile leaflets, and CIED-related TR are not typically exclusion criteria. For these devices, the main determinants of feasibility are current device sizes, as well as the ability to guide the device to achieve a coaxial implantation trajectory, largely determined by the size of the implant device itself and the available right atrial space. Although also described for T-TEER, acute changes in RV preload and afterload and the occurrence of ventricular decoupling can lead to left ventricular failure after reduction of massive and torrential TR and should be a concern in TTVR, given that ≤ mild TR can be achieved in > 90% of patients.

Table 3 displays the main anatomical and echocardiographic considerations that must be assessed in order to determine whether or not each of these types of implant is appropriate, bearing in mind that these criteria are constantly changing due to the technological evolution of prostheses.

Innovations and future perspectives

The expanding trend in percutaneous tricuspid valve interventions reflects both technological advances and the growing demand for less invasive alternatives in patients with significant regurgitation. This growth is expected to be driven by a reduction in complications associated with conventional surgery, increased familiarity of multidisciplinary teams with valve anatomy, and improved imaging techniques used in pre-procedure assessment.

In this context, appropriate candidate selection requires an integrated analysis of clinical and anatomical profile, considering factors such as age, comorbidities, degree of RV dysfunction, and tolerance to anticoagulation or contrast media, in addition to the structural characteristics of the valve, including annulus dimensions, degree of tethering, extent of coaptation, and leaflet number and integrity. It is also necessary to take into account the particular characteristics of each device, including compatibility with the tricuspid annulus, the viability of vascular access, and the technical complexity involved in implantation. This systematic approach contributes to defining the most appropriate therapeutic strategy for each clinical and anatomical profile.

During subsequent phases, new transcatheter replacement devices are expected to be introduced and expanded in Brazil, for example, EVOQUE (Edwards Lifesciences), which has already been approved in Europe (CE Mark in October 2023) and recently authorized by the United States Food and Drug Administration in February 2024. With its self-expandable design, multiple sizes, and transfemoral delivery, EVOQUE represents a viable alternative for cases with anatomy that is unfavorable to T-TEER.

Even though the initial results from the pivotal TRISCEND II study indicated a reduction in the degree of TR and functional improvement with implantation of the EVOQUE prosthesis, it will be necessary to monitor the device's performance regarding safety, durability, and clinical outcomes in local populations. The eventual incorporation of this technology into the Brazilian scenario should be accompanied by training programs and structured assessment protocols in order to ensure appropriate application to clinical and institutional realities.[13]

Conclusion

Appropriate selection of candidates for percutaneous tricuspid valve intervention requires a systematic echocardiographic approach, focused on the functional and morphological analysis of the valve complex and its adjacent structures. Characterizing leaflet anatomy, identifying points of effective coaptation, quantifying the degree of tethering, and assessing annulus dimensions are important steps in determining technical viability and expected clinical benefit. The integrated use of multiplanar windows and 3D reconstructions, when available, enhances diagnostic accuracy and contributes to individualized therapeutic planning. Accordingly, echocardiographic assessment has become not only a diagnostic tool but also a relevant step in the decision-making process for transcatheter tricuspid valve therapies.

Author Contributions

Conception and design of the research: Souza AC. Acquisition of data: Souza AC. Analysis and interpretation of the data: Silva H. Writing of the manuscript: Souza AC, Silva H. Critical revision of the manuscript for intellectual content: Felix AS.

Potential conflict of interest

No potential conflict of interest relevant to this article was reported.

Sources of funding

There were no external funding sources for this study.

Table 3 – Anatomical, technical, and clinical considerations for selecting between percutaneous edge-to-edge repair and orthotopic valve replacement strategies in the management of tricuspid regurgitation

	Edge-to-edge repair	Orthotopic replacement
Tricuspid valve anatomic considerations		
Flail or prolapse	Device appropriate	Device appropriate
CIED-related TR	Device not appropriate or use with caution	Device appropriate
No alternative pacing option possible (in cases of pacemaker dysfunction or impossibility of implantation)	Use with caution	Device not appropriate or use with caution
Coaptation gap > 10 mm	Device not appropriate or use with caution	Device appropriate
Tethering > 10 mm	Device not appropriate or use with caution	Device appropriate
> 3 leaflets	Use with caution	Device appropriate
Thick, short, or immobile leaflets	Device not appropriate	Device appropriate
Torrential TR	Use with caution	Device appropriate
Device-specific considerations		
Large valve annulus	Device appropriate	Use with caution
Small RV dimensions	Device appropriate	Use with caution
RV systolic dysfunction	Use with caution	Device not appropriate or use with caution
Suboptimal access or trajectory	Device not appropriate or use with caution	Device not appropriate or use with caution
Other considerations		
Contraindication to anticoagulation or high bleeding risk	Device appropriate	Device not appropriate or use with caution
Inadequate transesophageal echocardiography images	Device not appropriate or use with caution	Use with caution

Adapted from Madhavan et al.[12] CIED: cardiac implantable electronic device: RV: right ventricular; TR: tricuspid regurgitation.

Study association

This study is not associated with any thesis or dissertation work.

Ethics approval and consent to participate

This article does not contain any studies with human participants or animals performed by any of the authors.

Use of Artificial Intelligence

The authors did not use any artificial intelligence tools in the development of this work.

Data Availability

The underlying content of the research text is contained. within the manuscript.

References

1. Dahou A, Levin D, Reisman M, Hahn RT. Anatomy and Physiology of the Tricuspid Valve. JACC Cardiovasc Imaging. 2019;12(3):458-68. doi: 10.1016/j.jcmg.2018.07.032.
2. Pena JLB, Vieira MLC, editors. Ecocardiografia e Imagem Cardiovascular. Rio de Janeiro: Thieme Revinter; 2021.
3. Muraru D, Hahn RT, Soliman OI, Faletra FF, Basso C, Badano LP. 3-Dimensional Echocardiography in Imaging the Tricuspid Valve. JACC Cardiovasc Imaging. 2019;12(3):500-15. doi: 10.1016/j.jcmg.2018.10.035.
4. Jost ZT, Nooli NP, Ali AE, Jaganathan V, Nanda NC. Three-Dimensional Echocardiography of the Tricuspid Valve. Front Cardiovasc Med. 2023;10:1114715. doi: 10.3389/fcvm.2023.1114715.
5. Badano LP, Tomaselli M, Muraru D, Galloo X, Li CHP, Marsan NA. Advances in the Assessment of Patients with Tricuspid Regurgitation: A State-of-the-Art Review on the Echocardiographic Evaluation Before and After Tricuspid Valve Interventions. J Am Soc Echocardiogr. 2024;37(11):1083-102. doi: 10.1016/j.echo.2024.07.008.

6. Hahn RT, Weckbach LT, Noack T, Hamid N, Kitamura M, Bae R, et al. Proposal for a Standard Echocardiographic Tricuspid Valve Nomenclature. JACC Cardiovasc Imaging. 2021;14(7):1299-305. doi: 10.1016/j.jcmg.2021.01.012.

7. Stankovic I, Daraban AM, Jasaityte R, Neskovic AN, Claus P, Voigt JU. Incremental Value of the en Face View of the Tricuspid Valve by Two-Dimensional and Three-Dimensional Echocardiography for Accurate Identification of Tricuspid Valve Leaflets. J Am Soc Echocardiogr. 2014;27(4):376-84. doi: 10.1016/j.echo.2013.12.017.

8. Sugiura A, Tanaka T, Kavsur R, Öztürk C, Vogelhuber J, Wilde N, et al. Leaflet Configuration and Residual Tricuspid Regurgitation after Transcatheter Edge-to-Edge Tricuspid Repair. JACC Cardiovasc Interv. 2021;14(20):2260-70. doi: 10.1016/j.jcin.2021.07.048.

9. Hahn RT, Lawlor MK, Davidson CJ, Badhwar V, Sannino A, Spitzer E, et al. Tricuspid Valve Academic Research Consortium Definitions for Tricuspid Regurgitation and Trial Endpoints. J Am Coll Cardiol. 2023;82(17):1711-35. doi: 10.1016/j.jacc.2023.08.008.

10. American Society of Echocardiography. Key Echocardiographic Considerations for Transcatheter Edge-to-Edge Repair of the Tricuspid Valve (TriClip): Eligibility Criteria. J Am Soc Echocardiogr. 2023;36(11):1090-105. doi:10.1016/j.echo.2023.08.012.

11. Hungerford SL, Rye EE, Hansen PS, Bhindi R, Choong C. Key Echocardiographic Considerations for Tricuspid Valve Transcatheter Edge-to-Edge Repair. J Am Soc Echocardiogr. 2023;36(4):366-380.e1. doi: 10.1016/j.echo.2023.01.013.

12. Madhavan MV, Agarwal V, Hahn RT. Transcatheter Therapy for the Tricuspid Valve: A Focused Review of Edge-to-Edge Repair and Orthotopic Valve Replacement. Curr Cardiol Rep. 2024;26(6):459-74. doi: 10.1007/s11886-024-02051-4.

13. Hahn RT, Makkar R, Thourani VH, Makar M, Sharma RP, Haeffele C, et al. Transcatheter Valve Replacement in Severe Tricuspid Regurgitation. N Engl J Med. 2025;392(2):115-26. doi: 10.1056/NEJMoa2401918.

Review Article

Role of Transthoracic Echocardiography in Percutaneous Closure of Ventricular Septal Defect

João Batista Masson Silva,[1,2] *Cloves Geraldino da Silva Junior*[2,3]
Universidade Federal de Goiás (UFG),[1] *Goiânia, GO – Brazil*
Hospital das Clínicas da Universidade Federal de Goiás (UFG), Empresa Brasileira de Serviços Hospitalares (EBSERH),[2] *Goiânia, GO – Brazil*
Clínica MEDCORE,[3] *Goiânia, GO – Brazil*

Abstract

Ventricular septal defect (VSD) is the most common congenital heart defect, and its management has evolved with percutaneous closure, a minimally invasive alternative to surgery. In this context, echocardiography has established itself as the primary imaging tool, crucial in all phases of the procedure. Transthoracic echocardiography (TTE) is essential for diagnosis, anatomical classification (perimembranous, muscular, inlet and outlet), initial hemodynamic assessment, and long-term follow-up. Indication for closure is based on such criteria as the left ventricular (LV) volume overload, with Qp:Qs ≥ 1.5:1. For detailed planning and intraprocedural guidance, transesophageal echocardiography (TEE), especially with three-dimensional (3D) reconstruction, is the gold standard. 3D TEE offers an accurate measurement of defect diameters, a border analysis for safe device anchorage, and an assessment of the relationship with adjacent structures, such as the aortic and tricuspid valves. The success of the intervention, both in congenital VSDs and in the rare and complex post-infarction VSDs, depends directly on the quality of the echocardiographic evaluation. The multimodal approach, which integrates TTE and TEE, ensures appropriate patient selection and safe procedure management, optimizing outcomes and expanding the realms of percutaneous VSD treatment.

Introduction

Ventricular septal defect (VSD) is the most prevalent congenital heart defect, accounting for approximately 40% of all cardiac malformations. The global prevalence is approximately 9/1,000 live births, but the exact incidence may be underestimated due to the high frequency of spontaneous closure. The diagnosis and characterization of VSD depend on its location and hemodynamic consequences, with echocardiography being the primary tool for this assessment.[1,2]

Keywords

Ventricular Heart Septal Defects; Echocardiography; Transesophageal Echocardiography

Mailing Address: João Batista Masson Silva •
Hospital das Clínicas da Universidade Federal de Goiás (UFG). Primeira Avenida S/N. Postal Code: 74605-065. Goiânia, GO – Brazil
E-mail: jbmasson@ufg.br
Manuscript received August 25, 2025; revised September 8, 2025; accepted September 8, 2025
Editor responsible for the review: Marcelo Tavares

DOI: https://doi.org/10.36660/abcimg.20250065i

VSD classification is based on its anatomy, following the consensus of the International Society for the Nomenclature of Pediatric and Congenital Heart Diseases (*Sociedade Internacional para a Nomenclatura de Doenças Cardíacas Pediátricas e Congênitas* – ISNPCHD). VSDs are categorized into four main types, depending on their location and borders from the right ventricle (RV) perspective.[2-4]

- **Perimembranous VSD**:
  - ◇ The most common type (80% of all VSDs).
  - ◇ Located in the membranous septum (adjacent to the aortic and tricuspid valves).
  - ◇ Perimembranous VSD may extend to the inlet, outlet, or trabecular portions of the muscular septum.
  - ◇ May be associated with aortic valve leaflet prolapse (aortic regurgitation).
  - ◇ Often referred to as **infracristal** (located below the supraventricular ridge).
  - ◇ The proximity of the atrioventricular (AV) conduction system to the posteroinferior border of the perimembranous VSD makes it vulnerable to injury, with the risk of heart block, during surgery or percutaneous intervention.

- **Muscular (or trabecular) VSD**:
  - ◇ This type constitutes 5-20% of all VSDs.
  - ◇ Completely surrounded by muscle tissue.
  - ◇ They may be single or multiple ("Swiss cheese") defects.
  - ◇ This type of VSD has a high rate of spontaneous closure (up to 2/3 of muscle defects can close without intervention).

- **Outflow tract (or subarterial) VSD**:
  - ◇ Located in the RV outflow tract, adjacent to the pulmonary and aortic valves.
  - ◇ Least common type in the West (approximately 6%).
  - ◇ May represent up to 33% of cases in the Asian population.
  - ◇ Is frequently associated with aortic cusp prolapse and aortic regurgitation.
  - ◇ Also referred to as supracristal, as it is located above the supraventricular ridge.

SUMÁRIO

Central Illustration: Role of Transthoracic Echocardiography in Percutaneous Closure of Ventricular Septal Defect

1 – Diagnosis and Anatomic classification of the VSDs (2D and 3D TTE)				
Congenital				Acquired
Perimembranous	inlet	outlet	Muscular	Post-infarction
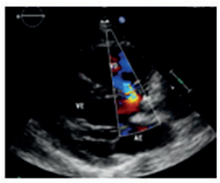	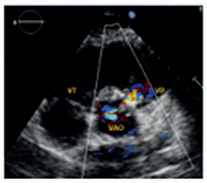	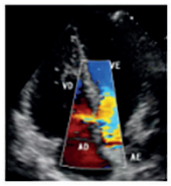	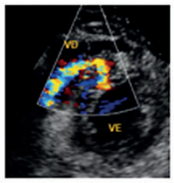	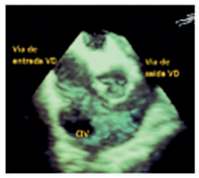
2 – Evaluation of the Hemodynamic Repercussion (2D and 3D TTE)				
QP:QS – pulmonary hyperflow	PH signs	Eisenmenger	LA and LV overload volume	
3 – Criteria for percutaneous closure (2D and 3D TEE/TTE)				
Muscular – Highly indicated	Perimenbranous – selected cases (VSD border – AO valve > 2-3 mm)	Outlet (not recommended)	Inlet (not recommended)	Pós-AMI Evaluate time of AMI, location, and tissue friability
4 – Intraoperative (2D and 3D TEE/TTE)				
Choice of Prosthesis		Implant		Pre-release
Congenital VSD – Overestimate 1-2 mm of the maximum measured diameter; Post-IM VSD – the degree of overestimation depends on tissue friability.		Evaluate: Passage of the catheters Opening of the discs Positioning of the septum		Check stability
5 – Post-release (2D and 3D TTE)				
Maintenance of positioning		Residual shunt	Reverse remodeling	

Arq Bras Cardiol: Imagem cardiovasc. 2025;38(3):e20250065

How to perform echocardiographic evaluation in a percutaneous closure of ventricular septal defect.

- **Inlet VSD (or atrioventricular canal-type):**
  - ◇ Located in the inlet of the RV (near the atrioventricular valves).
  - ◇ May be part of an atrioventricular septal defect (AVSD).
  - ◇ Less common type (approximately 8% of all VSDs).

The natural history of untreated VSDs varies considerably. Small VSDs (diameter of less than 1/3 of the aortic root diameter) and restrictive VSDs (peak pressure gradient greater than 64 mmHg), which do not cause left ventricular volume overload or pulmonary hypertension (PH), can remain asymptomatic for decades. However, an unknown percentage of patients may develop long-term complications. VSDs with large shunts can cause LV volume overload and PH, leading to ventricular dysfunction, arrhythmias, aortic regurgitation, and heart failure.[2,5]

A restrictive VSD that does not close spontaneously may be predisposed to late sequelae, such as LV dilation, arrhythmias, aortic regurgitation, PH, and endocarditis. By contrast, large and non-restrictive VSDs can lead to PH, with increased pulmonary vascular resistance (PVR), culminating in flow reversal (right-to-left shunt) and the development of Eisenmenger syndrome.[6]

Post-infarction ventricular septal defect (PIVSD) is a rare mechanical complication of acute myocardial infarction (AMI), with an incidence of approximately 0.17% to 0.34% in the reperfusion era. However, this represents a devastating condition, with mortality that can exceed 90% in the absence of intervention. The pathophysiology of the rupture results from transmural myocardial necrosis, typically occurring 3 to 5 days after the ischemic event. During this phase, inflammation and enzymatic degradation of the collagen matrix by metalloproteinases result in necrotic septal tissue, which is extremely friable and mechanically incompetent to withstand the interventricular pressure gradient. The echocardiographic report, in this context, should be more than descriptive and must be interpretive, offering the multidisciplinary team an opinion on the feasibility of anchoring the device, which directly impacts the choice between an immediate percutaneous approach or stabilization for delayed surgery.[8]

The immediate consequence is the formation of an acute left-to-right shunt, leading to biventricular volume overload, hemodynamic collapse, and often rapid progression to cardiogenic shock and multiple organ failure. The anatomical complexity of VSD is a critical factor, ranging from simple, apical defects associated with anterior infarctions to complex ruptures with serpiginous and irregular courses, located at the septal base in inferior infarctions. Therefore, detailed assessment of the defect morphology, the quality of the adjacent necrotic tissue, and its relationship to adjacent valvular structures is essential for prognosis and planning of the therapeutic approach.[8]

Transthoracic echocardiography (TTE) is the primary imaging method used for the diagnosis and characterization of VSDs, providing essential anatomical and hemodynamic assessments to guide clinical management. Three-dimensional (3D) echocardiography, in particular, enhances this assessment by allowing en face visualization of the interventricular septum, which is useful for accurate analysis of the size, shape, and relationship of the defect to adjacent structures. This technique allows for a more accurate assessment of maximum and minimum diameters, delineation of borders, and visualization of the defect's course through the septum, overcoming the limitations of two-dimensional imaging, especially in funnel-shaped VSDs. TTE can be complemented by other imaging techniques, such as transesophageal echocardiography (TEE), cardiovascular magnetic resonance (CMR), and cardiovascular computed tomography (CCT), especially in cases of complex anatomy, inadequate acoustic windows, or for a more detailed assessment of extracardiac and ventricular structures.[2,9]

Although TTE is an indispensable first-line tool for the initial diagnosis and follow-up of patients with VSD, its limitations must be recognized, especially in the adult population and in cases of complex anatomy. Suboptimal acoustic windows can compromise complete visualization of the interventricular septum, and accurate assessment of the defect's edges – particularly the aortic rim, crucial for planning percutaneous closure – can be challenging. In these scenarios, TEE becomes essential, offering superior image resolution for detailed anatomical delineation, and is considered the gold standard for intraprocedural guidance. 3D echocardiography, both transthoracic and transesophageal, further enhances this assessment by allowing en face visualization of the defect, precise measurements of its maximum and minimum diameters, and a clear understanding of its spatial relationship with the aortic and tricuspid valves. Thus, a multimodal approach is consolidated, in which TTE serves as the main diagnostic and monitoring tool, while TEE, often with 3D reconstruction, is essential for the definitive planning and safe conduct of percutaneous intervention.[2]

General criteria for indicating closure of ventricular septal defect

The decision to intervene in a VSD in adult patients is multifactorial, based on a careful assessment of the defect's anatomy, its hemodynamic repercussions, and the patient's clinical status. The main indication for VSD closure is the presence of left ventricular volume overload with a hemodynamically significant left-to-right shunt, defined by a pulmonary to systemic flow ratio (Qp:Qs) ≥1.5:1. Intervention is recommended regardless of symptoms, as long as pulmonary vascular resistance remains low (less than one-third of systemic vascular resistance [SVR] or <3 Wood Units) and pulmonary artery systolic pressure (PASP) is less than 50% of systemic systolic pressure.[9,10]

There are also specific indications that justify intervention even in the absence of significant volume overload:

- **Aortic valve dysfunction**: Surgical closure is reasonable in adults with perimembranous or supracristal VSDs that have prolapse of an aortic leaflet resulting in progressive aortic regurgitation.[10]
- **Infective endocarditis (IE)**: Closure may be considered in patients with a history of repeated episodes of infective endocarditis attributed to VSD, even if the shunt is not hemodynamically significant.[10]

The presence of pulmonary hypertension makes the decision more complex. Closure may be considered in patients with moderate PH (PVR 3–5 Wood Units or PASP ≥ 50% of systemic) if a significant left-to-right shunt (Qp:Qs > 1.5) persists. However, intervention is contraindicated in severe PH and advanced pulmonary vascular disease (Eisenmenger physiology), defined by a PVR > two-thirds of SVR (or ≥ 5 Wood Units), predominant right-to-left shunt, or oxygen desaturation during exercise.[1,9,10]

Treatment Modalities: Surgery vs. Percutaneous Intervention

Surgical closure continues to be the treatment of choice for most VSDs that require intervention, with low operative mortality and good long-term outcomes. However, percutaneous intervention has emerged as a viable and effective alternative for selected cases, avoiding the need for sternotomy and cardiopulmonary bypass.[5]

The choice of modality depends primarily on the anatomy of the defect:

- **Surgery**: This is the standard for most perimembranous, inlet, and outlet/supracristal VSDs, and for patients requiring concomitant cardiac procedures.
- **Percutaneous treatment**: This is preferred for specific defects, such as muscular VSDs, postoperative residual VSDs, and defects in difficult-to-access surgical locations.

Percutaneous Treatment: Indications and Contraindications[5,9-11]

Despite advances, percutaneous treatment of VSD has well-defined indications and limitations.

Indications:

Percutaneous closure is considered reasonable and effective in the following scenarios:

1. **Muscular VSDs**: This is the main indication, especially for defects located in the mid- or apical trabecular septum, provided there are adequate edges for device anchorage. The Amplatzer Muscular VSD Occluder is the only FDA-approved device for this purpose in the US.
2. **Postoperative residual VSDs**: This is an excellent option for treating residual shunts that persist after surgical closure.
3. **Selected perimembranous VSDs**: Although technically feasible, the percutaneous approach is controversial due to its risks. It is an option in selected cases, especially in the presence of a membranous septal aneurysm, which can facilitate device implantation and protect adjacent structures.

Contraindications and Limitations:

The main limitations of the percutaneous approach are anatomical and related to the risk of complications:

- **Defect location**: Inlet and outlet/supracristal VSDs are generally not considered suitable for device closure due to their proximity to the atrioventricular and semilunar valves.
- **Proximity to valve structures**: An inadequate distance between the defect edges and the aortic or tricuspid valves is a significant contraindication due to the risk of interfering with valve function, which may cause or worsen regurgitation.
- **Risk of complete atrioventricular block (AVB)**: This is the main concern and the greatest limitation for percutaneous closure of perimembranous VSDs due to their proximity to the cardiac conduction system. The rates of complete AVB requiring a permanent pacemaker after the procedure range from 2% to 22%, a considerably higher risk than with surgery.
- **Hemodynamic contraindications**: The same ones that apply to surgery, such as the presence of severe PH with elevated PVR and right-to-left shunt (Eisenmenger syndrome), are absolute contraindications for percutaneous closure.

Selecting the appropriate device is critical to the success of the procedure and depends on the specific anatomy of the defect. Table 1 summarizes the main available devices and their indications.

Detailed Echocardiographic Analysis for Percutaneous Closure of VSDs[3,4,10,11]

Echocardiography is the core and crucial imaging modality that governs all phases of percutaneous closure of VSDs, from strategic planning to confirmation of therapeutic success and long-term follow-up. The technical rigor of the evaluation and the choice of echocardiographic modality (transthoracic vs. transesophageal; 2D vs. 3D) are tailored to the etiology of the defect – congenital or post-myocardial infarction – and the phase of patient management.[3]

Pre-procedure Assessment: Anatomical and Hemodynamic Mapping for Therapeutic Decision-making

The pre-procedure phase is crucial in determining the feasibility of the percutaneous approach, selecting the ideal device, and anticipating technical challenges.

Congenital VSD (elective planning):

2D transthoracic echocardiography (TTE) with Doppler is the first-line tool for diagnosis and initial evaluation. Technical analysis should include:

- **Anatomical mapping**: Using multiple views (parasternal, apical, subcostal), the TTE classifies the type of VSD (perimembranous, muscular, outlet, inlet), defines the number of defects, and measures their diameter in at least two orthogonal planes.
- **Hemodynamic assessment**: The indication for closure is confirmed by shunt quantification. The pulmonary to systemic flow ratio (Qp/Qs) is calculated, and a value ≥ 1.5 is considered hemodynamically significant. Right ventricular systolic pressure (RVSP) is estimated by the VSD jet velocity or tricuspid regurgitation velocity, using the simplified Bernoulli equation ($\Delta P = 4v2$). Left ventricular volume overload is quantified by measuring its diameters and volumes.

2D, and especially 3D, transesophageal echocardiography (TEE) is essential for detailed planning of percutaneous interventions, especially in adults or when the TTE window is suboptimal. 3D TEE offers technical superiority for:

- **Accurate sizing**: 3D TEE allows for the projection of an en face view of the defect, enabling an accurate measurement of maximum and minimum diameters, regardless of its spatial orientation. This is crucial for complex or oval-shaped defects, where 2D imaging may underestimate the maximum diameter, leading to the selection of an undersized device and the risk of embolization.
- **Edge analysis**: 3D TEE allows for simultaneous visualization of all defect edges, providing a clear spatial assessment of the "anchoring zone." Measurement of the aortic edge is mandatory; a deficient edge (<2-3

Table 1 – Main devices used for percutaneous closure of ventricular septal defect

Prosthesis Model	Defect Type (Anatomical Location)	Specific Clinical Recommendations	Prosthesis Diameters (Waist / Discs)
Amplatzer™ Muscular VSD Occluder 	**Congenital Muscular VSD:** Muscular portion of the septum (apical, mid-septal, anterior). May be used to treat multiple defects ("Swiss cheese").	Patients with complex and significantly sized muscular VSD, who are considered high risk for conventional surgery.	**Belt Diameter:** 4-18 mm **Disc Diameter:** 9-26 mm **Disc Separation Height:** 7 mm
Amplatzer™ P.I. Muscular VSD Occluder 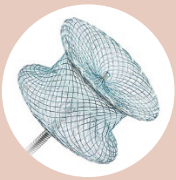	**Muscular VSD Post-Acute Myocardial Infarction (Post-AMI):** Defects that arise as a complication of an infarction.	Closure of post-AMI muscular VSDs in patients who are not satisfactory surgical candidates. This is contraindicated for congenital or perimembranous defects.	**Belt Diameter:** 16-24 mm **Disc Diameter:** 26-34 mm **Disc Separation Height:** 10 mm
Amplatzer™ Membranous VSD Occluder 	**Perimembranous VSD:** The most common type of VSD, located in the thin, membranous portion of the septum, near the heart valves.	Closure of perimembranous VSDs with significant hemodynamic repercussions. The asymmetric design seeks to avoid compression of the aortic and tricuspid valves.	**Belt Diameter:** 4-12 mm **Disc Diameters (Right):** 8-16 mm **Disc Diameters (Left):** 10-18 mm **Disc Separation Height:** 3 mm
Cera™ / CeraFlex™ VSD Occluders  **Perimembranous**  **Congenital muscular**  **Muscle post-AMI**	**Muscular and Perimembranous VSD:** Specific models are available for both types. For perimembranous defects, symmetrical, asymmetrical, and eccentric designs are available to adapt to complex anatomy.	Recommended for percutaneous closure of muscular and perimembranous VSDs. The variety of geometries for membranous defects allows for more precise selection to protect adjacent cardiac structures.	**Belt Diameter:** 4-24 mm **Disc Diameters:** Vary by model, from 8 mm to 31.6 mm **Disc Separation Height:** 3 mm

KONAR-MF™ VSD Occluder

Perimembranous and Muscular VSD:

Designed to be versatile, treating both types of defects, with a special focus on perimembranous defects.

Recommended for complex cases in which flexibility and low radial force are key to minimizing the risk of atrioventricular block (AVB). It is also a viable option for young children (<10 kg).

Belt Diameter (Right/Left):
3-12 mm / 5-14 mm

Disc Diameter:
10-18 mm

Cocoon® VSD Occluder

Muscular and Perimembranous VSD:

The availability of multiple waist lengths (4 mm, 7 mm, and 10 mm) makes the device adaptable to septal defects of varying thicknesses.

Occlusion of hemodynamically significant VSDs. The variety of waist sizes allows the physician to choose the prosthesis that best fits the thickness of the septum, whether muscular (thicker) or membranous (thinner).[6]

Belt Diameter:
3,25-12 mm

Disc Diameter:
10-18 mm

MemoPart™ VSD Occluder

Muscular

Muscular

Muscular and Perimembranous VSD:

Offers different models for each type of defect.

The recommendations are similar to those of the Amplatzer line.

The muscular model is for high-risk surgical patients, and the membranous model is for minimally invasive closure of perimembranous VSDs.

Belt Diameter:
4-20 mm

Disc Diameter E :
8-26 mm

Disc Diameter 4:
8-24 mm

Disc Separation Height:
2,6 - 7 mm

Perimembranous

mm) requires the use of an asymmetrically designed device to avoid interference with the aortic valve. The rule of thumb for device sizing is that its waist should be 1-2 mm larger than the maximum defect diameter.

Post-myocardial infarction VSD:

In this scenario, echocardiography is an emergency tool for diagnosis and risk stratification in a critically ill patient.

- **2D transthoracic echocardiography (TTE)**: This is the modality of choice for rapid bedside diagnosis. Its technical objectives are to confirm septal rupture with color Doppler, assess biventricular function, and, primarily, rule out other mechanical complications, such as papillary muscle or free wall rupture.
- **2D and 3D transesophageal echocardiography (TEE)**: This is essential for detailed anatomical characterization. Post-AMI VSD typically has an irregular and serpiginous course. 3D TEE is superior in assessing the quality of the surrounding tissue, identifying the extent of necrotic and friable myocardium, which is the main determinant of the viability of percutaneous device anchorage. Assessment of right ventricular function is of paramount prognostic importance, given the sudden volume and pressure overload.

  In the evaluation of post-infarction VSD, echocardiography transcends simple defect identification, assuming a key prognostic and strategic planning role. The echocardiographer's main priority is to assess the quality of the adjacent tissue, as the pathophysiology of the rupture involves transmural necrosis, resulting in an extremely friable and mechanically incompetent myocardium. TEE, especially with 3D imaging, is superior to TTE for this analysis, enabling a detailed characterization of the extent of necrosis and the integrity of the defect's edges. A wide, fragile edge is a strong predictor of percutaneous closure failure, increasing the risk of complications, including device embolization. Therefore, detailed echocardiographic assessment of the rupture morphology and the viability of the surrounding septal tissue is the determining factor in deciding whether a patient is a viable candidate for a percutaneous approach or whether hemodynamic stabilization for delayed surgery, allowing fibrotic maturation of the defect, would be the best strategy.[12]

Intraprocedural Assessment: Guiding the Intervention and Prosthesis Sizing[4,5,10,11]

Intraprocedural echocardiography is the cornerstone of implant safety and accuracy. Transesophageal echocardiography is traditionally considered the gold standard and the most widely used modality to guide the procedure, often described as "the interventionist's eye." Its superiority lies in its high image resolution, especially for posterior structures, and its ability to accurately assess defect edges and valve function, making it crucial in patients with limited transthoracic acoustic windows. In Brazil, most studies and position papers from societies such as the Brazilian Society of Cardiology (SBC) and the Brazilian Society of Cardiology (SBHCI) describe the procedure as being performed under TEE monitoring.

Regardless of the chosen modality, the role of intraprocedural echocardiography is multifaceted and governs the critical stages of the intervention:

- **Final prosthesis sizing**: Echocardiography (primarily TEE) performs the final and definitive measurement of the defect under the hemodynamic conditions of the procedure. The rule of thumb is to select a device whose waist is 1 to 2 mm larger than the maximum measured diameter to ensure secure anchorage. In post-AMI VSD, due to tissue friability, "significant oversizing" is often recommended. It is crucial to note that, unlike congenital VSDs, this "significant oversizing" is a qualitative, not quantitative, concept; the final decision depends on the intraprocedural assessment of defect morphology and tissue integrity, guided by the operator's experience rather than a fixed formula. It is important to note that the balloon sizing technique, common in ASD closure, is not used for VSDs due to the inelastic nature of the septum and the risk of widening the rupture in post-AMI cases.
- **Guidance and positioning**: Echocardiographic imaging actively guides every step, from the safe passage of guidewires and sheaths through the defect, avoiding injury to adjacent structures, such as the tricuspid valve chordae tendineae, to monitoring the sequential opening of the prosthesis discs and their correct positioning in the interventricular septum.
- **Pre-release critical evaluation**: Before definitive detachment of the prosthesis, echocardiography performs a crucial safety check, a true "point of no return." At this stage, the stability of the device, the presence of significant residual shunt, and, primarily, the absence of new aortic and tricuspid valve dysfunction are assessed.

Although TEE is the standard, TTE has emerged as a viable and effective alternative for guiding the entire procedure in selected cases. Studies have shown that, in patients with a good acoustic window (often children and young adults), TTE-only guidance can achieve success rates and residual shunt that are similar to TEE. The advantages of using TTE include the elimination of general anesthesia and intubation, as well as reduced procedure and fluoroscopy time. However, this approach is selective and requires considerable operator expertise, as it is best suited for patients weighing more than 10 kg and with defects smaller than 8 mm.

More recently, intracardiac echocardiography (ICE) has emerged as a promising emerging technology for procedural guidance. ICE also eliminates the need for general anesthesia and, in some cases, can offer superior visualization of certain defect edges when compared to TEE. Its adoption represents a significant advance in making percutaneous closure an even less invasive procedure.

Post-procedure Evaluation: Monitoring the Therapeutic Outcome

Post-procedure follow-up assesses the success of the intervention and monitors long-term progress.

- **2D transthoracic echocardiography and Doppler**: This is the primary modality for follow-up.
- **Immediate (pre-discharge) assessment**: A TTE is performed to confirm stable prosthesis position, quantify any immediate residual shunt, and rule out acute complications, such as pericardial effusion.
- **Short-term and long-term follow-up**: Serial echocardiographic follow-up (e.g., at 1, 6, and 12 months, and then every 2–5 years if stable) is recommended to monitor complete shunt occlusion (as device endothelialization occurs), ventricular function and remodeling (normalization of chamber dimensions), and valve function, as well as to detect late complications. Patients with significant residual findings require more frequent follow-up.

To emphasize the multifaceted role of echocardiography throughout the process, the Central Illustration presents a flowchart summarizing the main steps of the assessment.

Conclusion

Percutaneous closure of VSDs has established itself as an effective alternative to surgery in selected cases, and echocardiography is the core and crucial imaging modality in all phases of this procedure. Transthoracic echocardiography has established itself as the primary tool for diagnosis, classification, initial hemodynamic assessment, and long-term follow-up. However, for detailed intervention planning and, especially, intraprocedural guidance, TEE, especially with 3D technology, is the gold standard, ensuring the precision and safety necessary for therapeutic success. Careful patient selection, detailed anatomical characterization, and rigorous monitoring of adjacent structures, all guided by echocardiography, are the pillars that allow us to expand the realms of minimally invasive VSD treatment, in turn optimizing patient outcomes.

Challenges and future perspectives6

Despite remarkable advances, the field of percutaneous VSD closure still faces significant challenges that direct future innovations.

1. **Reducing the risk of atrioventricular block**: The main obstacle to the widespread adoption of percutaneous closure in perimembranous VSDs continues to be the risk of complete AV block. Future research should be focused on developing prostheses with more flexible designs and lower radial force, such as the *Nit-Occlud Lê VSD Coil* and the *KONAR-MF™ VSD Occluder*, which aim to minimize trauma to the conduction system.
2. **Improving imaging and guidance**: Although TEE is the standard, ICE is emerging as a promising alternative that eliminates the need for general anesthesia, potentially reducing procedure time and risk. The integration of fusion imaging, combining fluoroscopy and real-time echocardiography, as well as the development of artificial intelligence software to aid in implant sizing and simulation, are the next steps to further increase accuracy and safety.
3. **Development of bioresorbable devices**: The most transformative long-term prospect is the creation of fully bioresorbable occluders. Currently, research in this area is most advanced for the closure of low-pressure defects, such as atrial septal defects (ASD), with devices like the Carag Bioresorbable Septal Occluder already being used in clinical trials. Expanding this technology to VSDs is the next major challenge. This will require the development of polymers with greater mechanical strength, capable of withstanding the high interventricular pressure gradient and high shear stress, ensuring structural stability during the absorption and endothelialization process. Successful development of such devices would eliminate the risks associated with permanent implants, such as erosion and late thrombosis, representing the next frontier in the treatment of congenital heart disease.

Author Contributions

Conception and design of the research: Masson-Silva JB. Writing of the manuscript: Masson-Silva JB, Silva Junior CG. Critical revision of the manuscript for intellectual content: Masson-Silva JB, Silva Junior CG.

Potential conflict of interest

No potential conflict of interest relevant to this article was reported.

Sources of funding

There were no external funding sources for this study.

Study association

This study is not associated with any thesis or dissertation work.

Ethics approval and consent to participate

This article does not contain any studies with human participants or animals performed by any of the authors.

Use of Artificial Intelligence

During the preparation of this work, the author(s) used Gemini for grammar and agreement corrections in Portuguese, as well as for assistance with translations from other languages. After using this tool/service, the author(s) reviewed and edited the content as needed and take full responsibility for the content of the published article.

Data Availability

The underlying content of the research text is contained within the manuscript.

References

1. Sachdeva R, Valente AM, Armstrong AK, Cook SC, Han BK, Lopez L, et al. ACC/AHA/ASE/HRS/ISACHD/SCAI/SCCT/SCMR/SOPE 2020 Appropriate Use Criteria for Multimodality Imaging during the Follow-Up Care of Patients with Congenital Heart Disease: A Report of the American College of Cardiology Solution Set Oversight Committee and Appropriate Use Criteria Task Force, American Heart Association, American Society of Echocardiography, Heart Rhythm Society, International Society for Adult Congenital Heart Disease, Society for Cardiovascular Angiography and Interventions, Society of Cardiovascular Computed Tomography, Society for Cardiovascular Magnetic Resonance, and Society of Pediatric Echocardiography. J Am Coll Cardiol. 2020;75(6):657-703. doi: 10.1016/j.jacc.2019.10.002.
2. Fusco F, Borrelli N, Palma M, Sarubbi B, Scognamiglio G. Imaging of Ventricular Septal Defect: Native and Post-Repair. Int J Cardiol Congenit Heart Dis. 2022;7:100335. doi: 10.1016/j.ijcchd.2022.100335.
3. Nayak S, Patel A, Haddad L, Kanakriyeh M, Varadarajan P. Echocardiographic Evaluation of Ventricular Septal Defects. Echocardiography. 2020;37(12):2185-93. doi: 10.1111/echo.14511.
4. Tripathi RR. Ventricular Septal Defect: Echocardiography Evaluation. J Indian Acad Echocardiogr Cardiovasc Imaging. 2020;4(3):260-6. doi: 10.4103/jiae.jiae_42_20.
5. Turner ME, Bouhout I, Petit CJ, Kalfa D. Transcatheter Closure of Atrial and Ventricular Septal Defects: JACC Focus Seminar. J Am Coll Cardiol. 2022;79(22):2247-58. doi: 10.1016/j.jacc.2021.08.082.
6. Cox K, Algaze-Yojay C, Punn R, Silverman N. The Natural and Unnatural History of Ventricular Septal Defects Presenting in Infancy: An Echocardiography-Based Review. J Am Soc Echocardiogr. 2020;33(6):763-70. doi: 10.1016/j.echo.2020.01.013.
7. David TE. Post-Infarction Ventricular Septal Rupture. Ann Cardiothorac Surg. 2022;11(3):261-7. doi: 10.21037/acs-2021-ami-111.
8. Kurniawan A, Yogibuana V. Percutaneous Closure of Post-Infarction Ventricular Septal Rupture: A Review of Patient Selection, Techniques and Outcomes. Asian J Res Cardio Dis. 2025;7(1):191-210. doi: 10.9734/ajrcd/2025/v7i1131.
9. Stout KK, Daniels CJ, Aboulhosn JA, Bozkurt B, Broberg CS, Colman JM, et al. 2018 AHA/ACC Guideline for the Management of Adults with Congenital Heart Disease: A Report of the American College of Cardiology/American Heart Association Task Force on Clinical Practice Guidelines. Circulation. 2019;139(14):e698-e800. doi: 10.1161/CIR.0000000000000603.
10. Baumgartner H, De Backer J, Babu-Narayan SV, Budts W, Chessa M, Diller GP, et al. 2020 ESC Guidelines for the Management of Adult Congenital Heart Disease. Eur Heart J. 2021;42(6):563-645. doi: 10.1093/eurheartj/ehaa554.
11. Aboulhosn JA, Hijazi ZM. Transcatheter Interventions in Adult Congenital Heart Disease. Cardiol Clin. 2020;38(3):403-16. doi: 10.1016/j.ccl.2020.04.005.
12. Shafiei I, Jannati F, Jannati M. Optimal Time Repair of Ventricular Septal Rupture Post Myocardial Infarction. J Saudi Heart Assoc. 2020;32(2):288-94. doi: 10.37616/2212-5043.1120.

3D Printing of a Heart With Amyloidosis

Mariana de Paula Cruz,[1,2] Davi Shunji Yahiro,[1] Daniel Gama das Neves,[1] Renato Pereira Barbosa,[1] Alexandre Todorovic Fabro,[3] Pedro Manoel Marques Garibaldi,[3] Marcus Simões,[3] Claudio Tinoco Mesquita[1]

Universidade Federal Fluminense,[1] Niterói, RJ – Brazil

Health, Science & Education Lab, Radiology Department, Hospital Universitário Antônio Pedro, EBSERH,[2] Niterói, RJ – Brazil

Universidade de São Paulo,[3] Ribeirão Preto, SP – Brazil

Abstract

Cardiac Amyloidosis is a restrictive cardiomyopathy caused by the accumulation of amyloid protein in the heart. The advances in non-invasive diagnosis have been increasing its identification among patients with Heart Failure (HF), being previously considered to be a rare condition. Currently, it represents around 13% of the cases of Heart Failure with preserved Ejection Fraction (HFpEF). We report the case of a 72-year-old male patient who presented to the clinic reporting dyspnea and fatigue in low-effort activities. Laboratory exams were conducted, revealing increased cardiac markers, along with evidence of ventricular hypertrophy in electrocardiographic analysis. Cardiac imaging, serum free light chain (AL) assay, and endomyocardial biopsy indicated the diagnosis of AL amyloidosis. A three-dimensional model was constructed using magnetic resonance imaging (MRI) data. This model is intended to increase the awareness around amyloidosis as a possible differential diagnosis of HF, while also promoting patients' and families' education, demonstrating the typical structural abnormalities of the disease.

Introduction

Cardiac amyloidosis results from disorders in the folding of amyloidogenic proteins, leading to the formation of insoluble amyloid fibrils that accumulate in the extracellular matrix of the heart.[1] The most common variants are primary or light chain (AL) and transthyretin-related (ATTR) amyloidosis. AL amyloidosis is caused by the deposition of ALs of immunoglobulin, produced in excess by normal or malignant plasma cells.[2] Cardiac manifestations of amyloidosis include Heart Failure with preserved Ejection Fraction (HFpEF), arrhythmias, angina with non-obstructive coronary lesions, and thromboembolic events. Some cases of cardiac amyloidosis are associated with aortic stenosis, particularly in cases with low flow and low gradient.[3] The three-dimensional printing has been widely explored in the healthcare field for various applications, ranging from the production of surgical parts to educational models. This tool has stood out for allowing the creation of patient-specific materials, which aid in the study and understanding of complex pathological anatomies. We report a case of AL cardiac amyloidosis in which 3D printing was used to model the affected organ. This modeling was intended to increase the awareness of amyloidosis as a possible differential diagnosis of heart failure (HF) with preserved ejection fraction, while also promoting patients' and families' education.

Keywords

Amyloidosis; Heart Failure; Three-Dimensional Printing; Magnetic Resonance Imaging.

Mailing Address: Mariana de Paula Cruz •
Universidade Federal Fluminense. Avenida Marques do Paraná, 349. Postal code: 24030215. Niterói, RJ – Brazil
E-mail: m_cruz@id.uff.br
Manuscript received January 17, 2025, revised manuscript May 30, 2025, accepted July 27, 2025
Editor responsible for the review: Isabela Costa

DOI: https://doi.org/10.36660/abcimg.20250003i

Description

A 72-year-old male patient with a previous history of myocardial infarction presented to the cardiology department with progressive dyspnea and fatigue on exertion for the past year. He reported worsening over the last two months, affecting his usual activities, along with orthopnea, blurred vision, dizziness, and a sensation of imminent fainting upon standing. Physical examination revealed postural hypotension, lower limb edema (++/4), as well as distal hypoesthesia and hypopallesthesia. Cardiac auscultation revealed a holosystolic murmur at the tricuspid focus, with P2 hyperphonesis. Laboratory tests showed proteinuria (+++/4) in routine urine analysis, along with elevated cardiac markers NT-ProBNP and Troponin I, with no further abnormalities. An electrocardiogram indicated left ventricular hypertrophy and left anterior fascicular block. The evaluation was followed by an echocardiogram, which showed thickening of the right ventricle, interventricular septum, and valves. The Global Longitudinal Strain (GLS) displayed an apical sparing pattern. The ratio between the left ventricular ejection fraction (LVEF) and the GLS was elevated, suggesting cardiac amyloidosis. New suggestive findings were observed in Magnetic Resonance Imaging (MRI), which showed diffuse subendocardial late enhancement and confirmed the thickening of the chambers (Figure 1).

With the suspicion established, the investigation proceeded with the assays of free ALs of immunoglobulins. The results were as follows: free light kappa chain 18.1 mg/dL (6.7–22.4), lambda chain 168.4 mg/dL (8.3–27), with a ratio of Kappa to Lambda chains (K/L) of 0,11 (0.31-1.56). The finding of K/L ratio below the reference value is highly suggestive of AL Amyloidosis, due to the deposition of lambda ALs. Bone marrow and skin/subcutaneous biopsies did not show any infiltrations. An endomyocardial biopsy was performed (Figure 2), stained with Congo Red, which exhibited characteristic birefringence of amyloid infiltration under polarized light (Figure 3). Mass spectrometry confirmed the AL typing. The patient had clinical improvement after AL Amyloidosis-specific treatment.

Discussion

AL Amyloidosis

AL Amyloidosis, also known as primary amyloidosis, is the most common form of the disease among systemic variants. It

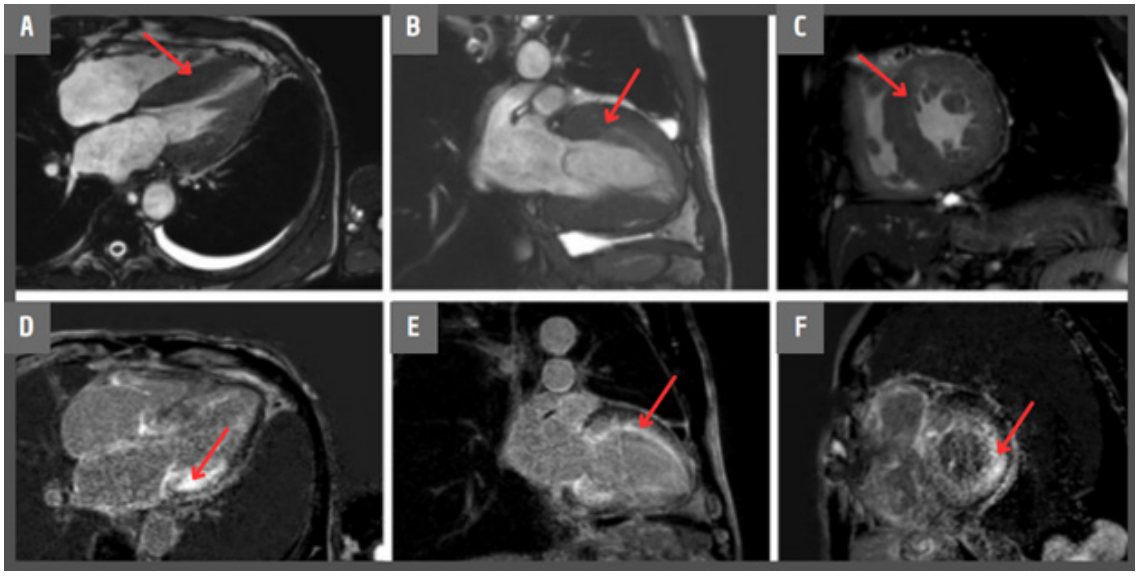

Figure 1 – *MRI showing thickening of the ventricular walls (panels A, B, and C) and diffuse late enhancement patterns in gadolinium contrast (shown in panels D, E, and F). This pattern arises from a difference in contrast uptake throughout cardiac tissue and may be found in various myocardial injuries.*

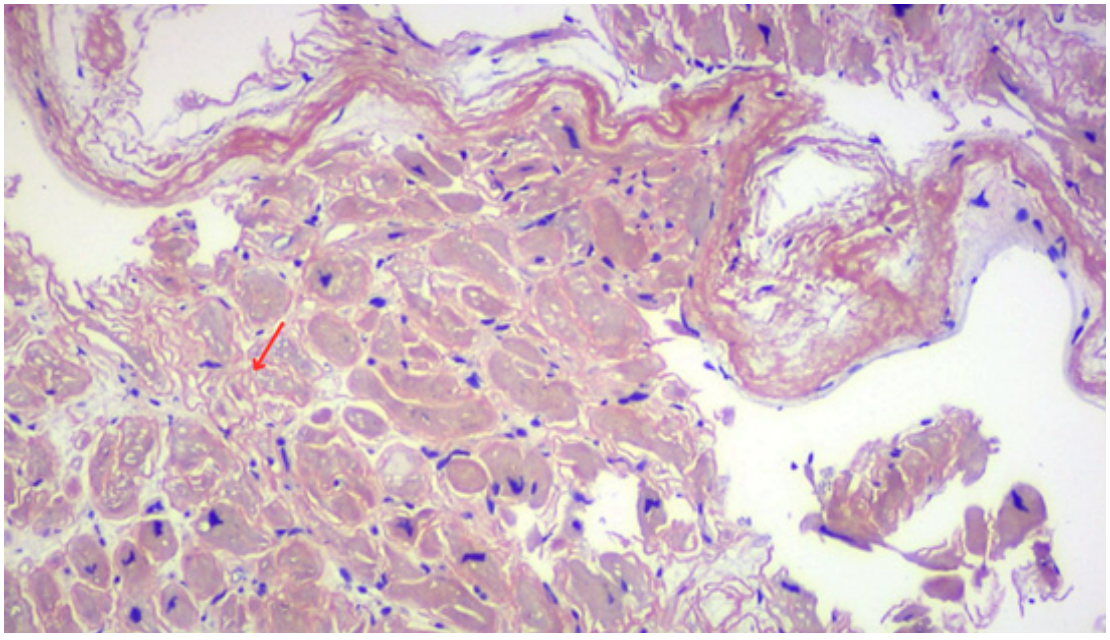

Figure 2 – *Endomyocardial biopsy of the left ventricle, stained with Congo Red, showing subtle red coloring of the amyloid protein deposits. Evaluation under polarized light can be utilized to increase sensitivity.*

arises from the tissue deposition of AL immunoglobulins in cardiac tissue, produced excessively by normal or malignant plasma cells. It is a rare condition, with 5.1 to 12.8 cases per million person-years worldwide. The vast majority of affected patients are over 40 years old, with a median age at diagnosis of 64 years. The progression of the disease is rapid and poses significant risks when not identified early.[2] The deposition of amyloid protein is characterized by significant thickening of the ventricular walls,

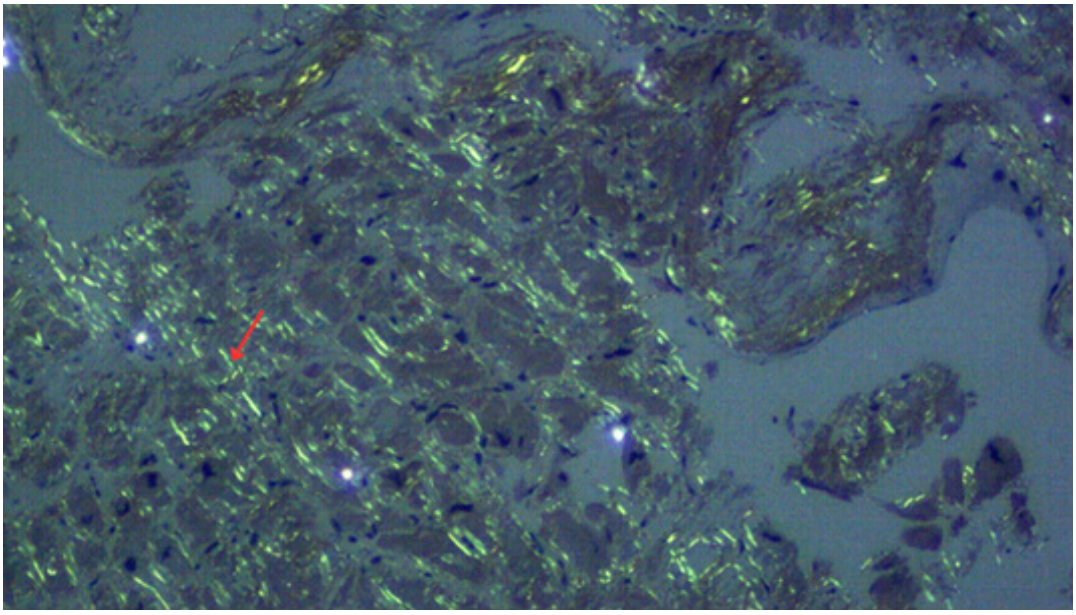

Figure 3 – *Endomyocardial biopsy of the left ventricle, stained with Congo Red, exhibiting a birefringence pattern under polarized light. The apple green birefringence is characteristically found in amyloid protein deposits, as the staining reacts with the misfolded proteins to form complexes that present optical reactivity. The polarized light evaluation enhances the sensitivity of the staining technique.*

septa, and valves, resulting in HF of a restrictive nature. Currently, cardiac amyloidosis accounts for about 13% of cases of HFpEF.[4] Diagnosis begins with the investigation of clinical findings consistent with HFpEF Symptoms may be more associated with left-sided HF (pulmonary congestion, dyspnea) or right-sided HF (edema, ascites). Other important alterations arise from amyloid infiltration in the atria, causing atrial fibrillation and other arrhythmias, and the cardiac conduction system, producing atrioventricular blocks.[5] Elevated serum levels of cardiovascular markers (especially troponin T and NT-ProBNP) should be present. The electrocardiogram of these patients typically shows low QRS voltage, inconsistent with the thickness of the ventricular wall, especially in AL Amyloidosis.

The investigation should continue with echocardiography and MRI, revealing more specific findings of the disease. The reduction in longitudinal strain with an "apical sparing" pattern is an important modification seen on echocardiography, along with thickening of the ventricles and valves. MRI may reveal a pattern of diffuse delayed enhancement using gadolinium-based contrast, with subendocardial or transmural distribution, consistent with the presence of amyloid deposits. Finally, the investigation of immunoglobulin ALs, combined with peripheral biopsy (or, if necessary, cardiac biopsy), will be conclusive for diagnosis. The assessment of ALs is best performed with the combination of three tests: immunofixation in blood and urine, which aids in their detection, and the measurement of the ratio between kappa and lambda chains, which yields a positive result when abnormal.[5]

The most important factor in determining prognosis is the extent of damage to the cardiac tissue. Understanding the physiopathology of amyloidosis and discussing its clinical and morphological manifestations are crucial for the early diagnosis of this increasingly understood yet still underrecognized condition in medical practice.

The 3D model

The three-dimensional model (Figure 4) was produced from the patient's imaging examinations (MRI). The processing of the files includes the steps of segmentation—isolating the desired anatomical structures—and slicing, which involves dividing the structure into printable layers. From these interventions, the final file (in STL format, Standard Tessellation Language) can be read by the machine as a sequence of two-dimensional planes, which are then built on top of each other by the printer (additive manufacturing). The material used in this process was plastic filament, a solid component that is melted by the machine and reshaped into the contours of the desired piece. This type of printer operates using the FDM (Fused Deposition Modeling) technique, which is the most accessible among the options for three-dimensional modeling. Filament modeling was chosen for this project to demonstrate the applicability of the technique even with the simplest forms of this technology.

The model displays the characteristic morphological changes of amyloidosis in cardiac tissue, reinforcing its similarity to the physiology of HF. Notably, there is left ventricular thickening, with a significant reduction in the ventricular lumen, as well as considerable thickening of the interventricular septum. To a lesser extent, the same modification is observed in the right ventricular wall. This type

Figure 4 – *Three-dimensional heart model with AL amyloidosis, produced using imaging data from MRI.*

of material, which has significant anatomical and pathological correspondence with the actual organ, can be applied in various contexts in medical practice. Its use for educational purposes, patient and family instruction, and especially guiding surgical approaches benefits from a more complete and consistent understanding of the studied organ structures. Furthermore, the dissemination and popularization of 3D printers have facilitated the development of more realistic and reproducible models without imposing significant financial costs.[6] Three-dimensional models can improve professional and patient education through the visual and tactile experience they allow.[7] In this regard, we emphasize the great potential for exploring this tool in the healthcare field, complementing imaging studies and possibly revealing new important information that enhances our understanding of diseases.

Author Contributions

Conception and design of the research: Cruz MP, Yahiro DS, Simões MV, Mesquita CT. Acquisition of data: Cruz MP, Yahiro DS, Neves DG, Barbosa RP, Fabro AT, Garibaldi PMM. Analysis and interpretation of the data: Cruz MP, Yahiro DS. Writing of the manuscript: Cruz MP, Yahiro DS. Critical revision of the manuscript for intellectual content: Cruz MP, Yahiro DS, Simões MV, Mesquita CT.

Potential Conflict of Interest

No potential conflict of interest relevant to this article was reported.

Sources of Funding

This study was partially funded by Fundação Carlos Chagas Filho de Amparo à Pesquisa do Estado de Rio de Janeiro (FAPERJ) and Conselho Nacional de Desenvolvimento Científico e Tecnológico (CNPq).

Study Association

This article is part of Mariana de Paula Cruz's Final Course Project at the Federal Fluminense University (UFF).

Ethics Approval and Consent to Participate

This study was approved by the Ethics Committee of the Faculty of Medicine of UFF under protocol number 6.594.419/CAAE:70417223.1.0000.5243. All the procedures in this study were in accordance with the 1975 Helsinki Declaration, updated in 2013. Informed consent was obtained from all participants included in the study.

Use of Artificial Intelligence

The authors did not use any artificial intelligence tools in the development of this work.

Availability of Research Data

All datasets supporting the results of this study are available upon request from the corresponding author: Mariana de Paula Cruz.

References

1. Porcari A, Fontana M, Gillmore JD. Transthyretin Cardiac Amyloidosis. Cardiovasc Res. 2023;118(18):3517-35. doi: 10.1093/cvr/cvac119.
2. Baker KR. Light Chain Amyloidosis: Epidemiology, Staging, and Prognostication. Methodist Debakey Cardiovasc J. 2022;18(2):27-35. doi: 10.14797/mdcvj.1070.
3. Jaiswal V, Agrawal V, Khulbe Y, Hanif M, Huang H, Hameed M, et al. Cardiac Amyloidosis and Aortic Stenosis: A State-of-the-Art Review. Eur Heart J Open. 2023;3(6):oead106. doi: 10.1093/ehjopen/oead106.
4. González-López E, Gallego-Delgado M, Guzzo-Merello G, de Haro-Del Moral FJ, Cobo-Marcos M, Robles C, et al. Wild-Type Transthyretin Amyloidosis as a Cause of Heart Failure with Preserved Ejection Fraction. Eur Heart J. 2015;36(38):2585-94. doi: 10.1093/eurheartj/ehv338.
5. Simões MV, Fernandes F, Marcondes-Braga FG, Scheinberg P, Correia EB, Rohde LEP, et al. Position Statement on Diagnosis and Treatment of Cardiac Amyloidosis - 2021. Arq Bras Cardiol. 2021;117(3):561-98. doi: 10.36660/abc.20210718.
6. Barros PHF, Borges CS, Ferreira CPDC, Hernani BL, Abreu IP Neto, Tastaldi L, et al. Hernia 3D Training Model: A New Inguinal Hernia 3D-Printed Simulator. Einstein. 2024;22:eAO0620. doi: 10.31744/einstein_journal/2024AO0620.

Late Discovery of Left Ventricular Pseudoaneurysm: A Rare Clinical Case

Angélica Pedreira da Silva,[1] *Gilson Soares Feitosa,*[1] *Gabriel de Castro Vaz Leal,*[1] *Rilson Fraga Moitinho,*[1] *Jorge Andion Torreão*[1]

Hospital Santa Izabel,[1] *Salvador, BA – Brazil*

Abstract

Left ventricular (LV) pseudoaneurysm is a rare complication of acute myocardial infarction (AMI). We report the case of a 67-year-old male patient seen in 2024. Following an AMI in 2019, the patient was diagnosed with a LV pseudoaneurysm after complaining of dyspnea and undergoing imaging tests including echocardiogram and magnetic resonance imaging. The patient underwent aneurysmectomy and revascularization surgery, progressing satisfactorily during the postoperative period.

Introduction

Left ventricular (LV) pseudoaneurysm is a clinicopathological entity that constitutes a rare mechanical complication of acute myocardial infarction (AMI).[1] It is formed when the cardiac rupture is contained by pericardium or scar tissue, without the presence of the myocardium as a tissue component.[1] It generally occurs in the inferior and posterior ventricular walls, given that ruptures of the anterior wall tend to lead to cardiac tamponade and sudden death, whereas the inferior-posterior face of the heart rests on the diaphragm, facilitating containment of the ventricular cavity by the pericardium.[2] Given its composition, there is a high risk of rupture, making surgical correction necessary.[3]

Case report

We report the case of a 67-year-old male patient, resident of the state of Bahia, Brazil, with hypertension for 10 years and diabetes for 5 years. He had been an ex-smoker for 32 years, with an estimated smoking history of 51 pack-years.

In 2019, he presented with AMI with ST-segment elevation in the anterior wall. However, he arrived at a unit with a hemodynamic service 8 days after diagnosis, without having received fibrinolytic therapy. Upon admission, he underwent coronary angiography, which showed 90% stenosis in diagonal branch and only parietal irregularities in the other coronary arteries. He underwent transluminal angioplasty and was discharged from the hospital. The patient was advised to undergo outpatient follow-up at the cardiology service, which he did not follow.

Five years later, the patient returned for a consultation requesting clearance for inguinal herniorrhaphy. He complained of dyspnea upon moderate exertion, such as walking uphill, but he stated that this symptom had been present since 2019, without progression. He denied association with chest pain or other anginal equivalents. The general surgeon reported that there was a mass in the LV on the chest tomography.

Upon physical examination, the patient had an active precordium, with an apparent, visible, and palpable apex beat in the fourth left intercostal space, between the left midclavicular line and the anterior axillary line, which was propulsive and measured 3 fingertips. The patient was using acetylsalicylic acid 100 mg/day, metoprolol succinate 50 mg every 12 hours, spironolactone 25 mg/day, atorvastatin 80 mg/day, enalapril 20 mg every 12 hours, and metformin XR 500 mg every 12 hours. The patient was admitted for diagnostic confirmation.

Radiography showed a mass adjacent to the LV (Figure 1), and electrocardiography indicated residual ST-segment elevation in the precordial leads (Figure 2).

Transthoracic echocardiography described akinesia of the middle and apical segments of the anteroseptal, anteroapical, apical LV walls and inferobasal and inferoseptal walls of the LV, in addition to the formation of a pseudoaneurysm in the inferolateral wall with important global systolic dysfunction and ejection fraction (EF) of 21%, by the Simpson method. We observed diastolic filling and tissue Doppler imaging compatible with type 3 diastolic dysfunction (restrictive pattern). The examination performed in 2019 revealed EF of 27% and segmental LV involvement with severe systolic dysfunction, with no mention of pseudoaneurysm formation.

Cardiac resonance imaging was performed, thus establishing diagnosis of LV pseudoaneurysm measuring 48 × 36 × 30 mm from the apical anterior segment, with neck size of 30 mm. Transmural late enhancement was greater than 50% throughout the apical and anteroseptal region (Figure 3).

The patient underwent a new coronary cineangiography according to the surgical intervention schedule, showing 75% stenosis in the bifurcation of the first marginal branch, 90% ostial stenosis of the second marginal branch, 75% to 90% stenosis middle third of the posterolateral branch, and 75% stenosis in the middle third of the right coronary artery (Figure 4).

The patient was referred for aneurysmectomy and revascularization of the marginal branch and the right

Keywords

False Aneurysm; Diagnostic Imaging; Post-Infarction Heart Rupture

Mailing Address: Angélica Pedreira da Silva •
Hospital Santa Izabel. Praça Conselheiro Almeida Couto. Postal code: 40050-410. Salvador, BA – Brazil
E-mail: angelica.pedreira@outlook.com
Manuscript received January 26, 2025, revised manuscript March 26, 2025, accepted April 27, 2025
Editor responsible for the review: Isabela Costa

DOI: https://doi.org/10.36660/abcimg.20250006i

coronary artery with saphenous vein graft. During surgery, the diagnosis of pseudoaneurysm was confirmed (Figure 5). During the postoperative period, he developed a stroke after an episode of atrial fibrillation with high ventricular response. Nonetheless, he was discharged approximately 7 days after the procedure without sequelae.

Discussion

AMI is the most common cause of LV pseudoaneurysm (55%). Less frequently, pseudoaneurysms occur as a complication of cardiac surgery, chest trauma, as a consequence of endocarditis, and, rarely, after suppurative pericarditis or tumor infiltration.[1,4,5]

Mechanical complications in the context of AMI are currently uncommon due to the effective implementation of early revascularization strategies. Although rare, cardiac rupture is one of the most feared events.[3] In the case of pseudoaneurysm, approximately 30% to 45% have a chance of rupture; in this context, surgical intervention can substantially reduce this risk.[1,4,5]

Some patients may present symptoms of heart failure due to LV dysfunction. However, approximately 10% are asymptomatic.[4]

Pseudoaneurysms can be detected on chest radiography as an area adjacent to the heart. On electrocardiography, there may be nonspecific repolarization changes.[6]

Echocardiography identifies changes in 90% of cases, but approximately 67% to 75% of cases are confused with aneurysm.[4,5,7] Left ventriculography, on the other hand, has been considered an important imaging modality, with a diagnostic accuracy of around 85%, given that it is possible to determine the neck of the pseudoaneurysm and the absence of surrounding coronary arteries.[3,7]

In 2005, Konen et al. assessed 22 cardiac resonance images of patients with pseudoaneurysm or LV aneurysm. Delayed enhancement of pericardium was more common in patients with pseudoaneurysm, leading to a sensitivity of 100% and specificity of 83.3%. For these patients, the end-diastolic volume was greater than in those with true aneurysm. Therefore, this test plays an important role in differentiating both pathologies.[8]

Treatment for acute and symptomatic cases is limited to surgical correction, taking patients' risks into consideration.[1]

In 1998, Yeo et al. followed 52 patients with pseudoaneurysm for approximately 4 years. The majority were diagnosed incidentally; 42 patients underwent surgical correction, and mortality reached 7%. Ten patients were treated conservatively; they did not undergo the procedure due to high risk. After 2.3 years of study, 19 patients died, 6 of them in the conservative group. There were no reports of rupture.[9,10]

Following this same model, in 2003, Moreno et al. followed 10 patients, all diagnosed with pseudoaneurysm and in conservative treatment, for 3.8 years, and none of

Figure 1 – *Chest radiography. Altered cardiac silhouette.*

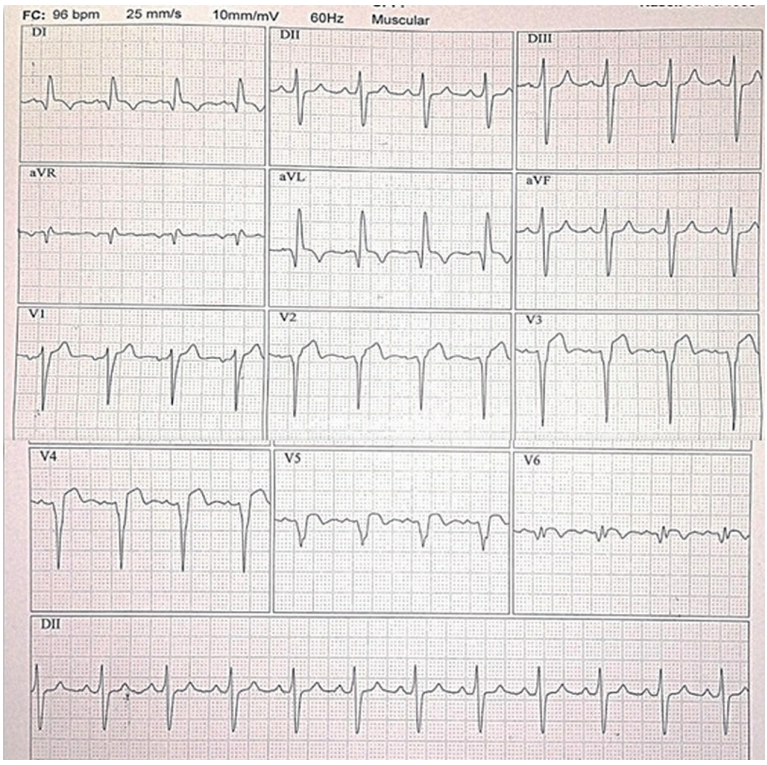

Figure 2 – *Electrocardiogram. ST-segment elevation in leads V1 to V5.*

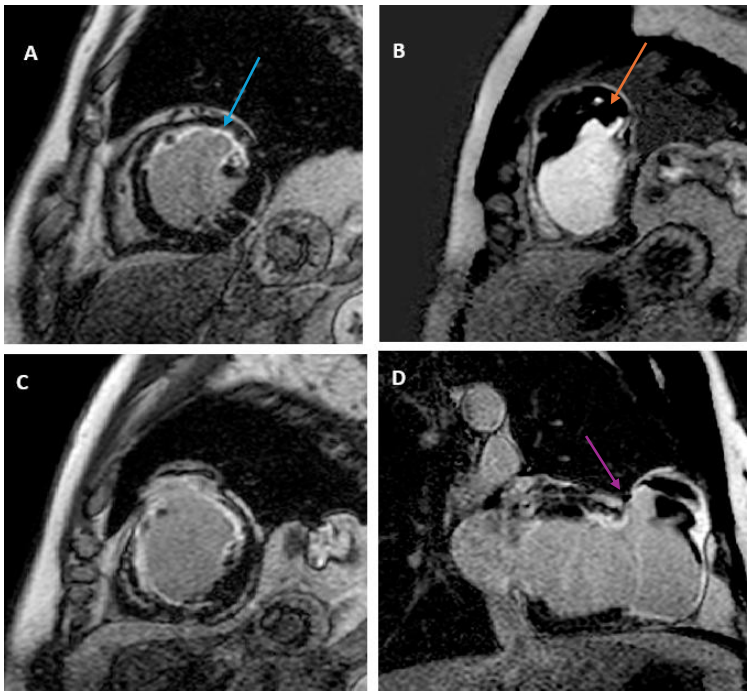

Figure 3 – *Cine cardiac magnetic resonance imaging. In image A, in the middle region of the heart, an area of anterior infarction can be observed due to the presence of late enhancement (blue arrow). In image B, in apical view, an intracavitary thrombus was found (orange arrow). In image D, the neck of the pseudoaneurysm is evident (purple arrow).*

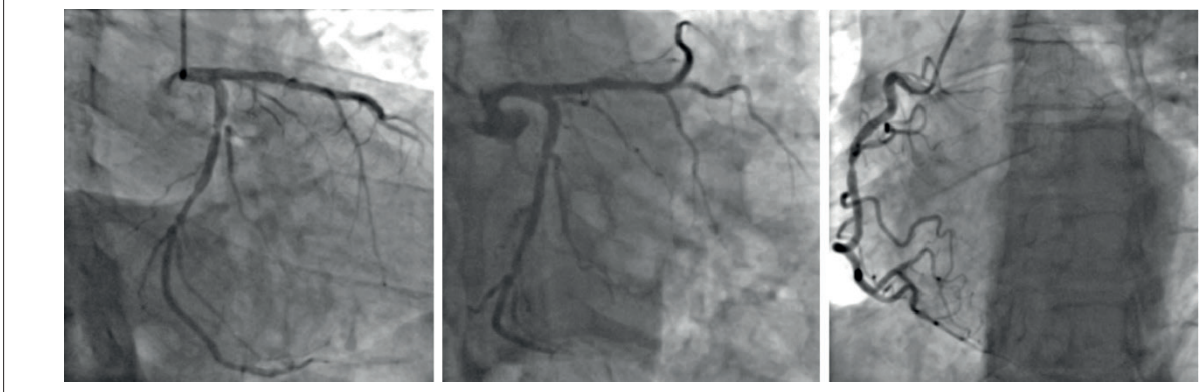

Figure 4 – *Coronary cineangiography. Residual two-vessel pattern, with significant lesions in the right and circumflex territories.*

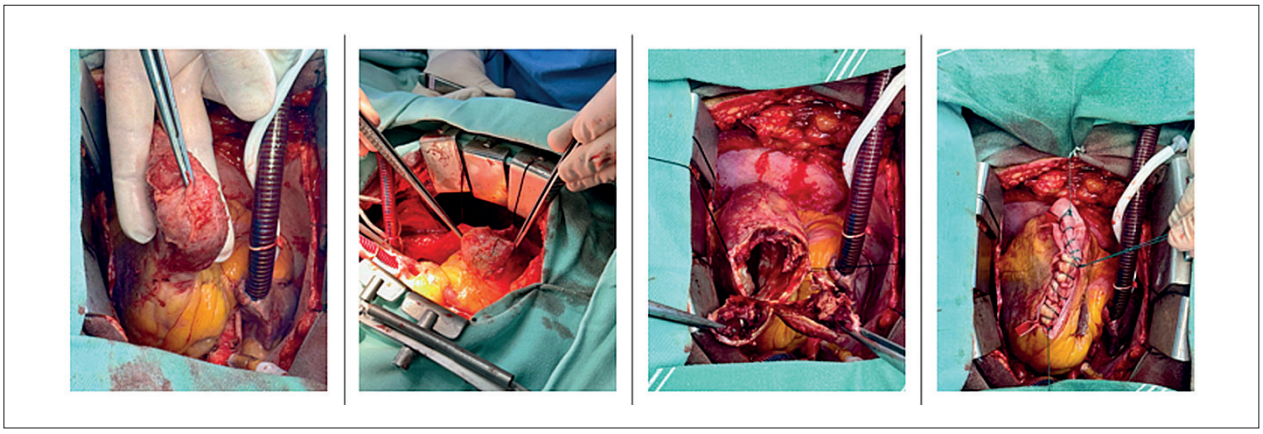

Figure 5 – *Cardiac surgery. Aneurysmectomy.*

them developed fatal rupture during this period. However, the incidence of stroke reached 33%, which suggests the possibility of chronic anticoagulation adjacent to treatment.[10]

According to Faustino et al., there is still no consensus on treatment for chronic cases, but surgical indication has become routine due to the risk of rupture and thrombotic embolization. In patients with pseudoaneurysms larger than 3 cm, procedure is indisputably necessary. In the case of patients with high surgical risk, the possibility of percutaneous procedure can be assessed. Since the condition may also be present in previously operated patients, the presence of adhesions makes intraoperative management difficult and increases mortality. Defects can be occluded with septal occluders, such as those used in congenital heart disease.[1,4,11]

Conclusion

This case illustrates the importance of diagnosing the LV pseudoaneurysm, which led to impaired EF. It is a rare condition that can remain asymptomatic for years, but it presents a significant risk of complications. Regular surveillance and follow-up are essential, especially in patients with a history of AMI. Diagnosis and surgical intervention are essential due to the high risk of rupture, even in the absence of symptoms. Imaging modalities, such as magnetic resonance imaging, are crucial for assessment and treatment planning.

Author Contributions

Conception and design of the research: Silva AP, Feitosa GS; acquisition of data: Silva AP, Moitinho RF, Torreão JA; analysis and interpretation of the data: Silva AP, Feitosa GS, Leal GCV, Moitinho RF, Torreão JA; writing of the manuscript: Silva AP; critical revision of the manuscript for intellectual content: Feitosa GS, Leal GCV, Torreão JA.

Potential Conflict of Interest

No potential conflict of interest relevant to this article was reported.

Sources of Funding

There were no external funding sources for this study.

Study Association

This study is not associated with any thesis or dissertation work.

Ethics Approval and Consent to Participate

This study was approved by the Ethics Committee of the Hospital Santa Izabel under the protocol number 90416125.4.0000.5520. All the procedures in this study were in accordance with the 1975 Helsinki Declaration, updated in 2013. Informed consent was obtained from all participants included in the study.

Use of Artificial Intelligence

The authors did not use any artificial intelligence tools in the development of this work.

Availability of Research Data

The underlying content of the research text is contained within the manuscript.

References

1. Inayat F, Ghani AR, Riaz I, Ali NS, Sarwar U, Bonita R, et al. Left Ventricular Pseudoaneurysm: An Overview of Diagnosis and Management. J Investig Med High Impact Case Rep. 2018;6:2324709618792025. doi: 10.1177/2324709618792025.
2. Coelho SG, Jorge CF, Carlos PB, Delgado A, Vicente L. Evolved Inferior Wall Myocardial Infarction with Left Ventricular Pseudoaneurysm: A Diagnostic Dilemma. Arq Bras Cardiol. 2020;114(4):730-1. doi: 10.36660/abc.20200029.
3. Oliveira SM, Dias P, Pinho T, Gavina C, Almeida PB, Madureira AJ, et al Giant Left Ventricular Pseudoaneurysm: The Diagnostic Contribution of Different Non-Invasive Imaging modalities. Rev Port Cardiol. 2012;31(6):439-44. doi: 10.1016/j.repc.2012.04.009.
4. Faustino M, Ranchordás S, Abecasis J, Freitas A, Ferreira M, Gil V, et al. Left Ventricular Pseudoaneurysm - A Challenging Diagnosis. Rev Port Cardiol. 2016;35(6):373.e1-6. doi: 10.1016/j.repc.2015.09.008.
5. Jacob JL, Buzelli G, Machado NC, Garzon PG, Garzon SA. Pseudoaneurysm of Left Ventricle. Arq Bras Cardiol. 2007;89(1):e1-2. doi: 10.1590/s0066-782x2007001300012.
6. Fialho GL, Fischer CH, Cordovil A, Campos O Filho. Chronic Left Ventricular Pseudoaneurism of Undetermined Etiology. Arq Bras Cardiol. 2010;94(1):e4-6. doi: 10.1590/s0066-782x2010000100024.
7. Frances C, Romero A, Grady D. Left Ventricular Pseudoaneurysm. J Am Coll Cardiol. 1998;32(3):557-61. doi: 10.1016/s0735-1097(98)00290-3.
8. Konen E, Merchant N, Gutierrez C, Provost Y, Mickleborough L, Paul NS, et al. True versus False Left Ventricular Aneurysm: Differentiation with MR Imaging--Initial Experience. Radiology. 2005;236(1):65-70. doi: 10.1148/radiol.2361031699.
9. Yeo TC, Malouf JF, Oh JK, Seward JB. Clinical Profile and Outcome in 52 Patients with Cardiac Pseudoaneurysm. Ann Intern Med. 1998;128(4):299-305. doi: 10.7326/0003-4819-128-4-199802150-00010.
10. Moreno R, Gordillo E, Zamorano J, Almeria C, Garcia-Rubira JC, Fernandez-Ortiz A, et al. Long Term Outcome of Patients with Postinfarction Left Ventricular Pseudoaneurysm. Heart. 2003;89(10):1144-6. doi: 10.1136/heart.89.10.1144.
11. Manica JLL, Bender LP, Borges MS, Prates PRL, Rossi-Filho RI. Percutaneous Treatment of Left Ventricle and Aortic Pseudoaneuryms: Three Case Series. Rev Bras Cardiol Invasiva. 2015;23(1):73-6. doi: 10.1016/j.rbciev.2015.02.002.

Turmoil of Symptoms: The Devastating Impact of Cardiac Lymphoma – Multiple Clinical Manifestations and the Lethal Causes of Cardiac Involvement

Gustavo Carvalho,[1] Maria Fernanda Miranda Carvalho,[1] Tiago Magalhães,[1,2] Alexandre Manoel Varela,[3] Kamila Fernanda Staszko,[1] Mariana Rie Hayashida[1]

Universidade Federal do Paraná,[1] Curitiba, PR – Brazil
Hospital do Coração,[2] São Paulo, SP – Brazil
Hospital Erasto Gaertner,[3] Curitiba, PR – Brazil

Abstract

Primary cardiac lymphoma (PCL) is a rare and highly lethal neoplasm, whose nonspecific clinical presentation makes early diagnosis difficult. This article reports the case of an elderly patient, previously healthy, who experienced dizziness and syncope for four months before the discovery of a large tumor mass in the heart. Imaging exams, such as echocardiography and magnetic resonance imaging, were crucial for tumor identification, and the biopsy confirmed it to be a B-cell lymphoma with high replication. However, given the severity of the condition and the family's refusal to proceed with treatment, the patient progressed to sudden death two weeks after diagnosis. Primary cardiac tumors (PCTs) are underdiagnosed, with varied symptoms that may include vascular obstructions, arrhythmias, and heart failure. PCLs account for only 1% to 2% of primary cardiac masses and are more common in elderly men. The diagnosis is challenging due to the absence of specific signs, making imaging exams and biopsies essential for disease confirmation. This case illustrates the complexity of managing PCLs, whose rapid progression limits therapeutic options. The lack of specific symptoms and silent progression highlight the importance of early diagnosis. The high mortality rate reinforces the need for greater medical attention to this condition, which frequently leads to fatal outcomes before an effective intervention can be implemented.

Introduction

Primary cardiac tumors (PCTs) are rare entities in clinical practice and can be classified as benign lesions (myxomas) or malignant tumors (sarcomas and lymphomas).[1,2] With the increasing life expectancy of the population, a higher incidence of these tumors is expected, highlighting the need for greater attention to their possible symptoms, especially considering their varied clinical manifestations.[2,3]

Considering this, it is important to emphasize that PCTs are often underdiagnosed, which may lead to fatal outcomes before an effective therapeutic approach can be implemented.[2] This article presents a case of primary myocardial lymphoma in an elderly patient, previously healthy, who experienced sudden death two weeks after diagnosis.

Thus, the objective of this study is to discuss the clinical and diagnostic characteristics of PCTs.

Case report

A 78-year-old man, previously healthy, presented with dizziness and syncope worsening over four months. The patient had been seen at other emergency care units, but his symptoms progressively worsened.

On physical examination, no significant findings were noted. The electrocardiogram showed sinus rhythm with diffuse ventricular repolarization abnormalities. A chest X-ray revealed a cardiac silhouette at the upper limit of normal and bilateral costophrenic angle blunting. A transthoracic echocardiogram detected a large tumor mass infiltrating the interventricular septum and the inferolateral wall of the right ventricle, extending into the right atrial and ventricular cavities, as well as the left ventricular cavity adjacent to the septum (Figure 1).

Given this, the patient was referred for a magnetic resonance imaging scan for a more detailed assessment of the neoplasm, which confirmed the echocardiographic findings (Figure 2). An endomyocardial biopsy was performed, guided by transthoracic echocardiography and fluoroscopy, conducted simultaneously in the hemodynamics room. The histopathological study and immunohistochemical analysis concluded that it was an invasive B-cell lymphoma with intense cellular replication (Figure 3).

After a detailed explanation of this complex and severe clinical case to the patient and his family, they refused the implementation of any form of treatment and requested discharge to his home, where he remained asymptomatic for approximately two more weeks, before experiencing sudden death.

Keywords

Heart Neoplasms; Echocardiography; Cardiac Arrhythmias; Biopsy

Mailing Address: Gustavo Carvalho •
CHC UFPR. Dionira M Klemtz, 201, casa 107. Postal code: 81320-390. Bairro Fazendinha, Curitiba, PR – Brazl
E-mail: gustavocarvalho1975@gmail.com
Manuscript received May 5, 2025; revised May 5, 2025 accepted May 5, 2025
Editor responsible for the review: Marcelo Tavares

DOI: https://doi.org/10.36660/abcimg.20250033i

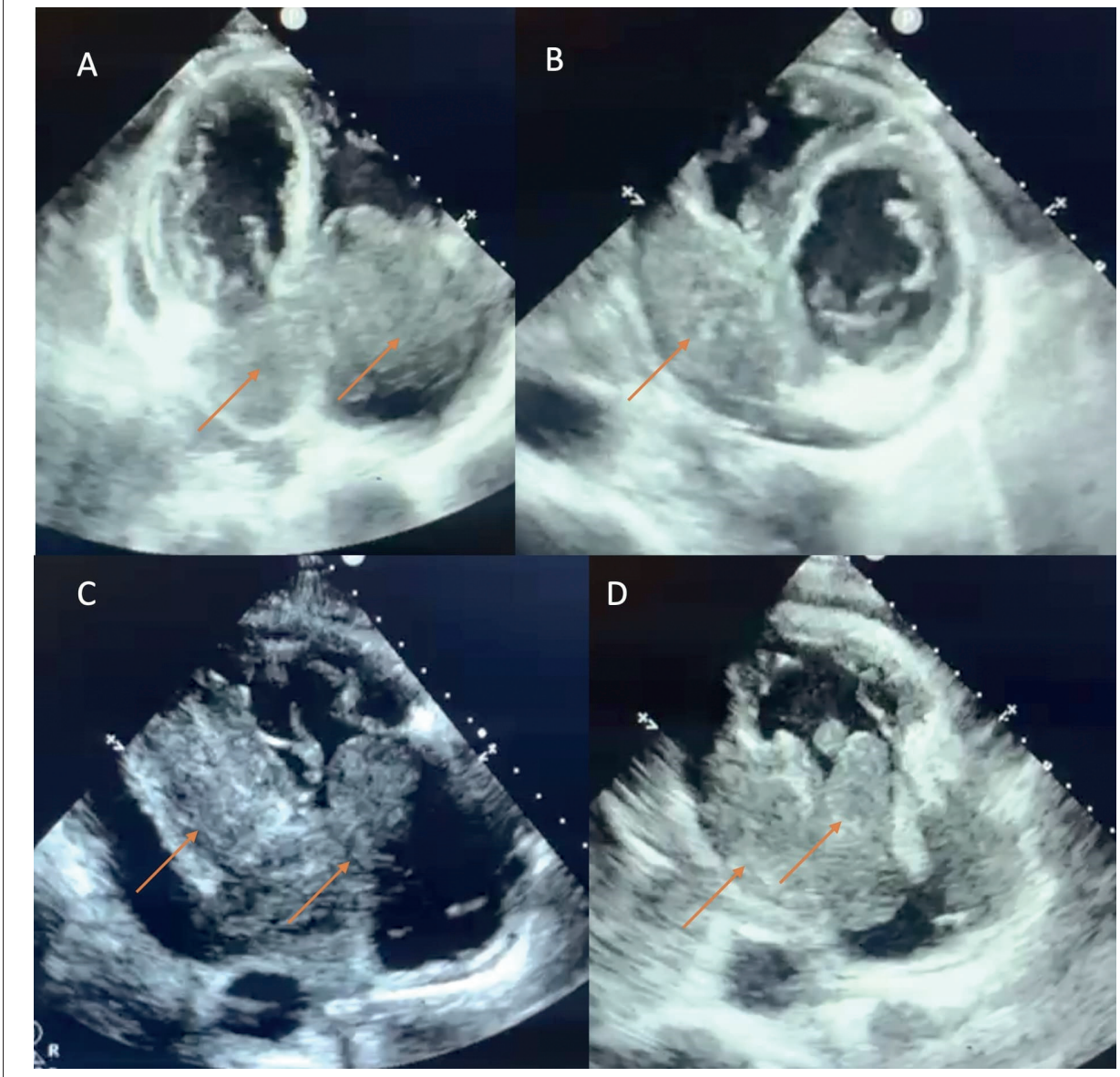

Figure 1 – *Transthoracic echocardiogram showing a tumor mass infiltrating the atrioventricular valves, the ventricular myocardium at the septal level, and the anterior and inferior walls of both ventricles. The tumor occupies the atrial and right ventricular cavities (arrows); pericardial effusion.*

Discussion

Although reported since the 16th century, PCTs are rare in clinical practice, with an incidence ranging from 0.0017% to 0.03% in autopsy studies.[1-3] PCTs can primarily manifest as benign lesions, with an incidence rate of 75%, or as malignant tumors, accounting for 25% of cases.[3-5]

On the other hand, primary cardiac lymphomas (PCLs) are classified as malignant neoplasms, representing 1% to 2% of all primary cardiac masses.[2-5]

Although PCTs generally affect more women, PCLs are more common in men over 60 years old, which is well represented by the patient described in this case report.[4-6]

PCLs often present nonspecific and multifaceted clinical manifestations.[14] Initially, the patients may be asymptomatic or oligosymptomatic, but as the disease progresses, they develop various signs and symptoms due to direct and/or indirect involvement of multiple organs and systems through heterogeneous, simultaneous, and diverse mechanisms. These include recurrent vascular obstructive phenomena caused by

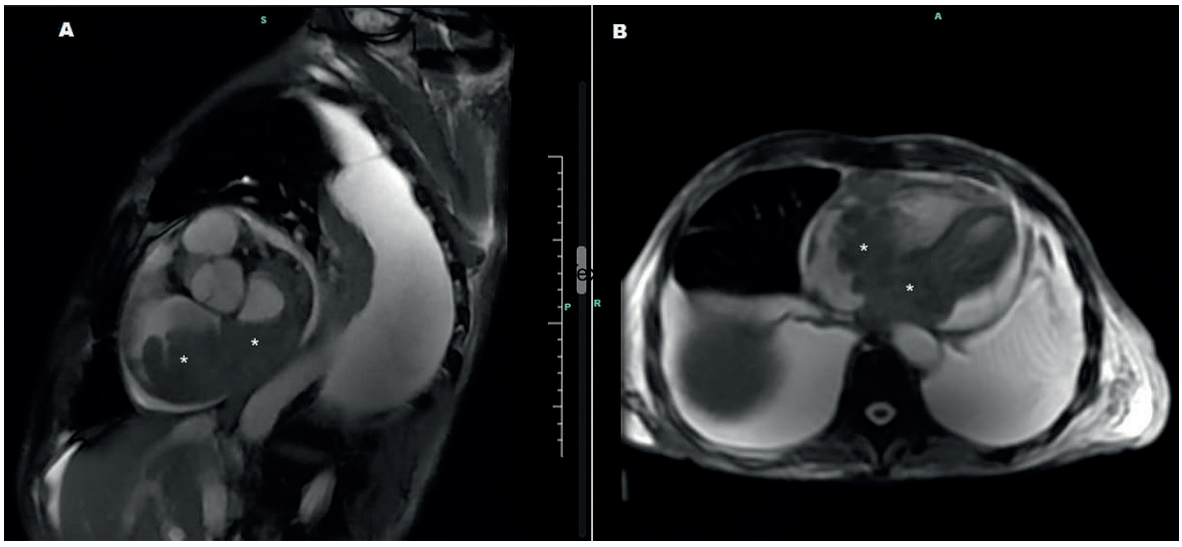

Figure 2 – *Magnetic resonance imaging showing the extent of cardiac involvement by lymphoma (*) demonstrated in the sagittal (A) and transverse (B) planes, along with pericardial and bilateral pleural effusion.*

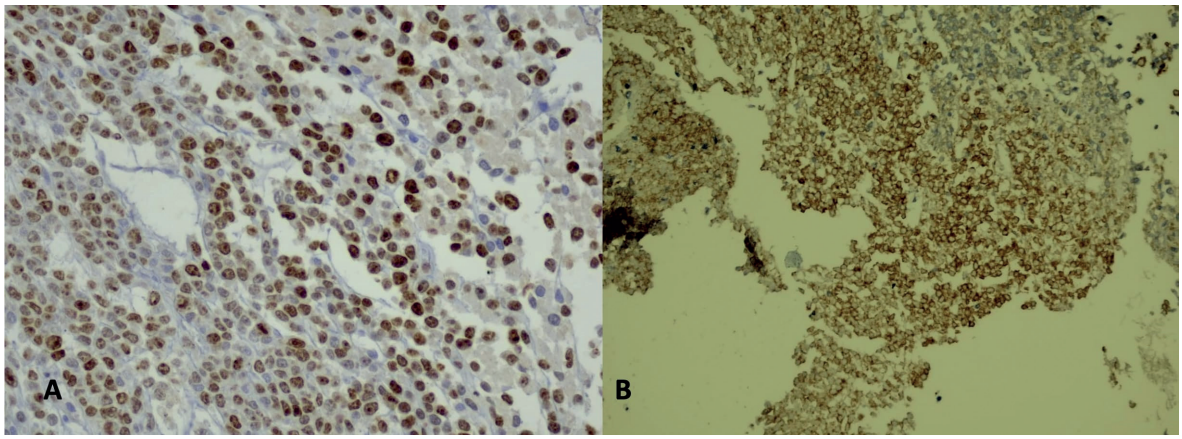

Figure 3 – *Histopathological and immunohistochemical findings demonstrating B-cell lymphoma with intense cellular proliferation in Ki-67 (A), and B lymphocytes marked in CD20 (B).*

thrombi and/or tumor fragments, leading to stroke, peripheral and visceral arterial embolism, and pulmonary thromboembolism.[4-7]

The tumor itself may cause fixed or transient intracardiac blood flow obstruction, depending on its size and morphology (intramural or pedunculated intracavitary), potentially compromising cardiac output.[2,4] When the myocardial electrical conduction system is affected, arrhythmia may occur, sometimes unexpectedly fatal, as possibly seen in the case presented here.[5-7]

Thus, in cases of cardiac tumors, it is undeniable that, due to their nonspecific symptoms, establishing a timely diagnosis to apply effective therapy is a challenge for the healthcare team, as demonstrated in this report.[6,7] Furthermore, it is essential to highlight the importance of imaging exams, such as echocardiography and cardiac magnetic resonance imaging, in the detection of these tumor masses and in performing endomyocardial biopsies to establish a histopathological diagnosis.[8-12]

Conclusion

PCL represents a rare but extremely severe condition, whose nonspecific clinical presentation and silent progression make its diagnosis a major challenge.

As discussed in this report, its multiple manifestations can mask the true extent of the disease, resulting in a discouraging prognosis. Cardiac involvement by lymphoma not only compromises organ function but also exposes the patient to a high risk of lethal events, such as fatal arrhythmias and critical vascular obstructions.

Given this scenario, the importance of early and thorough investigation using imaging exams, histopathological aspects, and immunohistochemical analysis for diagnostic definition is fundamental. However, as evidenced in the case described, even with the diagnosis established, therapeutic options may be limited due to the rapid progression of the disease and the patient's own decisions.

Thus, the devastating impact of cardiac lymphoma extends beyond its physiological repercussions, encompassing therapeutic limitations and abrupt outcomes, emphasizing the need for greater medical-scientific attention and understanding for future approaches to this unusual and fatal entity.

Author Contributions

Conception and design of the research: Carvalho G; acquisition of data: Carvalho G, Carvalho MFM, Magalhães T, Hayashida MR, Staszko KF; analysis and interpretation of the data: Carvalho G, Carvalho MFM, Varela AM; writing of the manuscript: Carvalho G, Carvalho MFM; critical revision of the manuscript for intellectual content: Carvalho G, Carvalho MFM, Magalhães T, Hayashida MR, Staszko KF, Varela AM; review of references: Carvalho MFM; magnetic resonance imaging: Magalhães T; pathological anatomy analysis: Hayashida MR; echocardiogram images: Staszko KF.

Potential Conflict of Interest

No potential conflict of interest relevant to this article was reported.

Sources of Funding

There were no external funding sources for this study.

Study Association

This study is not associated with any thesis or dissertation work.

Ethics Approval and Consent to Participate

This study was approved by the Ethics Committee of the Hospital De Clínicas Da Universidade Federal Do Paraná under the protocol number 90118225.4.0000.0096. All the procedures in this study were in accordance with the 1975 Helsinki Declaration, updated in 2013. The Free and Informed Consent Form was waived.

Use of Artificial Intelligence

The authors did not use any artificial intelligence tools in the development of this work.

Availability of Research Data

The underlying content of the research text is contained within the manuscript.

References

1. Leja MJ, Shah DJ, Reardon MJ. Primary Cardiac Tumors. Tex Heart Inst J. 2011;38(3):261-2.
2. Tyebally S, Chen D, Bhattacharyya S, Mughrabi A, Hussain Z, Manisty C, et al. Cardiac Tumors: JACC CardioOncology State-of-the-Art Review. JACC CardioOncol. 2020;2(2):293-311. doi: 10.1016/j.jaccao.2020.05.009.
3. Cresti A, Chiavarelli M, Glauber M, Tanganelli P, Scalese M, Cesareo F, et al. Incidence Rate of Primary Cardiac Tumors: A 14-Year Population Study. J Cardiovasc Med. 2016;17(1):37-43. doi: 10.2459/JCM.0000000000000059.
4. Carras S, Berger F, Chalabreysse L, Callet-Bauchut E, Cordier JF, Salles G, et al. Primary Cardiac Lymphoma: Diagnosis, Treatment and Outcome in a Modern Series. Hematol Oncol. 2017;35(4):510-9. doi: 10.1002/hon.2301.
5. Sarjeant JM, Butany J, Cusimano RJ. Cancer of the Heart: Epidemiology and Management of Primary Tumors and Metastases. Am J Cardiovasc Drugs. 2003;3(6):407-21. doi: 10.2165/00129784-200303060-00004.
6. Butany J, Nair V, Naseemuddin A, Nair GM, Catton C, Yau T. Cardiac Tumours: Diagnosis and Management. Lancet Oncol. 2005;6(4):219-28. doi: 10.1016/S1470-2045(05)70093-0.
7. Bruce CJ. Cardiac Tumours: Diagnosis and Management. Heart. 2011;97(2):151-60. doi: 10.1136/hrt.2009.186320.
8. Biersmith MA, Tong MS, Guha A, Simonetti OP, Addison D. Multimodality Cardiac Imaging in the Era of Emerging Cancer Therapies. J Am Heart Assoc. 2020;9(2):e013755. doi: 10.1161/JAHA.119.013755.
9. Zaragoza-Macias E, Chen MA, Gill EA. Real Time Three-Dimensional Echocardiography Evaluation of Intracardiac Masses. Echocardiography. 2012;29(2):207-19. doi: 10.1111/j.1540-8175.2011.01627.x.
10. Motwani M, Kidambi A, Herzog BA, Uddin A, Greenwood JP, Plein S. MR Imaging of Cardiac Tumors and Masses: A Review of Methods and Clinical Applications. Radiology. 2013;268(1):26-43. doi: 10.1148/radiol.13121239.
11. Jeong D, Patel A, Francois CJ, Gage KL, Fradley MG. Cardiac Magnetic Resonance Imaging in Oncology. Cancer Control. 2017;24(2):147-60. doi: 10.1177/107327481702400207.
12. Esposito A, De Cobelli F, Ironi G, Marra P, Canu T, Mellone R, et al. CMR in the Assessment of Cardiac Masses: Primary Malignant Tumors. JACC Cardiovasc Imaging. 2014;7(10):1057-61. doi: 10.1016/j.jcmg.2014.08.002.

Lutembacher Syndrome Associated With Pulmonary Hypertension: The Importance of Early Diagnosis for Enabling Surgical Treatment

Ana Luiza Caldeira Lopes,[1] *Maria Estefânia Bosco Otto,*[2] *Bianca Corrêa Rocha de Mello,*[1,3] *Michelle Bruna da Silva Sena,*[1] *Wagner Luis Gali*[1]

Hospital Universitário de Brasília,[1] *Brasília, DF – Brazil*

Universidade de Brasília,[2] *Brasília, DF – Brazil*

Instituto de Cardiologia e Transplantes do Distrito Federal,[3] *Brasília, DF – Brazil*

Introduction

Lutembacher syndrome (LS) is defined by the simultaneous presence of an atrial septal defect (ASD) and mitral stenosis (MS). Although it is a rare condition, its clinical significance lies in the considerable hemodynamic impact and the potential for early progression to irreversible pulmonary hypertension (PH).

The exact prevalence of LS remains unknown. However, for estimation purposes, MS is considered the most frequent manifestation of rheumatic fever (RF) in young women,[1] and the prevalence of RF in developing countries ranges from 5 to 10 cases per 1,000 children. Furthermore, the incidence of congenital ASD in patients with MS is estimated at 0.6% to 0.7%.[2]

The hemodynamic effects of LS vary according to the size of the ASD, the severity of the MS, the compliance of the right ventricle (RV), and the degree of pulmonary vascular resistance (PVR). When MS is severe and the ASD has significant hemodynamic impact, there is a left-to-right shunt of blood flow from the left atrium (LA) to the right atrium (RA), which prevents a proportional increase in LA pressure relative to the severity of MS. In such cases, the development of pulmonary venous hypertension tends to occur more slowly. However, progressive dilation of the right heart chambers and pulmonary hyperflow are observed, as in the case described here. If left untreated, PVR tends to rise progressively, eventually leading to RV failure. Pulmonary arterial hypertension (PAH) in these patients is usually hyperkinetic, resulting from volume overload in the right chambers and pulmonary overcirculation, in contrast to the PAH seen in isolated severe MS, where the predominant mechanism is retrograde pressure overload. In cases where the ASD has no significant hemodynamic consequences, the shunt is minimal, and the clinical course resembles that of isolated MS.[3,4]

This case report was submitted to and approved by the Research Ethics Committee at Universidade de Brasília under protocol number 86333025.3.0000.5558.

Case report

A 54-year-old woman sought medical attention with complaints of dyspnea on minimal exertion, palpitations, dry cough, and lower limb edema. She reported a history of heart disease since 2017, with multiple hospital admissions over the years. Physical examination revealed signs of systemic and pulmonary congestion, a 3+/6+ rumbling diastolic mitral murmur, and a fixed splitting of the second heart sound.

Electrocardiography (ECG) showed atrial flutter and signs of right heart chamber overload (Figure 1). Chest radiography revealed enlargement of the right chambers and pulmonary congestion (Figure 2). Transthoracic echocardiography demonstrated an ostium secundum-type ASD measuring 25 mm, with a pulmonary-to-systemic flow ratio (Qp/Qs) of 2.5 and evidence of a bidirectional shunt. Right heart chamber enlargement was observed, with a right atrial (RA) volume of 92 mL/m^2, a right ventricular (RV) basal diameter of 63 mm, and a mid-ventricular diameter of 44 mm. There was also moderate RV dysfunction with diffuse hypokinesia (TAPSE: 15 mm; FAC: 25%). Severe MS was also identified, with a mitral valve area of 1.2 cm^2 by planimetry and a mean gradient of 9 mmHg. The Block Wilkins score was 11 (thickness: 2; calcification: 2; mobility: 3; subvalvular: 2). The estimated systolic pulmonary artery pressure (SPAP) was 60 mmHg. The diagnosis of LS was then established (Figure 3 and Video 1).

In addition, as part of the ongoing investigation of PH, a pulmonary artery computed tomography angiography was performed to rule out chronic pulmonary thromboembolism as a potential associated mechanism. The examination revealed enlargement of the pulmonary artery trunk, dilation of the right heart chambers, and no evidence of obstruction in the pulmonary artery or its branches (Figure 4).

After clinical optimization with diuretics, a beta-blocker, and sildenafil, the patient underwent right heart catheterization, which confirmed PH of mixed etiology. Hemodynamic findings included a mean pulmonary artery pressure of 49 mmHg, a pulmonary artery wedge pressure of 20 mmHg, a PVR of 4.18 Wood units, and a pulmonary diastolic pressure gradient of 10 mmHg. During the procedure, a favorable vasodilator response to nitric oxide was observed, indicating that the PH was not fixed. Surgical correction

Keywords

Lutembacher Syndrome; Pulmonary Hypertension; Mitral Valve Stenosis; Atrial Heart Septal Defects.

Mailing Address: Ana Luiza Caldeira Lopes •
Hospital Universitário de Brasília. Campus Universitário Darcy Ribeiro, Asa Norte. Postal code: 70840-901. Brasília, DF – Brazil
E-mail: analuizacaldeira93@gmail.com
Manuscript received May 17, 2025; revised May 19, 2025; accepted June 21, 2025
Editor responsible for the review: Andrea Vilela

DOI: https://doi.org/10.36660/abcimg.20250043i

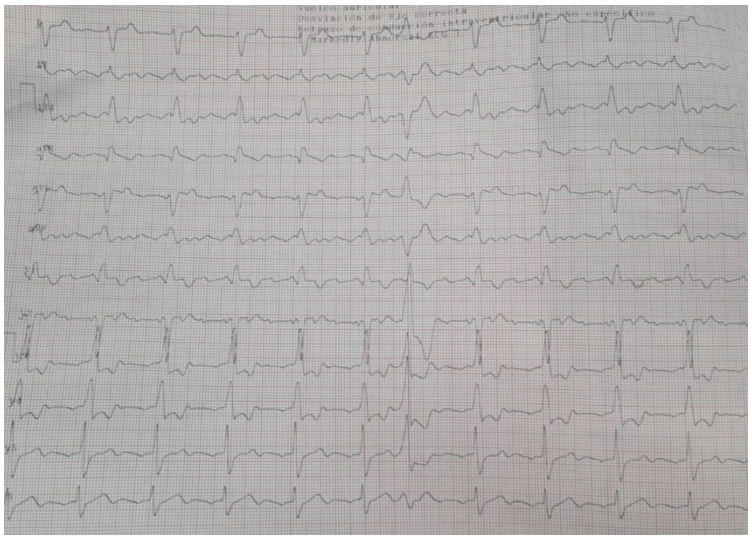

Figure 1 – *12-lead resting ECG showing atypical atrial flutter, right axis deviation, and right heart chamber overload. Source: Internal records of the Hospital Universitário de Brasília.*

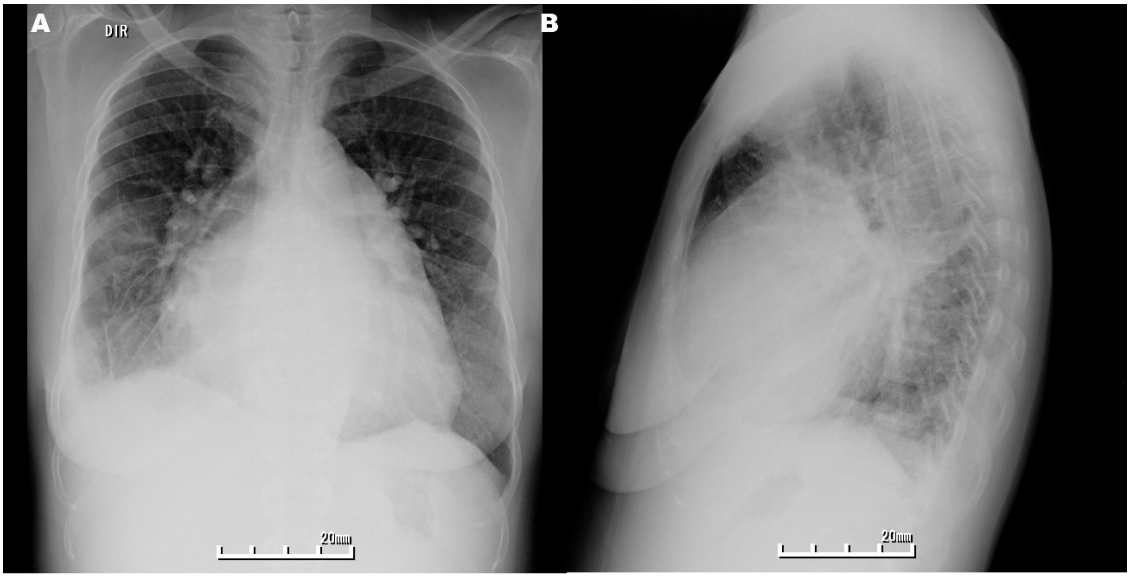

Figure 2 – *Chest radiography. A) Posteroanterior view and B) lateral view showing cardiomegaly and enlargement of the right heart chambers. Source: Internal records of the Department of Radiology, Hospital Universitário de Brasília.*

of the MS and ASD was therefore indicated. She is currently awaiting the procedure.

Discussion

The initial course of LS is often oligosymptomatic, as the presence of the ASD relieves LA overload caused by MS, delaying the onset of symptoms and the development of PH. However, chronic shunting leads to pulmonary overcirculation and progressive overload of the right heart chambers, as observed in the present case.[4,5] A favorable vasodilator response during right heart catheterization suggests the potential reversibility of PH and serves as a key criterion for indicating surgical treatment.[6,7]

Isolated MS is characterized by thickening of the valve leaflets and restricted mitral valve opening, resulting in increased LA pressure, postcapillary PH, and overload of the right

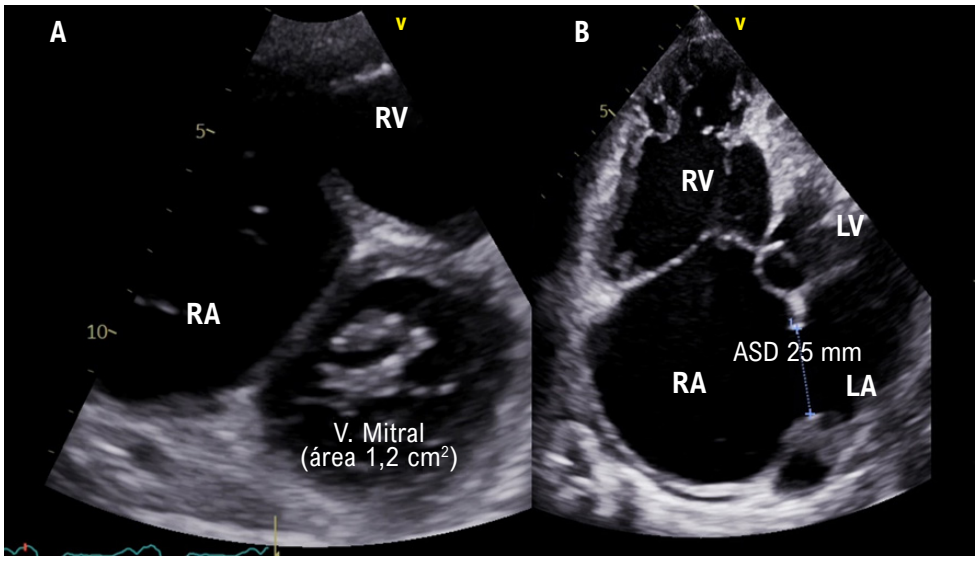

Figure 3 – *Transthoracic echocardiography. A) Parasternal short-axis view showing commissural fusion of the mitral valve and reduced valve area. B) Apical four-chamber view focused on the RV, showing a 25 mm ASD, biatrial enlargement, and RV enlargement. ASD: atrial septal defect; LA: left atrium; LV: left ventricle; RA: right atrium; RV: right ventricle; V: valve. Source: Internal records of the Department of Echocardiography, Hospital Universitário de Brasília.*

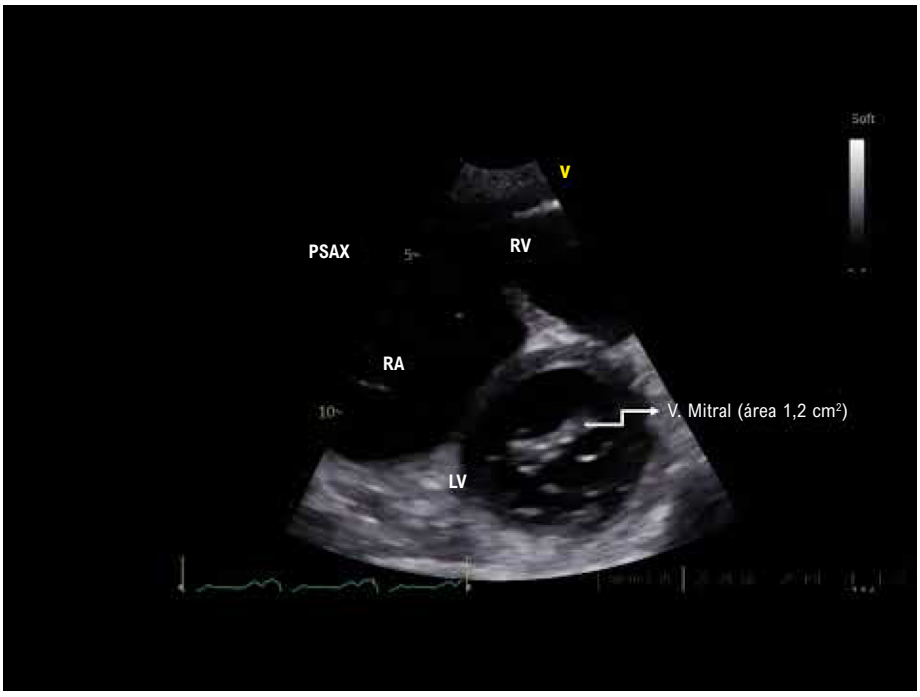

Video 1 – *ASD: atrial septal defect; LA: left atrium; LV: left ventricle; PLAX: parasternal long-axis view; PSAX: parasternal short-axis view; RA: right atrium; RV: right ventricle; V: valve. Source: Internal records of the Department of Echocardiography, Hospital Universitário de Brasília.*
Link: http://abcimaging.org/supplementary-material/2025/3803/2025-0043_video_01.mp4

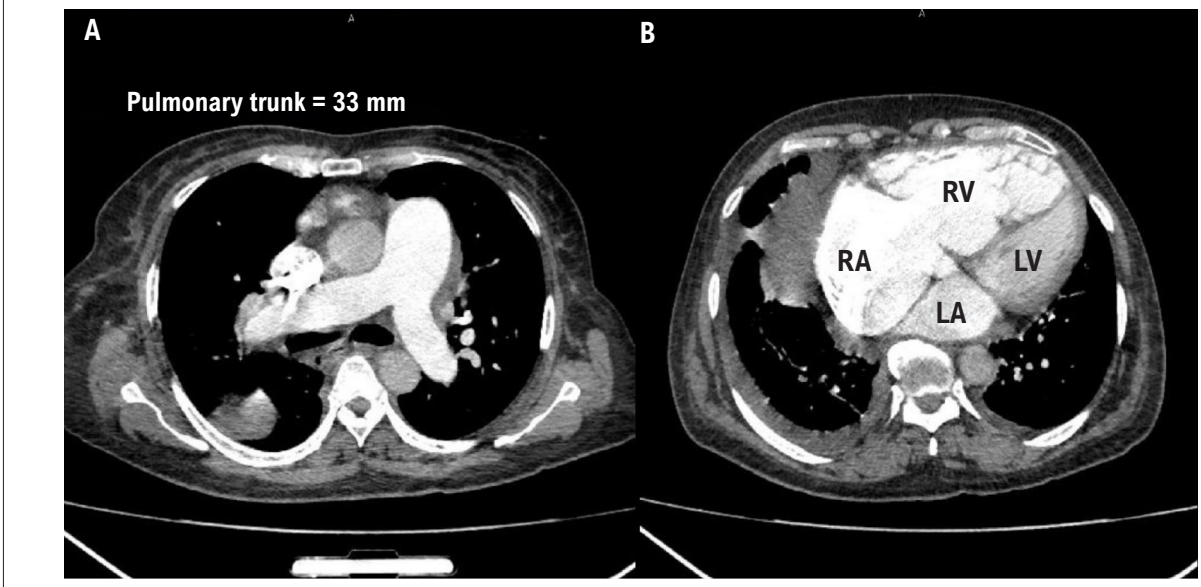

Figure 4 – *Pulmonary artery computed tomography angiography showing dilation of the pulmonary artery trunk and enlargement of the right heart chambers. LA: left atrium; LV: left ventricle; RA: right atrium; RV: right ventricle. Source: Internal records of the Department of Radiology, Hospital Universitário de Brasília.*

heart chambers. Intervention is indicated when MS is severe and symptomatic, or in asymptomatic patients with complicating factors.[8] Anatomical severity is defined by a mitral valve area less than 1.5 cm^2, a mean left atrioventricular diastolic gradient greater than 10 mmHg, and SPAP exceeding 50 mmHg. The main complicating factors include the development of PH and new-onset atrial fibrillation.[8] In LS, the ASD decompresses the LA, which may lead to underestimation of the transmitral gradient. In such cases, mitral valve area assessment by planimetry is considered more reliable.

ASD accounts for 5% to 10% of congenital heart diseases and is more prevalent in females. The ostium secundum type represents 50% to 70% of cases, with the defect located in the central portion of the atrial septum. This communication between atria creates a left-to-right shunt, which results in pulmonary overcirculation.[6] Both components of LS — MS and ASD — can individually lead to the development of PH; however, when combined, their hemodynamic effects are amplified.[7,9] Early diagnosis and timely intervention in LS are essential to prevent the progression of PH to irreversible forms.[5]

Surgical intervention for ASD is indicated in the presence of a left-to-right shunt, dilation of the right heart chambers, and a Qp/Qs ratio greater than 1.5. In addition, SPAP must be less than 50% of the systemic systolic pressure, PVR must be less than one-third of systemic vascular resistance, and there must be no cyanosis at rest or during exertion.[10] Closure of the ASD is contraindicated in the presence of Eisenmenger syndrome, which is characterized by irreversible PH with reversal of the shunt to right-to-left.[9,10]

Clinical management of LS includes the use of diuretics to relieve congestive symptoms, as well as beta-blockers and calcium channel blockers for heart rate control, particularly in cases with associated atrial arrhythmias. Prophylaxis for infective endocarditis should also be considered.[4,7]

Regarding interventional correction, the classical approach has been open-heart surgery. However, with advances in percutaneous techniques, transcatheter therapy — through valvotomy for MS and ASD closure using septal occluder devices — has emerged as a viable alternative.[7] In the present case, despite the lower morbidity and mortality associated with percutaneous treatment, open surgical correction was chosen due to a contraindication for balloon valvuloplasty.[10]

Conclusion

LS is a rare, frequently underdiagnosed condition. LS should be considered in the evaluation of patients presenting with signs of MS, PH, and disproportionate right heart chamber overload relative to the severity of the valvular lesion. Early diagnosis, combined with thorough hemodynamic assessment, is essential to determine the optimal timing for intervention and to help prevent the progression of PH to irreversible forms.

Author Contributions

Conception and design of the research, acquisition of data, analysis and interpretation of the data, statistical analysis, writing of the manuscript and critical revision of the manuscript for intellectual content: Lopes ALC, Otto ME, Mello BCR, Sena MB, Gali WL.

Potential Conflict of Interest

No potential conflict of interest relevant to this article was reported.

Sources of Funding

There were no external funding sources for this study.

Study Association

This article is part of Ana Luiza Caldeira Lopes' graduation thesis at the University Hospital of Brasília.

Ethics Approval and Consent to Participate

This study was approved by the Ethics Committee of the Faculdade de Medicina da Universidade de Brasília under the protocol number 86333025.3.0000.5558. All the procedures in this study were in accordance with the 1975 Helsinki Declaration, updated in 2013. Informed consent was obtained from all participants included in the study.

Use of Artificial Intelligence

The authors did not use any artificial intelligence tools in the development of this work.

Availability of Research Data

The underlying content of the research text is contained within the manuscript.

References

1. Zühlke L, Engel ME, Karthikeyan G, Rangarajan S, Mackie P, Cupido B, et al. Characteristics, Complications, and Gaps in Evidence-Based Interventions in Rheumatic Heart Disease: The Global Rheumatic Heart Disease Registry (the REMEDY Study). Eur Heart J. 2015;36(18):1115-22a. doi: 10.1093/eurheartj/ehu449.
2. Carapetis JR, Steer AC, Mulholland EK, Weber M. The Global Burden of Group A Streptococcal Diseases. Lancet Infect Dis. 2005;5(11):685-94. doi: 10.1016/S1473-3099(05)70267-X.
3. Phan QT, Nguyen HL, Le TD, Lee W, Won H, Shin S, et al. Combined Percutaneous Procedure in Patient with Lutembacher Syndrome: A Case Report and Real-World Experience Review. Cardiol Res. 2018;9(6):385-91. doi: 10.14740/cr776w.
4. Bari MA, Haque MS, Uddin SN, Shamsuzzaman M, Khan GK, Sutradhar SR. Lutembacher's Syndrome. Mymensingh Med J. 2005;14(2):206-8.
5. Kulkarni SS, Sakaria AK, Mahajan SK, Shah KB. Lutembacher's Syndrome. J Cardiovasc Dis Res. 2012;3(2):179-81. doi: 10.4103/0975-3583.95381.
6. Tezcan M, Isilak Z, Atalay M, Uz O. Echocardiographic Assessment of Lutembacher Syndrome. Kardiol Pol. 2014;72(7):660. doi: 10.5603/KP.2014.0142.
7. Aminde LN, Dzudie A, Takah NF, Ngu KB, Sliwa K, Kengne AP. Current Diagnostic and Treatment Strategies for Lutembacher Syndrome: The Pivotal Role of Echocardiography. Cardiovasc Diagn Ther. 2015;5(2):122-32. doi: 10.3978/j.issn.2223-3652.2015.03.07
8. Tarasoutchi F, Montera MW, Ramos AIO, Sampaio RO, Rosa VEE, Accorsi TAD, et al. Update of the Brazilian Guidelines for Valvular Heart Disease - 2020. Arq Bras Cardiol. 2020;115(4):720-75. doi: 10.36660/abc.20201047.
9. Calderaro D, Alves JL Jr, Fernandes CJCDS, Souza R. Pulmonary Hypertension in General Cardiology Practice. Arq Bras Cardiol. 2019;113(3):419-28. doi: 10.5935/abc.20190188.
10. Humbert M, Kovacs G, Hoeper MM, Badagliacca R, Berger RMF, Brida M, et al. 2022 ESC/ERS Guidelines for the Diagnosis and Treatment of Pulmonary Hypertension. Eur Heart J. 2022;43(38):3618-731. doi: 10.1093/eurheartj/ehac237.

Challenges and Implications of Uncorrected Atrioventricular Septal Defect in Adults: A Complex Case Report

Saulo Rodrigo Cunha,[1] Rafael Felipe Minotto,[1] Fernanda Pandolfo,[1] Fernando Colares Barros,[1] Pedro Tregnago Barcellos,[1] Ana Carolina Martins Mazzuca,[1] Eduardo Gatti Pianca[1]

Hospital Nossa Senhora da Conceição,[1] Porto Alegre, RS – Brazil

The prevalence of congenital heart disease in the adult population has shown continuous growth over recent decades. This is primarily due to significant advances in the diagnosis and treatment of congenital heart defects during childhood, which have been promoted by pediatric cardiology and congenital cardiac surgery. As a result, most children with congenital heart disease, including the most complex forms, now survive into adulthood. Currently, it is estimated that approximately 90% of children diagnosed with severe congenital heart disease reach 18 years of age. The growing clinical relevance of the adult congenital heart disease (ACHD) population stands out in this context. This is a heterogeneous group, both anatomically and pathophysiologically, as well as in terms of the different types of corrective or palliative surgical interventions to which they have been subjected. Although the overall number of individuals with ACHD continues to rise, the number of patients with certain specific anomalies or who have undergone specific types of repairs may still be relatively small.[1]

Atrioventricular (AV) septal defect is morphologically characterized by a common AV junction, with absence of the membranous and muscular AV septa. As a result, on echocardiographic examination, the AV valves are seen situated within the defect.[2] Atrioventricular septal defects (AVSDs) can be classified as partial or complete. Partial AVSD occurs when there is an opening divided by the superior and inferior bridging leaflets, which are connected by a tissue structure known as the "connecting tongue," separating the valve into two distinct orifices — one on the left and one on the right. On the other hand, complete AVSD is characterized by a single, undivided orifice encompassing the valvular structures on both the left and right sides.[2]

Case report

Male patient, 18 years old, admitted to a tertiary care hospital presenting with fever, cough, and dyspnea for the past seven days. According to the patient's mother, he sought medical attention on the second day of symptoms at an urgent care clinic, where he was prescribed ibuprofen and azithromycin to take at home. Due to lack of improvement, he sought hospital care.

Medical history includes congenital heart disease, specifically a surgically uncorrected AVSD, as he had lost follow-up at the reference hospital since childhood. On physical exam, he appeared in fair condition, with a productive cough, rapid breathing, and cyanosis around the lips and extremities. Hemodynamically stable, with blood pressure of 125 × 86 mmHg, heart rate of 105 bpm in atrial fibrillation rhythm, and oxygen saturation of 69% on room air.

Laboratory tests revealed: hemoglobin 16.2 g/dL, leukocytes 8,960/μL, CRP values over different days: 69.82 – 65.88 – 152.55 mg/dL (reference < 5 mg/dL), urea 20 mg/dL, creatinine 0.62 mg/dL, sodium 137 mEq/L, troponins 12 and 11.9 ng/L (reference < 14), NT-proBNP 4,377 pg/mL, and D-dimer 11,656 ng/mL. Blood cultures, urine culture, and rapid COVID-19 test were negative. The sputum smear showed some gram-negative diplococci, but the sputum culture was negative. The Mycobacterium tuberculosis DNA test also came back negative. Electrocardiogram showed atrial fibrillation, and a chest X-ray was ordered for further evaluation (Figure 1 and 2).

The patient was admitted to the Intensive Care Unit (ICU), where antibiotic therapy was broadened with the addition of amoxicillin/clavulanate, in combination with azithromycin. Blood and sputum cultures were collected, and an arterial blood gas test was performed. A chest CT angiography was also requested, which ruled out pulmonary embolism but contributed to the elucidation of congenital heart disease (Figure 3).

After 48 hours in the ICU, the patient was transferred to the general ward and remained under the care of the cardiology team. A transthoracic echocardiogram was performed, confirming the diagnosis of partial AVSD, as described below: Situs: Left isomerism. Cardiac position: Levocardia. AV connection type: Via two valves located in the same plane. Ventriculo-arterial connection type: Concordant. Mode of ventriculo-arterial connection: With normally related great arteries. It showed Large single atrium due to absence of the interatrial septum. Moderate-to-severe left AV valve regurgitation (EROA: 0.22 cm^2, regurgitant volume 16 mL, vena contracta 0.45 cm). Moderate right AV valve regurgitation (EROA: 0.23 cm^2, regurgitant volume 21 mL, estimated peak jet velocity of 3.95 m/s, and pulmonary artery systolic pressure of 72 mmHg). Pulmonary hypertension (PH). Pulmonary artery significantly dilated, measuring approximately 5.0 cm. Left ventricle with concentric remodeling and preserved systolic function (61%). Right ventricle enlarged with reduced systolic function (FAC: 27.5%, S' wave 9.3 cm/s) (Figures 4 e 5, Video 1).

Keywords

Atrial Heart Septal Defects; Congenital Heart Defects; Adult.

Mailing Address: Saulo Rodrigo Cunha •
Hospital Nossa Senhora da Conceição. Av. Francisco Trein, 596. Postal code: 91350-200. Bairro Cristo Redentor, Porto Alegre, RS – Brazil
E-mail: saulo_rodrigom@hotmail.com
Manuscript received February 16, 2025, revised manuscript April 30, 2025, accepted June 25, 2025
Editor responsible for the review: Andrea Vilela

DOI: https://doi.org/10.36660/abcimg.20250014i

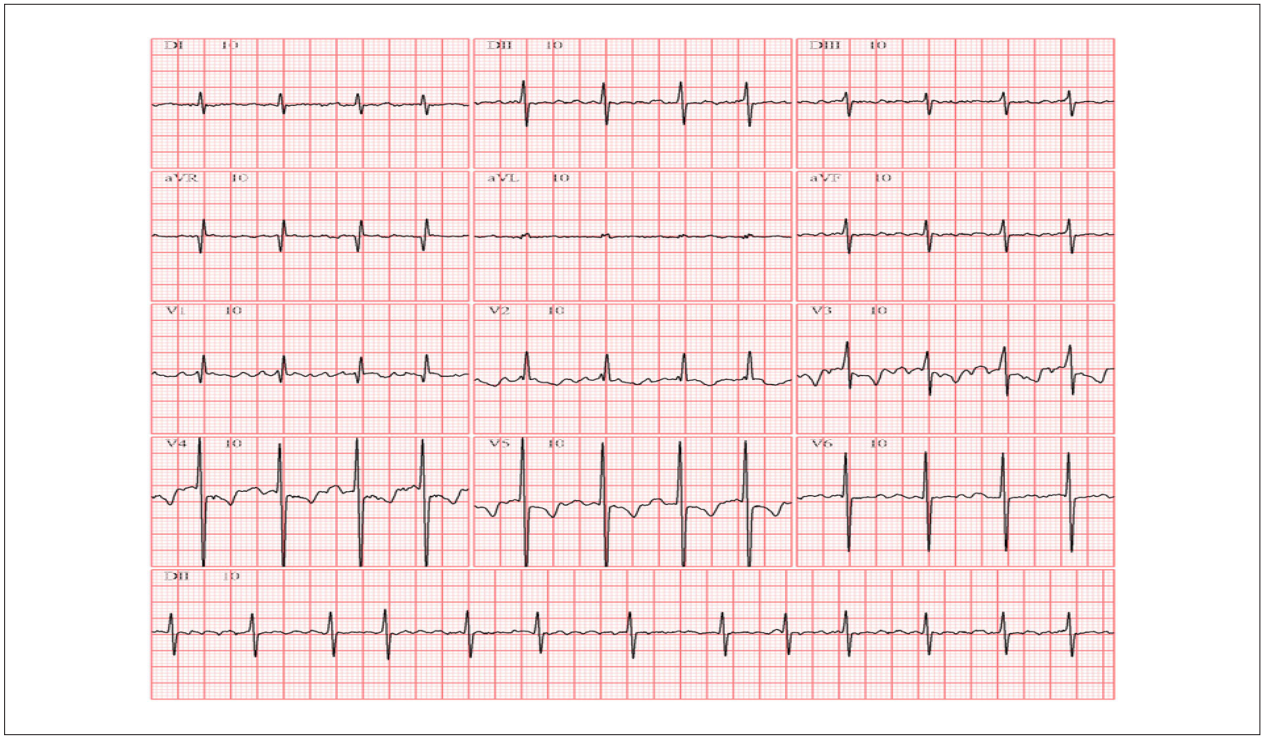

Figure 1 – *Resting Electrocardiogram: Atrial fibrillation rhythm, QRS axis +30°, secondary ventricular repolarization abnormalities.*

In this case report, a tissue tongue is observed connecting the two bridging leaflets, resulting in the separation of the AV valve into two distinct orifices — one right and one left. Additionally, the bridging leaflets are fused to the crest of the interventricular septum (Video 1).

Due to the clinical presentation, the working diagnosis upon admission was community-acquired pneumonia. Following antibiotic therapy, his fever and general condition improved, though he continued to experience exertional shortness of breath and maintained a resting oxygen saturation of 87%. He was discharged on rivaroxaban, sildenafil, carvedilol, enalapril, spironolactone, digoxin, and furosemide, and scheduled to start bosentan to improve functional class and quality of life.

While a recent right heart catheterization was not performed, echocardiographic findings strongly suggest Eisenmenger syndrome, indicating elevated pulmonary vascular resistance. As such, surgical correction of the AV septal defect is contraindicated. A combined heart-lung transplant may be considered for patients with complex cases, poor prognosis, and unresponsiveness to medical therapy.

Discussion

From a management standpoint, most adults with AVSD will have undergone surgical repair during childhood. In cases of complete AVSD — involving both a large Atrial Septal Defect (ASD) e Ventricular Septal Defect (VSD) —, failure to perform early surgical correction — typically before six months of age — can lead to irreversible pulmonary vascular disease and, eventually, Eisenmenger physiology, which rules out the possibility of complete repair.[3]

A 2014 study found that the overall prevalence of PH in adults with congenital heart disease was 3.2%, being more prevalent among older patients.[4] Among patients who previously underwent correction for simple congenital defects, such as atrial or ventricular septal defects, or patent ductus arteriosus, the prevalence of PH was found to be 3%. The risk increased significantly with older age at the time of surgical intervention.[5]

PH in ACHD presents a wide range of clinical manifestations. In this population, management encompasses both non-pharmacological strategies (such as patient education, dental care, vaccination, and psychosocial support) and pharmacological therapies. In recent years, treatment options have expanded with the advent of pulmonary vasodilators targeting various pathways, leading to significant improvements in quality of life.[6] Outcomes for those with PH have also improved, thanks to broader access to targeted PH therapies, advances in perioperative care, and the adoption of multidisciplinary management approaches.[7]

For patients who have undergone surgical repair, long-term follow-up is essential to monitor for potential complications such as left AV valve regurgitation or stenosis, left ventricular outflow tract (LVOT) obstruction due to anatomical distortion, and tachyarrhythmias or bradyarrhythmias. Left AV valve regurgitation is the most

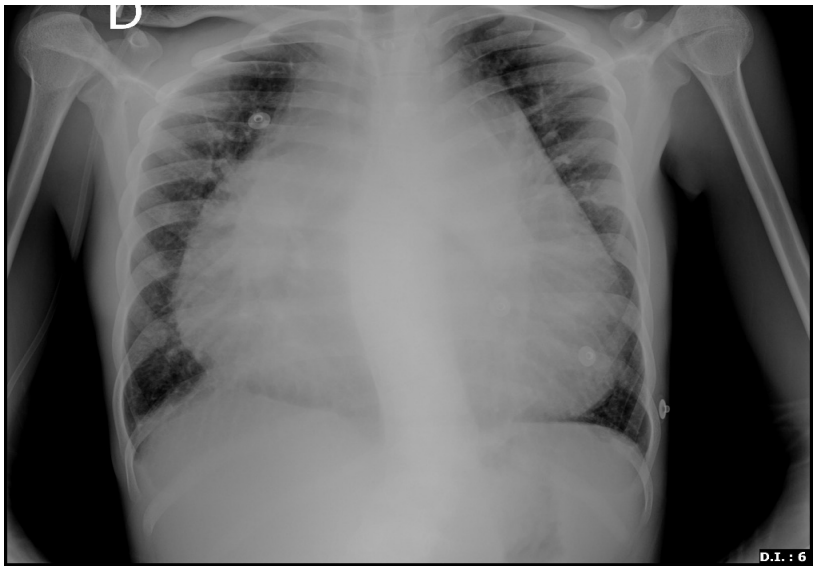

Figure 2 – *Posteroanterior Chest X-ray: Hospital admission. Significant global cardiomegaly.*

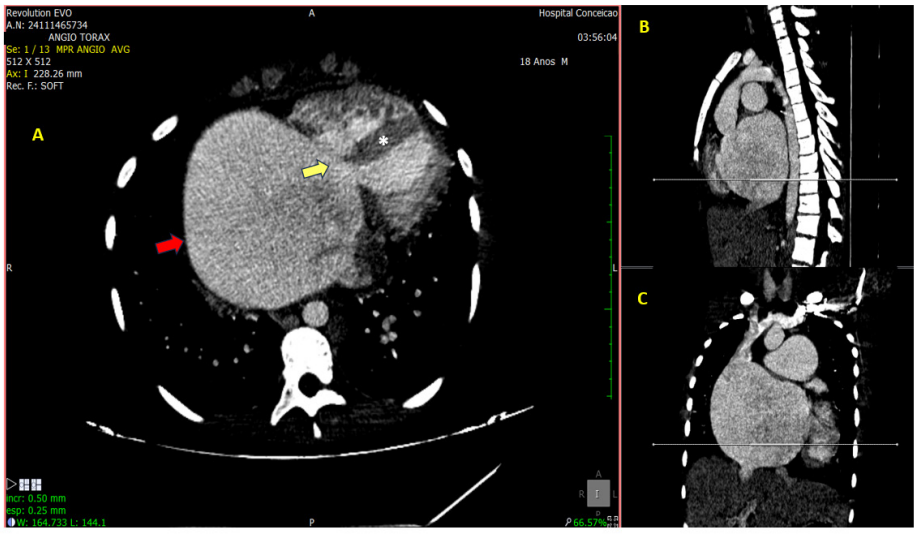

Figure 3 – *Chest CT with multiplanar reconstruction: A) Transverse view showing significant cardiomegaly and presence of AV defect. The red arrow identifies a single atrium with marked enlargement. The yellow arrow shows the AVSD. The asterisk identifies an intact interventricular septum. B) Sagittal view showing dilation of the pulmonary artery. C) Coronal view.*

common cause of late surgical reintervention. There are few long-term follow-up studies of patients after childhood AVSD repair; therefore, the most effective and efficient timing and method of monitoring are still under investigation.[8]

In this case, most AVSD features were successfully identified via 2D echocardiography. However, when surgical repair is a viable option, 3D echocardiography can provide a more detailed view of the AV valve anatomy, enhancing preoperative planning for valve reconstruction.[8,9]

Adults with uncorrected congenital heart disease represent a growing population, characterized by complex clinical scenarios that demand highly individualized therapeutic approaches. In this context, two-dimensional echocardiography becomes an essential tool, not only for accurate diagnosis but also for supporting the development of patient-specific therapeutic strategies.

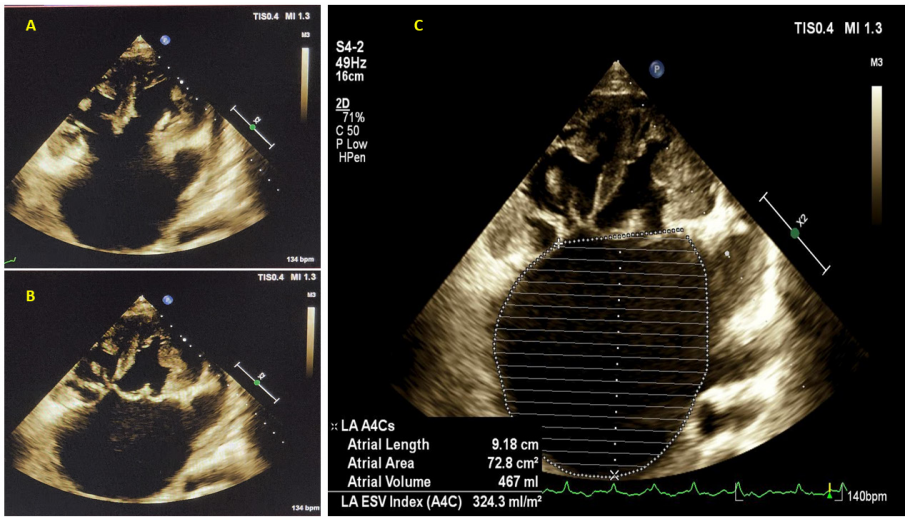

Figure 4 – *Apical 4-chamber (A4C) transthoracic echocardiogram: A) Left and right AV valves are open and aligned in the same plane. B) Left and right AV valves are closed. C) Image shows the single atrium volume.*

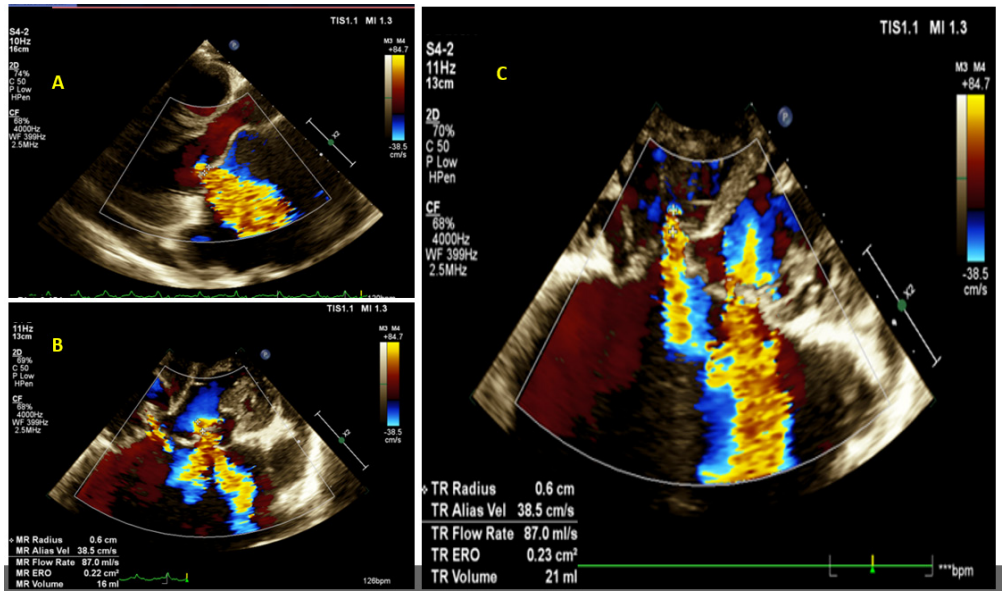

Figure 5 – *Transthoracic echocardiogram: A) Left AV valve in parasternal long-axis view with vena contracta measurement. B) Left AV valve in A4C view with measurements of jet radius, EROA, and regurgitant volume. C) A4C view showing single atrium and regurgitant jets from both AV valves, with right valve jet measurements including radius, EROA, and regurgitant volume.*

Author Contributions

Conception and design of the research: Cunha SR, Barros FC, Pandolfo F, Barcellos PT, Pianca EG; acquisition of data: Cunha SR, Minotto RF, Barros FC, Mazzuca ACM, Pianca EG; analysis and interpretation of the data: Cunha SR, Minotto RF, Barros FC, Pandolfo F, Mazzuca ACM, Barcellos PT, Pianca EG; writing of the manuscript: Cunha SR, Pianca EG; critical revision of the manuscript for intellectual content: Pandolfo F, Mazzuca ACM, Barcellos PT, Pianca EG.

Potential Conflict of Interest

No potential conflict of interest relevant to this article was reported.

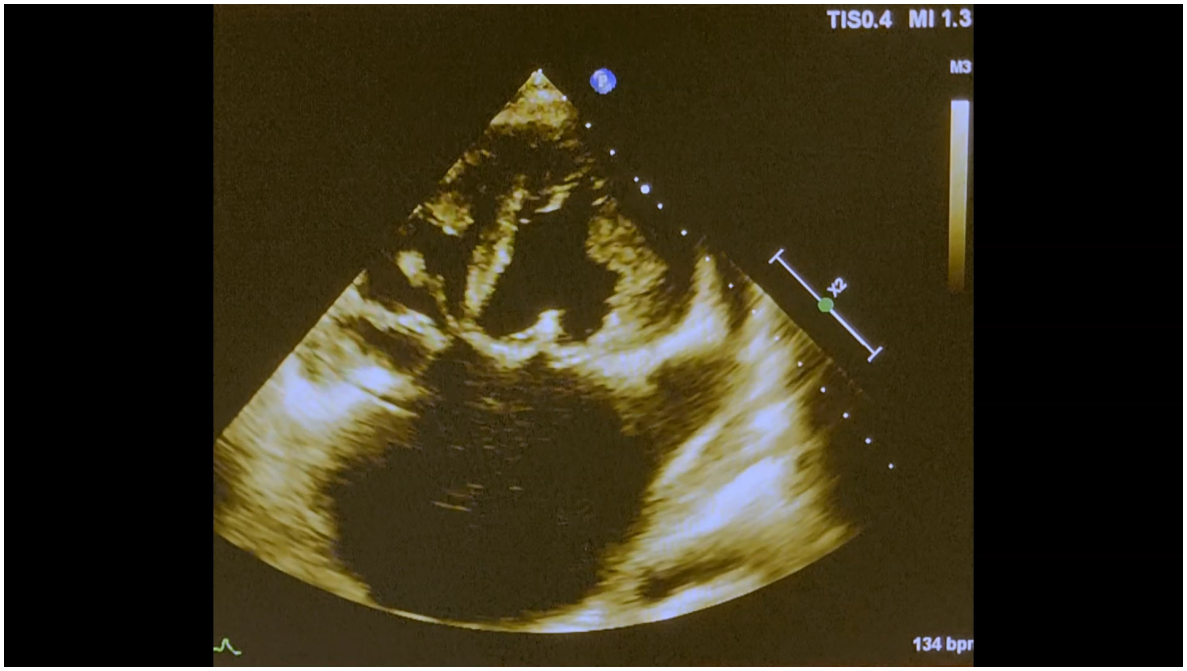

Video 1 – *Ecocardiograma transtorácico mostrando valvas AVs esquerda e direita no mesmo plano com ampla comunicação interatrial. Link: http://abcimaging.org/supplementary-material/2025/3801/2025-0014_video_1.mp4*

Sources of Funding

There were no external funding sources for this study.

Study Association

This article is part of the scientific output of the Medical Residency Program in Echocardiography, developed by the residents and preceptors of Hospital Nossa Senhora da Conceição.

Ethics Approval and Consent to Participate

This study was approved by the Ethics Committee of the Hospital Nossa Senhora da Conceição Sá under the protocol number CAAE: 91751125.8.0000.5530, Technical opinion: 7.974.789. All the procedures in this study were in accordance with the 1975 Helsinki Declaration, updated in 2013. Informed consent was obtained from all participants included in the study.

Use of Artificial Intelligence

The authors did not use any artificial intelligence tools in the development of this work.

Availability of Research Data

The underlying content of the research text is contained within the manuscript.

References

1. Stout KK, Daniels CJ, Aboulhosn JA, Bozkurt B, Broberg CS, Colman JM, et al. 2018 AHA/ACC Guideline for the Management of Adults with Congenital Heart Disease: A Report of the American College of Cardiology/American Heart Association Task Force on Clinical Practice Guidelines. J Am Coll Cardiol. 2019;73(12):e81-e192. doi: 10.1016/j.jacc.2018.08.1029.
2. Mann DL, Zipes DP, Libby P, Bonow RO. Braunwald – Tratado de Doenças Cardiovasculares. 10th ed. Rio de Janeiro: Elsevier, 2018.
3. Pena JLB, Vieira MLC, editors. Ecocardiografia e Imagem Cardiovascular. Rio de Janeiro: Thieme Revinter Publicações; 2021.
4. van Riel AC, Schuuring MJ, van Hessen ID, Zwinderman AH, Cozijnsen L, Reichert CL, et al. Contemporary Prevalence of Pulmonary Arterial Hypertension in Adult Congenital Heart Disease Following the Updated Clinical Classification. Int J Cardiol. 2014;174(2):299-305. doi: 10.1016/j.ijcard.2014.04.072.
5. Lammers AE, Bauer LJ, Diller GP, Helm PC, Abdul-Khaliq H, Bauer UMM, et al. Pulmonary Hypertension after Shunt Closure in Patients with Simple Congenital Heart Defects. Int J Cardiol. 2020;308:28-32. doi: 10.1016/j.ijcard.2019.12.070.
6. Martins AVV, Zorzanelli L, Thomaz AM. Pulmonary Hypertension in Adults with Congenital Heart Disease: Current Treatment. Rev Soc Cardiol Estado de São Paulo. 2023;33(1)22-8. doi: 10.29381/0103-8559/2023330122-8.
7. Humbert M, Kovacs G, Hoeper MM, Badagliacca R, Berger RMF, Brida M, et al. 2022 ESC/ERS Guidelines for the Diagnosis and Treatment of Pulmonary Hypertension. Eur Heart J. 2022;43(38):3618-731. doi: 10.1093/eurheartj/ehac237.

8. Moreno N, Almeida J, Amorim MJ. Atrioventricular Septal Defect in an Adult Patient: There are 'Clefts' and Clefts. Rev Port Cardiol. 2016;35(3):181.e1-4. doi: 10.1016/j.repc.2015.11.004.

9. Grewal J, Mankad S, Freeman WK, Click RL, Suri RM, Abel MD, et al. Real-Time Three-Dimensional Transesophageal Echocardiography in the Intraoperative Assessment of Mitral Valve Disease. J Am Soc Echocardiogr. 2009;22(1):34-41. doi: 10.1016/j.echo.2008.11.008.

Long-term Follow-Up of a Patient with FLNC Gene Mutation-Related Cardiomyopathy: A Case Report

Isabela Bispo Santos da Silva Costa,[1,2] Bruno Soares da Silva Rangel,[2] Antonio Tito Paladino Filho,[2,3] Bruno Normande Colombo,[2] Thamara Carvalho Morais,[2] Ludhmila Abrahão Hajjar[2,4]

Universidade de São Paulo, Instituto do Câncer do Estado de São Paulo,[1] São Paulo, SP – Brazil

Hospital Vila Nova Star,[2] São Paulo, SP – Brazil

Instituto Dante Pazzanese de Cardiologia,[3] São Paulo, SP – Brazil

Hospital das Clínicas da Faculdade de Medicina da Universidade de São Paulo,[4] São Paulo, SP – Brazil

Introduction

Heart Failure (HF) is estimated to affect approximately 26 million people worldwide.[1,2] In Brazil, prevalence is high, with about 2 million diagnosed patients and an incidence of roughly 240,000 new cases every year. Between 2011 and 2021, more than 2.5 million HF-related hospitalizations were recorded in the Brazilian Unified Health System (SUS), underscoring the relevance of the disease in the national context.[3] These figures highlight the need for early diagnostic strategies and etiological definition for the appropriate management of these patients. Establishing an etiological diagnosis is often challenging but essential to provide disease-specific treatments and improve prognosis. Diagnosis encompasses multimodality cardiac imaging, with Cardiac Magnetic Resonance imaging (CMR) being a useful tool for evaluating non-ischemic cardiomyopathy phenotypes and establishing an etiological diagnosis.[4]

Clinical Case

A 52-year-old male patient presented in 2017 with exertional dyspnea and chest pain and was initially investigated by echocardiography, which revealed new left ventricular dysfunction. The patient had no known previous comorbidities or family history of cardiomyopathy. Additional investigations included CMR, which showed left ventricular enlargement and systolic dysfunction with a Left Ventricular Ejection Fraction (LVEF) of 38%, along with multiple non-ischemic Late Gadolinium Enhancement (LGE) foci without myocardial edema, initially interpreted as previous inflammatory cardiomyopathy (Figure 1). The patient was then diagnosed with Heart Failure with Reduced Ejection Fraction (HFrEF), and treatment with beta-blockers and angiotensin-converting enzyme inhibitors was initiated.

Keywords

Cardiomyopathies; Genetics; Cardiac Magnetic Resonance Imaging; Arrhythmias, Cardiac; Sudden Cardiac Death

Mailing Address: Isabela Bispo Santos da Silva •
Rua Dr. Alceu de Campos Rodrigues, 46, 1º andar. Postal Code: 04544-000, São Paulo, SP – Brazil
E-mail: isabela.scosta@vilanovastar.com.br
Manuscript received September 9, 2025; revised September 10, 2025 accepted September 10, 2025
Editor responsible for the review: Marcelo Tavares

DOI: https://doi.org/10.36660/abcimg.20250071i

In 2024, the patient was referred to our service due to persistent HFrEF, now associated with frequent palpitations. Repeat CMR was performed. The exam revealed biventricular systolic dysfunction (LVEF 42% and RVEF 40%), diffuse hypokinesia, absence of myocardial edema, elevated native T1 mapping (1120 ms) and extracellular volume fraction (42%), as well as extensive areas of non-ischemic LGE (> 35% of LV mass) with a ring-like pattern (Figure 2), suggesting a genetic cardiomyopathy, with possible FLNC or desmoplakin mutation. Marked progression of LGE compared with the previous exam was observed.

Due to palpitations associated with the high burden of LGE, a 24-hour Holter monitor was performed:

- Total events: 102,754
- Heart rate: 57-74-141 bpm
- Ventricular ectopy 10,130 events (10%)
  - 9,323 isolated; 44 bigeminy; 402 couplets; one non-sustained ventricular tachycardia (NSVT) with three beats.

Genetic testing (Table 1) indicated a heterozygous pathogenic variant in the FLNC gene. Clinical therapy was optimized, family screening was recommended, and an implantable cardioverter-defibrillator (ICD) was placed for sudden cardiac death prevention.

Discussion

Genetic cardiomyopathies associated with mutations in the filamin C (FLNC) gene are rare and difficult to diagnose. Filamin C is a cytoskeletal protein that plays an essential role in maintaining the structural and functional integrity of cardiomyocytes. Pathogenic mutations in this gene are associated with a wide range of clinical manifestations. Truncating filamin C mutations are prevalent in dilated cardiomyopathy and Arrhythmogenic Right Ventricular Cardiomyopathy (ARVC). Non-truncating filamin C mutations are more common in Hypertrophic Cardiomyopathy (HCM) and Restrictive Cardiomyopathy (RCM). Two main pathogenic mechanisms in FLNC-related cardiomyopathy have been described: protein aggregation due to non-truncating mutations and haploinsufficiency caused by truncating mutations.[5]

FLNC-related cardiomyopathy, manifesting as a DCM phenotype, usually presents with LV dilation, LV systolic dysfunction, and areas of myocardial fibrosis identified as

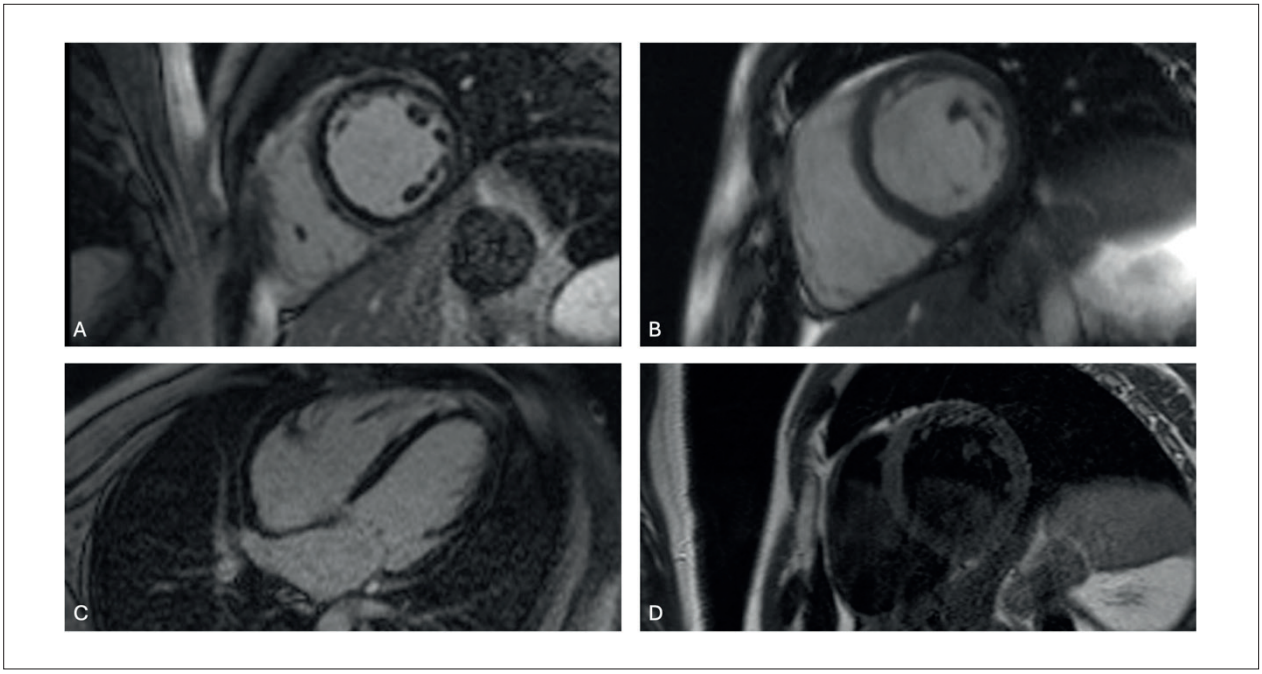

Figure 1 – *Cardiac magnetic resonance imaging performed in 2017. A and C: LGE images in short-axis and 4-chamber views. B: short-axis cine MRI image. D: dark-blood triple inversion recovery sequence image.*

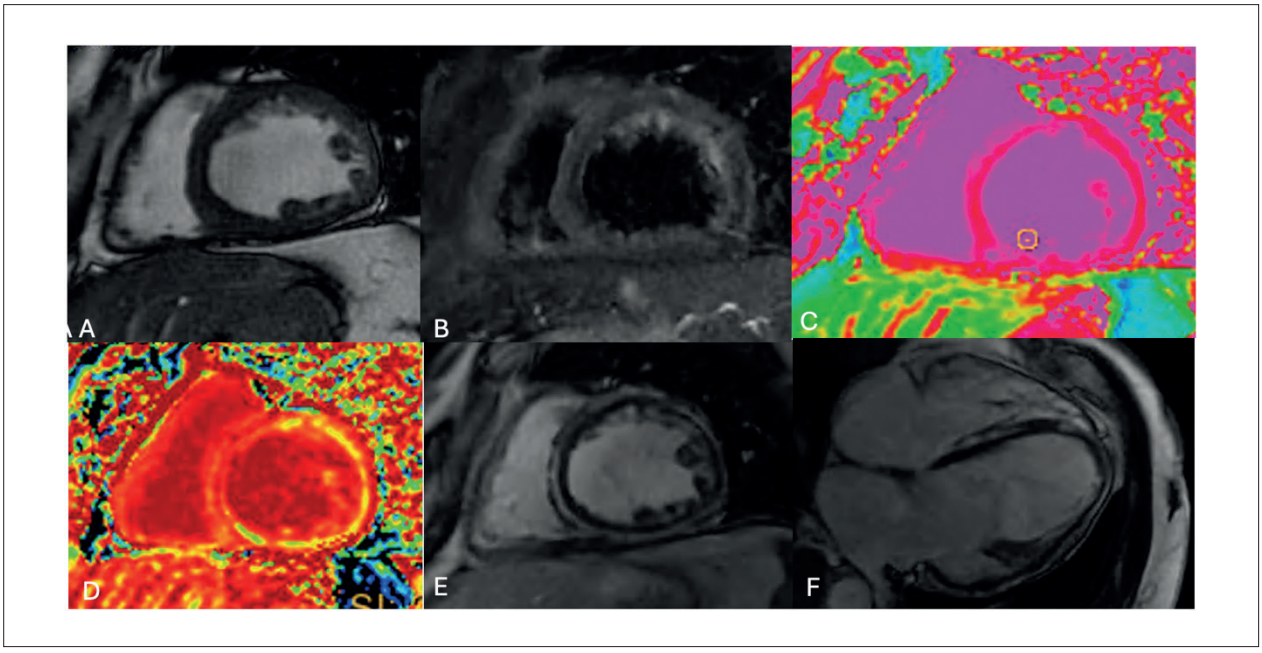

Figure 2 – *Cardiac magnetic resonance imaging performed in 2024. A: cine MRI image; B: dark-blood triple inversion recovery sequence image; C: native T1 map; D: extracellular volume map; E and F: LGE images in short-axis and 4-chamber views, respectively, showing extensive areas of non-ischemic LGE.*

LGE on CMR.[4] Clinical suspicion may arise in patients with recurrent or familial myocarditis, in patients with arrhythmias, or when CMR demonstrates progression of fibrosis. FLNC mutation-related cardiomyopathy is notable for its association with inflammatory pathways overlapping with classical myocarditis, representing a rare but increasingly recognized cause of arrhythmogenic cardiomyopathy.[6]

The risk of sudden cardiac death in these patients is high, mainly due to a predisposition to malignant ventricular arrhythmias such as sustained ventricular tachycardia or

Table 1 – Genetic testing

Gene/Transcript	Exon	Variant	Population frequency	Zygosity	Classification
FLNC (NM_001458.5)	4	C850+1G>A p.?	0%	Heterozygous	Likely Pathogenic

ventricular fibrillation. This risk justifies the early consideration of preventive strategies, such as implantable cardioverter-defibrillators (ICDs), particularly in individuals with a history of complex arrhythmias or significant ventricular dysfunction.[7] In the present case, ventricular dysfunction (LVEF < 45%), associated with extensive fibrosis, survival greater than one year, supported ICD implantation with a class IIa recommendation.[4,8]

CMR plays a fundamental role in the diagnosis of non-ischemic cardiomyopathies, including those related to FLNC mutations. This exam allows both morphofunctional evaluation and tissue characterization with identification of myocardial fibrosis. The location and pattern of myocardial fibrosis, such as ring-like or diffuse, may provide valuable information for differentiating ischemic and non-ischemic etiologies, as well as correlate with prognosis and arrhythmic risk. Moreover, CMR with T1 mapping and extracellular volume quantification may be useful for the early detection of tissue changes, even in the absence of overt morphological abnormalities.[4,6,9]

The integration of genetic, clinical, and imaging findings is essential for effective diagnostic and therapeutic approaches in genetic cardiomyopathies, particularly in patients such as the one described, in whom disease progression was significant. Identification of FLNC mutations should raise concern for the potential risk of refractory HF and SCD, making regular follow-up crucial for these patients.

Author Contributions

Conception and design of the research: Costa IBSS, Rangel BSS. Writing of the manuscript: Costa IBSS, Rangel BSS, Paladino Filho AT,Colombo BN, Morais TC. Critical revision of the manuscript for intellectual content: Hajjar LA.

Potential Conflict of Interest

No potential conflict of interest relevant to this article was reported.

Sources of Funding

There were no external funding sources for this study.

Study Association

This study is not associated with any thesis or dissertation work.

Ethics Approval and Consent to Participate

This study was approved by the Ethics Committee of the Hospital São Luiz, Rede D'Or, under the protocol number CAAE 91628425.0.0000.0087. All the procedures in this study were in accordance with the 1975 Helsinki Declaration, updated in 2013. Informed consent was obtained from all participants included in the study.

Use of Artificial Intelligence

The authors did not use any artificial intelligence tools in the development of this work.

Availability of Research Data

The underlying content of the research text is contained within the manuscript.

References

1. van Riet EE, Hoes AW, Wagenaar KP, Limburg A, Landman MA, Rutten FH. Epidemiology of Heart Failure: The Prevalence of Heart Failure and Ventricular Dysfunction in Older Adults Over Time. A systematic review. Eur J Heart Fail. 2016;18(3):242-52. doi: 10.1002/ejhf.483.
2. McDonagh TA, Metra M, Adamo M, Gardner RS, Baumbach A, Böhm M, et al. 2021 ESC Guidelines for the Diagnosis and Treatment of Acute and Chronic Heart Failure. Eur Heart J. 2021;42(36):3599-726. doi: 10.1093/eurheartj/ehab368.
3. Brasil. Ministério da Saúde. Comissão Nacional de Incorporação de Tecnologias no Sistema Único de Saúde (CONITEC) [Internet]. Brasília: Ministério da Saúde; 2024 [cited 2025 Nov 4]. Available from: https://www.gov.br/conitec.
4. Arbelo E, Protonotarios A, Gimeno JR, Arbustini E, Barriales-Villa R, Basso C, et al. 2023 ESC Guidelines for the Management of Cardiomyopathies. Eur Heart J. 2023;44(37):3503-626. doi: 10.1093/eurheartj/ehad194.
5. Song S, Shi A, Lian H, Hu S, Nie Y. Filamin C in Cardiomyopathy: From Physiological Roles to DNA Variants. Heart Fail Rev. 2022;27(4):1373-85. doi: 10.1007/s10741-021-10172-z.
6. Del Franco A, Ruggieri R, Pieroni M, Ciabatti M, Zocchi C, Biagioni G, et al. Atlas of Regional Left Ventricular Scar in Nonischemic Cardiomyopathies: Substrates and Etiologies. JACC Adv. 2024;3(10):101214. doi: 10.1016/j.jacadv.2024.101214.
7. Ortiz-Genga MF, Cuenca S, Dal Ferro M, Zorio E, Salgado-Aranda R, Climent V, et al. Truncating FLNC Mutations are Associated with High-Risk Dilated and Arrhythmogenic Cardiomyopathies. J Am Coll Cardiol. 2016;68(22):2440-51. doi: 10.1016/j.jacc.2016.09.927.

8. Towbin JA, McKenna WJ, Abrams DJ, Ackerman MJ, Calkins H, Darrieux FCC, et al. 2019 HRS Expert Consensus Statement on Evaluation, Risk Stratification, and Management of Arrhythmogenic Cardiomyopathy: Executive Summary. Heart Rhythm. 2019;16(11):e373-e407. doi: 10.1016/j.hrthm.2019.09.019.

9. Schoonvelde SAC, Ruijmbeek CWB, Hirsch A, van Slegtenhorst MA, Wessels MW, von der Thüsen JH, et al. Phenotypic Variability of Filamin C-Related Cardiomyopathy: Insights from a Novel Dutch Founder Variant. Heart Rhythm. 2023;20(11):1512-21. doi: 10.1016/j.hrthm.2023.08.003.